Holocene paleoenvironmental reconstruction in Galway Bay, a shallow coastal embayment along Ireland's North-East Atlantic margin

Joyce D. Novak, BA, MSc

2017

Thesis submitted for the degree of Doctor of Philosophy

Department of Geography
Mary Immaculate College
University of Limerick

Supervisor: Dr. Catherine Dalton
Co-supervisor: Dr. Caroline Cusack

Submitted to the University of Limerick December, 2016

For Dylan and Nathan

"For whatever we lose (like a you or a me), it's always ourselves we find in the sea."
E. E. Cummings

For Dave

For everything…and more. A chuisle mo chroí.

“These shores, so different in their nature and in the inhabitants they support are made one by the unifying touch of the sea. For the differences I sense in this particular instant of time that is mine are but the differences of a moment, determined by our place in the stream of time and in the long rhythms of the sea.”

Rachel Carson, 1951

Title of Thesis: Holocene paleoenvironmental reconstruction in Galway Bay, a shallow coastal embayment along Ireland's North-East Atlantic margin

Author: Joyce Novak

Coastal environments are highly dynamic and complicated systems that vary spatially and temporally over a range of timescales. This study explores the paleoenvironmental changes recorded in sediment cores taken from Galway Bay, located on the coast of western Ireland. Galway Bay is a large shallow bay, which is protected from ocean swells of the North Atlantic by the Aran Islands. The inner bay receives freshwater mainly from the Corrib River Catchment. Four c. 6 m sediment cores were extracted along an inner bay transect and are explored here in a multi proxy paleoecological study to track environmental change during the Holocene period. Physical proxies obtained using a Multi Sensor Core Logger (MSCL), geochemical signatures acquired with X-ray fluorescence (XRF) scanning and microfossils (diatom and foraminifera) were examined. A Holocene timeframe was established with 23 AMS ^{14}C dates across the four cores spanning c. 10000 cal years BP. A west-east progression is noted in the sediment stratigraphy. The western most sediment core contained no sediment post c. 8500 cal years BP while the eastern most sediment core, closest to the Corrib River outflow, contained the most complete sediment profile with sediments from the early, mid and late Holocene. A sedimentary hiatus spanning 5-7 ka is confirmed in two sediment cores. Change points in the sediment profiles are identified, reflecting known climatic events, including marine transgression, a possible 8.2 ka cooling event, freshwater phases and rising sea levels. The early Holocene encompassed the highest rate of sediment accumulation and marine transgression is captured in the proxy evidence. Coastal environmental change is postulated with water level rise and paleo tidal ranges varying from Highest Astronomical Tide to Mean High Water with high to middle marsh and mudflat development. The mid Holocene has a major break in sediment continuity with no complete mid Holocene sediment profile preserved. The innermost bay core retained sediment until c. 6000 cal years BP. The major hiatus is associated with a visible shell layer possibly reflecting a possible storm event and a sediment washout. The shell layer is overlain with late Holocene sediments (c. 500 years) in both inner bay cores reflecting either a return of conditions facilitating sediment deposition, or sediments that have not yet been washed out. The complex chronology and sedimentary profiles display a west to east progression along the inner Galway Bay transect reflecting a spatial trajectory of chronological, physical, chemical and biological change and thus environmental change as the rising sea made its way east into the Galway Bay.

Declaration

I hereby declare that this thesis represents my work and has not been submitted in whole or in part, by me or another person, for the purpose of obtaining any other qualification.

Signed: _____

Date: _____

Acknowledgements

I would like to thank Mary Immaculate College for awarding me the MIC Studentship which made this work possible. As well, for further research seed funding which was used for radiocarbon dating of material in this project. The Marine Institute, for granting me their Networking and Travel Award in 2012 and 2013.

My academic supervisor at MIC, Dr Catherine Dalton, for guiding me through the PhD process. For her exceptional skills as an editor and imparting her knowledge of the paleo world and academia to me. I am eternally grateful.

My supervisor at the Marine Institute, Dr Caroline Cusack, for sharing her enormous intelligence with me and opening the MI to me. Your advice regarding ocean sciences was invaluable and I could not have completed this without you. Your camaraderie as a working mother and regarding sick children made me feel human.

To my fellow geography postgrads Margaret Browne and Darren Barry who have battled in the trenches with me from Ireland to Italy (via Moneygall), provided countless hours of informed discussion, sci-fi and superhero discussion, Japanese food, map making, foram processing, stats confusion and who have cheered me on from the sidelines; I am not quite sure I would've crossed the finish line without them. The Geography Department at Mary Immaculate College: Dr Des McCaffrety, Dr Brendan O'Keefe, Dr Helene Bradley-Davis, Dr Angela Cloke-Hayes, Dr Shane O'Sullivan, Grainne Dwyer and Niall Walsh for continual support.

To the Marine Institute's INFOMAR programme through which the sediment cores for this project were obtained. Morris Clarke, Helen McCormick and Macdarra O'Cuaig in the Fishery Ecosystem Advisory Service at the MI; Kieran Lyons, Trevor Alcorn and Deirdre O'Driscoll in Data Services and Adam Leadbetter at the MI. Dr Mike Williams (NUIG), Bill Wood, Dr Rosaleen Mylotte (UL), Dr. Paula Reimer (Queens), Dr Jonathan Turner (UCD), Dr Steve McCarron (Maynooth), Dr Gil Scott, Dr Garrett Duffy (NUI Galway), Cathal Clarke (NUI Galway), Dr Jonathan Lewis (Loughboro UK).

Tobi and Otis Rapp & Séan O'Connor at the MI Fishery Science Unit in Castletownbere & Gavin Power, fisherman extraordinaire, for sharing your space with me for the past five years, for all the seafood, putting up with my messiness and especially for all the banter about life in this tiny little paradise at the edge of the world in West Cork.

Gretta Purcell for always minding the boys (and me).

The strong women on whose shoulders I stand: Catherine Martinez, Anita H. Martinez, Catherine Novak-Doyle, Dr. Carolyn Tricomi, Dr. Anita DeStefano, Josephine DeStefano – long stemmed American beauties all.

Colleen- for loving me more than her luggage.

Catherine Schnabel Martinez – for happily entertaining my endless stream of questions & nurturing my inquisitive nature – how I wish you were here to share this moment.

And most of all, my parents (Mom & Bill, Daddy & Kathy) who are my champions, my biggest fans and when need be, my financial backers. Your pride overwhelms me & your love is boundless. Your relentless pursuit of this achievement was as great as my own. Go raibh maith agat.

TABLE OF CONTENTS

List of Maps

List of Figures

Figure 6.7: Sediment cores VC001 and VC003 in the Glacoal Isostatic Adjustment (GIA) Model (Bradley *et al*., 2011). The green 'x' is the existing primary limiting point identified in Edwards and Craven (2017); the two red 'x' marks are VC001 and VC003. (a) Ireland RSL for 10, 9, 7 and 4 kyr BP; (b) Galway Bay RSL for 10, 9, 7 and 4 kyr BP.

Figure 6.8: The upper 200 cm of VC001 is shown showing possible evidence of the 8.2 ka cold with selected physical and geochemical proxies. A) Physical evidence: p-wave velocity (m/s), gamma density (g/cm^3), magnetic susceptibility (SI), organic carbon (%) and DI-salinity (PPM). B) Geochemical evidence: Ca/Ti, K/Ti, Si/Ti, Zr/Ti and Br/Cl.

Figure 6.9: Marine Institute LIDAR imagery of inner Galway Bay, accessed on 12/9/2016 from the INFOMAR bathymetry mapping system on the Marine Institute website. Sediment cores VC001, VC002, VC003 and VC004 are marked accordingly. (a) Drumlins identified by McCabe and Dardis (1989) are outlined in red and potential, unconfirmed drumlins are outlined in purple. (b) A potential paleo lagoon in Inner Galway Bay during the mid-Holocene is indicated with a yellow dashed line. This is a theoretical delineation and postulated here as one possible paleo lagoon barrier.

Figure 6.10: A schematic diagram of paleoenvironmental changes in Inner Galway Bay during the Holocene. Here, environmental changes, paleotidal changes, sea level and the 8.2K cold event are noted. Additionally water levels and sediment depths are indicated.

Figure B1: Age Depth Profile VC003

Figure B2: Age Depth Profile VC004

Figure C1: Single Elemental Profiles XRF VC001 (a): MSE, Mo inc, Mo coh, Si, Ca, Ti, Mn, Ni; (b): Zn, Pb, S, Cl, Ar, K, Cr, Ga, Br; (c): Rb, Sr, Y, Zr, La, Ce, Ta, W, Bl, U. The following elements are excluded due to extensive nil counts: Mg, Al, Cu, Ba, As.

Figure C2: Single Elemental Profiles XRF VC002 (a): MSE, Mo inc, Mo coh, Si, Ca, Ti, Mn, Ni; (b): Zn, Pb, S, Cl, Ar, K, Cr, Ga, Br; (c): Rb, Sr, Y, Zr, La, Ce, Ta, W, Bl, U. The following elements are excluded due to extensive nil counts: Mg, Al, Cu, Ba, As.

Figure C3: Single Elemental Profiles XRF VC003 (a): MSE, Mo inc, Mo coh, Si, Ca, Ti, Mn, Ni; (b): Zn, Pb, S, Cl, Ar, K, Cr, Ga, Br; (c): Rb, Sr, Y, Zr, La, Ce, Ta, W, Bl, U. The following elements are excluded due to extensive nil counts: Mg, Al, Cu, Ba, As.

Figure C4: Single Elemental Profiles XRF VC004 (a): MSE, Mo inc, Mo coh, Si, Ca, Ti, Mn, Ni; (b): Zn, Pb, S, Cl, Ar, K, Cr, Ga, Br; (c): Rb, Sr, Y, Zr, La, Ce, Ta, W, Bl, U. The following elements are excluded due to extensive nil counts: Mg, Al, Cu, Ba, As.

Figure E: Detrended Correspondence Analysis (DCA) for diatoms in sediment core VC001

List of Tables

CHAPTER 1: Introduction

1.1 Research rationale

Nicholls *et al*. (2007), estimates that over half of the world's human population resides within 60 km of a coastline. This makes the need for greater knowledge of coastal environments over time a priority. Understanding the natural forcings and changing climatic conditions which lead to regionally diverse coastal environments is imperative and one of the main drivers in coastal paleoenvironmental studies. In order to understand present day ecological processes, it is necessary to identify the base-line conditions that existed prior to anthropogenic influences (Delaney and Devoy, 1995). The Intergovernmental Panel on Climate Change (IPCC), in their inaugural report released in 1990, recognised that global recommendations for coastal areas, with specific reference to sea level and coastal conditions, should not be made. Instead the IPCC stressed the need for further study of individual, spatially unique coastal areas in order to make accurate regional assessments of climate change on coastal environments and future coastal defence planning. In their two most recently published assessment reports (IPCC, 2007; 2013) the IPCC looks at the Holocene and discusses, in part, changes in circulation, sea surface temperature, sea level rise and refers to various studies which utilise a multi proxy approach to determine coastal paleoceanographic change during the Holocene (e.g Juckes *et al.,* 2007; Loehle and McCulloch, 2008; Christiansen and Ljungqvist, 2012; Shi *et al.,* 2013).

Understanding contemporary coastal systems requires multiple sets of spatially and temporally compatible data that can integrate past climate conditions, natural variability, reference conditions and anthropogenic disturbances (Andersen *et al*., 2004). The coastal sediment record portrays amalgamated profiles of relative sea-level and the extent of land-based activities via sedimentation rates, time marker horizons, geochemical signatures and biological responses represented in fossil assemblages. The provision of information to help describe past climate regimes, define reference conditions, assess change of state and help anticipate ecosystem responses under new climate scenarios is vital. Additionally, coastal environments have high primary productivity; it is estimated that shelf seas house approximately 20% of all oceanic primary productivity (Behrenfeld *et al.,* 2005; Jahnke, 2010; Simpson and Sharples, 2012; Scourse, 2013) with the phytoplankton production rate

three to five times higher and a per unit carbon fixation rate approximately 2.5 times greater than in the open ocean (Simpson and Sharples, 2012). This makes these extremely important environments on various scales and for numerous reasons. Coastal environments are sensitive to changes in freshwater inputs, sea level and nutrient supply and as such, climate change and eutrophication of coastal waters over the coming century are major global issues (EEA, 2001; Clarke *et al.,* 2006; Borja *et al.,* 2006; Weckström *et al.,* 2007). Current European legislation (e.g.: The Water Framework Directive (WFD)) provides a framework for the protection of transitional waters (estuaries) and coastal waters. In Ireland, the WFD requires on-going data related to transitional waters and accurate baseline information is a necessity.

An example of an individual, spatially unique coastal area is Galway Bay on the Irish Atlantic seaboard. There has long been speculation of vastly different paleo environments in Galway Bay. Fahey (1900) in an article presented to the Galway Archaeological and Historical Society writes:

> "In our ancient annals we find the Corrib and the bay into which it flows…Lough Corrib is *Lough Orbson* and *the spacious bay into which the crystal waters of the Corrib are borne in rushing volume, was known to the ancients as Lough Lurgan'* And O'Flaherty tells us in his Ogygia that '*Lough Lurgan was one of the most ancient lakes in Ireland'*."

This legacy survives today in the gaeltacht in Galway where Lough Lurgan is still the name used when referring to Galway Bay and has led to an idea of a mythical lake where Galway Bay presently lies (pers comm. Macdarra Ó'Cuaig). While this image of a lake had persisted culturally, there was no published scientific research to this affect.

O'Carra *et al*. (2014) presents radiocarbon dates taken from a red deer (*Cervus elaphus* Linnaeus, 1758) and other animal remains found in the intertidal zone near An Spidéal and Williams and Doyle (2014) present radiocarbon dates taken from tree stumps in An Spidéal, exposed by storm surges in the intertidal zone in 2012. Brief speculation on paleoenvironmental conditions are suggested but no further research is published on these sites. Publications relating to geomorphology, specifically glacial landscapes and glacial

activity in Galway Bay exist (e.g.: Williams, 1980; McCabe and Dardis, 1989; Knight, 2014) but largely pre date the Holocene or are terrestrial-based. Paleo sediment transport and deposition in Galway Bay (e.g.: Hall *et al*., 2006; Williams, 2010; Cox *et al*., 2012) is also explored but largely discusses modes of boulder transport as a result of storm force.

Until 2007, there had been limited work on paleoenvironmental records from Galway Bay when an INFOMAR funded project resulted in the use of nine sediment cores in an unpublished Master's thesis (Wood, 2010). However, this work concentrated primarily on shallow marine sediments from the outer and southern bay regions, as well as terrestrial sites. The sediment sequences exhibited disturbed chronologies and interpretation was complicated. In 2009, the four sediment cores used in this research were extracted from a targeted transect including coastal water body Inner Galway Bay North (Code IE_WE_170_0000) and transitional waters in the Corrib Estuary (Code IE_WE_170_0700). Mylotte (2014) conducted doctoral studies on humic compound extraction methodologies using the same sediment cores. Subsurface seismic data was also collected and was included in an unpublished Master's thesis (Clarke, 2014).

1.2 Aims and objectives

The aim of this research is to track the environmental changes in inner Galway Bay during the Holocene, identifying coastal changes that occurred through time. The first objective in reaching this aim was to generate a chronological profile that would make this possible. Establishing chronologies in sediment cores can be problematic because sediment can become re-worked over time. Storm events, geomorphological changes and biological influences can all lead to the movement of sediment vertically through the profile that would cause recent sediment to be deposited below older sediment. This can lead to inconsistencies in resultant radiocarbon dates and conclusions.

The second objective of this research was to collect data from multiple proxies and create a comprehensive data set. Physical, geochemical and microfossil proxies were used in this research leading to an enormous amount of data. Sorting through the data to extract information that would provide the basis for useful and relevant conclusions regarding the changing coastal environment in inner Galway Bay was imperative. Multi-proxy

paleoenvironmental studies generate greater information than a single proxy approach and can be used to gauge subtle environmental responses. The integration of data can be used to quantify various environmental changes both regionally and spatially.

The location of the sediment cores used in this project run along an west-east transect in the inner Bay with the eastern-most point located close to the Corrib River outflow. The third objective of this project was to determine if there was a trajectory of change over a period of time between the transitional waters of the Corrib Estuary and the Inner, more saline modern bay. This would have implications for regional coastal evolution and allow for the identification of natural variability in these transitional and coastal water bodies. Included as part of this objective, was to identify any signals that may be associated with known climatic events. This would give even greater insight into the behaviour of regional coastal environmental changes during known climatic conditions.

Lastly, this research sought to establish baseline data to underpin effective management of coastal systems in Ireland. This objective would lend a historical perspective and therefore aid implementation of current legislation for Irish coastal waters. To achieve integrated coastal zone management there is a clear need for a combination of monitoring, modelling and paleoenvironmental studies to provide accurate explanations or predictions of aquatic system changes (Anderson *et al.*, 2006).

1.3 Structure of thesis

Numerous processes interact to control coastal environments thus making the land-sea interface a dynamic and challenging area to study. Chapter 2 will discuss coastal environments and the oceanic, estuarine and terrestrial processes that act together to produce coastal zone environments and their sediment deposits. Chapter 3 will discuss environmental change during the Holocene, delving briefly into the Last Glacial Maximum to set the scene of consequent conditions during the Holocene and moving on to the drivers of climate change, climatic conditions and relative sea level rise. Ireland lies on the edge of the European continental shelf and the coastal zone here is heavily affected by storm events as it is exposed to the full force of energy from the North Atlantic. Chapter 4 gives an account of the study area in Galway Bay, located on Ireland's Atlantic coast, and the methods employed

in this research. Chapter 5 details the results of this study. This includes 23 radiocarbon dates and data from physical, geochemical and biological proxies taken from four sediment cores on a west-east transect in north inner Galway Bay. Chapter 6 offers a discussion of confirmed paleoenvironmental conditions along this transect and postulates scenarios which may have led to such conditions. This includes a breakdown of changes as they occurred in the early, mid and late Holocene. Chapter 7 concludes this body of work giving the reader a concise list of research outcomes to advance the knowledge base of coastal paleoenvironmental science.

CHAPTER 2: Coastal Environments

Introduction

Coastal ocean environments are complex systems that are connected to land, the open-ocean and the atmosphere. The interaction of terrestrial and marine forces in the coastal zone produces a dynamic environment where constant change ensues. These changes vary on a temporal scale; water circulation responds to changes in salt and heat content and wind forcing on an hourly to daily time scale compared to changes in the open ocean which have weekly, monthly to annual response times. Key to understanding these dynamics are atmospheric, oceanic, estuarine and fluvial processes which act upon the coastal zone along with the local conditions. Together they determine how processes play out in a particular coastline. Coastal waters are a vital component of oceanic primary productivity; coastal oceans comprise only around 7% of the total ocean area yet they support 15–20% of total primary productivity (Simpson and Sharples, 2012). Sediment movement within this zone influences bathymetric changes and determines geologic evolution of the coastline through erosion, transport and deposition. Rivers and streams further supply fresh water, sediment and nutrients; sub-aerial weathering and erosion help to shape the coast. The resulting ecological habitats house distinct assemblages of flora and fauna. These key components, processes and conditions are now reviewed in the following sections to inform interpretations of coastal sediment deposits.

2.1 Coastal processes

Classifications used to distinguish coastal zones are grouped based on uniform physical characteristics such as substrate or depth of the water column. Anderson and Vos (1992) classify three coastal zones based on levels of seawater inundation: the subtidal zone, the intertidal zone and the supratidal zone (Figure 2.1). The subtidal zone has the highest level of inundation and the supratidal zone the lowest. Tidal ranges are highly variable geographically, both locally and globally, and are impacted by position, geomorphology, bathymetry and weather (Thurman, 1994). Tidal datums are used as references to measure local tides and outline the standard elevations defined by a certain phase of the tide (NOAA, 2016). When defining tidal ranges in the coastal zone with respect to specific parameters

(e.g.: ecological ranges of organisms) authors may use a water level associated with a specific tidal datum. Haslett *et al*., (2001) uses foraminifera as tidal indicators and relates the coastal zonation outlined by Anderson and Vos (1992), who discuss diatoms as coastal indicators, to tidal water levels on the shoreline. Hemphill-Haley (1995) also provides classic text on using diatoms to establish rising sea levels and outline tidal water levels. Tidal datums include: Highest Astronomical Tide (HAT), Mean Highest High Water (MHHW), Mean High Water (MHW) and Mean Low Water (MLW). The water level Highest High Water (HHW) (Haslett *et al*., 2001) is equivalent to HAT and Extreme High Water (EHW) (Hemphill-Haley, 1995) occurs above the extent of HAT, likely as the result of a storm event. The tidal datums HAT, MHW and MLW are indicated in Figure 2.1.

Coastlines are continually changing due in large part to the processes of erosion, transportation and deposition. Major movements of sediment take place here powered by processes generated by the ocean and its confluence with the terrestrial environment. Murray (2006) suggests that the two important physical factors affecting coasts are waves and tides; due largely to the fact that both processes impart high energy. Wave energy can generate a force that causes great and vigorous erosion on the shoreline and tidal forcing plays a significant role in sediment and nutrient exchange (Pidwirney, 2006).

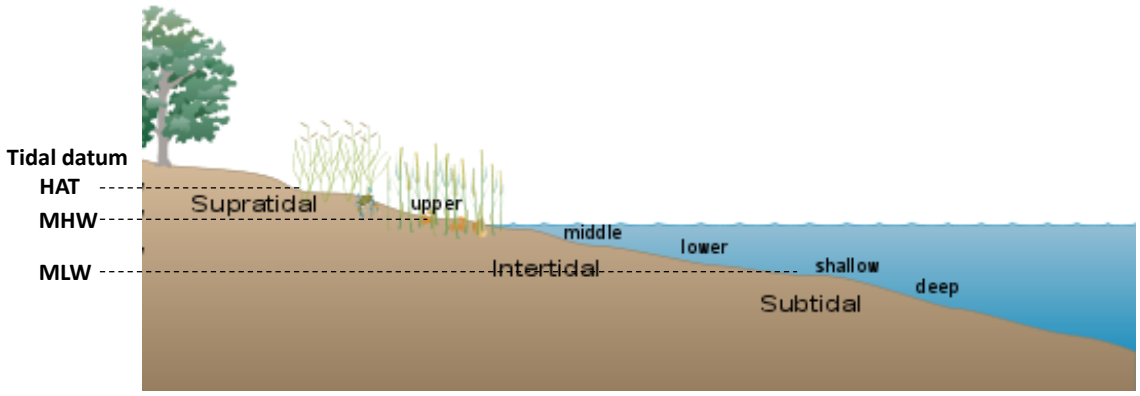

Figure 2.1: An illustration of the coastal zone based on seawater inundation as outlined by Anderson and Vos (1992). Included in the illustration are the markers for Highest Astronomical Tide (HAT), Mean High Water (MHW) and Mean Low Water (MLW); as defined by NOAA (2016) and Haslett *et al.*, (2001).

2.1.1 Oceanic processes

The North Atlantic Ocean has circulatory patterns dominated by two large gyres (subtropical and subpolar). The circulation of the subpolar gyre (SPG) changes on decadal time-scales (Curry and McCartney, 2001; Bersch, 2002; Hakkinen and Rhines, 2004), and influences water circulating on both sides of the North Atlantic. For example, an expansion of the SPG leads to cooler and fresher inputs from the west to east in the North Atlantic and a contraction of the SPG results in a higher transport of southern warm saline waters into the NE Atlantic region (Holliday, 2003; Hátún *et al.*, 2005; Hughes *et al*., 2012). The Atlantic Meridional Overturning Circulation (AMOC) is a key component of the global climate system and is responsible for a large fraction of heat transport in the Atlantic basin (Johns *et al.*, 2011; Boulton *et al*., 2014). The AMOC is characterised by northward flowing warm saline waters in the upper layer of the Atlantic Ocean, cooling and freshening of the waters in the Irminger Sea, Nordic and Labrador Seas, and a southward flow of colder waters at depth. This circulation transports heat from the Southern regions of the Atlantic to the polar North Atlantic, where heat is released to the atmosphere. This release of heat can have substantial impacts on climate over large regions (Bryden *et al*., 2005; Wunsch and Heimbach, 2006; Zhang, 2010). There is a relationship between the AMOC and the Atlantic Multidecadal Oscillation (AMO), observed as an oscillatory pattern of sea surface temperature (SST) in the Atlantic Ocean (Zhang and Wang, 2013).

Thermohaline circulation is a vital component of the global ocean nutrient and carbon cycles and is influenced by changes in temperature, salinity and freshwater influx that regulate water density and the continuance of the cycle (Jones, 1997). Warm surface waters are depleted of nutrients, but are enriched again as they mix with nutrient rich colder deep waters. The cause of this mixing is complicated. Recently, Lozier (2010) chronicles numerous studies which explore mixing in ocean currents and several methods have been identified including eddies in water transport and mixing (Dengler *et al*., 2004) and internal pathways (Bower *et al.*, 2009).

Atlantic MOC is represented by changes in SST and parameters such as salinity (Reverdin, 2010), sea level, and sea-ice transport (Frankcombe *et al.,* 2010). There is evidence that the signal of observed multidecadal variability can also be seen in ecosystem parameters such as coastal phytoplankton distribution (Dixon *et al.,* 2009), salmon recruitment (Friedland *et al.,* 2009) and cod populations (Drinkwater *et al.,* 2009). Ocean circulation is also influenced by geophysical characteristics including sea floor bathymetry and ridges that separate deep waters of the ocean into distinct basins and seamounts. (Stewart, 2008). In the North East Atlantic, the margin of the continental shelf spans the distance from northern Norway to Southern Iberia and includes the open-sea shoreline to the shelf break where the inclination of the sea floor increases with the passage to the continental slope. The physical energy of the inner continental shelves comes from tides, waves and storms (Murray, 2006).

The extensive processes including tidal currents, bottom friction on the water column, heat loss, freshwater inputs and discreet circulation patterns create different dynamics near the coast, from the shelf seas < 200 m to shorelines (Simpson, 2005). In particular, in the southern North Sea and most of the Irish Sea, tides are sufficiently strong to maintain a mixed water column throughout the year. Parts of the North West European Shelf have some of the largest tides globally: for example the Bristol Channel has a spring tidal range of over 14 m (Pelling *et al*., 2013). The large tides make this one of the most energetic areas (Egbert and Ray, 2001), which is about 5 – 6 % of the total present-day global tidal dissipation. Tides across the region are dominated by the semi-diurnal constituents (Uehara *et al.,* 2006) which are a response of the shelf seas to the tides generated in the Atlantic Ocean. Tides are a result of the position and gravitational attraction of the moon and to a lesser extent the sun, on the Earth causing the highest high tides (Spring tides) and the lowest high tides (Neap tides) at various lunar cycles. Tidal currents change in a very regular pattern making them predictable (Pinet, 1998).

Tidal mixing fronts on the continental shelf of the Northern Atlantic separate seasonally stratified waters from well mixed/sporadically stratified waters in shallow regions (nearer the coast or on banks and shoals). Offshore tidal fronts, like the Celtic Sea Front, play a significant role in circulation and tend to separate nutrient-depleted water from nutrient-rich

water, and cross frontal exchange processes can result in enhanced biological production (Holt and Proctor, 2008; Coughlan and Stips, 2015).

In other regions such as the shelf seas to the west of Ireland and in the Celtic Sea a well stratified water column develops in summer as a result of solar heating. In summer, circulation at depth in the shelf seas is forced by density-driven currents. These persistent sub-surface baroclinic jet-like flows are generated by bottom density fronts that develop as a result of competition between tidal mixing and seasonal heating of the upper water column (Hill, 2005). There is strong evidence to suggest that the presence of these subsurface currents (below the thermocline) play an important role in the transport of nutrients, phytoplankton and contaminants in the Irish Coastal Current northwards along the west coast of Ireland in the summer months. Off of the west coast of Ireland, the Irish Shelf Front, a thermohaline front, separates coastal shelf waters and the northward directed inshore Irish Coastal Current from offshore saltier Atlantic waters. Examples of coastal currents include the Scottish Coastal and the Irish Coastal currents, which transport water around Britain and Ireland and towards the southern North Sea, and the outflow from the Rhine and other rivers along the north coast of continental Europe that combine with the outflow from the Baltic to form the Norwegian Coastal Current, which flows north towards the Arctic (Holliday *et al.*, 2011).

Salinity, temperature and pressure are important oceanographic parameters in the pelagic and coastal zones (Tomczak and Godfrey, 2005). Salinity in Irish coastal waters ranges from 0 to 35, with 35 representing the most saline conditions. Salinity increases water density - a variable also influenced by fluctuations in temperature and pressure (Dietrich *et al.*, 1980). Temperature is an important parameter due, in part, to the impact it has on ecology. Distinct species assemblages are often associated with different water masses or niches defined by physical and chemical properties. Seawater density is a function of temperature, salinity and pressure and with these parameters measured and understood key processes can be examined (Millero and Poisson, 1981; UNESCO, 1981). At all trophic levels, indices derived from widely available datasets, such as those for sea surface temperature (SST), are frequently used as a measure of upper ocean conditions. As oceans cover the majority (70 %) of the earth's surface, understanding the long-term variability in SST has been a key issue in recent

research, notably climate change research (Smith *et al*., 2008), and the development of gridded SST products has been driven in part by the need to provide data input to general atmospheric circulation models (Hurrell *et al.,* 2008; Hughes *et al.,* 2009).

Coastal geomorphology is affected by wave action as energy released by waves can be more significant on certain parts of the shoreline than others and this is evident in coastal landforms. Waves are generated by aeolian processes with wave height affected by wind speed, wind duration and fetch (Duxbury *et al*., 2002). As waves approach the shoreline, the water depth decreases and the wave begins to touch bottom. Friction occurs resulting in a high energy wave of turbulent water both impacting the shoreline and the intertidal zone; where incoming waves meet back flowing water (Pidwirny, 2006). For example, cliffs are formed when wave refraction causes a higher concentration of wave energy on headlands and bays form when deeper waves are refracted to adjacent areas (Tomczak and Godfrey, 2005).

2.1.2 Coastal sedimentation

Coastal sedimentary processes are complex and include erosion, transportation and deposition. Coastal areas are subject to the varying influences of riverine and atmospheric inputs, coastal and seafloor erosion, and biological activities. Grain size of sediments is one of the major controlling factors for sediment distribution in coastal areas (Ip *et al*., 2007). Ocean currents and waves continually exert force on landmasses and energy is constantly being expended along coastlines making them dynamic systems (Jones, 1997). Wave energy can generate a force that causes vigorous erosion as the wave connects with the shore with the majority of coastal erosion taking place in the surf zone (between the shoreline and breakers). Waves break at depths between 1.0 and 1.5 times wave height and rock particles are carried in suspension by the waves as they collide with each other thus causing a reduction in particle size. These smaller particles are carried away by the retreating surf causing an increase of the depth to the bottom. On rocky coastlines, wave impact continually undercuts the rock resulting in a mass wasting processes where rocky material from above can slide and fall into the water to be carried away by further wave action (Pidwirny, 2006). Coastal sediment deposition occurs primarily in two ways: sediment

that is created by wave action and sediment that is deposited by rivers and streams and transported by waves and currents. Finer grained sediment is carried offshore and deposited on the continental shelf or in offshore sandbars. Coarser grained sediment can be transported by longshore currents and beach drift further along the coastline (Pugh, 1982). If wave energy and sediment supply are constant, then a steady state is reached. If any one of these factors change, then the shoreline will adjust. Coastal erosion varies based on the level of resistance offered by the coastal type; hard rock coasts experience low levels of erosion while soft cliffs and sedimentary coast are far less resilient. Human modification also play a role interrupting natural forces, for example coastal defences and river damming, however, the impacts are often not visible for decades or centuries and can be difficult to quantify in the short term (European Commission, 2004).

Storm events and their associated wave activity and sediment transport have a significant impact on coastal landscapes. Understanding the distribution and force of storm and tsunami wave energy on the continental shelf and associated coastlines is an important factor in determining sediment movement (Hall, 2011). Storm wave energy strong enough to move boulders > 256 mm heights up to 50 m above mean sea level are documented (Williams 2010). These wave emplaced megaclasts can be found on cliff tops along the coasts of Ireland (Williams, 2010; Hall *et al.*, 2010; Cox *et al*., 2012) and the Faroe Islands (Williams and Hall, 2004). Relatively recent tsunami activity and paleo tsunamis have been postulated (Knight 2011; Williams 2011; Cox *et al*., 2012). Boulder displacement is a key indicator of paleo storms and storm forces additionally have major implications for patterns in sediment displacement.

2.1.3 Estuarine processes

It is difficult to define an estuary because of the variety of geomorphologies, water inputs and outputs and climatic conditions. A classic definition was produced by Donald Pritchard in 1967 who defined an estuary as "*a semi-enclosed coastal body of water which has a free connection with the open sea and within which sea water is measurably diluted with fresh water derived from land drainage*." In an estuary, marine and freshwater inputs maintain an exchange of salts and tidal energy which influences density and water circulation patterns. Wind energy, tidal energy and river inflow work together to produce the motion and mixing

of water in the estuary (Pritchard, 1967; Palmer *et al.*, 2011). Shallow, open systems, estuaries have transitional zones between the freshwater and marine and exhibit distinct salinity gradients and are characterised by a large variability in physical, chemical and biological properties (Lancelot and Muylaert, 2011).

2.1.3.1 Estuarine water circulation

Water circulation patterns in estuarine environments are identified by density induced water column stratification (McDowell and O'Connor, 1977; Dyer, 1986), which is controlled by the interaction of saline marine inputs and freshwater riverine inputs (McManus, 1998; 2000). At the mouth of the estuary, dense shelf water is drawn in below the outflowing surface layer. This exchange flow occurs in fjords, drowned river valleys, bar-built estuaries, and rias (Valle-Levinson, 2010; Geyer and MacCready, 2014). The resultant horizontal salinity gradient is the key driving force for estuarine circulation, which in turn plays a key role in maintaining salinity stratification in estuaries. The combined influence of the estuarine circulation and stratification determines the volume of estuarine water and the fluxes of salt and fresh water within the estuary, and their intensity varies with the strength of the freshwater inflow. Because of these dynamics, estuaries are often the most strongly stratified aquatic environments, but they also tend to have vigorous water and salt exchange, due to the estuarine circulation (Geyer, 2010). The inflow of river water at the head of the estuary maintains well developed salinity stratification and in many estuaries this produces a relatively fresh upper layer and a lower layer of near oceanic salinity. These variations in physico-chemical parameters form frontal systems where two regions of water with differing properties meet along a horizontal gradient (Largier, 1993; Duck and McManus, 2003). Coastal bathymetry and the placement and behaviour of currents, shoals and channels also impact water circulation and density in the estuarine environment, thus affecting frontal formation and behaviour (Valle-Levinson and O'Donnell, 1996).

2.1.3.2 Estuarine sedimentation

Estuary morphodynamics reflect the relative balance between competing marine and fluvial processes (Cooper, 2001). Sedimentation in estuarine areas is related to frontal systems; where the deposition of sediment is a response to frontal system processes. Driven primarily

by tidal and wave forces, water entering the estuary sinks along the frontal edge pulling sediment down onto the sea bed. The relatively sheltered character of estuarine environments, in particular where tidal currents are weak, allows sediments to flocculate and fall out of suspension. This process has resulted in the development of mudflats and sandflats in European estuaries, though there is considerable variability among estuaries in the pattern and distribution of their sedimentary structures including bathymetry, sediment supply, turbidity and current flows (Healy and Hickey, 2003). The ebb and flood phases of the tide build up the sand in varying positions and these two are re-worked until they meet in a zone of accumulation i.e. longitudinal frontal systems subdivide marine and fresh water leading to accumulations of sediment parallel to the frontal interface thus creating sandbanks (McManus, 2000). The rate at which sediment is deposited in this environment varies based on the type of particulate matter. Silt has a slow settling velocity and can be transported long distances before it settles out of the water column in places where the current is too weak to carry it away when the tide turns (Bartholdy, 2000). Coarse sediment has a high settling velocity and deposition corresponds to the direction of peak current velocities. This compares to fine sediment deposition, transported largely in suspension, with a lag effect based on the relationship of the time it takes the sediment in suspension to adjust to changes in the water velocity (Pritchard and Hogg, 2003). It is the circulation within the estuary that drives the sediment accumulation rate, effectively trapping particles that sink such as sediment or particulate organic matter with high sediment accumulation rates (Traykovski *et al.*, 2004; Geyer and MacCready, 2014).

2.1.4 Terrestrial processes in the coastal zone

The main terrestrial processes which affect coastal zone structure and function are fluvial processes; rivers and streams supply fresh water with its load of sediment and nutrients into estuaries (Keller, 1985). A catchment is the entire area contributing to the stream-flows of a main river and its tributaries. Topographic characteristics influence the pathways and processes that occur in a given catchment area including the amount and rate of water yield (Gregory and Walling, 1976). Fluvial discharge in the coastal zone acts as a transport system for sediment and nutrients. The transport and discharge of riverine inputs in the near shore environment can introduce anthropogenic pollutants (e.g.: high loads of nutrients from

agricultural and industrial practices (Harrington and Harrington, 2014). Nutrient concentrations in rivers are controlled by biogeochemical reactions in the pelagic zone during transport and nutrient exchange events at the sediment–water interface (House, 2003). For example, ammonium and phosphate can attach to sediments in the water column and be transported and deposited down-stream in the estuary. Inorganic particulate nutrients attach to the surface of suspended inorganic sediment particles and the co-precipitation of phosphate with calcite can enhance sediment storage (Walling *et al*., 2003; Evans *et al*., 2004; Withers and Jarvie, 2008). Conversely, sediments can also become a nutrient source through the release of dissolved chemical species under well-defined pH and redox conditions (House and Denison, 2002; Chahinian *et al.*, 2011).

2.1.4.1 Terrigenous sedimentation and its effect on the coastal zone

Sediment flux to the coastal zone is governed largely by geomorphic and tectonic influences in drainage basins, by the geography and geology of the basin and by human activities. The interplay of these factors is complicated and our understanding of what controls sediment discharge into the ocean is a topic of extensive research (Hay, 1994). A recent survey (Syvitski *et al*. 2005a) found globally that soil erosion is accelerating due to factors such as deforestation, agriculture and mining, while at the same time, sediment flux to the coastal zone is decelerating due to such occurrences as channel bank hardening, water diversion and reservoir storage. Another factor that complicates our understanding of a river's conveyance of sediment to the coast is a lack of long term data, as many parameters are measured in years rather than decades (Syvitski, 2003). Despite these complications, the importance of understanding fluvial delivery of sediment is paramount. Understanding the redistribution of terrigenous material in a fluvial system and the processes of water velocity and its relationship to climatic processes is an essential part of this type of research. The transport of particulate material down a river relies on the velocity of the river. In general, the faster the river velocity, the larger the sediment load it can transport. However, this is not always the case. Sand is more easily eroded than smaller silt particles and once in motion sand can have lower transport velocities. The smallest particles may never be deposited on the riverbed and are transported into the estuary. Once a certain velocity has been achieved these small particles tend to move as a suspended load. The suspended sediment increases down

river) and is at its maximum at the outflow of an estuary (Smith and Stopp, 1978). The detailed pattern of sediment production within an area is the result of many conditions, including meteorological, physiographic and environmental spatial controls. The sediment load of a river is generally reduced significantly when catchment rainfall is low; sediment transported in such a low energy system will consist of fine material. Conversely, high rainfall conditions produce a high energy sediment transport system and an increase of coarse material is transported and deposited in the basin. Grain size of the deposited material reflects the environmental conditions during the time of deposition (Bloemsma, 2010).

Deposition of sediment from freshwater catchment systems in intertidal environments has varying effects on the coastal zone. Geomorphology and hydrodynamic features of the receiving coastline play a part in the sediment behavior. For example, low energy coastal environments, where waves and tides are small and currents slow, have accumulations of fine grained material that can redistribute across the intertidal zone. High energy coastal environments are more susceptible to processes such as erosion and transport. This is most obvious on rocky shores where there is little or no visual build-up of fine grained sediment (Woodroffe, 2002; Edwards, 2013). Climate has an effect on fluvial sediment transport; with increased temperatures the atmosphere holds and transports more water vapour and this can enhance the hydrological cycle and increase precipitation. This would lead to higher river flows and a greater means for large sediment relocation into the coastal zone and reworking of sandy sediment in the estuaries. Quantifying this occurrence is difficult, and records are sparse and incomplete. Trends in ocean salinity data can, however, be linked to increased precipitation and higher fluvial discharge into nearshore environments (Durack and Wijffels, 2010; Helm *et al*., 2010). Investigations of the global water cycle are likely to become an important focus of future coastal research as the climate changes. There is a need to increase the volume and quality of salinity data collected in the ocean in order to fully understand and measure terrestrial inputs into the coastal zone (Lagerloef *et al.,* 2010; Hughes, 2012).

In summary, the key oceanic, estuarine and terrestrial processes reviewed here all serve to highlight the complex sequence of interactions that produce coastal zone environments and their sediment deposits. Ocean circulation, in part, regulates temperature and salinity and

impacts sedimentation and zonation in more discreet coastal zones. Land based catchment formation affects fluvial behaviour and freshwater input in terms of quantity and biogeochemical inputs into the coastal zone. Estuaries have a variety of geomorphologies and are heavily influenced by salinity and the resulting water density structures produced. The dynamic coastal environment and the ecological communities therein are a subject of great interest in research.

CHAPTER 3: Holocene environmental change

Introduction

Coastal systems are dynamic over a range of timescales from seasonal to annual, decadal, centennial and millennial scales. One of the most relevant long term periods of interest in terms of environmental change is the Holocene geological epoch or the last 11.7 ka calendar years. This period encapsulates the era since the last glaciation up to the present day and resulted in the formation of our current land and seascapes. Long term development of coastal environments through time can be reconstructed using paleoenvironmental study of aquatic sediments. Paleoenvironmental examination utilises evidence of past environmental change which helps with interpretation of past climatic conditions within the coastal zone. Sediments in coastal zones are a potential archive of past changes in salinity, sea level and climate variations. An overview of the significance of the Holocene period in terms of climate change its driving forces, important change points and key research is described in this chapter. This is followed by a review of paleoenvironmental study and applications of different proxies in coastal environments.

3.1 The Holocene

The Holocene geological epoch is the current interstadial period and follows on from the Pleistocene or last glacial period within the overall Quaternary Period (Figure 3.1). The last glacial period ended with the cold Younger Dryas sub-stage European cooling event which is dated to c. 11-10 ka in radiocarbon years or 12.9-11.7 ka in calendar years (Rasmussen *et al.*, 2006; Carlson, 2013), and thus gave rise to the onset of the Holocene. During the first 1,000 years of the Holocene, global temperatures began to rise and the ice sheets of northwest Europe began to retreat. Due to the thickness and extent of these ice sheets it took approximately 2500 years for them to melt away completely and they remained extensive until 9000-6000 years ago, varying regionally (Roberts, 1998). The climatic shift which brought about the Holocene is significant because of the impact it had on most elements of the environment such as ecological distributions, sea level changes and sedimentation rates. Climate change during the Holocene is a composite of external forces plus feedbacks within the climate system (Bradley, 2005). In order to understand present day processes, it is

necessary to understand conditions in the past prior to the major landscape modifications by man in recent years (Delaney and Devoy, 1995).

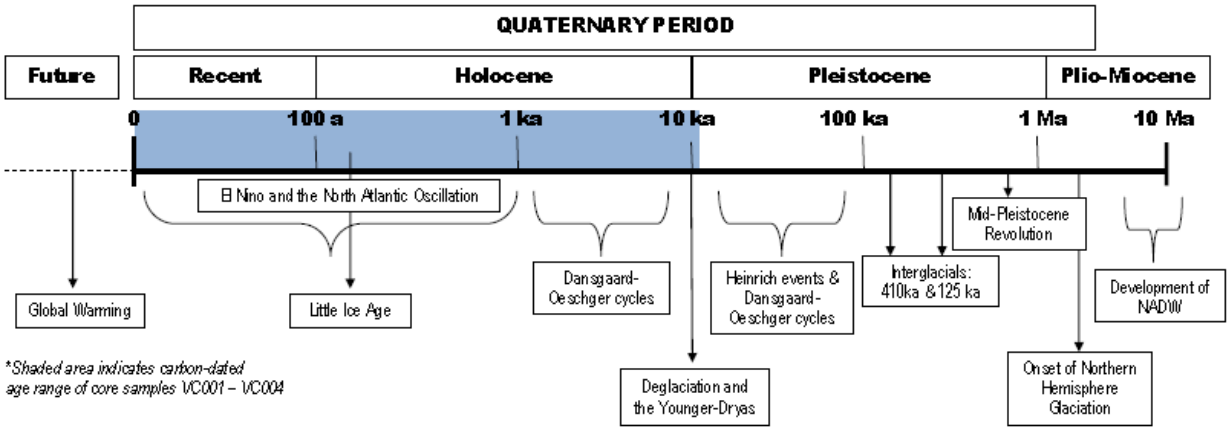

Figure 3.1: Based on Maslin *et al* (2001; 2005), this chart outlines major climate events of the Quaternary Period. Highlighted in blue are the relevant Holocene events.

3.2 Glacial activity as a precursor to Holocene environmental conditions

The Quaternary period is characterised by the effects of glaciation (Woodcock, 2000). During the Last Glacial Maximum (LGM, 26-19 ka) (Clark *et al.*, 2009), global ice sheets reached their last maximum integrated volume (Peltier and Fairbanks, 2006; Chiverrell and Thomas, 2010). The maximum extension of each individual ice sheet worldwide varied due to local factors such as variation in ice source regions, ice divides and varying degrees of isostatic depression (Clark *et al.*, 2009; Barth *et al.*, 2016). One of the results of the continual expansion and retreat of the ice sheets was the addition and retraction of water from the hydrological cycle which caused ocean volumes to fluctuate (Tooley and Shennan, 1987). This resulted in a lowering of sea levels during the LGM facilitating the spread of flora and fauna in Northern Europe and other areas via the creation of land bridges that connected areas like Britain to continental Europe (Bennett *et al.*, 1991; Roberts, 1998).

It is important to understand the behaviour of ice sheets and patterns of retreat during deglaciation because as ice sheets retreated, certain geophysical characteristics remained. Drumlins, trim lines, glacial irratics, moraines, emergent coastal landforms and other

geomorphological characteristics resulting from glaciation impacted the processes and ecological conditions that occur in the Holocene (Clark *et al*., 2012). An example of this is the laterally extensive ice sheet which extended out onto the continental shelf that existed over the UK and Ireland (e.g.: Evans *et al.,* 1980; Warren, 1992; Sejrup *et al.,* 1994; McCabe and O'Cofaigh, 1995; Clark and Meehan, 2001). Referred to collectively as the British and Irish Ice Sheet (BIIS), it is thought to have existed from ca. 70 ka through to deglaciation (Peck *et al.,* 2007; Hibbert *et al.,* 2010; Scourse *et al.,* 2009, Scourse, 2013). There is some debate as to the extent of the ice sheet over Ireland (the Irish Ice Sheet, IIS) (See Figure 3.2), with all agreeing that central and northern Ireland was completely covered by the IIS but differing in the extent of the western and southern margins (Sejrup *et al.,* 2005, Shennan *et al.,* 2006 and Brooks *et al.,* 2008; Greenwood and Clark, 2009 and Clark *et al.,* 2012) and whether southwestern Ireland was the centre of an independent ice cap (the Kerry-Cork Ice Cap, or KCIC) (Bowen *et al*., 1986, McCabe, 1987 and Ballantyne *et al.,* 2011) or was completely overridden by a contiguous IIS (Barth *et al*., 2016). Further evidence suggests that ice cover reached beyond the south of Ireland Moraine (O'Cofaigh and Evans, 2001, Evans and O'Cofaigh, 2003; Hegarty, 2004; Ballantyne *et al.,* 2006) and into the Celtic Sea south of the Isles of Scilly (Scourse *et al.,* 1990; Scourse, 1991; Hiemstra *et al.,* 2006). Ballantyne *et al.* (2006) suggests that only mountain areas with peaks above 725 m remained ice free. An accurate reconstruction of the LGM IIS is critical for characterizing its response to climate forcing, particularly the abrupt changes in the North Atlantic (Clark *et al*., 2012) and sea level rise estimates (Lambeck *et al*., 2014 and Peltier *et al*., 2015) require an accurate reconstruction of the extent and the height (or thickness) of the ice sheet.

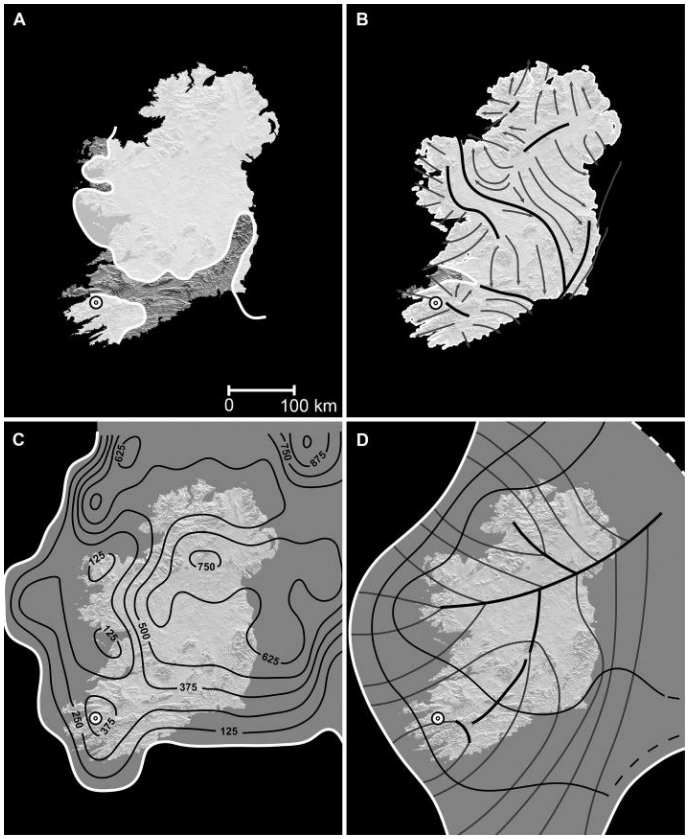

Figure 3.2: Source (Barth *et al*., 2016): LGM Irish Ice Sheet reconstructions from A) Bowen *et al.* (1986), B) Ballantyne *et al*. (2011), C) Brooks *et al*. (2008) (for 21 ka), and D) Greenwood and Clark (2009) (for 24 ka) showing varying interpretations of the IIS extent. White shaded areas indicate ice cover. Thick black lines represent ice divides. Thin black lines represent ice thickness contours and numbers indicate topography corrected ice-sheet thickness. Gray lines represent proposed ice flow lines.

As the ice sheets began their retreat, the geomorphology of both inland and coastal landforms in this region underwent changes. This occurred, in part, due to eustatic changes; those resulting from increasing volume of water in the ocean. In Ireland, isostatic crustal rebounding occurs in the deglacial period after 20 ka from the unloading of glacial ice and this process has an effect on coastlines causing relative sea levels to fall. Five to six thousand years later, c. 15 ka to 14 ka, rapidly melting ice sheets in this area caused sea levels to remain stable as the freshwater input into coastal areas levelled out the crustal rebounding effects of a retreating shoreline. This ice retreat was interrupted by a large scale ice re-advance which affected much of the country (McCabe *et al.*, 1998, 2005; Brooks *et al.*, 2007). This ice re-advance was most likely due to a Heinrich Event and affected areas of

Ireland as far south as the Shannon Estuary (Thomas *et al.,* 2004). This was a brief event and ice retreat resumes leaving the region ice free by 15000 BP (McCabe *et al.,* 2005). Edwards and Brooks (2008) discuss Irish landforms in relation to glacial retreat stating that between 15000 and 14000 years ago rapid ice melts had left Ireland surrounded by water. In the first thousand years of the Holocene, c.10 ka, eustatic sea level rise from the retreat and melting of ice sheets world-wide was faster than the isostatic coastal rebounding. In the mid to late Holocene, sea level rise is regional; for example, areas of the Eastern coast of Ireland experienced static sea level rise for the past 6000 years but the southern and western coastlines of Ireland experienced continuous sea level rise throughout the past 6000 years with the highest rates occurring in the southwest (Edwards and Brooks, 2008). Some recent modelling indicates that a gradual end to the melting of the ice sheet in Britain and Ireland during the mid Holocene resulted in a general 3 m sea level rise commencing 7000 years ago but there is further debate as to whether the melting ended by 4000 years ago or continued slowly until pre-industrial times (Lambeck *et al.,* 1998, 2002; Peltier, 1998, 2004; Shennan *et al.,* 2000b, 2002; Peltier *et al.,* 2002; Shennan *et al.,* 2006; Bradley *et al*., 2011). Establishing the impact of an ice sheet on regional and global climate (Hostetler *et al.,* 2000; Braconnot *et al.,* 2012) and sea level (Bradley *et al*., 2011; Lambeck *et al.,* 2014 and Peltier *et al.,* 2015) requires an accurate reconstruction. As well, determining the resultant geomorphology accurately assists in the reconstruction of physical processes during the Holocene (Clark *et al.,* 2012).

3.3 Drivers of climate change in the Holocene

The reactions of the atmosphere and the oceans to internal and external forcing vary on a temporal scale. The atmosphere responds relatively quickly with a response time from days, months or a few years. Likewise, surface ocean waters can change over months and years, but deep oceans can take decades to centuries to respond to various forcings and this makes oceanic processes significant factors in long term climate change on centennial and millennial time scales (Maslin *et al.,* 2005). Paleoclimatic variability during the Holocene involved the combination of specific external forcings and internal modes of climate variability.

3.3.1 External forces

External forces, such as solar radiation, orbital forcing and volcanic activity all played a part in the unfolding of climatic conditions during the Holocene. Hayes *et al.* (1976) demonstrated that climatic oscillations during the Quaternary were driven by regular changes in solar insolation brought about by Milankovitch cycles and regulated by orbital forcing, the parameters of which have varying effects on cyclicity (Imbrie and Imbrie, 1979; Armstrong and Brasier, 2005).

Orbital forcing was a primary factor in Holocene climate changes from 11000 to 6000 years ago and was a result of changes in the Earth's orbit relative to the sun. This change altered the amount of radiation the Earth's surface received on a seasonal basis and how such radiation was redistributed. This redistribution, in turn, helped to regulate the temperature gradient globally, therefore having an effect on atmospheric and ocean circulation (Bradley, 2008; Yu, *et. al*., 2005). In the mid to late Holocene (6000 to present), as orbital forcing reduced its effect on earth systems, glacial retreat had levelled off and smaller more localised changes started occurring. Solar irradiance affects both the atmosphere and oceans; acting on an 11 year cyclic pattern, it varies regionally and creates climatic variation on the earth (Rindi, 2002; Maslin *et al.,* 2005). When solar irradiance is high, heating rates in the upper atmosphere are increased, affecting stratigraphic winds and in turn surface climates (Shindell *et al.,* 1999; Dunkerton, 2001; O'Hanlon, 2002). Studies have suggested a link between solar variability and North Atlantic climate (Bond *et al*., 2001) and in Asia (e.g.: Asian monsoons, Neff *et al*., 2001; Fleitmann *et al*., 2003; Wang *et al*., 2005). Volcanic forcing has well known effects throughout the Holocene and single events can result in a direct radiative effect on overall hemispheric or global mean temperatures producing short-term cooling effects. Aerosols released during an eruption reduce the energy receipts on the Earth's surface and can affect atmospheric wave circulation and temperatures (Bradley, 1988; Robock, 2000).

3.3.2 Internal modes of climate variability

The oceanic, poleward transport of heat is a fundamental driver of the climate system. In the Atlantic Ocean, wind-driven gyres and MOC are the dominating drivers of circulation (Holliday *et al*., 2011). Many studies have been carried out to define the size of the

variability in MOC in order to understand changing climate (Gherardi *et al*., 2005; Biastoch *et al*., 2008; Trouet *et al*., 2012; Pillar *et al*., 2016). The North Atlantic Oscillation (NAO) is an atmospheric process influenced by pressure and is most pronounced in the winter months from February to December (Hurrell, 1995; Labudova *et al*., 2013). Air pressure at the Earth's surface varies spatially and atmospheric circulation occurs as air moves from areas of high pressure to areas of low pressure. The NAO is further influenced by the deflection of wind caused by the Coriolis force which influences ocean water currents creating a directional change in surface currents and affecting upwelling and downwelling events in intertidal environments. This is significant for coastal ecology because cold, nutrient rich waters rise and alter sediment composition and food web dynamics (Ross, 1995; Stewart, 2008). Variations in the NAO index result in climate oscillation with active and passive phases of decadal variation peaking every six to ten years and correlating to changes in climate and sea surface temperatures over time (Appenzeller *et al.,* 1998; Jennings *et al.,* 2000a; Folland *et al*., 2009). For example, a positive NAO index is associated with an increase in occurrence of westerly winds and increased wind speeds, temperature and rainfall in northern Europe (Daultry, 1996; Butler *et al.,* 1999). In Ireland, winter precipitation has been recorded as above average when the NOA index is highly positive (Jennings *et al.,* 2000a). In addition, NAO phases in the Atlantic have been linked to survival rates of Atlantic salmon smolts and marine zooplankton production (Jennings *et al.,* 2000b).

The idea that slow changes in ocean circulation influence climate variability in the North Atlantic region goes back half a century (Bjerknes, 1964; Knudsen *et al*., 2011). There are several lines of evidence suggesting that SST variations related to the AMO drive climate and precipitation patterns over North America (Endfield *et al*., 2001; Sutton and Hodson, 2005; Hu and Feng, 2008), droughts in the Sahel region of Africa (Folland *et al*., 1986), variability in Northeast Brazilian rainfall (Folland *et al*., 2001) and tropical hurricane frequency and intensity (Goldenburg *et al*., 2001). However, because the instrumental SST records only span ~150 years, studies of corals (Kilbourne *et al*., 2008), tree rings (Gray *et al*., 2004), estuarine fossil pigments (Hubeny *et al*., 2006) and sea-spray in Greenland ice cores (Fischer and Mieding, 2005) have been carried out to fill this void and indicate that 60 to 100 year oscillations were also present in the North Atlantic region during the latest

centuries preceding the instrumentally observed AMO. However, the available evidence for a pre-industrial AMO remains inconclusive. These oscillatory climate variations have been attributed to internal variability of the ocean related to changes in the Meridional overturning circulation (Vellinga and Wu, 2004), a notion that has been supported by numerical studies showing that SST is the primary carrier of the multidecadal signal (Delworth, and Mann, 2000; Knight *et al*., 2005).

3.4 Climatic conditions in the Holocene

The early Holocene in Europe is marked by a warm period initiated by the pre-Boreal Oscillation leading to the Holocene Thermal Maximum (HTM). The pre-Boreal Oscillation persisted until 10750 cal years B.P. (Fisher *et al.,* 2002) and signified the end of Late Glacial type environments in Ireland. The input of meltwater into the North Western Atlantic eventually led to changes in pack ice position on the North Atlantic and Arctic Oceans that likely affected ocean circulation and caused a rapid increase in atmospheric temperatures in North West Europe (Diefendorf, 2005); heating over the land caused low pressure increasing precipitation over land masses. The HTM was not a uniform phenomenon, however, and seems to vary spatially in Europe (Kaufman *et al*., 2004) with studies from Sweden (Laroque and Hall, 2003), North-West Russia (Ilyashuk *et al.,* 2005), the Austrian Alps (Ilyashuk *et al*., 2011) and Ireland (McKeown, 2013; Ghilardi and O'Connell, 2013) putting the HTM between 10000 and 9000 cal years BP. One study from Ireland (Deifendorf, 2005) suggests a thermal maximum at 10800 cal years BP while other European studies in Norway (Velle *et al.,* 2005), Fennoscandia (Seppa *et al*., 2002), Northern Sweden (Rosen *et al.,* 2001), Iceland (Caseldine *et al.,* 2006) and Scotland (Edwards *et al.*, 2007) give the time frame for the HTM earlier between 8000-7000 cal years BP.

The warm temperature, newly available habitat and soil formation saw the expansion of vegetation and forest biomes (Roberts, 1998; Woodcock, 2000). Within this period are several distinct oscillations or climate cooling events, which occur c. 8.2 ka, 5.5 ka, 4.2 ka and between 1200 and 1650 AD (Maslin *et al.,* 2005; deMenocal *et al.,* 2006). The 8.2 ka cold event lasted approximately 200 years and created widespread cool and dry conditions ending with a rapid return to generally warmer and moister climates than at present. Marine records indicate cold and arid conditions in parts of NW Europe during this event (Alley *et*

al., 1997). The mid-Holocene, from c. 6000 cal years BP to c. 2600 cal years BP, sees the climate shift into the cooler Sub-Atlantic period which experiences oscillations between cool-wet and warm-dry conditions taking place every 260-520 years (Barber *et al.,* 1994). The 5.5 ka cooling event is marked by a sudden and widespread shift in precipitation causing many regions to become either drier or moister. Changes in dust and SST records in Africa show a higher humidity at the onset of this event and ending with a 300 years transition to current arid conditions (de Menocal *et al.,* 2000b). In Europe, a shift in vegetation, specifically the decline of *Ulmus* sp., is attributed, in part, to climate change during this event (Maslin and Tzedakis, 1996). The mid to late Holocene sees a period of relative sea level stability and coastlines begin to take the forms we see today. Estuaries and bays adjacent to river catchment outflows start to experience sediment deposits as marine incursion reduces. Sedimentation creates new alluvial habitat and landforms along the coastlines. Human settlements begin to spread during this time as well, having implications for increased sedimentation and/or erosion in adjacent coastal areas (Berglund *et al.,* 1996). At 4.2 ka, a strong cold and arid event occurred across the North Atlantic, northern Africa and southern Asia (Bradley and Jones, 1993; Bond *et al.,* 1997; Bianchi and M^{c}Cave, 1999; de Menocal *et al.,* 2000a; Cullen *et al.,* 2000; Maslin *et al.,* 2005). This event coincides with major shifts in anthropogenic activity (e.g.: collapse of the Mesopotamian Empire, collapse of the Old Kingdom in Egypt, the rise of early Bronze Age civilizations in Greece, Israel and India) (Peiser, 1998; Cullen *et al.,* 2000; de Menocal, 2001). Marine sediment cores indicate a large and extreme drought took place c. 4000 years BP with a significant increase in the amount of dust in the ocean for the 300 years that follow (Cullen *et al.,* 2000; de Menocal, 2001; Maslin *et al.,* 2005).

The Little Ice Age, occurring from 1200 to 1650 AD, is the most recent Holocene cold event and is possibly the most rapid and largest change in the North Atlantic during the Holocene as indicated by ice cores and marine cores (Mayewski *et al.,* 1997; de Menocal *et al.,* 2000b). It is characterised by a temperature decrease of 0.5-1.0 °C in Greenland, (Dahl-Jensen *et al.,* 1998), significant shift in ocean currents in the North Atlantic (Jennings and Weiner, 1996; Andrews *et al.,* 2001) and a SST fall of 4°C off the coast of West Africa (de Menocal *et al.,* 2000b). This period is also marked by significant anthropogenic changes

including the extinction of Norse colonies on Greenland and mass migrations and famine across Europe (Bradley and Jones, 1993; Barlow *et al.,* 1997).

3.4.1 Holocene climatic cyclicity

Holocene climate events are considered millennial scale quasi-periodic climate changes that occur in c. 1500 (+/- 500) year cycles (Maslin *et al.,* 2005). Thought to be similar to Dansgaard - Oescher cycles (D-O cycles) (Bianchi and M^c Cave, 1999; de Menocal *et al.,* 2000; Maslin *et al.,* 2005), there is uncertainty regarding the periodicity of these cycles. D-O cycles are high-frequency climate oscillations with 1000-, 1450- and 3000-year cyclicities (Dansgaard *et al.,* 1993; Grootes, 1993; Leuschner and Sirocko, 2000). Often linked to a reduction in the North Atlantic Deep Water (NADW) (Bond *et al.,* 1997; Maslin *et al.,* 2005), these Holocene cycles cause surface water temperatures of the North Atlantic to be c. 2-4°C cooler than during the warmest intervals (Bond *et al.,* 1997; de Menocal *et al.,* 2006b). Recent marine sediment cores have indicated that there are, indeed, millennial scale climate cycles throughout the Holocene but whether these are quasi-periodic or have a regular cyclicity is not absolute. Many theories have been postulated regarding the cause of these Holocene climate cycles, the majority of which include a variation in the deep water circulation system of the ocean. The internal instability of Arctic Sea ice, based on the theories behind glacial Heinrich cold events, is one theory for these climate cycles. This suggests that large areas of sea ice have their own internal waxing and waning rates (Jennings *et al.,* 2002) which may cause melt water in the Nordic Seas which, in turn, reduces deep water formation leading to Holocene cyclic cold events (Kreveld *et al.,* 2000; Jennings *et al.,* 2002; Sarnthein *et al.,* 2001). Surface ocean waters can change over months and years, but deep oceans can take decades to centuries to respond to various forcings and this enables it to be a significant factor in long term climate change on centennial and millennial time scales (Bond *et al.,* 2001; Maslin *et al.,* 2005).

3.5 Relative Sea Level (RSL) during the Holocene

At the onset of the Holocene, as the ice sheets melted and water was returned to the ocean, the sea had begun to transgress across the continental shelves forming shelf seas and shallow marine margins (Scourse, 2013). Understanding changes in sea level over geological time scales is vital. These changes represent important controls in the evolution of coastal environments and their adjacent landforms (Mastronuzzi *et al.*, 2005). Relative Sea Level (RSL) changes are reconstructed from physical features and biological organisms whose distributions are related to sea level in a consistent manner (Edwards, 2007b; 2013; Lambeck *et al*., 2010; Edwards and Craven, 2017). Some of the most marked Holocene paleogeographic effects have been shifts in coastlines (Woodcock, 2000) and the effect on shoreline geomorphological change has been highly variable spatially. Changes in beach morphology in Northern Ireland where isostatic uplift temporarily outstripped eustatic sea level rise resulted in emergent shorelines (Cooper *et al*., 2009) and isostatic adjustment led to uplifted shorelines that can be traced around Scotland (Smith *et al*., 2000; 2011). An occurrence on some Northern European coastlines, these stranded raised shorelines are remnants of late Holocene regression. By contrast, southern England is experiencing gradual subsidence (Woodroffe and Murray-Wallace, 2012) and the Bay of Biscay and South Western coastlines in Europe been affected by eustatic sea level rise creating inundation coastlines seen today (Leorri and Cearreta, 2004; Leorri *et al.*, 2012).

Several models have been generated to create a 'curve' which represents RSL rise over time (e.g.: Shennan *et al*., 2006; Brooks *et al*., 2008;Edwards and Craven, 2017). The models incorporate observational data based on Sea Level Index Points (SLIPs), known points of position and elevation that have been radiocarbon dated to provide information on paleo sea levels. These models are often linked to data from ice sheet retreat models (e.g.: Bradley *et al.,* 2011; Kuchar *et al.,* 2012). Edwards and Craven (2017) give additional RSL models using SLIPs from four sites in Ireland. In models generated in Brooks and Edwards (2008) a broad scale geographical change is demonstrated in Ireland and some of the most marked Holocene paleogeographic effects have been shifts in coastlines (Woodcock, 2000). Figure 3.3 shows sea level rise along the Irish coastline (Brooks and Edwards, 2008) at various intervals (8000, 6000, 4000 and 1000 years before present). These models were generated to demonstrate broad scale geographical changes in Ireland and not to determine detailed

localised events (without other correlating evidence). However, it can be assumed that in the Galway Bay region, a change in the hydrology has taken place; the level of inundation of salt water, freshwater or both has altered its state to the saline Bay we know today. In fact, Edwards and Brooks (2008) go on to state that c. 8000 years ago the Aran Islands, Clare Island, Inisturk and Inisboffin were most likely part of the mainland and the shallow embayment of Galway Bay and Clew Bay probably had large expanses of terrestrial or littoral environments.

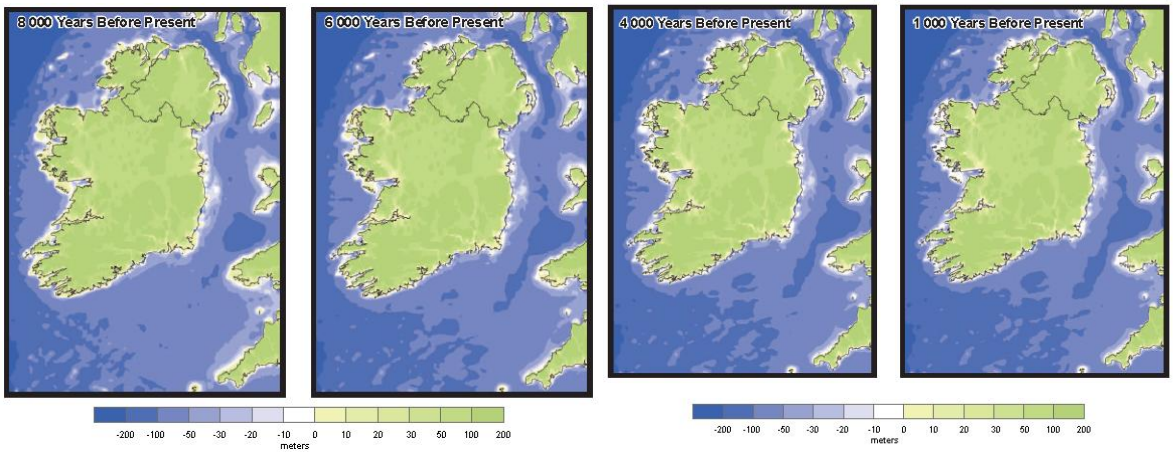

Figure 3.3: Sea level rise in Ireland in the latter part of the Holocene (Edwards and Brooks, 2008).

Glacial isostatic rebound models (e.g.: Shennan *et al.*, 2006 and Bradley *et al.*, 2011; Kuchar *et al*., 2012) relate to marine transgression and RSL as well. These models help to understand the thickness of ice sheets and the rates of ice sheet retreat and therefore the onset of Holocene conditions; in coastal areas inferences regarding marine transgression can be made from glacial isostatic rebound models. Sea level rise is, in part, a result of the mass redistribution of water which occurred as ice sheets melted globally. Redistribution of water was changeable on both spatial and temporal scales and relied, largely on the glacial isostatic response of the earth – or the response of the land to change in pressure as the ice sheets melted (Milne *et al*., 2014). In the UK and Ireland, several studies relating to RSL as a result of glacial isostatic response have been carried out (e.g.: Peltier *et al*., 2002; Shennan *et al*., 2000, 2002, 2006; Brooks *et al*., 2008; Bradley *et al*., 2011; Kuchar *et al*., 2012).

Geomorphological studies which focus on Holocene Relative Sea Level (RSL) changes have helped us understand that there is considerable geographic variation in the pattern of sea level rise (e.g.: Lambeck *et al.*, 2010; Woodruff and Murray, 2012; Edwards, 2013; Shennan *et al.*, 2015; Edwards and Craven, 2017). Figure 3.4 displays the RSL curves produced by Bradley *et al.* (2011) and Kuchar *et al.* (2012) with recent SLIPs in Ireland (as published in Edwards and Craven (2017).

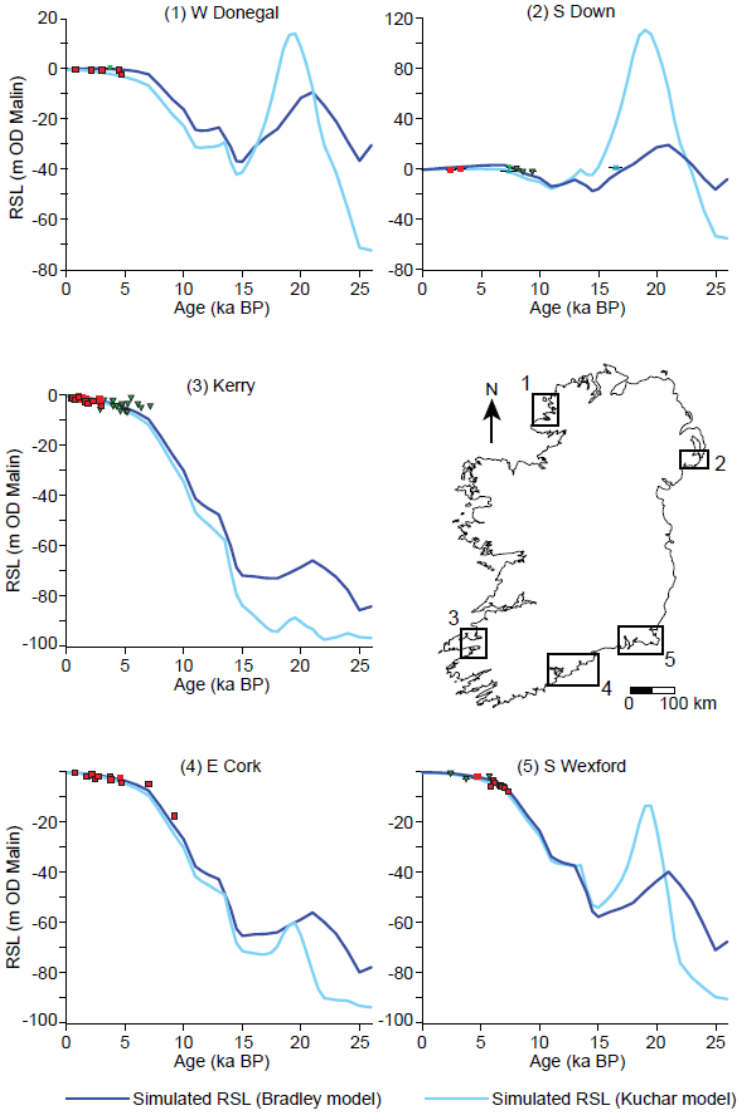

Figure 3.4: Relative Sea Level curves from Ireland as published in Edwards and Craven (2017). Included here are the SLIPs (represented by the red points) in relation to existing curves produced by Bradley *et al.*, (2011) (indicated by the dark blue line) and Kuchar *et al.*, (2012) (indicated by the light blue line).

Variation in the models from c. 25-15 kya is likely due to the difference in model parameters where Bradley *et al*. (2011) uses a global ice reconstruction and Kuchar *et al*. (2012) combines ice modelling techniques with glacial isostatic adjustment modelling. However, this figure is effective in showing that there are differences along coastlines within close proximity of each other and that geographic variation is an important variable when examining sea level rise.

In the early Holocene sea level rise was a key factor in environmental changes to coastal areas, particularly low energy coastal environments. RSL change during this time was largely the product of variations in ocean level (eustatic) and vertical land movements (isostatic) (Edwards, 2007a; 2013). Rising temperatures acted as a catalyst for eustatic sea level rise, which accounted for most shoreline changes as the coastal response was nearly instantaneous. During the mid-Holocene, eustatic sea level rise experienced a distinct decline. Previously, isostatic changes occurred in proportion to the amount of ice overburden that had depressed the lithosphere and the resulting effects were more localised than eustatic effects. In some areas which had been compressed under ice, the land raised forming marine platforms that drastically altered the coastal landform and coastlines with shallow gradients underwent the most change as it was these areas that were most affected by inundation of the sea and the incoming tide (Chappell and Pollach, 1991; Roberts, 1998). Sea level rise combined with several other factors, such as, coastal geography and geomorphology, sediment transport and sediment accretion played a prominent role in Holocene coastal landscape development (Anderson and Vos, 1992).

3.6 Paleoenvironmental applications

Holocene sediments deposited in estuarine and coastal environments are archives of paleoenvironmental information (Colman *et al.*, 2002). Applied paleoenvironmental research using stratigraphical, chronological, geochemical and microfossil evidence can offer valuable data on past changes in salinity, sea level and climate variations. Environmental reconstructions supported by radiocarbon dating have helped validate the timing of events and rates of change in environmental proxy records since it was developed in the late 1940s (Libby *et al*., 1949; Reimer *et al*., 2013). Geochemical sedimentary features, both organic

and inorganic, are widely used in paleoenvironmental study to describe and quantify the source environment while key biological remains in coastal sediments include silicious diatom microfossils and calcareous foraminiferal tests. Diatoms have been used as salinity indicators and elevation markers in paleo research on coastal wetlands, tidal marshes and tidal flats (Patterson *et al*., 2000; Nelson *et al*., 2008; Roe *et al* 2009 and Smith *et al*., 2010). Foraminifera are widely used as proxies for Holocene marine transgression and sea level rise (Edwards and Horton, 2006; Wright *et al*., 2011; Edwards and Wright, 2015; Plets *et al*., 2015). The key components of paleoenvironmental study in terms of chronological, stratigraphical, geochemical and microfossil tools and their applications in the coastal zone are outlined in the next sections.

3.6.1 Radiocarbon dating

Radiocarbon dating has become an essential component in the interpretation of paleoecological data by allowing for a better understanding of the timing of events and rates of change in environmental proxy records (Reimer *et al.,* 2013). Radiocarbon dating of organic material is a core method of obtaining age estimates for Holocene chronologies and is based on measurement of the decay rate of the radioactive isotope ^{14}C; a chemical element that is isotopically unstable and undergoes radioactive decay with time (Roberts, 1998; Bradley, 1999). In the 1980s the Accelerator Mass Spectrometer (AMS) methodology was developed and can date samples as small as 5 mg (Pilcher, 2005). Radiocarbon dating estimates can be obtained on wood, charcoal, marine and freshwater shells, bone and antler, and peat and bulk organic-bearing sediments. They can also be obtained from carbonate deposits such as calcite, marl, dissolved carbon dioxide, and carbonates in ocean, lake and groundwater sources (Bradley, 1999). Each sample type has specific issues associated with its use for dating purposes, including contamination and environmental effects (Jones *et al.,* 1989; Heier-Nielsen *et al.,* 1995). Additionally ^{14}C years do not directly equate to calendar years (de Vries 1958; Stuiver and Suess 1966; Reimer *et al.,* 2009) and a calibration of radiocarbon dates needs to be carried out (Reimer *et al.,* 2013).

Dating of macrofossils is preferable to bulk sediments, as the latter may be complicated by the presence of old organic matter in the sediment matrix, and is subject to a variety of effects that can produce inaccurate radiocarbon ages (Olsson, 1979; Sutherland, 1980). This

dating complication can become exacerbated in northern latitudes where organic matter decomposes slowly and may reside in permafrost for long periods of time before being eroded into fluvial of coastal systems. The usage of plant macrofossils potentially avoids problems associated with dating mixtures of contemporaneous and older organic matter in bulk sediment (Oswald *et al*., 2005).

Marine carbonate materials are subject to various effects that require the initial radiocarbon age reported by the laboratory to be corrected or calibrated. Marine shells are subject to the marine reservoir effect, a delay in incorporation of atmospheric radiocarbon into oceanic deep water. This delay, combined with the variable strength in deep water upwelling at coastal zones, results in spatial and temporal variation in the marine reservoir effect, where marine samples appear older than terrestrial samples of equivalent age (Bard, 1988). A second potential source of variation associated with shell ageing is the feeding strategies, ecology and behaviour of molluscan taxa. For example, epifaunal species such as oysters may yield older ages than infaunal species such as clams at the same stratigraphic level, due to burrowing habits (Ingram and Southon, 1996) or the variation of feeding strategies between organisms where the age of the ingested carbon is reflected in the apparent age of the shell (Dyke *et al.*, 2003). A further source of variation is the differential seasonal growth patterns displayed by different molluscan taxa. Those species growing in spring or summer, for example, may display older ages than those whose growth is limited to winter, because of variations in the strength and position of upwelling water masses through the year (Hutchinson *et al*., 2004). However, radiocarbon ages on marine shells have provided important information on glacial and sea level history and have become an essential tool in paleoecological studies.

3.6.2 Sediment stratigraphy

Syvitski and Milliman (2007) describe sediment flux to the coastal zone as being conditioned by geomorphic and tectonic influences (basin area and relief), geography (temperature, runoff), geology (lithology, ice cover), and human activities (reservoir trapping, soil erosion). Paleoenvironmental reconstructions attempt to track these occurrences, forces and changes over time through analysis of the sediment record. Geographical position in the coastal zone (e.g.: estuaries, lagoons, tidal marsh) provide a variety of conditions for organic

and inorganic deposits suitable for stratigraphic reconstructions. Stratigraphic tools include particle size analysis, x-ray imaging and visual observations.

In the coastal zone, low energy environments such as estuaries act as sediment traps for both fluvial and marine sediments and tend to accumulate sediment rapidly. A high sedimentation rate has great potential for high temporal resolution in proxy reconstructions (Coleman, 2002). Paleoenvironmental evidence from estuaries and coastal low lands can provide important information for RSL studies and coastal evolution (Innes and Frank, 1988; Shennan, 1992, Shennan *et al.*, 2000a). Coastal lagoons provide a suitable sedimentary environment for paleoecological studies because they are relatively sheltered from wave and tidal forcings (Bennion and Battarbee, 2007) and provide information of atmospheric and terrestrial changes over time (Cassina *et al*., 2013). Studies of sediment sequences from tidal marshes provide quantitative reconstructions of late Holocene relative sea level and land level movements worldwide (Watchman *et al*., 2013). In North Western Europe, sea level rise is one of the most significant factors affecting coastal development (Kennett, 1982; Vos and de Wolf, 1988) and therefore plays an important role in paleoecological reconstructions of tidal areas. Salt marsh sediment has been used widely as a proxy for RSL studies (Gehrels *et al*., 2005 (Western Atlantic); Kemp *et al*., 2011 (South Eastern United States); Kemp *et al*., 2014 (Eastern Atlantic)). Patterns of sediment transport and deposition on a temporal scale can reveal paleo landscapes and shed light on storm activity regionally (Cooper and Jackson, 2003). Stratigraphical examinations can reveal coastal geomorphological changes and explain the interplay between marine incursion and excursion in the coastal zone as seen in the sediment record (Cooper *et al*., 2009). Sedimentary coasts and associated lithostratigraphies reveal regional tidal frames. The use of radiocarbon dating in conjunction with established sediment sequences allows for a collection of 'sea-level index points' which enable the development of records of relative sea-level change from sedimentary coasts (Edwards, 2006; Horton and Edwards, 2006). This sedimentary information can be used collectively to make important inferences about ecological changes in spatially expansive coastal areas during the Holocene.

3.6.3 Geochemical proxy analysis

Traditional methods of acquiring geochemical data from sediment cores involves incremental sampling to obtain gram quantities of material and further processing it for elemental composition as needed. This process is time consuming and results in the destruction of the samples (Kido *et al.,* 2006; Croudace *et al.,* 2015). During the last fifteen years, X-ray fluorescence (XRF) core scanning technologies have been developed and have made possible high resolution, non-destructive measurements of elemental composition in sediment cores (Croudace *et al.,* 2006; Francus *et al.,* 2009). A major advantage of XRF core scanning over conventional geochemical analysis is that element intensities are obtained directly at the surface of a split sediment core. In addition, the spatial resolution of XRF core-scanning devices is much higher than that of conventional destructive methods, and allows the extraction of near-continuous records of element intensities from sediment cores (Richter *et al.,* 2006; Rothwell *et al.,* 2006; Thomson *et al.,* 2006; Weltje *et al.,* 2008). Modern XRF methods provide useful, high resolution geochemical records from terrestrial and marine sources (e.g.: Jansen *et al.,* 1998; Rothwell *et al.,* 2006; Thomson *et al.,* 2006). The advantages of XRF core scanning over conventional destructive techniques indicate that this tool has great potential for paleo-environmental research (Calvert and Pedersen, 2007; Weltje *et al*., 2008).

It is common for element ratios, as opposed to single, downcore element composition, to be used in cross core comparisons and for higher accuracy in statistical analysis of geochemical data (Croudace *et al*., 2006; Richter *et al.,* 2006; Weltje and Tjallingii, 2008; Goudeau, *et al*., 2014). Numerous elemental ratios are used in paleoecological studies and a number of elemental ratios salient to coastal and marine paleo studies are discussed here. An indicator of marine biogenic carbonate versus terrestrial input is Ca/Ti (Richter *et al*., 2006; Rothwell and Rack, 2006; Goudeau *et al.,* 2014). This ratio can also be used as a preliminary overview of downcore sedimentary variability and for stratigraphic correlation in marine cores (Hennekam and deLange, 2012; Lacka *et al.,* 2015). K/Ti can indicate terrigenous input into a system and reflects temporal changes in sediment sources from acidic (more K) and basaltic (more Ti) source rocks. Increased K/Ti ratios are observed at times of enhanced terrigenous matter supply (Richter *et al.,* 2006; Riethdorf, *et al*., 2016). Elevated K/Ti have

also been associated with coarser grain size, as well as, with changes in provenance (Rothwell and Rack, 2006; Goudeau *et al.,* 2013). Goudeau *et al.* (2014) suggests climate may be reflected in the K/Ti ratio due to the presence of illite (a mica-like clay mineral) because more illite is eroded in cold environments (Yarincik *et al.,* 2000). K/Ti values are usually high in sediments that have a relatively high illite (Goundeau *et al.,* 2014). The ratio of Si/Ti can indicate the deposition of biogenic silica (BSi) in diatom rich sediments. Diatoms extract dissolved silica from the surrounding waters in which they live (Hendey 1964) indicating that a higher Si/Ti relates to increased diatom productivity; possibly due to the availability of essential nutrients in the water column (Cantarero, 2013; Goundeau *et al,*. 2014).

High Zr/Ti ratios can represent coarse-grained sedimentation and strong physical degradation possibly resulting in the breakage of diatom valves in the sedimentation process. Fe/Mn has been used as a proxy for several things including: source heterogeneities in oceanic basalt content (Qin and Humayun, 2008; LeRoux *et al.,* 2010) and oxic conditions at the sediment/water interface or in the sediment (Kastner *et al.,* 2010). This is because as water depth increases, Fe/Mn ratios decrease as more oxidized MnO_2 is fixed to the sediment surface. Some studies show that when sediment re-distribution takes place, there is an increase in the Fe/Mn ratio (Haberzettl *et al.,* 2006; 2007; Kastner *et al.,* 2010) and another shows a high Fe/Mn ratio generally indicates a stable catchment with low perturbation by erosional fluxes (Terasmaa *et al.,* 2013). The Br/Cl ratio is used as an indicator of saline water when marine sediments display a constant Br/Cl ratio therefore implying sea-water presence. High Br/Cl ratios may also indicate organic-rich layers as Br and S are high in organic-rich sediments (Croudace *et al.,* 2006; Rothwell *et al.,* 2006; Thomson *et al.,* 2006). A high Sr/Ca ratio may indicate the presence of high-Sr aragonite which requires a shallow-water source (Croudace *et al*., 2006).

3.6.3.1 Applications of geochemical markers in sediment cores

XRF core scanning has successfully been applied to sediment sequences to reconstruct paleo-environmental changes. For example, environmental forcings and changes occurring in a 14 ka long sequence from Chile (Moreno *et al.,* 2007; Giralt *et al.,* 2008); variations in aeolian inputs linked to the East Asian monsoon over the last 16 ka (Yancheva *et al.,* 2007);

paleo-flood events over the last 2 ka in Spain (Moreno *et al.*, 2008); and changes in sediment input linked to movement of the Intertropical Convergence Zone over the last 55 ka in tropical Africa (Brown *et al.*, 2007; Kylander *et al.*, 2011). X-Ray Fluorescence core scanning is commonly used to reconstruct paleoenvironments in both marine and lacustrine sediments and identify diagenetic processes. The reconstruction of paleo sedimentary sequences, specifically paleo vertisols (Ashley and Driese, 2000); shifts in the hydrological cycle over the past 90,000 years (Peterson *et al.*, 2000); paleoclimatology in Cariaco Basin (Haug *et al.*, 2001); paleo climate and sedimentary histories (Bahr *et al.*, 2005); paleoclimatology in sub-tropical ocean basins (Peterson and Haug, 2006); and paleolimnological studies in Mexico (Cantarero, 2013) and elsewhere (Löwemark *et al.*, 2011). The contents of biogenic silica, biogenic carbonate, and terrigenous material can be estimated from major element composition, and examination of temporal or spatial variations in the contents of these components is useful for reconstructing paleoclimatic and paleoceanographic changes (e.g.: Sirocko *et al*., 1991 (circulation and upwelling in the Arabin Sea); Tada, 1991 (paleoceanographic change in the Sea of Japan); Irino and Tada, 2000 (paleoceanographic change in the Sea of Japan). The variation in concentrations of certain metal species such as iron, manganese and calcium are a result of changes in hydrological processes, climate, and ecology (Boyle, 2001).

3.6.4 Microfossil analysis in paleoecological reconstruction

Rashid *et al*., (2013) describes microfossils, including diatoms and foraminifera, as the most useful paleoenvironmental indicators for coastal change because they occur in large numbers in small diameter in Holocene submerged coastlines. Diatoms are used as proxies for a variety of research themes including: climate change; sea level rise; long term environmental change; paleo-oceanic, estuarine and coastal reconstructions. Planktonic foraminifera are indicative of open ocean environments and benthic foraminifera, while found in near shore and deep sea environments, characterise coastal and intertidal environments; living at the sediment to water interface.

3.6.4.1 Diatoms

Diatoms are algae; microscopic unicellular eukaryotic organisms in the Kingdom Protista (Round *et al.*, 1990; Hoek *et al.*, 1995), which range in size from approximately 5 µm to 500 µm and live wherever there is moisture and adequate light for photosynthesis to occur (Barber and Haworth, 1981). There are over 250 genera and 10,000 taxa, globally distributed, dating back to the early Cretaceous period. Occupying both marine and freshwater systems, diatoms are used as environmental indicators with applications including reconstruction of past climate changes and modern anthropogenic impacts (Battarbee *et al.*, 2001). Planktonic species, those living freely or as colonial chains in the water column are largely controlled by nutrient concentration in marine environments. Benthic diatoms are those associated with a substrate and live mostly in littoral zones (Hendey, 1964; Battarbee *et al.*, 2001). In an estuary, freshwater diatoms may be transported in by river systems and marine diatoms may arrive via tidal action while true estuarine species occur in the mixing zones (Cooper, 1999). Each specific diatom habitat can be defined by physical and chemical conditions that support varying diatom assemblages. In the littoral zone, habitats are more accurately defined as a series of microhabitats that interact due to the strong forcing of tides and weather and the competition for appropriate substrate to allow for photosynthesis. Predation, temperature, bacterial epidemics and anthropogenic influences are all stressors on these diatom populations and can affect their appearance in the fossil record (Hendey, 1964).

The earliest use of diatoms as salinity indicators in paleoecological studies was in Scandinavia (Cleve-Euler, 1923; 1943; Lundqvist and Thomasson, 1923; Halden, 1935). Stemming from a debate on land uplift and resulting lake isolation, a progression from marine to brackish to freshwater diatoms emerged as evidence of the changing landforms in the Baltic region (Berglund, 2003). Diatom species were found to have an individual affinity for specific levels of saline water and were classed ecologically using the Halobian system (Table 3.1). Diatom assemblages are also sensitive to changes in pH and trophic conditions (Smol, 1990; Lowe and Walker, 1997).

Table 3.1: Originally derived from Kolbe's (1927) work in Germany and later modified by Hustedt (1953, 1957) and Simonsen in 1962. The Halobian scale divides diatom species into five categories of salt tolerance (Vos and de Wolf, 1993; Lowe and Walker, 1997; Berglund, 2003; Zong *et al*., 2003; Roe *et al.*, 2009).

Category	Ecological group	Salt concentrations
Polyhalobous	Marine	>30
Mesohalobous	Brackish	0.2 - 30
Oligohalobous (halophilous)	Salt tolerant freshwater	
Oligohalobous (indifferent)	Slightly to salt tolerant freshwater	<0.2
Halophobous	Freshwater	0 (salt intolerant)

3.6.4.1.1 Diatom paleoecological applications

Interpreting diatom assemblage data for paleoecological reconstruction can be complex. While the siliceous form of diatoms preserve well under a range of sedimentary environments (Anderson and Vos, 1992) issues of breakage and dissolution of the silicia frustules can cause differential preservation and misleading results (Lowe and Walker, 1997; Ryves *et al*., 2001; Ryves *et al*., 2006; Ryves *et al*., 2009). Fossil diatoms undergo various processes during their transformation from living organisms to fossils; these processes are termed taphonomy (Flower and Ryves, 2009). In the coastal zone, taphonomic limitations are often enhanced by exposure to semi-terrestrial conditions; for example, in salt marshes, often only a small portion of species which actually lived in this environment remain (Sherrod *et al*., 1989; Denys and de Wolf, 1999). Determining the origin of the taxa and whether it is indicative of the area from which it was found or has been transported is core to any investigation. Diatoms that have lived at the place of deposition (autochthonous) and those that were transported by wind or water (allochthonous) provide different information about the local environment or the input waters into the system (Vos and de Wolf, 1988; Anderson and Vos, 1992; Lowe and Walker, 1997). Excessive valve breakage due to the high energy nature of coastal zones is typical as well (Beyens and Denys, 1982) but also results from grazing effects (Turner, 1991) and, after deposition, by compaction and drying of sediments (Flower, 1993). This combined with individual taxa morphology and response to tidal flushing can make it difficult to accurately recreate paleoenvironmental conditions in the coastal zone. In salt marsh and marginal peat areas, paleo environments that were well

drained through time, a resulting fossil record predominated by *Paralia* and *Pseudopodosira* have little to do with the actual paleoenvironment and more to do with individual species robustness (Denys, 1989; 1994; Hemphill-Haley, 1995; Denys and de Wolf, 1999).

In coastal environments, specifically the littoral zone, diatoms appear throughout the year (as opposed to seasonal fluxes which occur in the open ocean). While individual species experience seasonal periodicity, a disappearance of one species is quickly replaced with the appearance of another. That is not to say that population densities have no variation; while small numbers are present on most shores at all times of the year, seasonal density distribution varies from place to place and from year to year. Some species have a precise vegetative period and others can be found at varying quantities throughout the year. This leaves open, the possibility of false interpretations of population densities for some species in the littoral zone and as such, careful attention needs to be paid to sampling protocols for benthic diatoms (Hendey, 1964; Denys, 1985; Weckstrom and Juggins, 2005). Vos and de Wolf (1988) recognise that in coastal areas, the tide is the most important factor for the classification of varying sedimentary environments and that an indirect relationship exists between sedimentary environments: sub-, inter-, and supra-tidal environments in macro-, meso-, and microtidal systems and tidal lagoons in microtidal and non-tidal systems; and ecological groups: planktonic and benthic (and their sub-divisions).

3.6.4.1.2 Diatom applications in the coastal zone

Tidal Zones

Diatoms are recognised as a valuable tool in paleoecological reconstruction (Hustedt 1957; Juggins, 1992; Vos and de Wolf, 1993). As diatoms are often the dominant microphyte in estuaries and marine littoral areas (Palmer and Abbott, 1986; Cooper *et al*., 2010) their presence in the sediment record over time create an environmental history of coastal zones as indicator species that respond to environmental variation in the tidal zone (Pilarczyk *et al*., 2014). Certain diatom taxa predominantly inhabit particular inter-tidal zones and can therefore be employed to identify small-scale sea level changes by quantifying the vertical range of the assemblages associated with each zone (Vos and de Wolf 1988; Nelson and Kashima, 1993; Hemphill-Haley, 1995; Anderson and Vos 1997; Roe *et al* 2009). This

relationship between diatoms and the environmental gradients that control their distribution can reflect the highest point of marine influence and therefore provide stratigraphic markers used for shoreline displacement and the determination of the sea level history of coastal areas (Palmer and Abbott, 1986; Anderson and Vos, 1992; Lowe and Walker, 1997; Berglund, 2003; Roe *et al.*, 2009). Quantifying the magnitude and frequency of transgressive and regressive events and thus localized sea level changes, can be carried out by looking at changes in fossil diatoms assemblages in combination with alterations in sediment and landform (Denys and de Wolf, 1999). In paleotidal reconstructions, the same idea applies, using general assemblage composition to allow for gross distinction of subtidal, lower and higher intertidal and supratidal conditions. Here, however, problems arise with a direct association between vertical diatom zonation and tidal reconstructions because of the numerous environmental characteristics involved including light, salinity, stability of substrate, type of substrate, water movement, degree and duration of substrate desiccation, plant cover and nutrient supply (Denys and de Wolf, 1999).

Storms

High energy storm events can also be read in the diatom record. For example, diatoms found in sandy deposits occurring between fine grained estuarine sediments can be storm indicators. *Paralia sulcata*, a robust tychoplanktonic diatom, is abundant in the water column in stormy weather. The presence of *P. sulcata* together with sessile species from the sublittoral zone can be an indicator of stormy conditions or events (Haggart, 1988; Smith *et al.*, 1992; Hemphill-Haley, 1996; Denys and de Wolf, 1999). De Wolf *et al* (1993) discuss how storm activity can be tracked from wave disturbance of off -shore tidal laminations consisting of sand with *Delphineis minutissima* and clay with *Cymatosira belgica*. Diatoms have been widely used as indicators of storm events in the Gulf of Mexico (Horton *et al*., 2009; Lane *et al*., 2011 and Hawkes and Horton, 2012; Pilarczyk *et al*., 2014), earthquakes in Alaska (Shennan *et al*., 2009, 2014) and Japan (Sawai *et al*, 2012) and tsunamis in Alaska (Briggs *et al*., 2014) and Chile (Horton *et al*., 2011).

Ecological conditions

Diatoms recovered from sediment cores reflecting upwelling events can be used to track sea surface temperature changes and periods of high and low bio-productivity through varying

time periods. As well, evidence of sediment bioturbation and varying degrees of diatom preservation for specific species (e.g.: *Delphines karstenii*; *Fragilariopsis doliolus*) can be used as indicators of upwelling events and periods of high and low paleoproductivity (Schrader and Sorkness, 1991; Schrader *et al.*, 1993; Kennington *et al.*, 1999). Nutrient concentration in coastal waters is reflected in fossil diatom assemblages and used as a paleo indicator (Weckstrom and Juggins, 2006; Clarke *et al*., 2006; Liu *et al*., 2008). The use of diatoms to track changes in pH has also been widely used (Battarbee *et al*., 1999; Tiffs *et al*., 2008; Cassina, 2012).

Glacial activity

The reconstruction of glaciostatic recovery following the last ice age and resulting glacier rebound and coastline formation can be extrapolated using diatom based reconstructions (Battarbee, 1986; Long and Shennan, 1994). Diatom calibration sets from high latitude sediments in the Arctic and Antarctic oceans have enabled paleoceanographers to interpret the limits of glacial coverage and timing of ice ages and warming periods throughout the Quaternary (Kennington, 2002). Tracking Antarctic diatom assemblages and their association with open-ocean or sea-ice conditions and specific climatic conditions has allowed the reconstruction of varying glacial periods and the extent of sea ice in the Quaternary (Fryxell, 1991; Kaczmarska *et al.,* 1993; Cunningham *et al.,* 1999). As well, diatoms have been used in North America to track ice sheet regression and meltwater patterns (Gil *et al*., 2015).

3.6.4.2 Foraminifera

Foraminifera are unicellular protists (Protozoa) existing primarily in the marine environment as either benthic or bottom dwelling and planktonic or free floating in the water column (Murray, 1991). There are an estimated 6800 species of foraminifera (Hayward *et al*., 2014). The external skeleton of the foraminifera, referred to as the test, is comprised of either calcareous material, where the organism secretes a calcium carbonate ($CaCO_3$) test or agglutinated material, where the organism forms their tests by adhering detrital material to their body. The test type is dependent on whether or not the organism's environment is conducive to carbonate preservation (Scott *et al.,* 2001). Foraminifers can be epifaunal

(attached to a surface) and or infaunal (burrowers); and their feeding patterns are fundamental limiting factors which control distribution patterns. In marginal marine settings most primary production is from benthic algae; in intertidal zones microphytobenthos (including diatoms and flagellates) produce a film that moves through the sediment; in shallow lagoons and tidal marshes higher plants form essential parts of the food source of foraminifera (Murray, 2001; 2006).

When observed in the fossil record, foraminifera and other rhizopod remains are often the only proxy information regarding the spatio-temporal nature of transitional environments (Scott *et al.*, 2001). The accumulation rate of inorganic sediments in coastal environments has a bearing on the concentration of fossil foraminiferal tests. For example, in areas of high fluvial sediment input taxa count numbers may be very low due to the type of sediment and some deep-sea sediments may be almost pure concentrations of foraminiferal tests. In general, tests are scarce in coarse sands but are often abundant in silts and fine sands (Haynes, 1981). Boomer and Horton (2006) comment that brackish water conditions can pose certain problems in paleoenvironmental reconstructions. The shells of some agglutinated species are susceptible to disaggregation causing them to break up and therefore not appear in the fossil record. In addition, some calcareous species can become dissolved under acidic conditions and this too can alter faunal composition.

3.6.4.2.1 Foraminiferal applications

Foraminifera are important in paleoclimatic, paleo-sea-level, paleo-depth and paleoceanographic studies. They are also used in age determinations using oxygen isotopes and in petroleum assessment (Albani *et al*., 2001). The use of foraminifera to determine paleo tidal ranges is based, in part, on Scott and Medioli (1980) who carried out the first detailed study to accurately reflect vertical tidal zonation in coastal habitats. Hass (1997) used foraminifera to carry out paleoclimatology reconstructions and Nees (1997) used foraminifera to look at paleoceanographic and paleo- climatology research; Cearreta *et al.* (2003) studied foraminifers in lagoons in Portugal to assess modern assemblages and establish a dataset for transfer functions. Ruiz *et al.* (2005) looked at foraminifera in estuaries and their relationship to sediments as paleo-geographies changed over time; Edwards and Horton (2006) carried out paleotidal and paleo-sea level studies based on

foraminiferal assemblages in Norfolk, UK. Cronin *et al*. (2010) looked at paleo-climate reconstructions in Chesapeake Bay, USA. In the coastal zone, sea level rise studies using foraminifera as a proxy are widely accepted and paleoceanographic studies in the tidal zone have resulted in a large body of work dedicated to sea level changes during the Holocene. Scott and Medioli (1980) use foraminifera to infer sea level rise in Nova Scotia, Canada and Thomas and Varekamp (1991) looked at coastal marsh sequences in Connecticut, USA to establish paleo tidal ranges. In Australia, Cann *et al.* (2002) discusses changes in biofacies, including changes in foraminiferal assemblages to infer Holocene sea level change and in New Zealand, Hayward *et al.* (2002; 2004) uses foraminifera to infer paleo tides and salinity in coastal areas. Gehrels *et al*. (2006) establishes Holocene sea level changes in Iceland. Edwards and Horton (2000) researched salt mash foraminiferal assemblages in the UK to establish sea level rise. Also in the UK, Gehrels *et al*. (2002); Horton and Edwards (2006); Shennan *et al*. (2006) and Edwards (2007a) all used foraminifera to establish Holocene sea level changes and climate change. Scourse (2013) gives a comprehensive review of Holocene paleoenvironmental change and sea level rise globally.

Additionally, foraminifera have been widely used in glacial and interglacial studies. For example, Fretwell *et al.,* (2010) looked at isostatic uplift in Shetland islands and Southern Antarctic peninsula; Edwards and Brooks (2008) researched glacial formation in Ireland; Chiverrell and Thomas, (2010) looked at the extent of the BIIS over the UK and Ireland and Scourse (2013) investigated glacial activity and sea level rise in the UK during the Quaternary). Multi-proxy studies, which include foraminiferal data, can also result in paleotidal information and sea level rise models.

3.6.4.3 Transfer functions

Transfer or calibration functions are mathematical functions where a biological response acts as proxy data for reconstructing past environmental variables. Imbrie and Kipp (1971) devised the first procedure involving a transfer function for quantitative reconstruction of past environmental variables from fossil species assemblages and use marine foraminifera as a proxy for ocean surface temperatures and salinity. Since then different regression and calibration techniques have been developed for different types of proxy data including diatoms. Transfer functions are now routinely used in paleoecological studies (e.g.: Horton

et al., 1999; 2000 (UK transfer function data base); Gehrels *et al.*, 2001; 2002 (UK salinity); Horton and Edwards, 2005 (UK sea level rise with foraminifera as proxy); Edwards, 2007a (UK sea level rise using sedimentary proxy data); Patterson *et al.*, 2004; Scourse, 2013 (glacial extent and change)). Understanding and quantifying modern distributions of microfossil indicators relative to target variables can enable use of microfossils as proxies for former tide and sea levels (Gehrels *et al*., 2001; Patterson *et al*., 2005, Roe *et al.,* 2009). These relationships can also then be used to establish quantitative predictions of future tide and sea level change.

Increasing interest in freshwater acidification was the driving influence in the development of diatom transfer function models for pH, however differences in affinities for salinity, substrate and inter-tidal exposure make diatoms particularly suitable for reconstructing paleo sea level changes (Palmer and Abbott, 1986; Vos and de Wolf, 1988; Shennan *et al.,* 1994; Roe *et al*., 2009). Analysis of the diatom composition in sediment cores extracted from the coastal zone can be undertaken using qualitative (presence/absence), semi-quantitative (estimated abundance class) and quantitative (relative abundance or concentration by counting) methods. Here, abundances of individual taxa can be extremely high and the preservation state of the diatoms can vary greatly and decisions regarding methodological approaches to taxa determinations should be considered on a case by case basis. However, when applying these methods to paleoecological reconstructions a statistically reliable and reproducible approach is most suited (Denys and de Wolf, 1999). Cassina (2012) uses diatoms to infer pH in coastal lagoons in Ireland during the Holocene and Lewis (2011) uses a diatom based salinity transfer function in the Baltic Sea to recreate environmental conditions in the Holocene in Northern Europe. McKeown (2013) uses fossil chironomids from sediment cores in lakes in Ireland to document climatic change in Western Europe over the last 10,000 years.

In summary, our understanding of Holocene coastal environmental change has largely been derived from paleoenvironmental studies of key physical, chemical and biological components of aquatic sediments. Each proxy record provides important contribution to environmental inferences; however, knowledge of their limitations is vital.

CHAPTER 4: Methodology

Introduction

A paleoenvironmental, multi proxy approach was undertaken to assess environmental change in Inner Galway Bay North. This chapter describes the Galway Bay study area, field methods employed for the extraction of sediment cores and laboratory methods utilised in the project. Radiocarbon dating was carried out and sedimentological, geochemical and biological materials were extracted and analysed.

4.1 Study Area

Galway Bay is an indentation on the west coast of Ireland facing out into the North Atlantic Ocean with a surface area of c. 800 km^2. Map 4.1 shows the study area in relation to Ireland with water depth in the Bay represented and the lower Corrib catchment delineated. The sediment core sampling points are labelled. The Bay lies along the 53° 11′ north latitude and is bounded by the 8° 55′ and 9° 55′ west longitudes. Geologically the entire northern shoreline of the Bay is within the Galway granite batholith and to the east of Galway City the granite is overlain by Carboniferous limestone, which also forms the bedrock of the southern shores (Lei, 1995). Galway Bay is a drowned glacial landscape exhibiting drumlins, meltwater channels and other glacial formations (NPWS, 2013). INFOMAR (Integrated Mapping for the Sustainable Development of Ireland's Marine Resource) surveys of Galway Bay began in 2006 as a joint venture of the Marine Institute and the Geological Survey of Ireland and have mapped the bathymetry of the Bay (Marine Institute, 2016). Galway Bay is partially sheltered from the prevailing south-westerly winds by the Aran Islands and can be divided into the Inner and Outer Bay. Map 4.2 shows the divisions of Galway Bay: Outer Galway Bay, Inner Galway Bay North and Inner Galway Bay South. The Corrib Catchment is defined and the EPA (2014) delineation of transitional waters is shown with the sampling points in red. The Inner Bay is shallow with water depths <30 m and the outer Bay considerably deeper with depths up to 70 m (O'Donncha *et al., 2015*). Surface sediments consist of layers of Holocene silty-clay material to varying depths and coarser material deposited by storm surges in the Bay (Erdmann *et al*., 2015). The largely glacial derived substrate of inner Galway Bay from Oranmore Bay to Kinavarra Bay results in a wide range

of sediments (NPWS, 2013). Intertidally this ranges from cobbles and pebbles with fucoids, to mixed sediment, sand and sandy mud and a very heterogeneous substrate within the depositional environment of east Galway Bay. The northern shoreline of Galway Bay is highly indented and characterised by an irregular series of rocky bays with small sandy beaches with the Northern Sound having a maximum depth of 69 m and width of 13 km (O'Donncha *et al., 2015*).

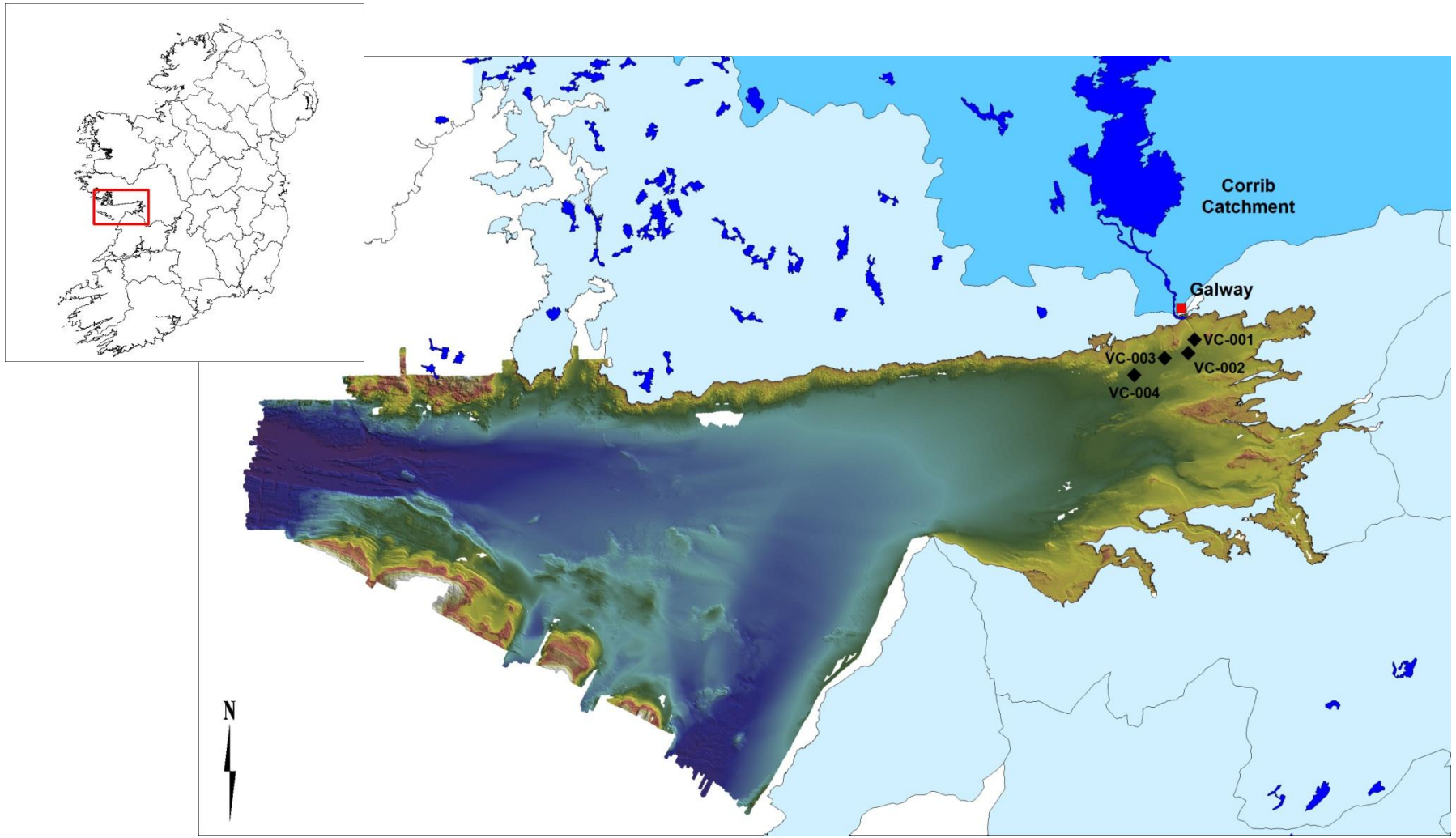

Map 4.1: Map of Galway Bay, Ireland showing water depth. The locations of the four sample sediment cores are noted in black and labelled (VC001, VC002, VC003 and VC004). The small map of Ireland indicates the position of Galway Bay nationally.

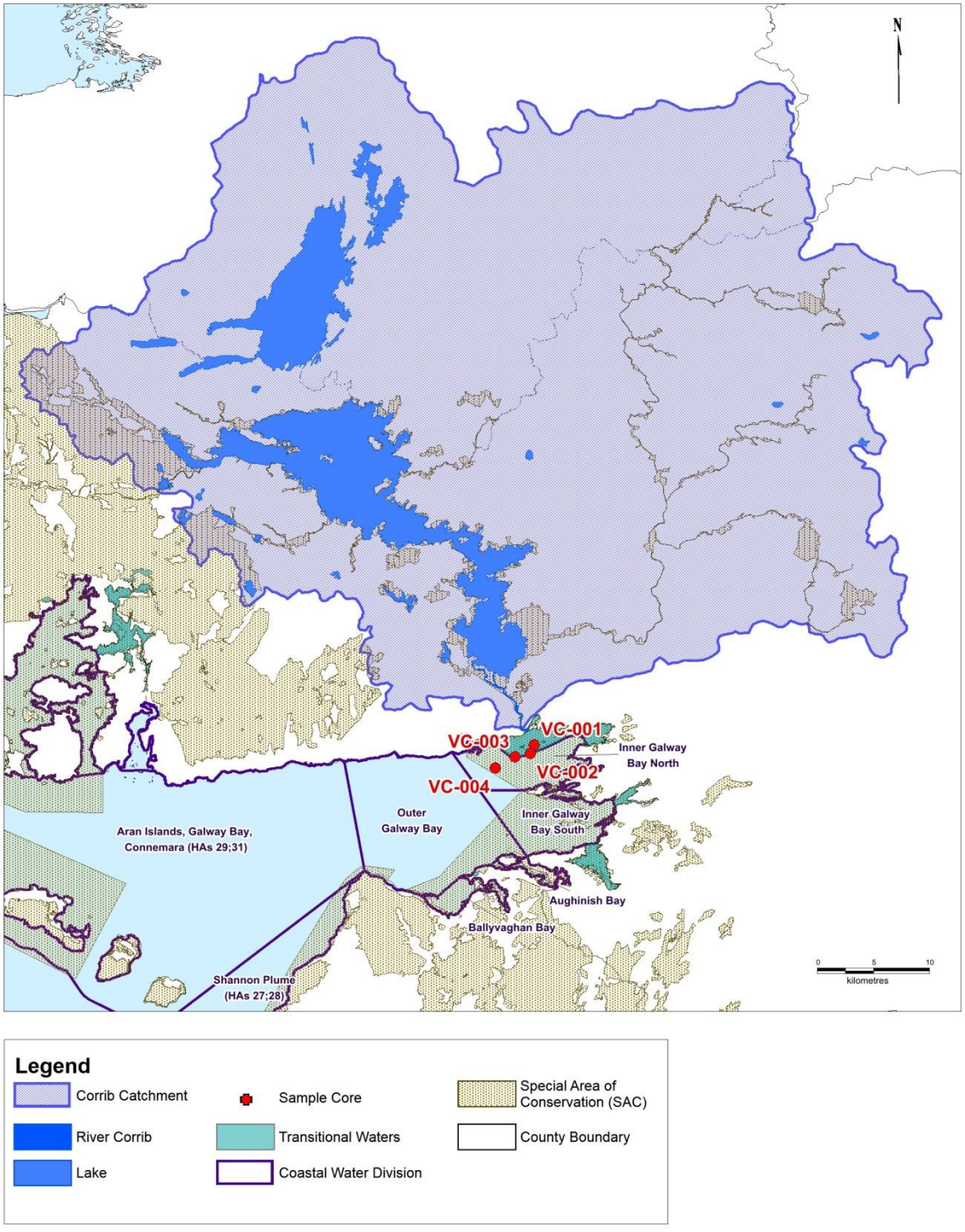

Map 4.2: The delineation of the Corrib Catchment with the Transitional Waters, Inner Galway Bay and Outer Galway Bay marked (delineation as per EPA, 2014). The sample sediment cores are labelled in red (VC001 and VC002 in the transitional waters and VC003 and VC004 in Inner Galway Bay North).

4.1.1 Modern hydrological conditions in Galway Bay

Hydrodynamics in Galway Bay are influenced by several factors including oceanic flows from the North Atlantic as they enter the Bay from the continental shelf; freshwater inflow, mainly from the Corrib River and the wind driven processes affecting the water. General circulation is governed by a strong north-easterly inflow through the South Sound, both at the surface and at the bottom and there is outflow through the North Sound (Booth, 1975; Fernandes, 1988). Donncha *et al*. (2015) notes a possible gyre in the outer Bay (as postulated by Booth, 1975 and Fernandes, 1988) with varying reports of the direction of circulation. Recent Marine Institute (MI) data (Map 4.3) of the north Inner Bay shows various discreet circulatory patterns, most notably two small gyres west and east of Mutton Island and likely driven by the Corrib River outflow where density driven currents are tied to the freshwater inflow and the waters of Salthill, west of Mutton Island. The Corrib, which enters the Bay at the north-eastern corner, is the primary driver of reduced salinity here and as a result reduced density of water in the Inner Bay and along the north shore (Anninou and Cave, 2009). A major influence in the north Inner Bay, the Corrib River drains approximately 70% of the catchment area around Galway Bay with an average flow of 99 m^3 s^{-1} (BIM, 2012). The direction of the winds and to a lesser extent the tide, are the main driving forces for mixing in Galway Bay (Anninou and Cave, 2009). Atlantic tidal waves begin as generally small waves and increase in size as they move eastward across the continental shelf and are further enhanced as they enter bays and estuaries in western Europe. The west coast of Ireland experiences and average tidal range of 4.5 m and Galway Bay is highly variable. Map 4.4 shows the Mean High Water and Mean Low Water delineation in the north Inner Bay. A low energy coast comprising small waves, tides and slow currents, Galway Bay is dominated by silty sand to clayey sediment, with accumulations of fine grained sediment that may gather forming intertidal flats. The lowest-energy coastal areas are typically found in sheltered embayments, lagoons and estuaries with low fetch (Woodroffe, 2002). The general physical characteristics of the sediment in low energy intertidal areas combined with the biological components are indicative of environmental conditions in intertidal zones (Edwards, 2007b).

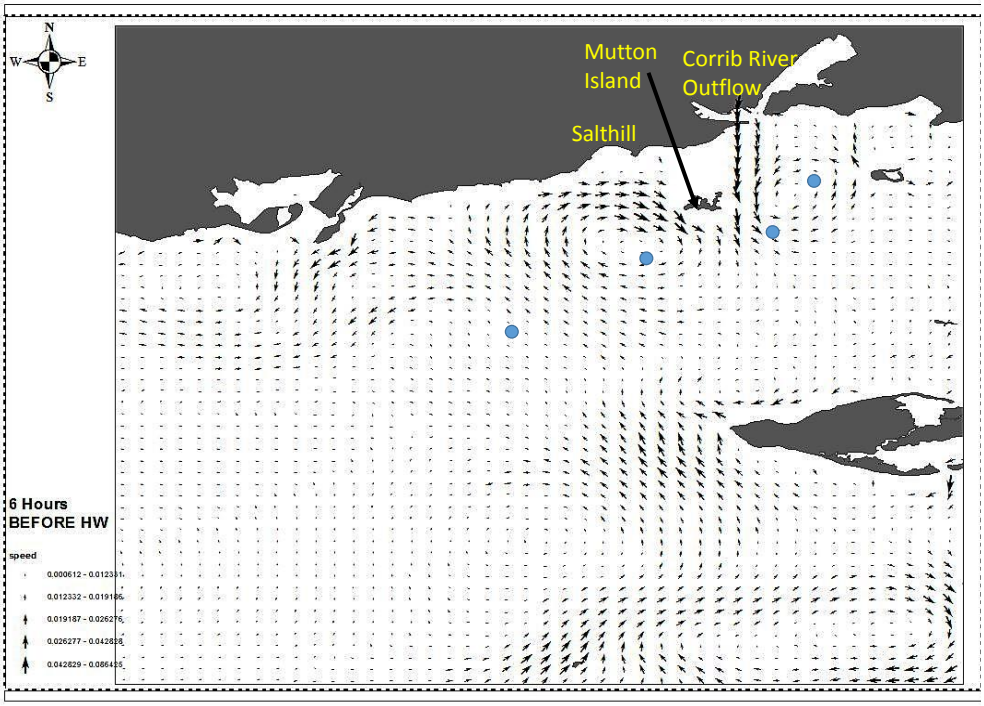

Map 4.3: Circulation in the north Inner Galway Bay. This map displays an average of surface and bottom currents at all sampling points collected by the Marine Institute in 2015 (unpublished data) in this area. Arrows indicate direction and shading of the arrows indicates the speed of the flow: darker arrows having a faster flow than lighter arrows.

Map 4.4: North Inner Galway Bay showing Mean High Water line (blue) and Mean Low Water line (green) (www.marine.ie accessed 14/7/2016).

4.1.2 The Corrib catchment

The Corrib Catchment (hydrometric area no. 30, OS catchment no. 143) is located in Counties Galway, Mayo and Roscommon in the Western River Basin District (Map 4.2). It has a total catchment area of 3,101 km^2 (McGinnity *et al.*, 2003). Loughs Corrib (17,000 ha), Mask (8,000 ha), Carra (1,500 ha) and numerous tributaries, are included in this catchment with the total lake and river area in the catchment estimated at 277.67 km^2 and 6.87 km^2 respectively (McGinnity *et al.,* 2003). The River Corrib drains Lough Corrib and runs for 7.7 km before entering the sea in Galway City. To the east of Loughs Corrib and Mask, the land is low-lying with moderate rainfall and karst limestone geology where underground karst conduits contribute to the freshwater system. The smaller tributaries flowing into the Loughs from the west are much steeper, draining impermeable mountainous catchments with high rainfall. The management of Lough Corrib has changed over the years. For example, in the 12th century, the Friars Cut was built to provide another outlet from the Lough into the River Corrib in an attempt to allow boats to access the Lough from the sea. Between 1846 and 1850 the lake was lowered to reduce flooding of surrounding farm land (Freeman, 1957).

4.2 Sediment coring

On February 27th 2009, as part of the Marine Institute Research Vessel (RV) Celtic Explorer Cruise No. CE09-04 and funded by INFOMAR (Project # INF-09-19DAL), four sediment cores were obtained across a transect in inner Galway Bay North. Figure 4.1 summarises the journey of the sediment cores from extraction to analysis at the laboratories of project partners. Sediment core extraction was carried out using the vibrocore technique; developed in the 1960's for use in marine, coastal and shelf oceanographic investigations (Sanders and Imbrie, 1963; Bouma 1969; Glew *et al.,* 2001). Widely used and cost effective, this method allows for the acquisition of cores over 1 m in length where at least a portion of the sediment is unconsolidated (Lansky *et al.,* 1979) and as a continuous sediment sequence, uninterrupted by over overlapping or missing sections at core tube breaks (Glew *et al.,* 2001). The Geological Survey of Ireland's Geo-Core 6000 was utilised for all core extraction. A four kilometre NE-SW transect between transitional water body Corrib Estuary (IE_WE_170_0700) and coastal waterbody Inner Galway Bay North

(IE_WE_170_0000) consisting of the inner bay silt/clay depositional areas and less than 1.8 km from the coast was targeted for core extraction. Careful attention was paid to ensuring cores were extracted outside known navigation channels which would have experienced dredging in the past. As per standard methodology laid out in Benetti (2007), six metre core liners were inserted into the core barrel and the vibrocorer rig was lowered by winch from the ship to the sea-bed and electrically driven hammer drills enabled the core barrel to penetrate the sediment. Coring duration was between 10 and 30 minutes for each core. Core liner tubes were sub-sectioned into 1 m lengths and sealed using caps. Caps were sealed using hot wax and tubes were clearly labelled. Each core section was marked with an arrow towards the top, the cruise number (CE09-04), corer label (VC), core site (e.g.: 001) and core section number (e.g.: 1 of 6, with progressive numbers for each core section).

Geo-references of the cores were originally recorded in decimal degrees and later adjusted to degrees, minutes, seconds. Table 4.1 shows the original recordings and subsequent adjustment along with water (m) and field core section (cm) depths and actual sediment lengths (cm).

Table 4.1: Georeferences of the four sediment cores with their respective assigned codes, depth of water, core length and sediment length of each vibrocore; acquired aboard the Celtic Explorer CE09-04 28th February 2009.

Code (Core)	Degrees & Decimal Minutes		Degrees, Minutes, Seconds		Water Depth (m)	Core Depth (cm)	Actual Sediment Length (cm)
	Latitude (N)	Longitude (W)	Latitude (N)	Longitude (W)			
VC001	53°15.373′	09°02.234′	53°15′22.21″	09°02′14.40″	11.2	550	535
VC002	53°14.951′	09°02.562′	53°14′57.20″	09°02′33.41″	12.4	580	554
VC003	53°14.793′	09°03.801′	53°14′47.30″	09°03′48.30″	13.4	600	542
VC004	53°14.262′	09°05.365′	53°14′15.44″	09°05′21.54″	13.5	500	478

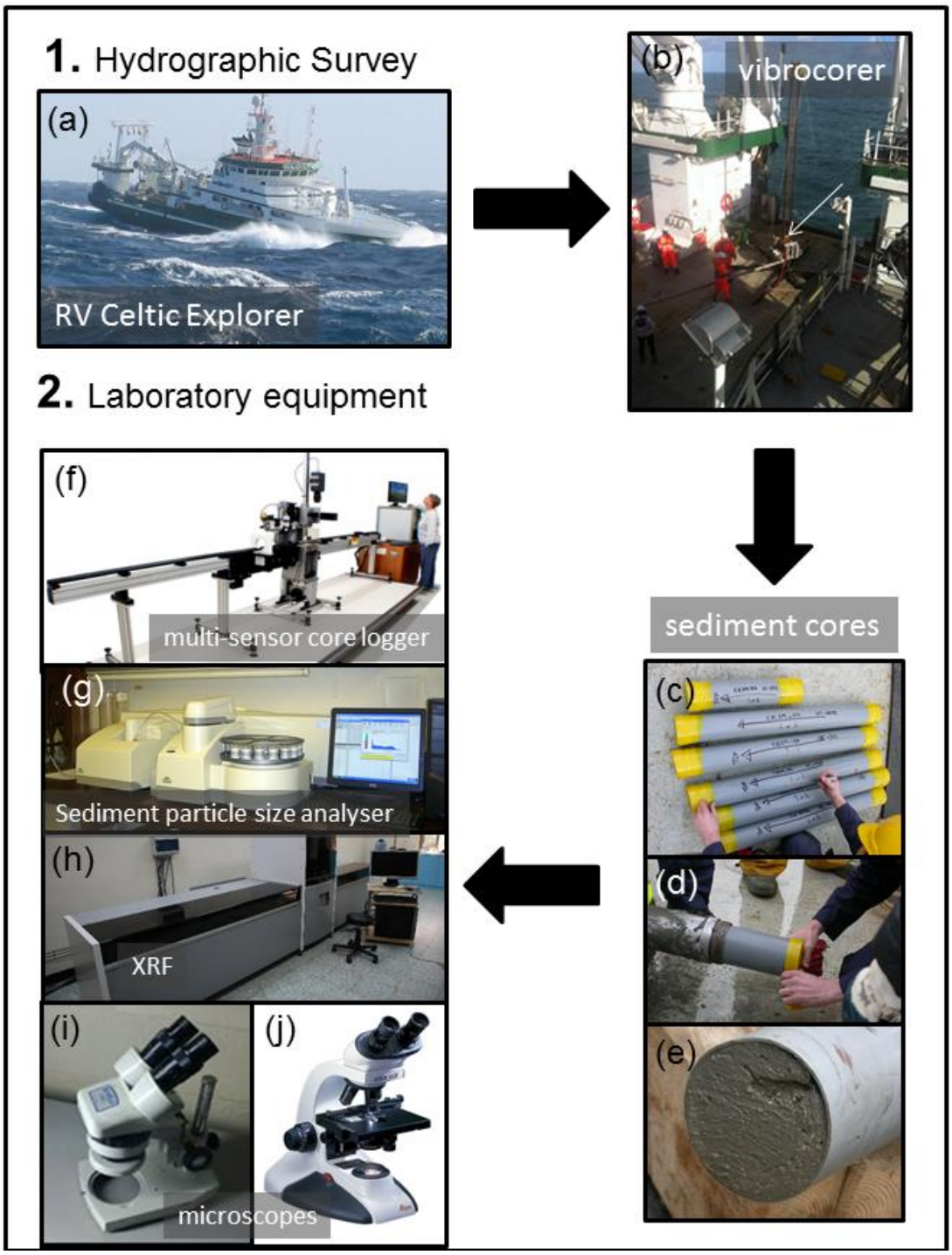

Figure 4.1: Flow diagram shows sample recovery through to laboratory analyses where (a) Research Vessel *Celtic Explorer*; (b) vibrocorer; (c -e) sediments cores; (f) multisensor core logger; (g) Malvern mastersizer 2000 sediment particle size analyser; (h)) XRF; (i) stereoscope used to identify foraminifera; (j) light microscope with phase contrast used to identify diatoms.

4.3 Laboratory analysis

A range of physical, chemical and biological analysis was conducted on the sediment samples. Table 4.2 shows the sediment parameters analysed, sample resolution and methods and equipment utilised. The receipt of four Mary Immaculate College Research Directorate awards made the procurement of 23 radiocarbon dates possible. These dates were acquired on all four sediment cores. The Multi Sensor Core Logger at NUI Maynooth allowed for whole core sedimentological analysis at a one centimetre sample resolution. The Malvern Mastersizer at Trinity College allowed for particle size analysis at a 20 cm resolution to be carried out on two of the vibrocores (VC001 and VC003). The use of the X-ray fluorescence scanner at University College Dublin yielded 2 mm sample resolution obtaining 32 elemental profiles on all four cores. Microfossil analysis (diatoms and foraminifera) was carried out at Mary Immaculate College with a diatom sample resolution of 2-20 cm on sediment cores VC001, VC003 and VC004 while foraminifera were sampled at 20 cm intervals on sediment cores VC001 and VC003. A PhD project at the University of Limerick used these vibrocores, in part, to calculate the percent organic carbon in all four sediment cores on cumulative 25 cm sections (Mylotte, 2014). Additionally a seismic profile of the study area was generated in a MSc project at NUI Galway using the seismic data obtained during this research cruise (Clarke, 2014).

Table 4.2: Sample resolution, methods and equipment utilised, radiocarbon dates and sedimentological, geochemical and microfossil proxies analysed for Galway Bay sediment cores.

Proxy	Resolution	Method Details	Equipment used and location of analysis	State of Core	Cores Targeted	Analysis
Radiocarbon Dates	As needed at change points	Shell, Wood and bulk sediment targeted, cleaned, sent to ChronoLab to process.	Accelerator Mass Spectrometer at Queens University Belfast	Split core	VC001,VC002 VC003,VC004	^{14}C dates run with a Marine Calibration
Sedimentological	1 cm (ten sec count rates)	One meter core sections for 30 minutes – whole core (prior to splitting).	Geo-tek Multi Sensor Core Logger (MSCL) at NUI Maynooth	Whole core	VC001,VC002 VC003,VC004	Gamma density, Magnetic Susceptibility, P-wave velocity
	20 cm	A laser-target obscuration of 15–20% was selected. Two gram sub-samples of wet sediment achieved required obscuration	Malvern Mastersizer with a Hydro G accessory unit and 36-pot Malvern auto-sampler in Trinity College	Split core	VC001, VC003	Particle size analysis
Geochemical	2 mm	Molybdenum tube operated at 60 kV and 50 mA with a sampling resolution of 2 mm and a 4 sec exposure time produced count rate of 20K	Itrax X-ray fluorescence (XRF) scanner at University College Dublin	Split core	VC001, VC003	32 element profiles Salient elemental ratios used for analysis
Microfossils						
Diatoms	Ranges from 2 to 20 cm	Samples prepared as per Battarbee *et al.,* (2001)	MEIJI Techno ML2000 phase contrast light microscope with camera at Mary Immaculate College	Split core	VC001, VC003 VC004	PCA, DCA, CA, Cluster Analysis, DI-Salinity
Foraminifera	20 cm	Samples prepared as per Armstrong and Brasier (2005)	A MEIJI-EMZ-TR stereoscopic microscope at Mary Immaculate College	Split core	VC001, VC003	PCA, Cluster Analysis,
Other data						
% Organic Carbon	25 cm	Data generated by R Mylotte	Various techniques at UL	Split core	VC001,VC002, VC003, VC004	Data produced by R. Mylotte
Seismic profile	n/a	Data generated by Cathal Clarke	High-freq single channel seismic reflection from ship	n/a	VC001, VC002 VC003, VC004	Data produced by C. Clarke

4.4 Sedimentology

4.4.1 Core logging

Sediment cores were transported to the Department of Geography at NUI Maynooth to undergo analysis using a Geotek multi-sensor core logger (MSCL). The MSCL enables non-destructive high resolution measurement of physical parameters on the each core. Measurements of core thickness (cm), p-wave velocity (m/s), gamma density (g/cm^3) and magnetic susceptibility (SI) were conducted on intact whole core sections. One metre core sections were scanned for c. 30 minutes at 1 cm spatial resolution and count rates of 10 seconds (n = 2230 records).The length of each core was calculated as they were run through the *Geotek* MSCL conveyor; the ends of core sections were covered in caps and no measurements were recorded in capped ends of the cores. Subsequent to the MSCL investigation, all four cores were split in half and digital images were recorded using a conventional tri-pod mounted camera.

Stratigraphical observations and physical core descriptions were completed through visual inspection of the digital imagery obtained from NUI Maynooth (high resolution TIFF images) as required. Physical descriptions and recording of core sediment followed Benetti (2007) and Last (2001). Lithology of bedding structures (e.g.: thickness of beds and lamination form) and sediment fabric features (e.g.: texture and grain size of material) were determined throughout the four cores following Benetti (2007) and Kemp *et al.* (2001). Disturbances in the sediment structure, mottling (iron deposits) and inclusions (e.g.: pebbles, shells, wood) were noted, measured and described before inclusion in the final sediment log. Sediment colours were described using Munsell colour charts. Other materials or changes in the stratigraphy of the core, as well as, areas of possible previous deposition and/or turbidity were noted and transcribed for visual presentation in the same manner.

A sediment log was generated using a combination of the above visual descriptions of the physical sediment cores and textural classification. The textural classification of sediments was determined using the particle size analysis results (VC001 and VC003 only; Table 4.1) and following the Shepard (1954) classification system. This system is based on the Wentworth (1922) particle size scale and was chosen due to the low level of sediment larger

than 2 mm. The Shepard system is designed for fine sediment grains containing less than 2% gravel (sediment >2 mm). Shepard classification was obtained using the SedClass program available via the United States Geological Survey website (www.usgs.gov). Classification for sediment cores VC002 and VC004 was performed visually and manually using the Troels-Smith scheme (1955) and VC001 and VC003 as a reference. Adobe Illustrator 10 was used to create sediment log images.

Laser Diffraction Grain Size Analysis (LDGSA) was performed on VC001 and VC003 at systematic 20 cm intervals (VC001, n=27; VC003, n=27) following methodologies outlined in Eschel *et al.* (2004) and Sperezza *et al.* (2004). The grain-size analysis, which was undertaken at Trinity College Dublin, used a Malvern Mastersizer 2000 in combination with a Malvern Hydro G accessory unit and a 36-pot Malvern auto-sampler. This instrument is capable of analysing a size range from 0.02 to 2000 μm. Test samples indicated that 2 g subsamples of wet sediment achieved the required obscuration (time required for the laser to pass over the sediment particle to achieve the particle diameter). Results are displayed as mean grain size (μm) per 20 cm section of sediment core and percent of total core.

4.5 Radiocarbon dating

Radiocarbon dating took place at the Chrono laboratory at Queens University, Belfast using Accelerator Mass Spectrometry (AMS). Table 4.3 presents a summary of the 23 samples targeted for radiocarbon dating. Preliminary dates suggested that sediment core VC001 contained a relatively complete Holocene sequence and thus was the focus of ten radiocarbon dates. Macrofossil shells were targeted as they generally yield the true age of sediment in coastal and shallow marine sediment cores (Heier-Nielsen *et al.,* 1995). Nine intact macrofossil shells were sampled throughout the core and in the lower 35 cm where no shell was available, woody material was used (taken at 525 cm). In sediment core VC002, three shells were used for radiocarbon dating and in sediment core VC003, four visible woody samples were sub-sampled for dating along with two bulk samples for comparative test purposes; one in the lower core at 458 cm and one in the middle core at 354 cm. Bulk sediment samples can pose dating accuracy issues due to the broad provenance of materials, bioturbation and microfossil accumulation (Jones *et al.,* 1989). Sediment core VC004 was

targeted to see if zones of major change were concurrent across the coastal transect. As such, four samples were taken from areas of the core which displayed a visual change in sediment. All four samples taken from VC004 were shell. As per the guidelines issued by Queens University laboratory, small shell and wood samples were sent to the laboratory in glass vials. Shells were cleaned and dried. Larger fossil samples were wrapped in foil and packaged in a padded envelope for shipping. No species data was attainable for the wood samples and only limited shell samples could be identified. Bulk sediment samples were kept cool in the dark and submitted in sealed plastic bags.

Table 4.3: Summary of sediment core samples targeted for AMS ^{14}C dating; VC001, VC002, VC003 and VC004.

Core	Number of Samples	Sample Location (cm)	Sample material
VC001	10	5, 37, 66, 111, 115, 197, 322,342, 464, 525	Shell
		525	Wood
VC002	3	9, 56, 361	Shell
VC003	6	89, 252, 373, 507	Wood
		353-354, 457-458	Bulk
VC004	4	16, 55, 192, 450	Shell

4.5.1 Calibration

Marine samples have radiocarbon dates older than terrestrial samples with an accepted variance or 'offset' of typically 400 years (Pilcher, 2005). The marine offset can vary in different places depending on ocean mixing, upwelling and perturbations occurring from melting glacial ice and in the North Atlantic the offset can be as high as 700-800 years in Late Glacial times (Lowe and Walker, 2000). Marine calibration was undertaken using the Marine13 programme, part of the Calib (Rev. 7.1.0) suite of software (Reimer and Reimer, 1986-2014; Reimer *et al.*, 2013). To ensure higher accuracy, a marine radiocarbon reservoir correction (ΔR) was taken from the weighted mean of twenty of the closest sites published in

Harkness (1983); Blake (2005) and Butler (2009) available via Calib. The ΔR value is defined as the offset of a local marine reservoir from the global ocean age, R (Stuiver *et al.*, 1986; Rick *et al.*, 2012) and the value of -24 was used in this calibration. As part of the weighted average of ΔR, Calib provides the weighted uncertainty or the standard deviation as the weighted average error; the larger of the two was used in the current marine calibration (Stuiver *et al.*, 1986; Stuiver and Reimer, 1993; Culleton, 2006; Jones *et al.*, 2007; Petchy *et al.*, 2008; Rick *et al.*, 2012) with a value of 64.

4.6 Geochemistry – X-Ray Fluorescence (XRF)

Geochemical data from XRF core scanning has been used successfully to reconstruct environmental variability (e.g.: Haug *et al.*, 2001; Richter *et al.*, 2006; Hennekam and De Lange, 2012; Goudeau *et al.*, 2014). The XRF scanning system allows for a qualitative determination of the bulk geochemical composition (Jansen *et al.*, 1998). XRF determination was conducted at The Earth Institute at University College Dublin on all four sediment cores. Operational procedures of the Itrax XRF are outlined in Croudace *et al.* (2006). Measurements were conducted on the split cores as they provide higher resolution readings and a better control of the scanning process (e.g.: sediment disturbances like slumps, gaps or coring artefacts are recognisable) (Zolitschka *et al.*, 2001). Split core surfaces were gently smoothed and covered with a thin (4 µm) Ultralene film to avoid contamination of the measurement prism of the core scanner (Richter *et al.*, 2006). The Ultralene film can partially absorb the XRF intensities for lower fluorescence energies (Kido *et al.*, 2006; Tjallingii *et al.*, 2007). However, because the film is thought to have a constant thickness, the limited absorption by the film will cause a constant intensity decrease of the influenced elements (Al, Si, Cl) over the whole depth domain. Therefore, no correction for this foil absorption is required (Hennekam and De Lange, 2012). Figure 5.1 illustrates the various instruments used during the course of analysis of these sediment cores.

The Itrax XRF provided results for 32 elements as follows: Mg, Al, Si, P, S, Cl, Ar, K, Ca, Ti, V, Cr, Mn, Fe, Ni, Cu, Zn, Ga, As, Br, Rb, Sr, Y, Zr, Ba, La, Ce, Ta, W, Pb, Bi and U. Measurement of 1 m core sections with a 2 mm resolution and count rates of approximately 20,000 took between 7-8 hours producing approximately 12,000 data points. The element

profiles were examined in conjunction with the mean square error (MSE), a parameter of data quality. All counts per second (kcps) were greater than 100 and can be treated with certainty; all validity scores of 0 were stripped from the final data set.

The data generated by the XRF scan is the result of high resolution measurements over a short period of time (Jansen *et al.,* 1998) and in its original form is presented as unprocessed intensities (count per unit time per unit area). Several studies, however, have shown XRF count data to be semi-quantitative (Croudace *et al*., 2006; Richter *et al.,* 2006; Weltje and Tjallingii, 2008; Goudeau, *et al*., 2014), therefore elemental ratios have been used rather than direct counts. The elemental ratios relevant to this research were chosen and are displayed in table 4.4.

Table 4.4: Summary table of elemental ratios used as proxies to reconstruct past sediment chemistry changes in paleoclimate and paleoceanographic studies. All elements were generated by the XRF and initial ratios and Log ratios were generated in Excel.

Elemental Ratio	Indicators	References
Ca/Ti	• marine biogenic carbonate versus terrestrial input • downcore overview of sedimentary variability and stratigraphic correlation in marine cores • detrital input	Richter *et al*., 2006; Rothwell and Rack, 2006; Hennekam and deLange, 2012; Goudeau *et al.,* 2014; Lacka *et al.,* 2015
K/Ti	• coarser grain size • changes in provenance • climate variation (cold, arid environments) • terrigenous input	Bonatti and Gartner, 1973; Yarincik *et al.,* 2000; Richter *et al.,* 2006; Rothwell and Rack, 2006; Goudeau *et al.,* 2013; Riethdorf, *et al*., 2016
Si/Ti	• presence of quartz, • deposition of biogenic silica	Kemp *et al.,* 1999; Johnson *et al*., 2002; Cantarero, 2013;Goudeau *et al.,* 2014
Zr/Ti	• provenance (marine (decrease)/terrestrial sources) • grain size	Rothwell and Rack, 2006; Goundeau *et al.,* 2014;
Fe/Mn	• source heterogeneities in oceanic basalt content • conditions at the sediment / water interface • sediment redistribution • deposition of iron-sulphides which are typically formed under limited water circulation and possible anoxia • stable catchment with low perturbation by erosional fluxes (high ratio)	Engstrom and Wright 1984; Schaller and Wehrli 1996; Cohen , 2003; Humayun *et al.,* 2004; Haberzettl *et al*. 2007, 2006; Sobolev *et al*.,2007; Qin and Humayun, 2008; Enters *et al*. 2010; LeRoux *et al* 2010; Kastner *et al.,* 2010; Terasmaa *et al.,* 2013
Br/Cl	• constant ratio implies sea-water ratios. • high ratios may indicate organic-rich layers	Croudace *et al .,* 2006; Rothwell *et al.,* 2006; Thomson *et al.,* 2006
Sr/Ca	• presence of high-Sr aragonite which requires a shallow-water source	Croudace *et al .,* 2006; Ziegler et al., 2008

4.7 Diatoms

Diatom investigations were carried out on VC001, VC003 and VC004. Diatoms from the sediment cores were prepared using the hydrogen-peroxide method as per Battarbee *et al.* (2001). Initial diatom investigations were carried out at 20 cm intervals on all three cores and additional areas were targeted based on changes in resulting assemblages coupled with sedimentary variations. Quantities of sediment were placed in either 100 ml or 250 ml beakers and weighed (g). Samples were then digested using 30% hydrogen peroxide (H_2O_2) on a hot plate, in a fume cupboard, until organic material was oxidised. Beakers were

monitored to ensure desiccation did not take place. Beakers were removed from the heat and 2-3 drops of HCl 10% were added to remove any remaining H_2O_2 and the sides of the beaker were washed down with distilled water. After cooling, the liquid was transferred to 12 ml centrifuge tubes and centrifuged at 1200 rpm for four minutes. The supernatant was decanted off and the tubes were refilled with distilled water. This washing process was repeated four times.

4.7.1 Diatom identification and enumeration

Microscopic markers or microspheres were added to the final mixture prior to making slides. Divinylbenzene spheres (DVB) with a mean diameter of 8.1 µm were added to a known amount of sediment using a micropipette at a concentration of 100 µl of a 6.23 x 10^6 microspheres / ml suspension. A small amount of the sample mixture was diluted with deionised water and transferred onto microscope slide cover slips to prepare the diatom slides. The cover slips were dried over-night and then placed on the microscope slide with mounting medium Naphrax and heated. Completed slides were left to cool fully before enumeration was carried out. Diatom identification and enumeration was carried out using a MEIJI Techno ML2000 phase contrast light microscope with oil immersion objective at 1000x magnification. A Nikon Coolpix 4500 digital camera attached to the microscope was used to verify taxonomic features digitally and to record specimen samples. Where possible a minimum of 300 diatom frustules was counted per slide. Some core sections had a high level of diatom dissolution and breakage that prevented a target count of 300 frustules. Microspheres were also counted in the samples. Species counts were transformed into percentage abundances and taxa with relative abundance >1% in at least two samples through the core formed the working dataset. Species counts of individual diatom taxa were converted to percentage abundances of total sample. Working datasets with a relative abundance of greater than 1% of each sample were generated in all four sediment cores. Diatom frustule concentration was calculated using the method in Battarbee *et al.* (2001) as follows:

$$Frustule\ concentration = \frac{total\ microspheres\ introduced \times total\ diatoms\ counted}{microspheres\ counted}$$

Identification of diatoms was based on cell shape and detailed structure of the frustule (Figures 4.2 and 4.3). Taxonomic identification was conducted using Hendey, 1964; Hartley *et al*., 1986; Krammer and Lange-Bertalot, 1986-1991; Vos and de Wolf, 1992; Snoeijs *et al.*, 1993-1998; Witkowski, 1994; Hasle *et al.*, 1996; Hasle and Syvertsen, 1997; Pyle *et al.*, 1998; Witkowski *et al.*, 2000; Cremer *et al.*, 2007; Al-Yamani and Saburona, 2011 and following workshops with Dr Catherine Dalton and Dr. Jonathan Lewis held at Mary Immaculate College.

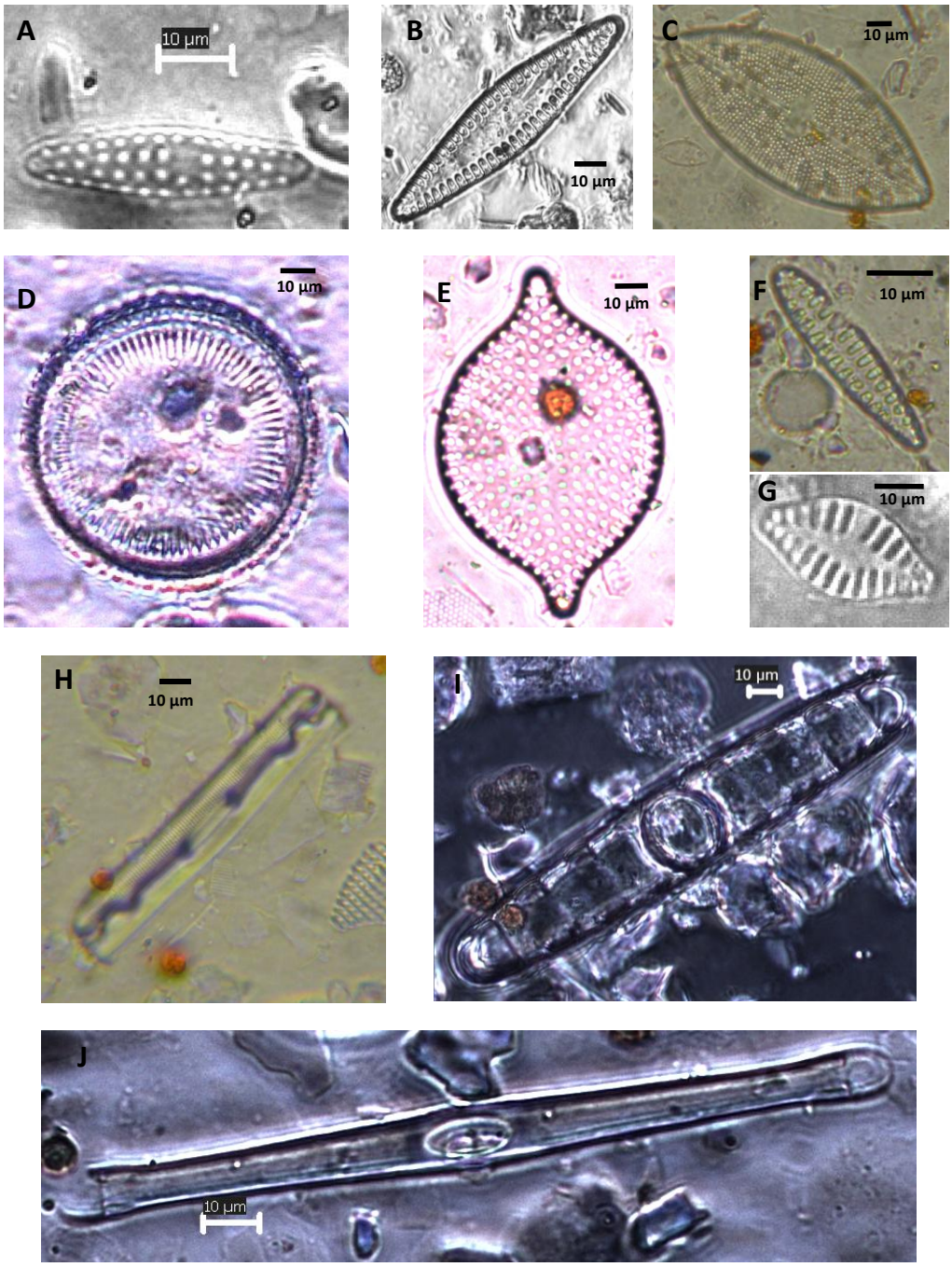

Figure 4.2: A sample of brackish diatoms: A.*Cymatosire belgica*, B. *Glyphodesmis distans*, C. *Petroneis marina* D. *Paralia sulcata*, E. *Rhaphoneis amphiceros*, F. *Opephora pacifica*, G. *Planothidium delicatulum*, H. *Grammatophora oceanica* (girdle view), I. *Grammatophora serpentine* and J. *G. oceanica*.

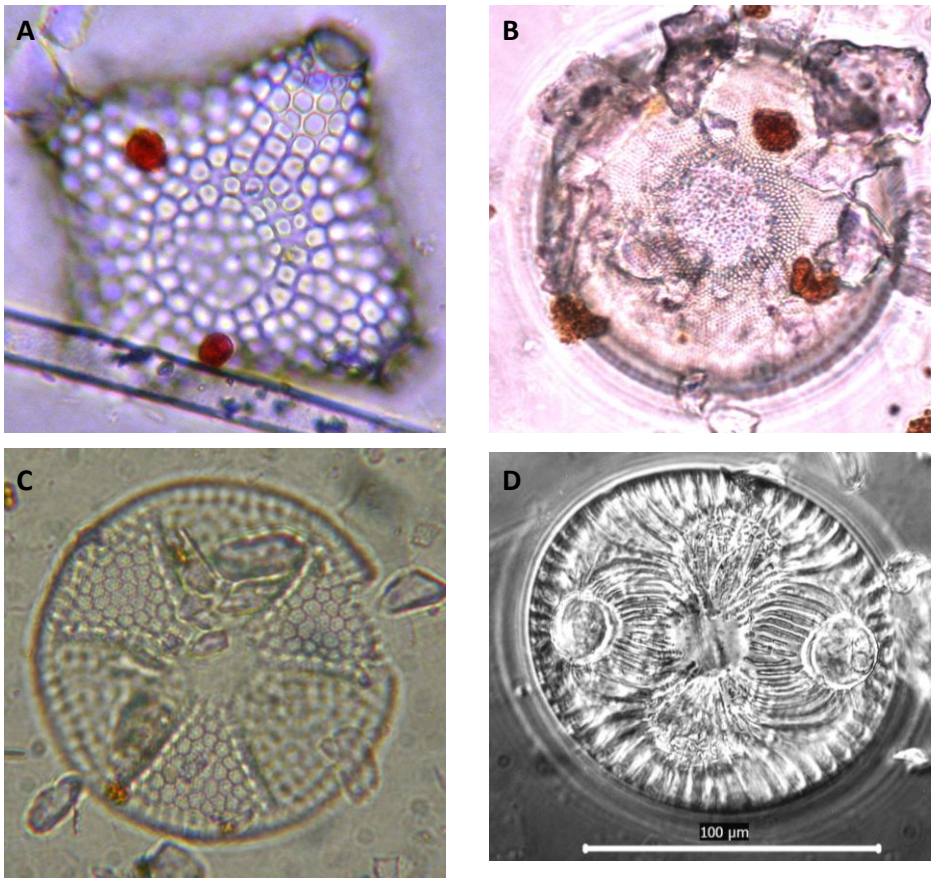

Figure 4.3: A sample of marine diatoms: A. *Triceratum archangelskianum*, B. *Hyalodiscus scotius*, C. *Actinoptychus scenarius*, and D. *Auliscus caelatus*.

4.7.2 Diatom dissolution and breakage

A diatom morphological dissolution index, the fractional index (F index) (Flower & Lokhoshway, 1993; Ryves *et al.,* 2001; Ryves *et al.,* 2006) was calculated. The F index estimates the proportion of pristine valves to all valves that can be classed and ranges from 0 to 1 where F=1 implies perfectly preserved valves and F=0 implies all valves are appreciably dissolved (Ryves *et al.,* 2001; Ryves *et al.,* 2006). The F index is calculated as follows:

$$Fi = \sum_{j}^{m} nij \Big/ \sum_{j}^{m} Nij$$

Where *nij* is the number of pristine valves of species *j* (of *m*) counted in sample *i*, compared to *Nij*, the total number of classifiable valves of species *j*.

Diatom valve breakage is linked to dissolution, as dissolved valves tend to break more easily (Ryves *et al.,* 2001). Coastal diatoms experience a higher degree of breakage than those from planktonic marine or freshwater environments due to exposure to higher energy systems. Therefore a breakage index was developed, by applying the F index to broken and intact valves (breakage degree in pristine or broken valves). Identification of valves was sometimes limited due to high breakage and the index was used here, in part, to quantify this occurrence. Where high breakage occurred, entire slides were counted to ensure counts accurately reflected the diatom assemblages.

4.8 Foraminifera

Sediment cores VC001 and VC003 were targeted for foraminiferal fossil investigation and methodology follows Armstrong and Brasier (2005). Due to the extremely low or complete lack of diatom microfossils in VC004, no foraminiferal samples were processed in this sediment core. As previously discussed, no microfossils were targeted in VC002. In both VC001 and VC003, samples were extracted at 20 cm intervals and 1 cm^3 were cut from the core and placed in a labelled plastic bag and sealed until processing occurred. Samples were placed on a weighted petri dish and dried at a low drying temperature (<40° C) in an oven overnight. Low drying temperatures decrease the chance of damage to the foraminiferal

tests. After drying, samples were weighed to obtain a dry sample weight. Samples were then washed in deionised water and wet sieved through a 63 μm sieve, placed in a petri dish and then dried again in a low temperature oven (<40° C). The dried sample was sieved through 150 μm sieve and stored in labelled glass vials; foraminiferal analysis was carried out using the >150 μm size fraction of sediment (Scott and Medioli, 1980; Kucera *et al.*, 2005).

Individual samples were poured into a random micro-splitter and divided into aliquots of ~300 foraminiferal specimens per sample. Statistically this ensured a 95% probability of not encountering an additional species comprising at least 1% of the faunal. Each sample was emptied onto a sorting tray and using a fine tipped paint brush (000) and a Leica Zoom 2000 stereo microscope (20 X objective lens) with a Volpi Intralux 5000-1 cold fiber optic light source equipped with dual moveable light guides, individual foraminifera were "picked" and placed onto a Cushman slide.

Taxonomic identification was accomplished primarily using; Murray (1991; 2006); Jones and Brady (1994); Scott *et al.* (2001); Sen Gupta (2003) and Brooks and Edwards (2006). In addition, localised knowledge (Barrett, 1998 unpublished; Wood, 2010 unpublished) of foraminifera and personal knowledge of foraminifera gained while attending the International School of Foraminifera at Collegio Internazionale at the University of Urbino, Italy were used to assist in species identification. Qualitative ecological analysis was also carried out based on Scott *et al* (2001), Murray (2006) and Horton and Edwards (2006). Ecological evidence was collected and put in a table and placed in Appendix G.

4.9 Data Analysis

In radiocarbon dating, an age depth model produces estimates of accumulation rates over time (Blaauw, 2010). The age depth models were run using the R console version 3.0.1 with the Bacon software (Blaauw and Christen, 2011); an age-depth model that uses Bayesian statistics to reconstruct sediment accumulation histories for deposits using known radiocarbon dates. This model incorporates a student-t distribution with wide tails so as to minimise the effect of outlying dates.

The geochemical data was transformed using log-ratios in order to avoid undesirable asymmetrical properties and because log-ratios of count data tends to correlate in a straightforward linear function. In addition, log-ratios allow the application of multivariate statistics with higher accuracy when correlating multiple sediment cores (Aitchison and Egozcue, 2005; Weltje and Tjallingii, 2008; Bloemsma, 2010; McKillup and Dyar, 2010; Hennekam and De Lange, 2012). Log ratio transformation was carried out using Microsoft Excel and analysed graphically using C2. Seven elemental log ratios which are known to be indicators of relevant parameters were chosen for proxy use. These are outlined in Table 5.4 and are as follows: Ca/Ti, K/Ti, Si/Ti, Zr/Ti, Fe/Mn, Br/Cl and Sr/Ca. A principle component analysis (PCA) was employed to determine if there were patterns in the data and the relevance of the individual geochemical ratios. PCA transforms the original variables into a smaller set of linear combinations that account for most of the variance in the original data (Dillon and Goldstein, 1984) in order to explain as much of the total variation in the data as possible with as few components as possible. The total sum of squares of regressions is the eigenvalue and is expressed as percentage of total variance in species data. The eigenvalue is equal to the maximized dispersion of the species scores on the ordination axis and is a measure of importance of the ordination axis (ter Braak, 1987). The first PCA axis has the highest eigenvalue and the second axis has the second highest eigenvalue and so on. The PCA was run using C2 software version 1.5 (Juggins, 1991-2007).

The parametric method, linear correlation, was used to statistically analyse the relationship of physical and geochemical proxies between sediment cores for the purpose of core comparison. Correlation is an exploratory technique used to examine whether the values of two variables are significantly related or change together in a consistent way and expressed as the Pearson correlation coefficient (r) (McKillup and Dyar, 2010). All correlations were carried out in Excel.

Microfossil data analysis involving stratigraphic plots, Hill's N2 diversity index, mean and median numbers, pennate:centric ratios (diatom), Benthic:Pelagic:Tychoplanktonic ratios (B:P:T, diatoms) and agglutinated:calcareous ratios (foraminifera) were generated using C2 software version 1.5. The diatom and foraminiferal species dataset was explored using cluster and ordination techniques. Zonation sequences were generated with constrained

cluster analysis on the working datasets using PAST 3.06 (Hammer *et al.*, 2001). Detrended Correspondence Analysis (DCA) is employed to ascertain if species data is suited to a linear or unimodal model and provides an estimate of the gradient length in relation to the underlying environmental gradients. The DCA is reported in standard deviation units (SD) for each axis model (ter Braak and Prentice, 1988) and if the gradient length is short (<2 SD units) taxa are generally behaving monotonically along the environmental gradient and therefore linear methods are appropriate (Birks, 1995), if the gradient is longer (>2 SD units) unimodal based methods are appropriate. DCA yielded a unimodal response for both diatoms and foraminifera. This gave cause for using Correspondence Analysis (CA), a technique that constructs the theoretical variable that best explains the species data using weighted averaging (ter Braak, 1987). Both ordination techniques were run through PAST 3.06.

Because diatoms are reliable indicators of salinity conditions (Balascio and Bradley, 2012), the diatom ratios (pennate:centric and B:P:T) were first examined to qualitatively assess the change in marine influence throughout the core. As well, ecological data was compiled for all species, including habitat preference, general environmental preference and life form and these full records are in Appendix D. Salinity reconstruction was carried out quantitatively using a diatom-based transfer function based on the Molton/Define training set from the Molten and Define Project (http://craticula.ncl.ac.uk/Molten/jsp/; Andrén *et al*., 2007; Lewis *et al*., 2013). The reconstruction was carried out by Dr Jonathan Lewis (Loughborough University) for sediment cores VC001 and VC003. Fossil diatom taxa representation in the modern training set for VC001 was >50% and was used with confidence, however, representation was poor for the taxa found in VC003 and results are unreliable and not presented. Prior to application of the transfer function (for salinity reconstruction) to the fossil diatom datasets, weighted average-partial least squares (WA-PLS) were tested. This model was evaluated using r2boot and RMSEP scores, following internal validation (via bootstrapping x1000 cycles) using the modern training set. Final diatom inferred (DI) salinity reconstructions are based on a component-2 model as it performed best under internal validation and exhibited a similarly high predictive power to other published salinity-based transfer functions (Lewis *et al*., 2013).

CHAPTER 5: Results

Introduction

In this chapter, results from the sediment core analysis are presented. Originally it was anticipated that the results would be ordered based on physical, chemical and biological measurements with horizontal comparisons across the four cores. When the results for the radiocarbon dating were finalised, however, it was apparent that cross-core comparison was complex. As a result, the chapter first outlines sediment core stratigraphies and chronologies for all four vibrocores. Subsequent to this, the multiple proxy results are presented for sediment core VC001. This is followed by the results for sediment cores VC002, VC003 and VC004, which are presented in tandem.

5.1 Sediment core extraction

The water depths' of the vibrocore extraction points ranges from 11.2 m for VC001 in the inner transitional waters to 13.5 m for VC004 in Inner Galway Bay. Table 5.1 gives water, core tube length and actual sediment depths of the vibrocores and Figure 5.1 shows a schematic of the water and sediment depths for each vibrocore extracted. The sediment shelves by 1.2 m between estuary cores VC001 (11.2 m) and VC002 (12.4 m) while water depths are similar at c. 13 m for the two inner bay cores (VC003, 13.4 m; VC004, 13.5 m). Core sediment depths ranged from 478 cm (VC004) to 556 cm (VC003).

Table 5.1: The depth of water at the time of sediment cores extraction for vibrocores VC001, VC002, VC003 and VC004 along with the depth of the core tube and actual sediment length.

Sediment Core	Water Depth (m)	Core Tube length (cm)	Sediment Length (cm)
VC001	11.2	550	535
VC002	12.4	580	554
VC003	13.4	600	556
VC004	13.5	500	478

The sediment core tube length varied from the actual amount of sediment acquired in each vibrocore. Tube lengths ranged from 500 cm (VC004) to 600 cm (VC003) with actual sediment lengths varying from 478 cm to 554 cm. The sediment found in the four vibrocores ranges from gravel to silty clay with areas of fine shell hash, dense shell hash and shell material.

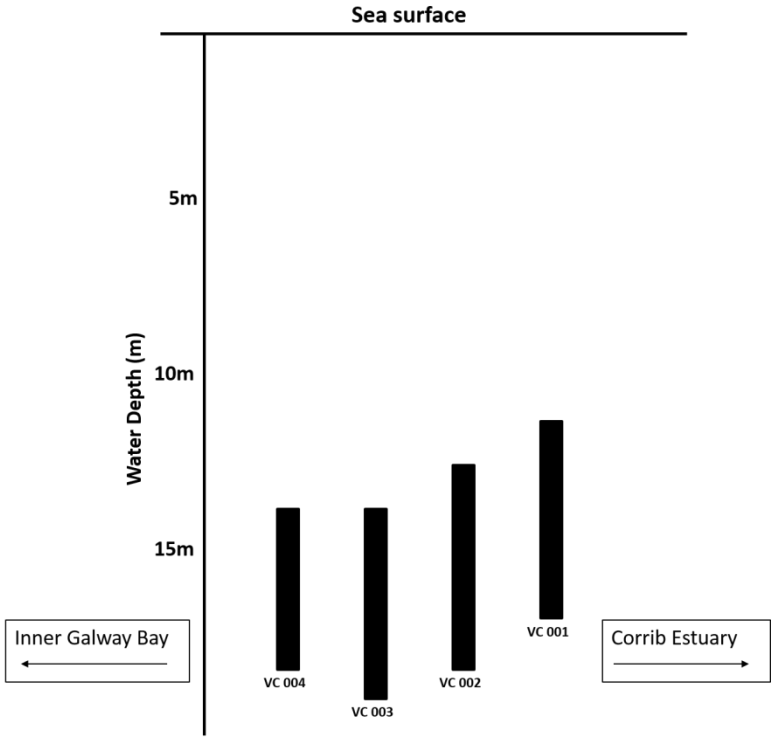

Figure 5.1: Schematic of vibrocores VC001, VC002, VC003 and VC004 and the sediment and water depth at which they were extracted (axis not to scale). VC001 is the innermost core located in the Corrib Estuary and VC004 is the outermost, located in Inner Galway Bay.

5.2 Core Lithology

The colour, texture and composition of all four sediment cores were recorded to gain a full lithological profile. A summary description of physical characteristics is presented in Table 5.2. Additionally, Laser Diffraction Grain Size Analysis (LDGSA) was conducted on cores VC001 and VC003. The full results of the LDGSA for cores VC001 and VC003 with their corresponding textural classification can be found in Appendix A. All sedimentological results (lithology and grain size analysis) were combined to produce a complete sediment log for inner Galway Bay. Figure 5.2 displays the sedimentary logs for VC001, VC002, VC003 and VC004.

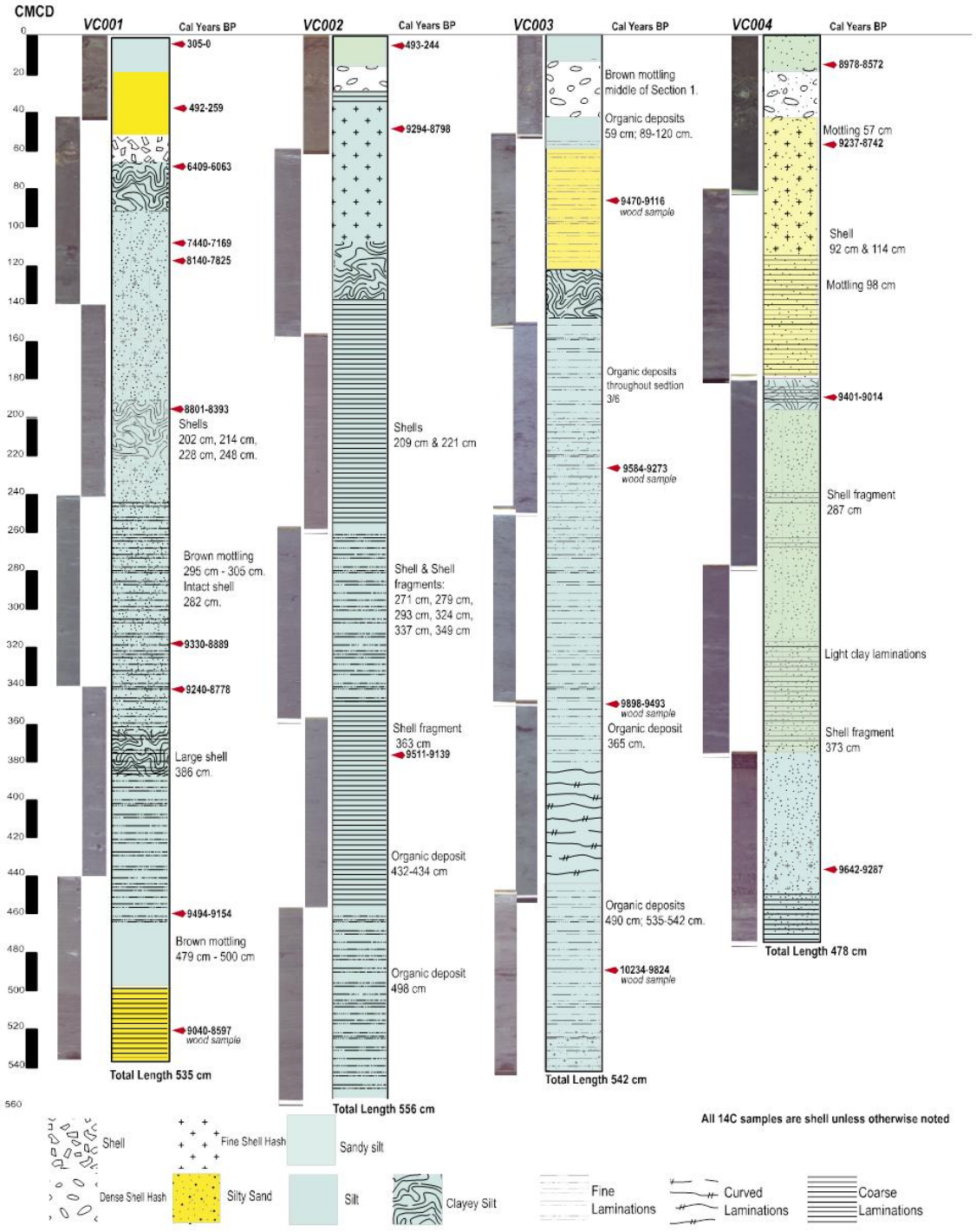

Figure 5.2: Sediment logs for VC001, VC002, VC003 and VC004

Variation between cores is evident with vibrocore VC001 having a generally sandier profile and cores VC002, VC003 and VC004 having a higher silt content with more clay present. Variability in sediment consistency is evident at the bottom of the cores while at the top of the sediment cores, a clear change can be seen in both in cores VC001, VC002 and VC003.

In sediment core VC001, the lower core from the base (535 cm) to 493 cm is classed as a silty-sand with heavy laminations and has a Munsell colour class of 5/2 Gray. The grain size analysis carried out on sediment core VC001 confirms that the lowest 45 cm is a silty sand material that changes to sandy silt at 490 cm (see Appendix A). The elevated levels of sandy material in this section and lower percentages of clayey material marks a difference in this section of the sediment core from material deposited above this area. LGDSA suggests the core continues to exhibit sandy silt material up-core to 50 cm with intermittent points of clayey silt at 374 cm, 210 cm and 58 cm. The uppermost 50 cm of VC001 is silty sand and sandy silt with the largest grain size occurring here at 32 cm. A distinct disturbance layer is prominent in VC001, located in the upper sediment core from 70 to 55 cm, comprised of intact and broken marine *Spisula* cf *subtruncata* shells. This layer is overlain by markedly different sediment made up of dense shell hash in sandy substrate with a Munsell colour class of 3/1 Gray.

Sediment core VC002 displays a disturbance layer (30-18 cm) overlain with a sandier sediment (18-0 cm) in the upper core similar to that found in VC001 but less pronounced; in sediment core VC002 this presents itself as several whole shells mixed with dense shell hash and sediment. Shell condition was too poor for identification. This disturbance layer over lays a relatively uniform sediment profile in the lower core with the exception of the base of the core (554-450 cm) where a band of sandy-silt material, with shell hash and fine white laminations, is present.

Table 5.2: Results of the lithological analysis of all sediment cores.

Depth(cm)	Lithology
VC001	
0-45	Dense shell hash in sandy substrate with a Munsell colour class of 3/1 Gray.
45-55	Clayey silt layer with no shell hash; a Munsell colour class 4/1 Gray; sediment compaction appears high
55-68	Disturbance layer comprised predominately of *Spisula* cf *subtruncata*.
68-116	Silty material with fine sand. Munsell colour class is 4/1 Gray; sediment compaction appears high, no shell or deposits appear.
116-128	Sandy silt sediment appears disturbed with white, broken laminations
128-210	Uniform silty material with fine laminations and fine shell hash; Munsell colour class is 4/1 Gray.
210-225	Clay band/heavy clay lamination
225-370	Uniform silty material with fine to medium sand. There are fine laminations throughout with brown organic mottling from 295-305 cm. Fine shell hash is observed from 225 to 240 cm; Munsell colour class is 4/1 Gray.
370-387	Clay band/heavy lamination
387-454	Sandy silt with fine sand throughout and fine laminations. Brown organic material 295-305 cm Munsell colour class 4/1 Gray.
454-500	Sandy-silt, no laminationst. Brown mottling throughout 497-500 cm. Munsell colour class is 5/2 Gray.
500-535	Sandy material with some silt content; Munsell colour class of 5/2 Gray. Heavy laminations are visible.
VC002	
0-18	Silty-sand with dense shell hash and a Munsell colour classification 7.5YR 3/3.
18-30	Disturbance layer comprised of several whole shells mixed with dense shell hash
30-132	From 30-34 cm is a small layer of course dark laminations and a Munsell colour classification 7.5Y/2. From 34 – 132 cm fine white laminations are present and the sediment is silty- clay. Scattered shell hash is observed from 58 to 105 cm. The Munsell colour class is 4/5GY from 55 to 132 and changes slightly to 4/7.5Y from 34 to 55 cm.
132-452	A silty sediment with some clay content and heavy dark laminations is visible from 320 to 452 cm and again from 132 to 268 cm. Between 268 to 320 cm the laminations become fine and light in colour. The Munsell colour classification for this section is 5/5Y from 352 to 452 cm and 4/5GY from 132 to 352 cm. Dark, organic deposits are present at 432 cm and shell fragments are found at 363 cm, 349 cm, 337 cm, 324 cm, 293 cm, 279 cm, 271 cm, 221 cm and 209 cm.
453-554	This section is comprised of silt with fine white laminations throughout the section. Munsell colour class is 5/5Y. Dark, black organic deposits are present at 498 cm and shell material is found at 481 and 520 cm.
VC003	
0-20	Sandy-Gravel material with 5/2 Gray Munsell colour class; brown mottling appears from 25 to 35 cm.
30-40	Possible disturbance layer; broken shells and shell hash present and pronounced laminations.
40-80	Silty material with small shells and shell hash; Munsell colour class is 5/2 Gray. Organic deposit at 59 cm.
80-130	Silty-sand material with a Munsell colour class 5/2 Gray and laminations are visible throughout. Organic deposits visible from 120-180 and woody deposit recorded at 90 cm.
130-150	Clayey silt band with pronounced, wavy laminations; Munsell colour class 5/2 Gray.
150-220	Silt material with little to no sand present; laminations pronounced with darker colour than surrounding sediment; Munsell colour class 5/2 Gray
220-270	Sandy silt –re-appearance of sand with a woody deposit at 253 cm and the laminations disappear; Munsell colour class 5/2 Gray
270-520	Silt material with little or no sand; laminations through most of this section and from 385-444 cm they become curved; organic deposits visible at 365 cm and 490 cm and woody material present at 374 cm and 508 cm. Munsell colour class 5/2 Gray.
520-542	Sandy silt section with organic deposits throughout and Munsell colour class 5/2 gray.
VC004	
0-53	Sandy Gravel with shell hash and broken shell material present throughout.
53-181	Sandy silt with a Munsell colour classification 4/7.5 Y. Coarse laminations appear from 128 to 181 cm and from 53 to 128 cm fine shell hash is present with mottling of organic material at 57 and 98 cm.
181-193	A band of silty-clay
193-478	Sandy-silt material throughout. From 449 to 478 coarse dark laminations are present and from 416 to 449 cm is fine shell hash. The Munsell colour class is 4/7.5 Y from 478 to 429 cm and becomes slightly lighter for 45 cm changing to 4/10 Gray from 429 to 384 cm. From 379 to 317 cm there are coarse laminations composed of a clayey material and the Munsell colour class returns to 4/7.5 Y. Shell fragments found at 373 and 287 cm.

Similarly, sediment core VC003 exhibits a sandier sediment core base (510-490 cm) layer and has a shell laden section in the upper core (50-30 cm) but in VC003 there is less distinction in the disturbance layer and higher levels of shell hash than those found in corresponding areas of VC001 and VC002. LDGSA confirms that sediment core VC003 has a silty profile with three bands of sandy silt; at the base of the core in the lower 25 cm of sediment, 265-205 cm and 120-90 cm. One band of clayey silt exists at 170-140 cm. The upper sediment core displays a different profile with gravel sediment occurring 40-0 cm.

Sediment core VC004, the westerly-most core, is largely uniform and lacks the base layer and disturbance layer seen in sediment cores VC001, VC002 and VC003. As well, VC004 is sandier through most of the core (478-55 cm) with a clayey band (195-180 cm) and shell hash intermittently throughout the sediment core.

5.3 Chronology

The sediment chronology established is based on the results of AMS ^{14}Carbon results of a range of sample materials (Table 5.3). In total, 23 ^{14}C AMS radiocarbon dates were obtained: ten from VC001, three from VC002, six from VC003 and four from VC004. Radiocarbon dating from the Corrib Estuary (sediment core VC001) revealed a relatively complete Holocene profile with a clear sediment change point evident in the lowest section of the core (525 cm) and a hiatus in the upper core (68-50 cm). In VC002 the sediment represents early Holocene material throughout most of the core with the exception of the upper core where recent material has been deposited. Sediment core VC003 and VC004 are comprised of early Holocene sediment.

Ten samples from core VC001 ranged in date from 8662±34 BP (9494-9154 cal BP) to 535±22 BP (305-0 cal BP). The shell dates obtained are in chronological order with the exception of an overlap between 344 cm and 322 cm with dates of 9240-8778 cal BP and 9330-8889 cal BP respectively. The fibrous wood sample from the bottom of the core at 525 cm gives a date of 9040-8597 cal BP. The shell date above this at 464 cm is 9494-9154 cal BP. A major change in sediment accumulation is evident within the top 2 m of the sediment core. Shell samples from 117 cm (8140-7825 cal BP), 111 cm (7440-7176 cal BP) and 66 cm (6409-6063 cal BP) appear to represent c. 1,000 years of material between samples. A date of 492-259 cal BP was obtained for a shell fossil at 37 cm suggesting a hiatus in sediment deposition. The most recent date of 305-0 cal BP was obtained at 5 cm sediment depth. Three dates were obtained from sediment core VC002 ranging from 8670±52 (9139-9511 cal BP) at 361 cm to 8425±48 (8798-9294 cal BP) at 56 cm and 692±27 (244-493 cal BP) in the top 9 cm of the core. All dates obtained were from shell material and occur in chronological order. Sediment core VC002 points to a hiatus of a larger time expanse of c. 8500 years.

Table 5.3: AMS ^{14}C dating for vibrocores including laboratory codes, the position of the sample in the core by section and depth, uncalibrated ages, the marine calibration, material and AMS $\delta^{13}C$.

Laboratory Code	Core Placement by section	Core Depth (cm)	^{14}C Age BP	Calibrated Age (cal BP)	Sampling Material	AMS $\delta^{13}C$
VC001						
UBA15741	1/6 5-7	5	535±22	0-305	Shell	-0.4
UBA18091	1/6 37-38	37	706±25	259-492	Shell	-0.9
UBA18096	2/6 26-27	68	5808±37	6063-6409	Shell	0.3
UBA18093	2/6 71-72	111	6775±29	7176-7440	Shell	-3.8
UBA15742	2/6 75-77	118	7485±32	7825-8140	Shell	2.3
UBA15743	3/6 58-59	197	8083±33	8393-8801	Shell	0.5
UBA15744	4/6 83-85	322	8452±44	8889-9330	Shell	2.8
UBA15745	5/6 3-5	344	8392±33	8778-9240	Shell	-2.9
UBA15746	6/6 26-28	464	8662±34	9154-9494	Shell	-6.0
UBA18094	6/6 93	525	8279±42	8597-9040	Wood	*
VC002						
UBA31051	1/6 9	9	692±27	244-493	Shell	*
UBA31052	1/6 56	56	8425±48	8798-9294	Shell	*
UBA31053	5/6 62	361	8670±52	9139-9511	Shell	*
VC003						
UBA15622	2/6 40-41	89	8630±34	9116-9470	Wood	-29.3
UBA15623	3/6 92-93	252	8761±35	9273-9584	Wood	-30.5
UBA15624	5/6 12-13	373	8966±36	9493-9898	Wood	-25.6
UBA15625	6/6 46-47	507	9236±38	9824-10235	Wood	-26.4
UBA15747	4 /6	353	11699±41	13032-13372	Bulk	-26.5
UBA15748	5 /6	457	11607±49	12899-13295	Bulk	-24.7
VC004						
UBA18088	1/5 16-17	16	8218±34	8572-8978	Shell	-1.1
UBA18089	1/5 55-57	55	8377±42	8742-9237	Shell	-2.7
UBA18090	3/5 11-12	192	8547±41	9014-9401	Shell	-3.0
UBA18092	5/5 60-61	450	8783±45	9287-9642	Shell	1.4

***CHRONO stopped reporting $\delta^{13}C$ in 2013**

A relatively short chronological period is suggested for cores VC003 and VC004. In core VC003 dates range from 9236±38 BP (10235-9824 cal BP) to 8630±34 BP (9470-9116 cal BP) based on four samples of woody material extracted across the 6 m core. Two additional dates obtained from bulk sediment samples suggest dates in the region of c. 11600 BP (113295-12899 cal BP). The dating results from four samples of shell material from VC004 reveal a short chronological timeframe with dates ranging from 8783±45 BP (9642-9287 cal BP) to 8218±34 BP (8978-8572 cal BP) for core sample depths between 451 cm and 16 cm. The dates are in chronological order.

As VC001 was the only sediment core to encompass a comparatively more complete Holocene profile, age depth models were run using R and the Bacon package provided by Blaauw and Christen (2011) and are presented in Figure 5.3. The calibrated ages generated from radiocarbon dating were used to establish a time frame to help interpret change through time (Lowe and Walker, 1997; Blaauw and Christen, 2011). Modelling sediment accumulation rates (Figure 5.4) creates a coherent evolution of deposition for the total core depth and can help identify areas of discontinuous deposition. For VC001, the model clearly displays the hiatus between 68-50 cm in the upper core, giving a frame of reference for changes in sediment constituents.

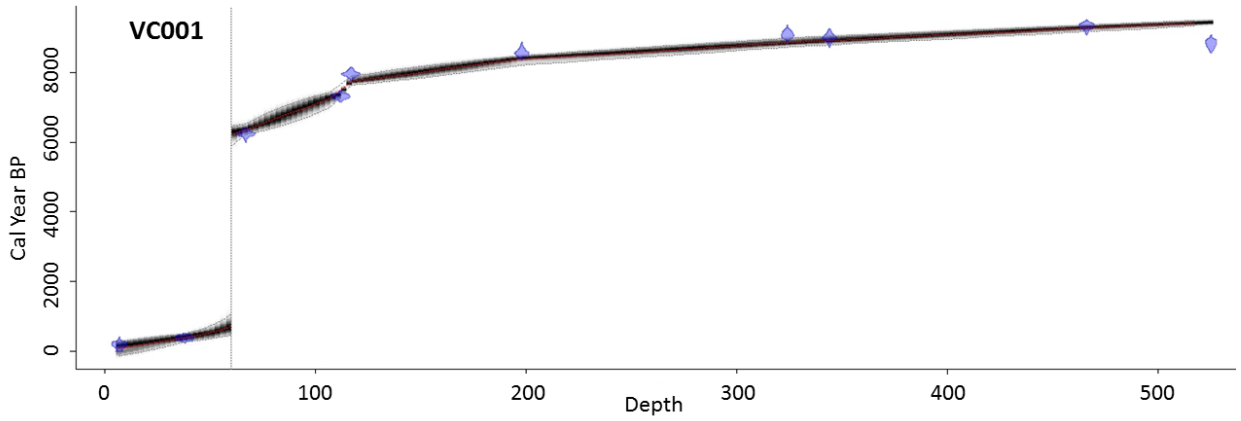

Figure 5.3: Age-depth profile of sediment core VC001

The age depth profile of sediment core VC001 shows a slow sediment deposition rate below 68 cm where approximately 457 cm of sediment was deposited over 3000 years. The hiatus occurs at c. 6000 cal years BP and is clearly marked in the core lithology (Table 5.2) with a disturbance layer consisting mostly of *Spisula cf subtruncata*. The recent material at the top of the core encompasses c. 1,000 years in 50 cm. The sedimentation rates varied considerably in core VC001 with the highest rates representing c. 30 yrs/cm and the lowest c. 4 yrs/cm. Before the hiatus, sediment accumulation rates are slow and steady while after the hiatus greatly accelerated accumulation rate occurs undoubtedly signalling a major change in the environment.

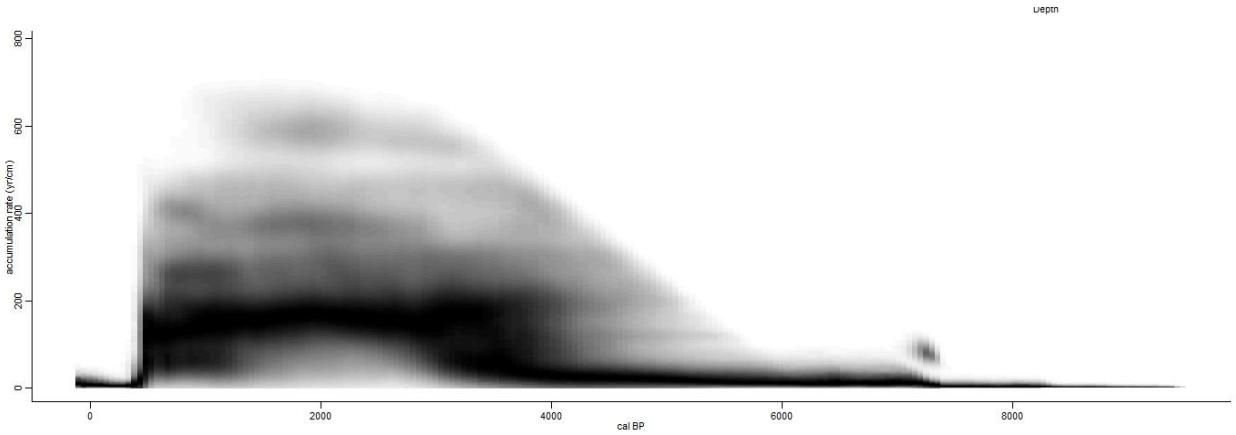

Figure 5.4: Sediment accumulation rates of sediment core VC001

Sediment core VC002, VC003 and VC004 had largely linear age depth profile with VC002 exhibiting a c. 8000 year hiatus at the top of the core. The age depth profiles and sediment accumulation rate graphs for these sediment cores can be found in Appendix B. As expected the truncated age profiles generated for sediment cores did not reveal extensive information. Sediment cores VC002, VC003 and VC004 have similar sediment accumulation rates with the highest accumulation rate of 6 yr/cm and the lowest less than 1 yr/cm. The VC004 results reveal a slower accumulation rate with the highest level of sediment accumulation at 3 yr/cm and the lowest falling below 0.5 yr/cm.

Figure 5.5 shows a schematic representation of the approximate chronological relationship between the four sediment cores. Core VC001 spans the Holocene and ranges from 9000 to 200 years cal BP while cores VC002, VC003 and VC004 appear to encompass just 1,500 years from 10000 to 8500 years cal BP. While VC002 has a recent sediment deposit (244-493 cal BP at 9 cm) overlaying early Holocene sediment, this core has a less complete Holocene profile relative to VC001 and only the upper 30 cm is comparable. The chronologies established therefore suggest that direct cross core stratigraphic comparisons are redundant as the age ranges of VC002, VC003 and VC004 coincide with only the lower 200 cm of sediment core VC001. The upper 20 cm of VC001, 18 cm of VC002 and 40 cm of VC003 have a composition of less cohesive gravelly material. Dates for these sediments from VC001 and VC002 confirm relatively recently deposited material. The top section of VC003 was targeted for radiocarbon dating but no suitable material was found to analyze. As well, radiocarbon dating suggest that both sediment cores VC002 and VC003 exhibit a c. 8500 year hiatus. As a result, physico-chemical and biological proxies will be described in full first for the VC001 Holocene record in the next section followed by a cross core comparison of the contemporaneous early Holocene sediments.

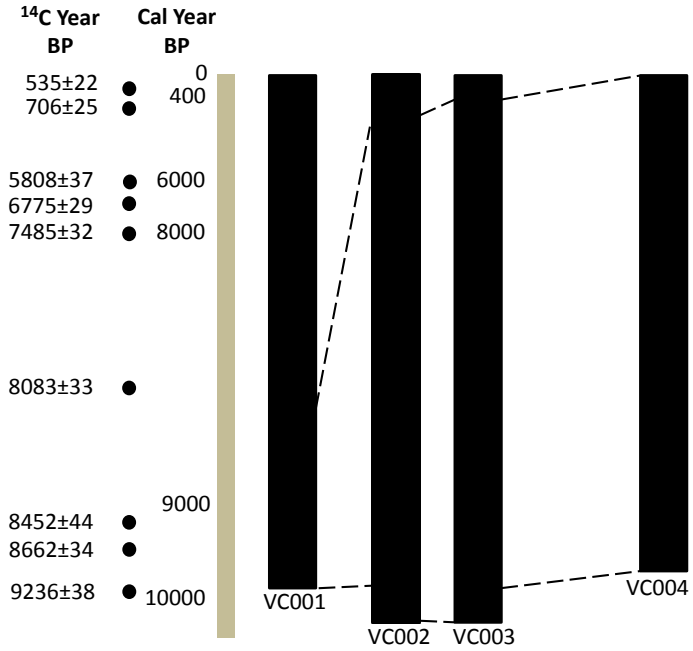

Figure 5.5: Schematic illustration demonstrating the estimated Galway Bay sediment core chronology. Sediment cores VC002, VC003 and VC004 approximate the first 1500 years of VC001. Dates listed are Cal Year BP (primary axis) and relevant uncalibrated radiocarbon age points (secondary axis).

5.4 Sediment core VC001

Physical, chemical and biological proxies were investigated for sediment core VC001. The core was divided into six sections with a total length of 535 cm. The use of a Multi Scanner Core Logger (MSCL), X-Ray Fluorescence scanner and standard laboratory processing techniques for diatoms and foraminiferal fossils were employed to obtain a range of data for paleoenvironmental reconstruction.

5.4.1 Physical properties

The MSCL produced data on physical components of sediment core VC001 including, p-wave velocity, gamma density and magnetic susceptibility (Figure 5.6). Measurements of % Organic Carbon (OC) content are also presented here with the mean grain size. The shell layer between 68-50 cm (comprised predominately of *Spisula* cf *subtruncata*) confounds measurements of magnetic susceptibility, gamma density, p-wave velocity and is clearly evident in the sediment profile.

The p-wave velocity is an acoustic property used to estimate grain size as it parallels changes in coarse fraction and is proportional to grain size and inversely proportional to porosity. The p-wave velocity ranges for VC001 are from 1030.67 m/s to 1828.06 m/s with the areas of highest fluctuation in the lower 10 cm and the upper 150 cm of the core. The bottom of the core sees a drop in the p-wave velocity, reaching its lowest reading in the oldest sediment at 9000 cal years BP (528 cm) but remains static upcore with a mean value of 1549.3 m/s until c. 8200 cal year BP (120 cm) when there is a sharp increase to 1721.88 m/s for a brief 25 cm interlude. The shell disturbance layer sees extreme fluctuation in the p-wave reading and this is determined to mean these readings are unreliable as porous gaps in shell layers can affect p-wave readings. The recent sediment at the top of VC001 is relatively stable with two areas of fluctuation which may be the result of gravel in the sediment in this area (Figure 5.2).

Gamma density indicates pore water content, areas of saturation and sediment compaction. The gamma density ranges from 1.46 g/cm^3 to 2.09 g/cm^3 with areas of fluctuation in similar core positions as the p-wave velocity; in the lower 10 cm and upper 150 cm of the core. There is a general decreasing trend upcore in density indicating that sediment compaction is

generally higher in the lower core with definite changes occurring from c. 8500 to 6500 cal years BP (150-70 cm). Gamma density sees a peak at 124 cm (c. 8500-8000 cal years BP).

Magnetic susceptibility can lead to inferences regarding sediment provenance, marine transgression and global sediment correlations. Sediment core VC001 has magnetic susceptibility levels ranging from 1.01 to 5.48 SI with a decreasing trend up core from 535 cm to 25 cm where there is an abrupt increase measured in recent sediment (400 cal years BP), possibly reflecting the significant amounts of sand in the sediment profile. Organic carbon levels affect biogeochemical processes, nutrient cycling, biological availability, chemical transport and interactions. The % Organic Carbon content ranges from 0.54 to 3.79 with the highest levels occurring in the recent sediment at the top of VC001. There is a general increasing organic carbon trend up the sediment core with areas of low measurements occurring in the oldest sediment c. 9000 cal years BP and again c. 8500-8000 cal years BP.

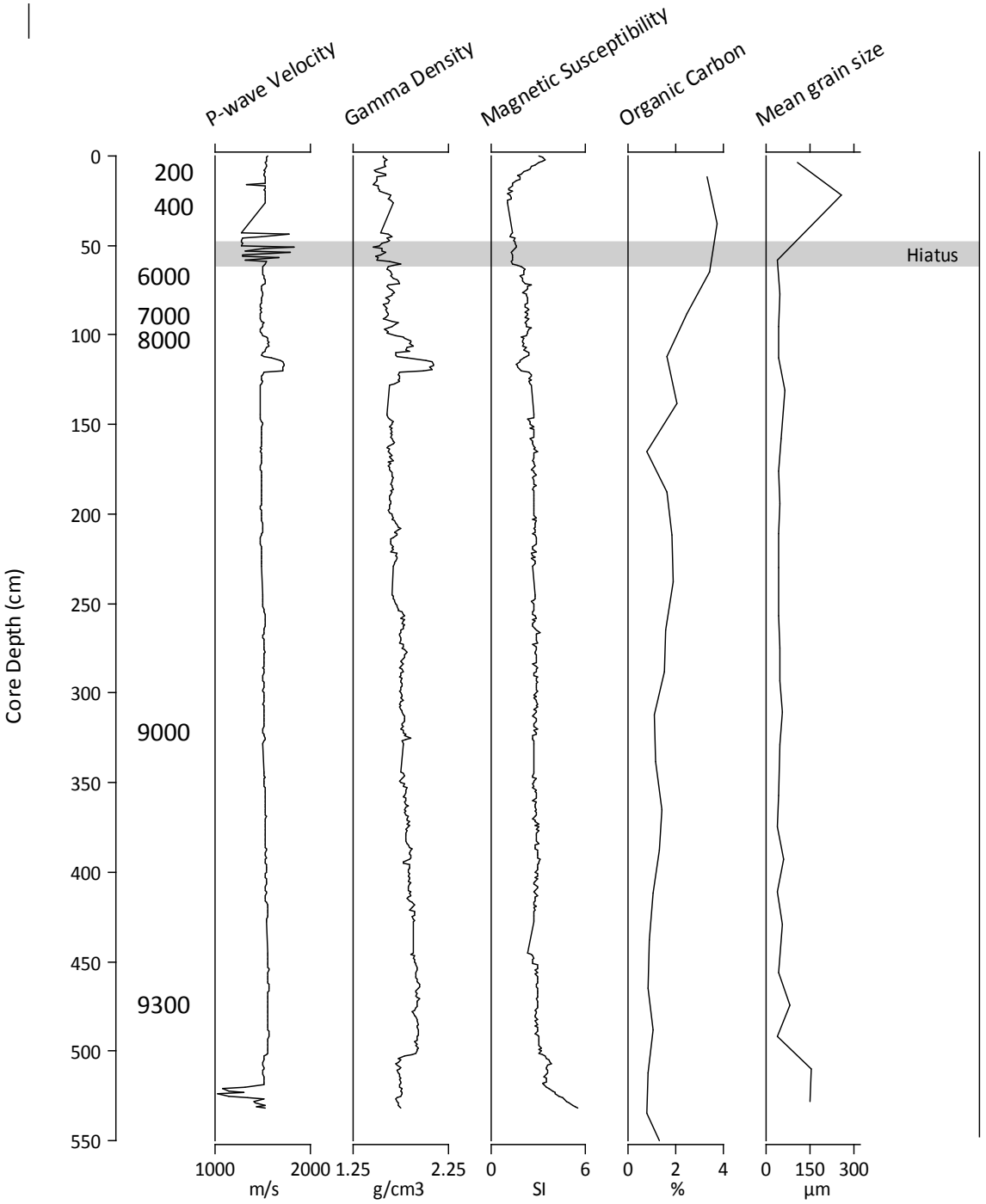

Figure 5.6: Results of the physical analysis carried out using the Multi Scanner Core Logger (MSCL) for vibrocore VC001, % Organic Carbon and mean grain size. The hiatus is highlighted in grey.

5.4.2 Geochemical properties

Geochemical analysis was carried out using XRF and produced a profile of 32 elements for sediment core VC001. Single elemental profiles are included in Appendix C while log-ratios for Sr/Ca, Ca/Ti, Si/Ti, K/Ti, Zr/Ti, Br/Cl, Fe/Mn are illustrated in Figure 5.7. Here four of the elemental ratios use Ti for the normalisation and other known ratios, which are indicative of biogenic and/or minerogenic inputs outlined in the methodology (see Table 5.4). The mean square error (MSE) is higher in the upper sediments reflecting poorer detection quality for the elements in this part of the core.

The Sr/Ca ratio, indicative of calcium carbonate mineralogy, is highest in the lower core from the base of the core c. 9000 cal years BP (508 cm), reaching its highest level with a ratio of 0.97. Ratios stabilise upcore with smaller peaks at 483, 374, 264, 159, 106 and 25 cm. The lowest points are experienced c. 6000 cal years BP (0.04) with an additional dip c. 8000 cal years BP (0.07). Conversely, the Ca/Ti ratio, which is indicative of detrital input, is lowest from the base of the core c. 9000 cal years BP (508 cm) and stabilises up core displaying peaks from 146-116 cm and highest values c. 6000 cal years BP (70-60 cm). The Si/Ti ratio often inferred as a proxy for biogenic silica, reveals five points with low values at 484, 369, 354, 264 and 107 cm and a peak in levels occurring c. 8000 cal years BP. The K/Ti ratio, utilised sometimes as a proxy for sediment provenance and climate variation, remains relatively stable upcore ranging from 0.63 to 1.1 until it reaches a peak area c. 8500-8000 cal years BP (from 135 to 120 cm) where the highest level of 2.07 occurs. The upper 120 cm ranges from 0.6 to 1.6, fluctuating throughout. The Zr/Ti indicative of changes in grain size fraction and sediment provenance, exhibits a slight decreasing trend in the lower core c. 9000 cal years BP and ranging from 3.7 to 0.7. From 483 cm upcore to 160 cm Zr/Ti does not exhibit much change with the exception of low points at 374, 349, 264 and 212 cm. From 8500 to 7000 cal years BP ratios are low and from 120-0 cm (mid-Holocene to recent sediment deposit) there is a distinct further downward trend with one high value spike at 65 cm where the highest ratio occurs (5.37). The Br/Cl ratio, often representative of sea water ratios, shows a similar pattern to Zr/Ti with a decrease in values in the lowest part of the core. However from 480 to 140 cm there is a steady increase in the Br/Cl ratio and a sudden dip from c. 8500 to 8000 cal years BP and again a steady increase up the top of the core into

the recent sediment. The Fe/Mn ratio can suggest variation in the sediment-water interface, remains relatively stable throughout the core. There is little change in Fe/Mn levels throughout the core. Measurements range from 51.63 to 270.04 and a mean of 103.23.

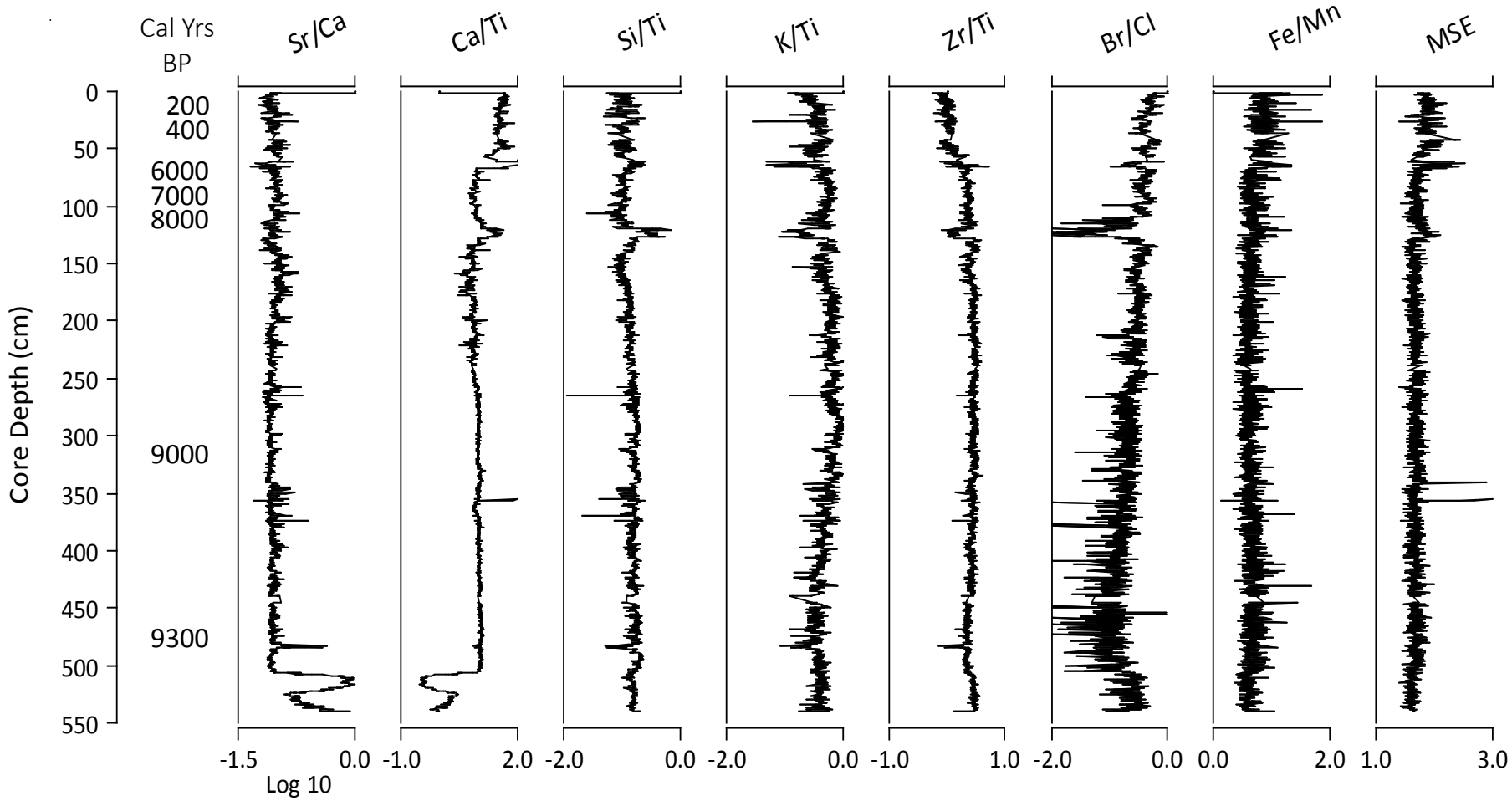

Figure 5.7: Seven elemental ratios for sediment core VC001: Sr/Ca, Ca/Ti, Si/Ti, K/Ti, Zr/Ti, Br/Cl, Fe/Mn. MSE is the mean square error and reflects the quality of fit for the elements.

A principle component analysis (PCA) was employed to determine if there were patterns in the data and the relevance of the individual geochemical ratios (Figure 5.8). The PCA loading was highest for Ca/Ti on axis 1, with an axis 1 eigenvalue of 0.4698, which gives an indication of terrigenous sediment deposition. Sr/Cl had the second highest PCA loading in axis 1 and can indicate shallow water. The axis 2 eigenvalue is 0.2743 and Br/Cl had the highest PCA loading here. Br/Cl is a proxy for marine organic sediments. Axis 1 represents the proxies with the highest influence on the sample and as such, these results indicate Ca/Ti and Sr/Ca is the driving geochemical parameters in VC001.

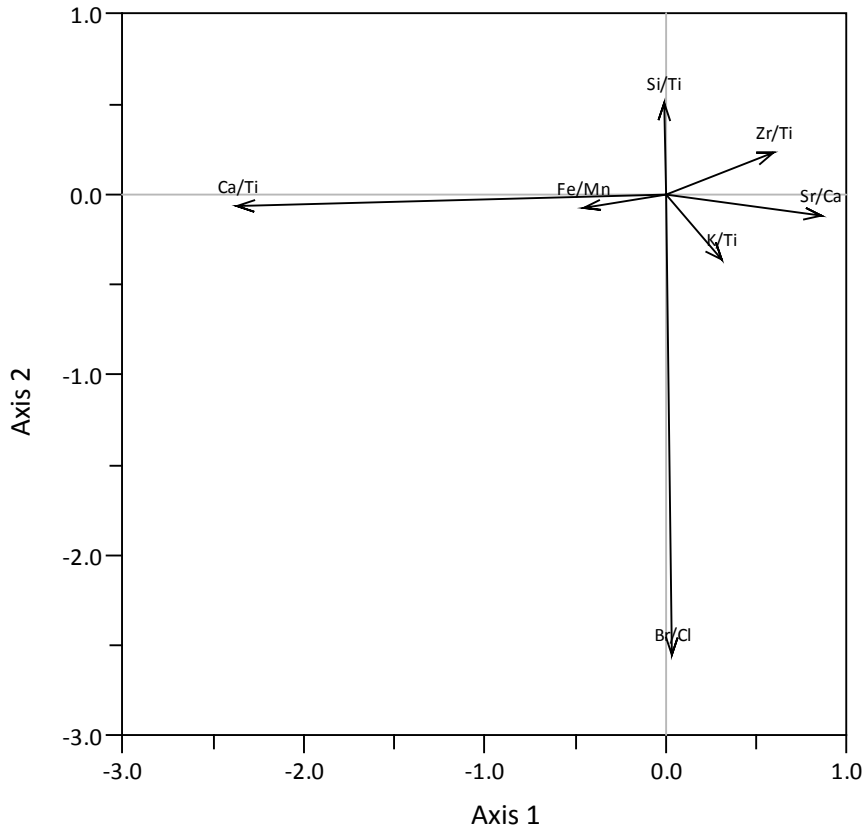

Figure 5.8: Principle component analysis of the geochemical ratios for VC001.

5.4.3 Diatoms

A total of 108 samples were counted for VC001 with 135 species identified. Diatom counts were transformed to percentages of total counts per sample. A summary diatom profile is presented in Figure 5.9 for 20 taxa which represent the most abundant species (>5% abundance in more than one sample). A full list of diatom species identified and their taxonomic authority is provided in Appendix D.

No diatoms were found in the bottom 5 cm (9040-8597 cal years BP) where the sampling frequency was 2 cm (535 to 530 cm) and low count numbers (<300) occurred from 529-497 cm; <50 individuals were counted at 529 and 527 cm (9595-9154 cal years BP). Upcore, from 496-74 cm (c. 9000-6500 cal years BP) all diatoms counts are greater than 300 with the exception of samples at 254 and 245 cm which had counts <100. No samples were taken from the disturbance layer (68-55 cm) as this area was considered to be the result of reworking of material and no accurate dates or conditions could be assessed from this section. Above the disturbance layer, from 55 to 40 cm (c. 400 cal years BP) where the sampling frequency was between 2-8 cm, there were very low frustule counts (<25) and no diatoms were present from 40 to 14 cm (c. 200 cal years BP). In the uppermost sample at 6-5 cm a low count of 161 individuals was tallied.

CONISS onstrained cluster analysis (Grimm, 1987) was used to determine diatom biological zones based on taxa occurrances >1% . The results of the cluster analysis are presented in Figure 5.9. Five major zones were identified and are used here to describe the floristic diatom changes throughout the sediment core. No zone is identified for the hiatus between 68-50 cm.

Zone 1 (c. 9000 cal years BP) (535 to 499 cm)

Diatom fossil assemblage in Zone 1 encompasses 36 cm of sediment and clear differences are evident in the diatom assemblages compared to the rest of the sediment core. All individual diatom counts in Zone 1 were less than 300 valves and poor frustule preservation was evident. Zone 1 is dominated by *Paralia sulcata* (35%) and *Podosira corolla* (21%). *P. sulcata* is heavily silicified, preserves well and is associated with a wide range of environmental conditions; thus it can be complicated to use for paleoenvironmental

reconstruction as it can be abundant in the fossil record because of its resilient structure, not as a result of an ecological parameter. Other taxa present here are *Tryblionella navicularis*, an epipelic, mesohalobian species; *Tryblionella compressa*, a polyhalobian, benthic species, *Grammatophora serpentina*, a pelagic, marine species that can also live attached to marine life and *Rhaphoneis amphiceros*, a mesohalobian, tychoplanktonic species.

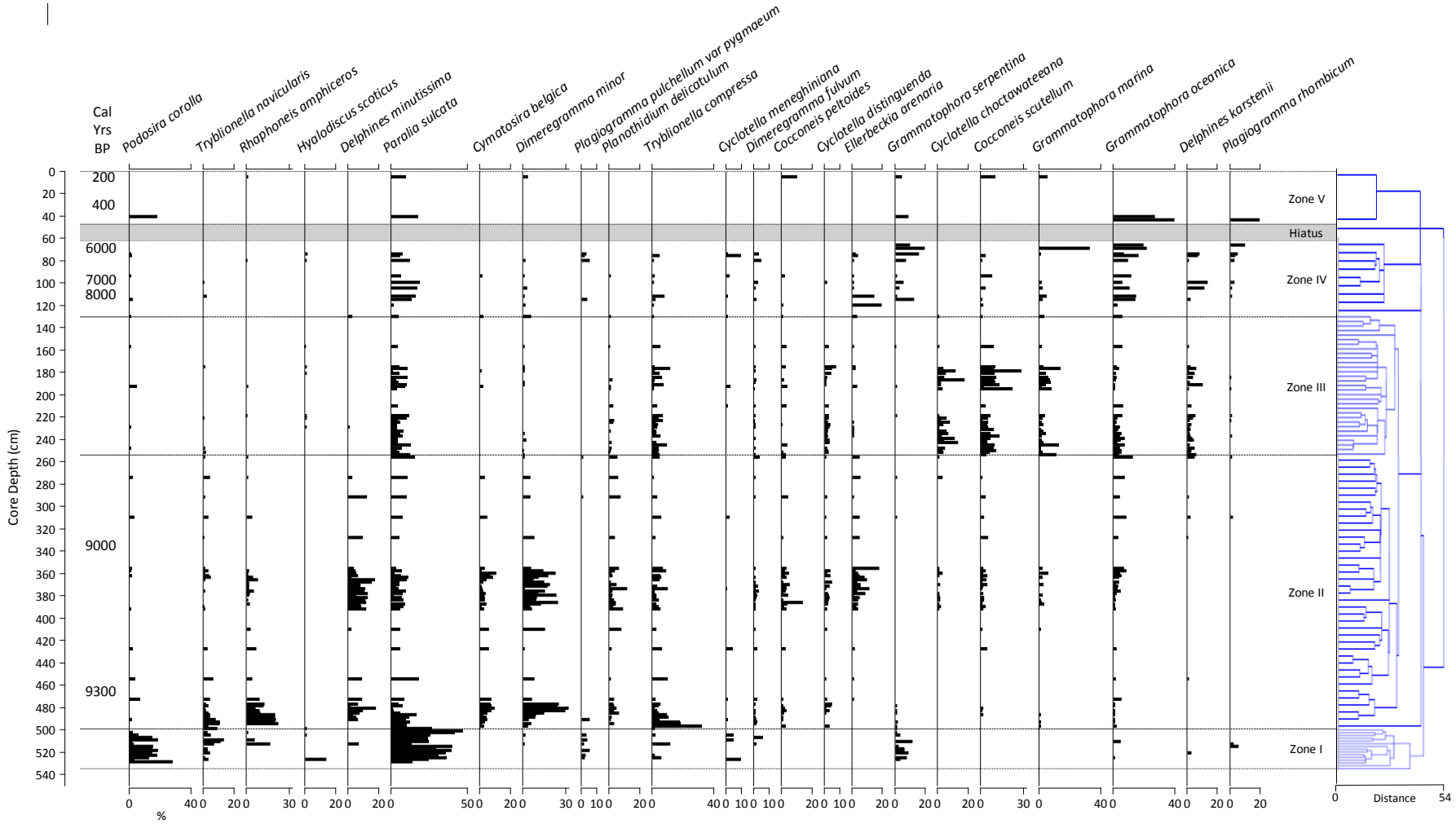

Figure 5.9: Diatom results for VC001. Here is a representative sample of diatom taxa appearing as greater than 5% of the total diatoms and in more than one sample. Radiocarbon dates are presented along the y- axis. Constrained cluster analysis with paired-group (UPGMA) using PAST is displayed.

Zone 2 (c. 9000-8800 cal years BP) (499-254 cm)

Diatom preservation was good in Zone 2 with valve counts >300 per sample for all but three samples which had counts between 250-300 frustules. *Dimeregramma minor* (12%) is a marine, episammic species the most dominant species and is an intertidal species. The cosmopolitan species *P. sulcata* (8%) is present here as well, but as a much lower proportion of the assemblage. *Rhaphoneis amphiceros, Tryblionella compressa Cymatosira belgica, Planothidium delacatulum* and *Grammatophora oceanica* are all intertidal, episammic or epipelic species and are represented as 3-7% of the assemblage. *Ellerbeckia arenaria* (4%) is a freshwater Oligohalobian indifferent species present here. Particularly, *E. arenaria* occurs from 400-350 cm consistently and in other samples intermittently in Zone 2 indicating times of increased freshwater into the environment. This zone is a departure from Zone 1 which had low individual frustule counts and was dominated primarily by two species; an assemblage most likely occurring due to occasional inundation as denoted by the presence of pelagic and tychoplanktonic species and those which entered the region attached to marine life.

Zone 3 (c. 8800-8200 cal years BP) (254-130 cm)

Diatoms in this zone between 254 and 130 cm were dominated by *Cocconeis scutellum* (9%) and *Tabularia fasciulata* (7%) both mesohalobian, epiphytic species associated with brackish lagoonal and muddy environments; *P. sulcata* (7%) has a strong showing in this zone as well. Diatom preservation was good. *Cocconeis placentula var euglypta (*epihytic, oligohalobian indifferent*) , Cyclotella choctawateeana* (mesohalobian, planktonic) and *T. compressa* have 4-5% of the assemblage while *G. oceanica*, *Grammatophora marina* (polyhalobian), *Eunotogramma leave* (mesohalobian, episammic) and *Delphines karstenii* (marine, polyhalobian) have c. 3% of the assemblage. Zone 3 is dominated by epiphytic, mesohalobian species indicating a higher level of macrophytes and seawater inundation.

Zone 4 (c. 8200-6000 cal years BP) (130-68 cm)

P. sulcata (11%) and *G. oceanica* (10%) have the highest occurrence in Zone 4. *E. arenaria* represents 7% of the assemblage and *D. karstenii*, *G. serpentina* and *E. leavis* constitute 3-4% of the diatoms represented in this zone. Zone 4 is comprised of diatoms similar to those found in Zone 2 and, therefore, a possible return to previous environmental conditions.

Zone 5 (c. 400-200 cal years BP) (50-top)

Zone 5 represents the sediment directly above the hiatus in VC001. The zone has low diatom concentrations (50-44 cm; <50 diatoms enumerated) and no diatoms encountered in several samples. Diatoms enumerated in the top 6 cm resulted in <200 individuals. *G. oceanica, P. sulcata, Cocconeis peltoydes, C. scutellum* and *Plagiogramma rhombicum* comprised the majority of this assemblage.

Diatom metrics including concentrations, total counts, Hills N2, F-index, breakage index, B:P:T ratio, organic carbon, CA results and DI salinity are presented in Figure 5.10. Additionally a table of diatom morphology (frustule group), habitat, general environment and life form were compiled for each species recorded in this research to get initial qualitative assessments of diatom assemblages; this can be found in Appendix D.

Diatom concentrations are represented as frustules x 10^5 g^{-1} WW. Diatom concentrations are variable throughout VC001 and range from 5.9 x 10^3 g-1 WW (44 cm) to 1.4 x 10^6 g-1 WW (370 cm). The lowest concentrations occur at the top and bottom of the sediment core and the highest concentrations of frustules are between 400 and 200 cm (c. 9000-8000 cal years BP). Hill's N2 diversity rating is presented along-side diatom concentrations to assess the relationship between these factors. A similar pattern emerges here with low species diversity found at the top and bottom of VC001 but increased fluctuation of diversity exists throughout the core from 450-80 cm (9000-7000 cal years BP) and a high level of broken diatoms found in samples. Breakage is found not only in the expected larger pennate diatoms (*Navicula digitoriata* and *Bacillaria paxillifera*) but also in smaller, more strongly silicified species (*Rhaphoneis amphiceros* and *Dimeregramma minor*) and centric diatoms not usually associated with broken frustules (*Paralia sulcata* and *Cyclotella distinguenda*).

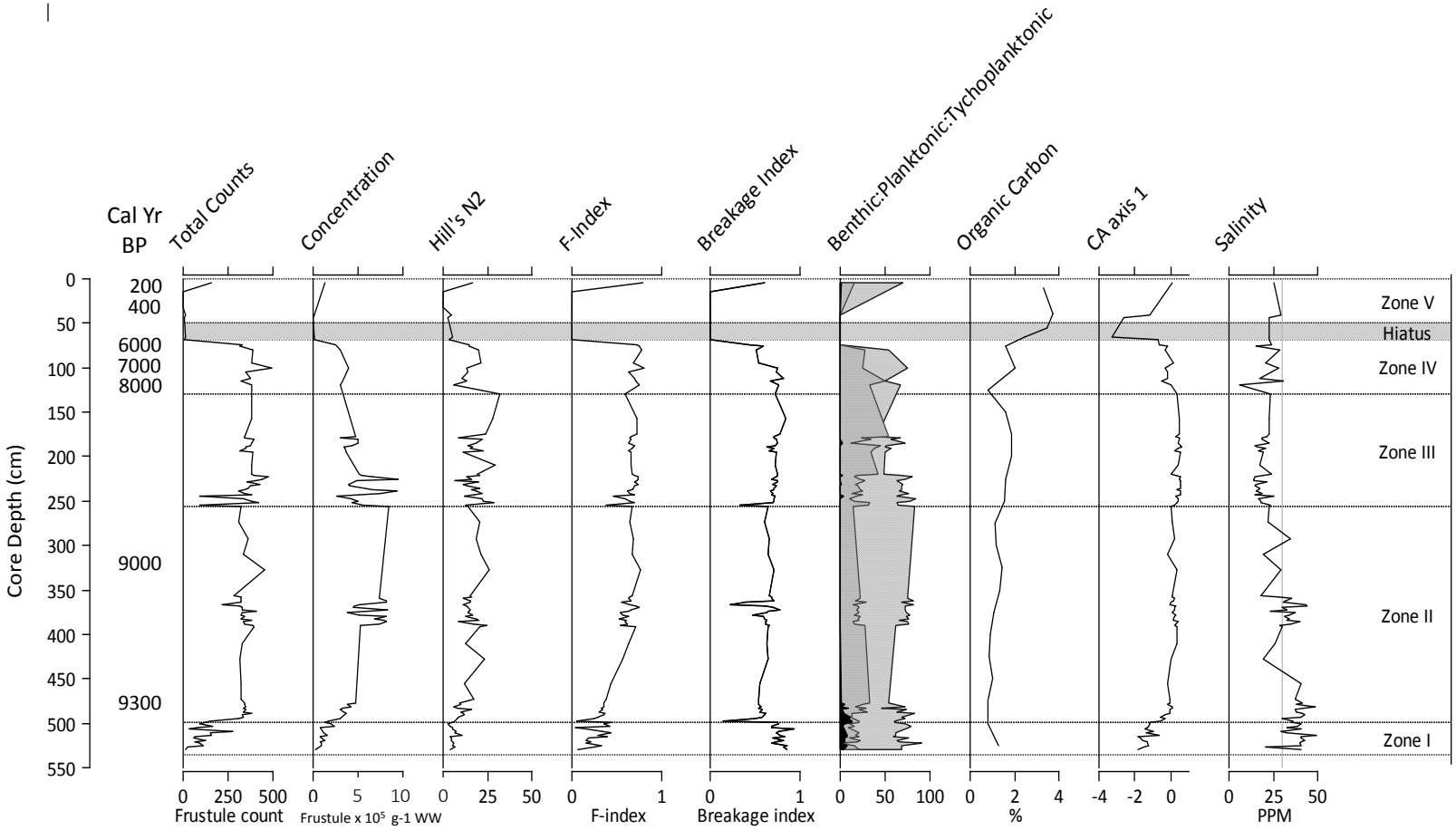

Figure 5.10: The results of the diatom metrics for VC001. Shown here are diatom counts (in count numbers), diatom concentrations, Hill's diversity index, F-index, breakage index, total unknown (%), benthic:planktonic:tychoplanktonic ratio (B:P:T), CA axis scores and Diatom inferred (DI) salinity (PPM). Diatom zones determined using CONISS and displayed on the right.

The morphological dissolution F-index was used to quantify the effect of silica dissolution in the samples and the breakage index is presented to assess if there is relationship between dissolution and breakage in this sediment core. The mean morphological dissolution F-index for VC001 is 0.49 and is lowest at the bottom of the core from 535 cm to 500 cm with a value of 0.07 indicating poor preservation (Figure 5.10). The F-index increases up the core where it reaches its highest level of 0.80 at 100 cm (c. 7000 cal years BP) indicating very good preservation during this time. Dissolution and breakage events therefore are clearly evident at the bottom of the sediment core c. 9000 cal years BP and between 400-350 cm and 275-225 cm; while no samples were analysed from the shell hash between 70-50 cm. The uppermost samples (<25 cm; c. 400 cal years BP) have a high F index averaging 0.79. The breakage index displays a contrary pattern to the dissolution index in the bottom of core VC001 with high breakage 525 to 500 (breakage index 0.94 at 507 cm) and a drop to the lowest breakage point at 497 cm (0.14). Upcore from 495 cm, however, it has a similar pattern as the F-index with the same areas of variation.

The division of diatom taxa into their habitat preferences (benthic:planktonic:tychoplanktonic) revealed a system dominated by benthic taxa for most of its history. The benthic:planktonic:tychoplanktonic ratio (B:P:T) sheds light on ecological parameters which might influence the results of the other indices and also indicate a shift in salinity levels. The ratios show higher percentages of planktonic diatoms in the bottom of the core (Zone 1) while above 500 cm (Zones 2-5) is dominated by benthic diatoms (Figure 5.10). Tychoplanktonic diatoms only appear substantially in Zone 1 as well. Dating is not straightforward in this area as the calibrated radiocarbon age in Zone 1 is 9040-8597 cal years BP and the date above this, at the base of Zone 2, is 9494-9154 cal years BP. This is likely due to a variation in dating material as discussed previously.

The ordination technique detrended correspondence analysis (DCA) revealed unimodality in the dataset with an axis 1 length greater than 2. All DCA results are in Appendix E. This axis length suggests that the diatoms have a unimodal species-environment relationship so correspondence analysis (CA) was applied (Figures 5.10 and 5.11). CA was used to determine the major patterns of variation in species composition data. The two outlier points, 68 cm and 44 cm represent the sampling points immediately prior to and after the hiatus.

Diatom clusters are grouped with a circle and Zones 1-4 are clearly indicated. Zone 5 is not clearly indicated here, most likely due to the low diatom concentrations and samples with no diatoms present. CA axis 1 sample scores were plotted stratigraphically (Figure 5.10). Basal sediments in Zone 1 contain low numbers of broken and highly dissolved diatoms indicative of occasional marine influence such as *P. sulcata* and *P. corolla.* The floristic composition of Zone 2 changes to species that prefer intertidal, muddy conditions such as *D. minor* and *T. compressa* with period of freshwater influence denoted with the presence of *E. arenaria*. Zone 3 shows diatoms with an affinity for increased inundation and lagoonal conditions, such as *C. scutellum* and *T. fasciulata.* Diatoms in Zone 4 exhibit a return to intertidal conditions with more marine species like *G. oceanica* and *P. sulcata* and with a freshwater pulse seen in the upper zone with the appearance of *E. arenaria*. Diatom assemblages in Zone 5 are dominated by *G. oceanica, P. sulcata, C. peltoydes, C. scutellum* and *P. rhombicum.*

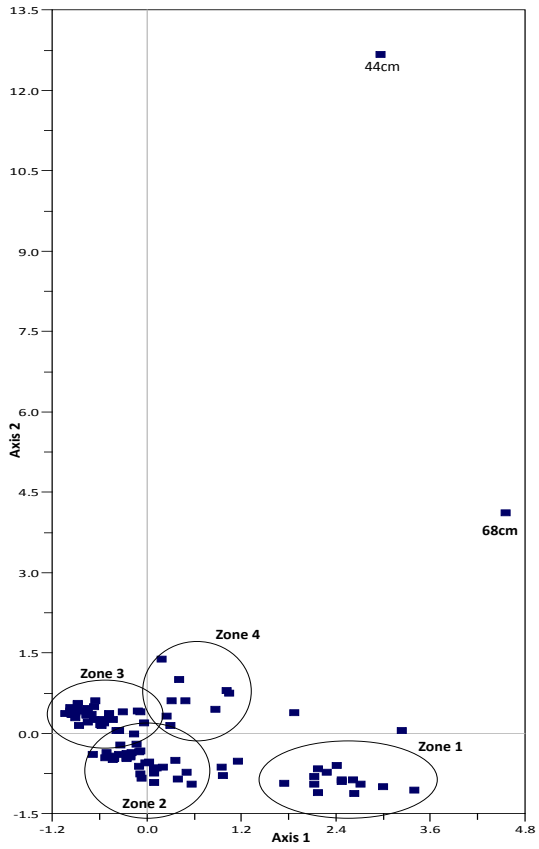

Figure 5.11: Results of the Correspondence Analysis (CA) of diatom assemblages for sediment core VC001.

Diatom salinity tolerances were classified into five groups based on the halobian scale (Figure 5.12). *Paralia sulcata* has been omitted from classification due to its variable salinity tolerance. Marine and brackish diatom taxa dominated sediment core VC001 with freshwater species making two significant appearances c. 9000 cal years BP and c. 8000 cal years BP. Freshwater/brackish species had the highest percentages 8801-8393 cal years BP.

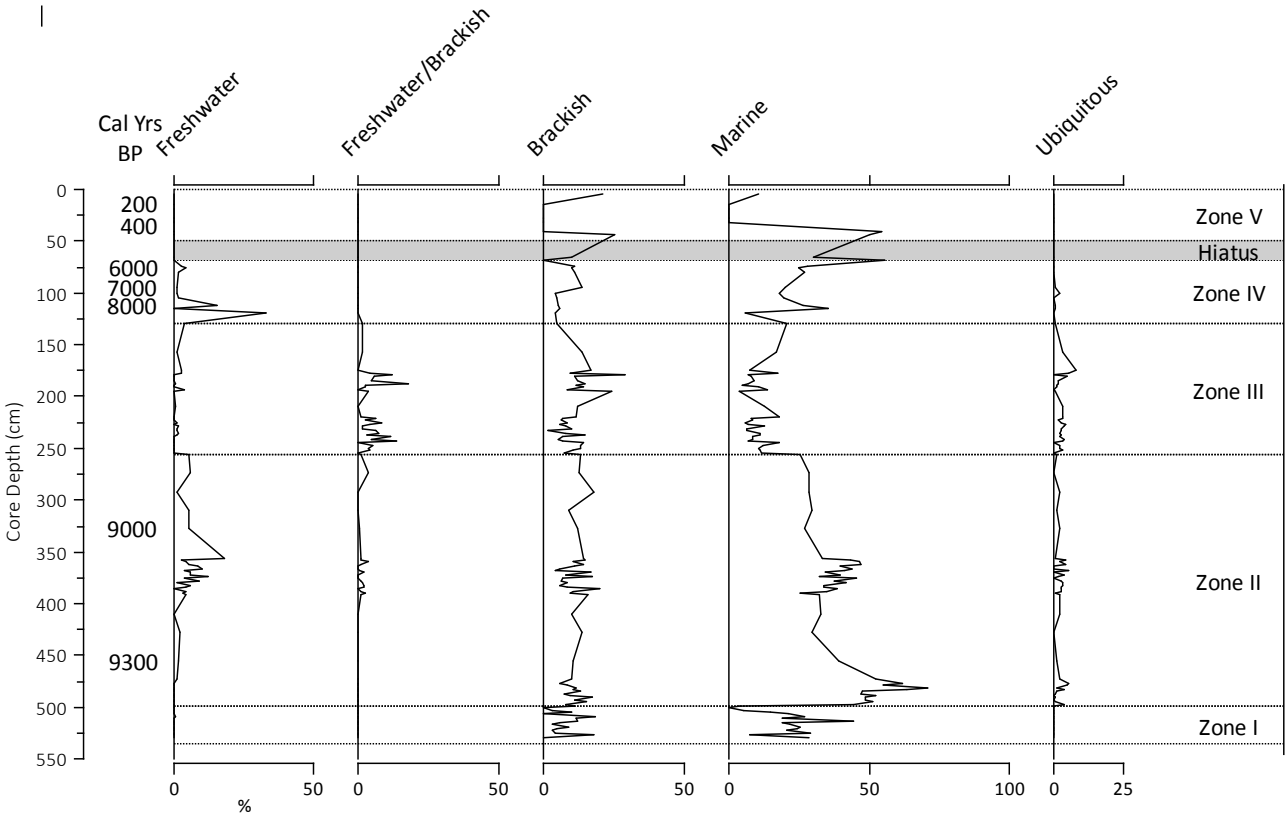

Figure 5.12: Diatom salinity groups in sediment core VC001 shown with radiocarbon dates on the left and diatom zones in th right column, The sediment hiatus is indicated in grey.

Quantitative analysis of diatom salinity was carried out using a transfer function. Diatom inferred (DI) salinity was assessed from the MOLTEN training set and is presented in Figure 5.10. A salinity optimum (g L^{-1}) for 51 species from the MOLTEN training set was used (average % coverage is >50% of the dataset >1% of the total diatoms). A table of these species and their respective salinity optimum is presented in Appendix F. Results in the lower 25 cm of the core are viewed cautiously. In this area diatom counts were very low (14-125 frustules) and dominated by *P. sulcata*; a thickly silicified species which does not

dissolve as easily as other species. WA-PLS DI salinity produces very high estimates (over 35, often around 40 g L^{-1} or PPM), which can happen due to a mathematical artefact incorporated into the deshrinking tool of the transfer function. DI salinity decreases up the core with the highest levels 9494-9154 cal years BP and the lowest at 120 cm (between 8140-7825 and 8801-8393 cal years BP) and freshwater influences evident from 400 to 100 cm with two large freshwater pulses apparent c. 9100 cal years BP and 8200 cal years BP, reflecting the dynamic and changing nature of this environment.

5.4.4 Foraminifera

In total, thirty samples were processed in sediment core VC001 at systematic 20 cm intervals throughout the core. All samples produced foraminiferal counts greater than 300 tests with the exception of samples from below 491 cm (c. 9000 cal years BP) where there were no foraminifera present and at 94 cm (c. 7000 cal years BP) where the count was < 200 tests. 57 species were encountered in VC001 samples. Figure 5.13 shows 33 taxa present in abundances of >2% and occurring in more than one sample. A full list of species and their taxonomic authority is provided in Appendix G. Biological zones were established based on percent foraminiferal individuals of all taxa >1% using CONISS contrained cluster analysis (Figure 5.13). Four zones were identified.

Zone 1 (535 – 491 cm) (c. 9000 cal years BP)

No foraminifers were observed in three samples taken from this zone. This coincides with woody material which was extracted from this area (525 cm) and low (<50 individuals) diatom presence.

Zone 2 (491-256 cm) (c. 9000-8500 cal years BP)

This zone is dominated by *Haynesinia germanica* (37%), *Ammonia aberdovenysis* (11%), calcareous species representative of tidal/mudflats with *A. aberdovenysis* in particular indicating estuarine, low salinity conditions. *Elphidium* spp. (10%) includes *E. excavatum*, an extremely versatile species and *E. williamsonii*, a species associated with mid to low marsh and tidal flats. *E. williamsonii* appears at 328 cm (9330-8778 cal years BP) along with *Bulimina elongata* (1%). Other calcareous species including infaunal species *Bolivina spathulata* (6%) and *Stainsforthia fusiformis* (5%) are associated with mid to low marsh conditions. Calcareous foraminifera are dominant here but agglutinated species, such as

Textularia sagittula (5%), *Haplophragmoides bradyii* and *Siphotextularia flintii* (2%) are present representing 10% of the total zone.

Zone 3 (256 – 32 cm) (c. 8500-6000 cal years BP)

H. germanica (30%) and *Ammonia beccarii* (26%) comprise >50% of Zone 3. *A. aberdovenysis* disappears from the sediment record at 175 cm (between 8393-8801 and 8140-7825 cal years BP). Agglutinated species *Haplophragomoides bradyii* disappears from the record after the first sample at 256 cm. *Aubigyna hamblensis* appears in the sediment record and *Bulimina spatulata, S. fusiformis* and *Fissurina* spp. all disappear from the sediment record at 130 cm (c. 8200 cal years BP). Additionally, from 130-68 cm *Elphidium* spp have a low percentage (3%) representation and *Haynesina depressula* has its only showing in the sediment core, although at low percentages. *Fissurina subformosa* has its strongest presence in this zone and calcareous species *Stainforthia fusiformis* and agglutinated species *T. sagittula* are also present. The upper part of this zone from 68-55 cm includes the disturbance layer and this area was not sampled for microfossils. One sample directly above the hiatus (32 cm; 492-259 cal years BP) is included in this zone and sees the only occurrence of *Bolivina spatulata, Bulimina elongata* and *Bolivinellina pseudopunctata* at <2% in this zone. This sampling point is viewed with caution due to the proximity to the disturbance layer as this may mean sediment has experienced reworking.

Zone 4 (27-0 cm) (c. 400-0 cal years BP)

The upper core zone consists of recent material, from 492-259 to 305-0 cal years BP. Three samples (27, 19 and 5 cm) are included in this zone. *H. germanica* (25%), *Lobatula lobatula* (19%), *Cibidies reflugens* (20%) and *A. beccarri* (14%) dominate this zone. Species diversity is lower in this zone with only 14 taxa recorded. The presence of the epifaunal species *L. lobatula* is a marked difference as it can indicate the presence of coarse grained sediments and high energy environments; similarly, *C. reflugens* (epifaunal) is found in deeper water, ranging from the intertidal zone to shelf seas. *Epistominella exigua* (8%), an epifaunal species, has its most prominent presence in Zone 4 and can reflect deeper, more oxygenated waters. Also noted in this zone are *Rosalina anomala* (3%), *Textularia tenusa* (2%) and *Quinquelocina seminulum* (2%).

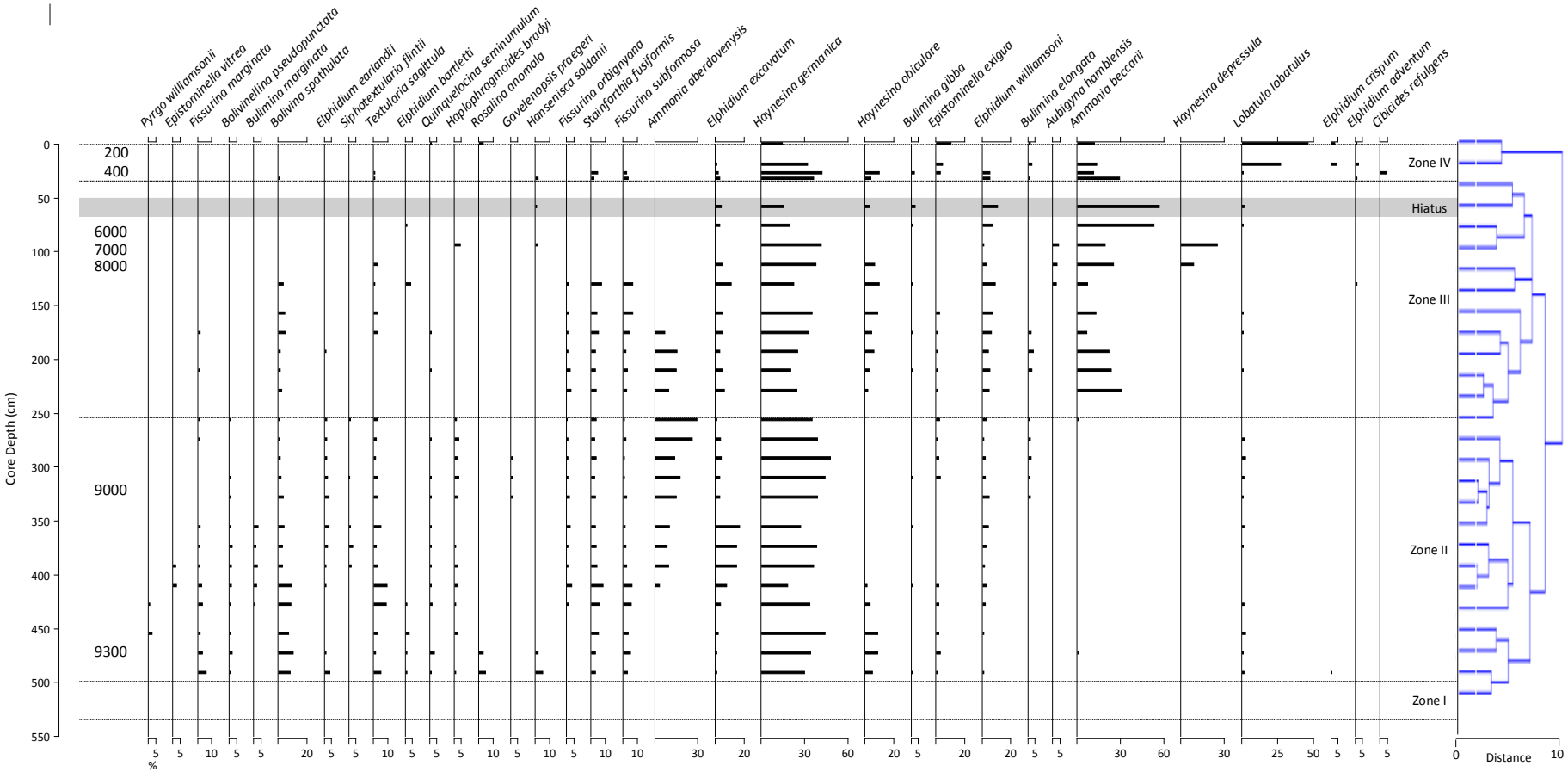

Figure 5.13: Foraminiferal taxa >2% occurrence in sediment core VC001. Radiocarbon dates are also presented along the y- axis. Constrained cluster analysis using PAST is also displayed.

Relevant foraminiferal metrics, including test counts, concentrations, diversity and agglutinated/ calcareous ratios, were explored to help interpret the data and results are presented in Figure 5.14. Foraminiferal concentration reflects the total number of tests in the individual sample and is variable throughout the core but sees the highest concentration levels of 4,707 per g^{-1} WW at 473 cm (c. 9000 cal years BP) and the lowest concentration of 727 per g^{-1} WW occurring at 94 cm (c. 6500 cal years BP). Hill' N2 diversity index was explored to assess stratigraphical species diversity and sees the lowest diversity occurring from 328 to 229 cm (c. 8500 cal years BP), 94 cm (c. 6500 cal years BP) and to 32 cm (c. 400 cal years BP). The highest diversity occurs in the lower core at 410 cm (c. 9000 cal years BP). Agglutinated species such as *Textularia saggitula* and *Haplophragmoides bradyii*, represent less than 10% of the total species in all samples except in the lower core where they are 13% (491 and 410 cm, c. 9000 cal years BP) and 11% (428 cm, c. 9000 cal years BP). Calcareous species, such as *Ammonia beccarii, Haynesina germanica, Elphidium* spp. and *Lobatula lobatula*, dominate the assemblages in this sediment core and in some samples in the upper core (76-58 cm, c. 6000 cal years BP), the assemblage is dominated by *Ammonia* spp. where this species represents >50% of the taxa. This area corresponds to the lowest levels of Hill's diversity index.

CA indicates patterns of variation in species composition data most notably within Zone 3 where samples from 112 and 94 cm (from 7440-7176 to 6409-6063 cal years BP) are distinct from others in the same zone (Figures 5.14 and 5.15). This variation is most likely driven by the presence of *Aubigyna hamblensis* and *Haynesina depressula* exclusively in this zone (4% of assemblage).

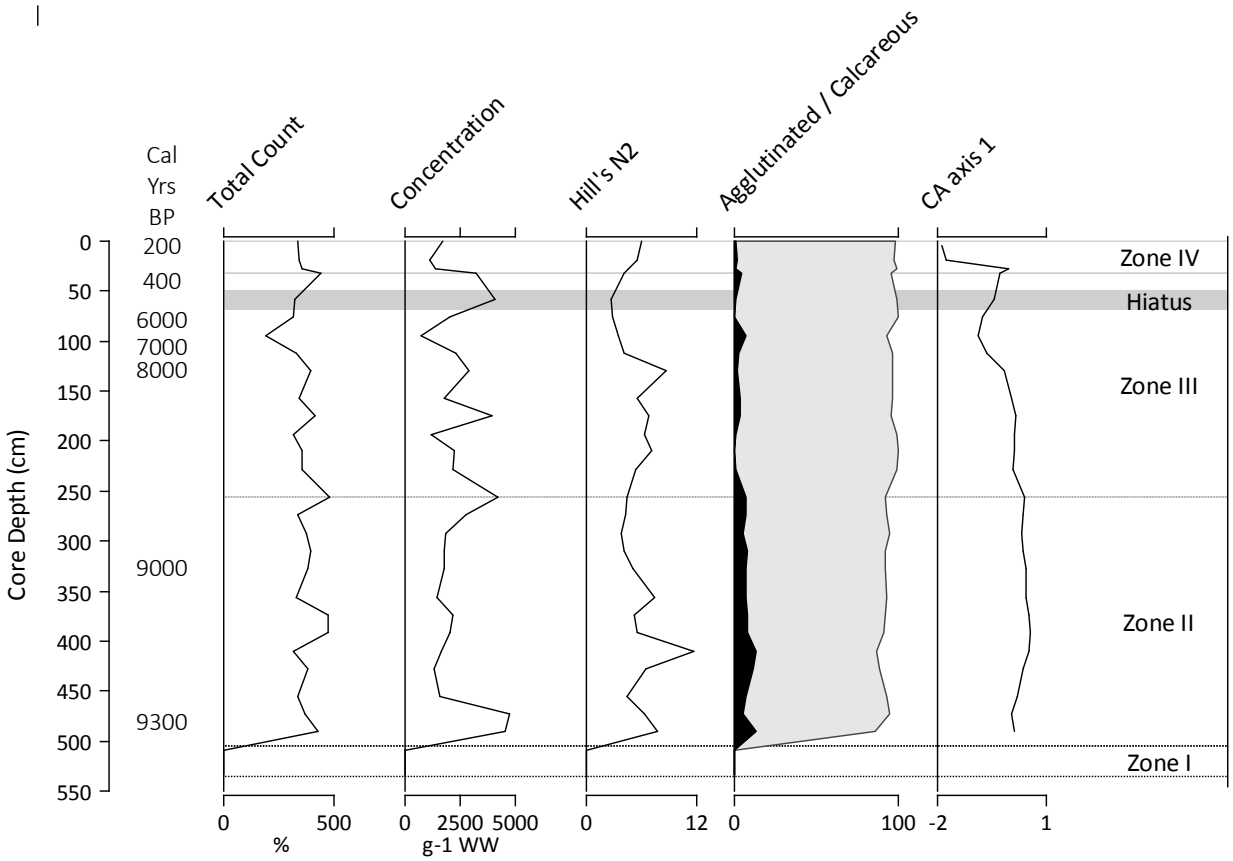

Figure 5.14: Foraminiferal metrics for sediment core VC001. Included here are the total counts, concentrations per sample, Hill's N2 Diversity Index, agglutinated vs calcareous taxa ratio, CA axis 1 sample scores.

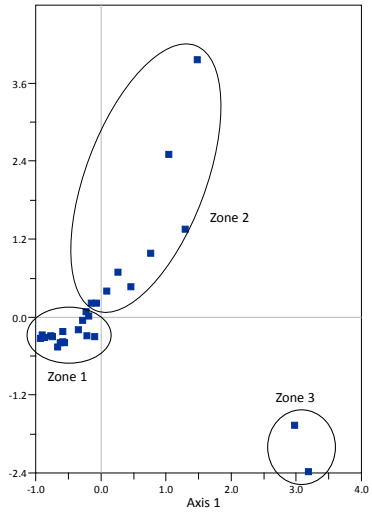

Figure 5.15: Graphic of the correspondence analysis (CA) of foraminifera from VC001. Zones previously identified from CONISS cluster analysis are circled and labelled.

5.4.5 Synthesis of data for sediment core VC001

Sediment core VC001 was extracted from the eastern-most location in this study, located in the Transitional Waters (Map 4.1) of the Corrib Estuary. Radiocarbon dating revealed a Holocene profile that records the early and mid-Holocene and a depositional hiatus overlain with recent sediment (Table 5.3). Results of multiple proxies reveal a major environmental change at the base of the core in (c. 9000 cal years BP) as recorded in grain size, magnetic susceptibility (Figure 5.6), selected geochemical ratios (Figure 5.7) and microfossils (Figures 5.9 and 5.13). Between c. 9000-8000 cal years BP little variation is evident in most proxies with the notable exception of the DI-salinity, which is highly variable throughout but with an overall decreasing trend. From c. 8800 to c. 8200 cal years BP little change is apparent in physical and geochemical proxies but the microfossils indicate an ecological response, seen most prominently in the diatom assemblages. Between c. 8200 and c. 6000 cal years BP notable pulses in magnetic susceptibility, geochemical proxies and the lowest levels of % OC are apparent, possibly reflecting the 8200 cold event (Figures 5.6 and 5.7) and a major freshwater pulse (Figure 5.9). A change in microfossil assemblages is observed here as well (Figures 5.9 and 5.13). Sediment deposition rates accelerate with just c. 60 cm of sediment representing c. 3000 years (Figure 5.4). The depositional hiatus is clearly defined by a thick shell layer composed largely of *Spisula* cf s*ubtruncata* from 68-50 cm and with dates of 6409-6063 cal years BP below and 492-259 cal years BP above the hiatus (Figure 5.2). The top of the core is comprised of modern material and notable differences are apparent in the high mean grain size (Figure 5.6) and % OC levels (Figure 5.10), increased Br/Cl and Ca/Ti and decreased Zr/Ti levels (Figure 5.7). Microfossil assemblages here, as well, change to more modern marine environmental conditions as evinced by the foraminiferal dominance of *L. lobatulus*, *E. exigua* and *H. germanica* and diatom floristic profile including *G. oceanica, P. sulcata* and *C. peltoydes* (Figures 5.9 and 5.13).

5.5 Sediment cores VC002, VC003 and VC004

The results of the radiocarbon dating revealed that sediment cores VC002, VC003 and VC004 largely have an early Holocene chronology with a dating range of c. 2,000 years (c. 10000 cal years BP to c. 8000 cal years BP). While VC002 has a recent date of c. 350 cal years BP at 9 cm, overlaying a hiatus, the majority of this sediment core (56-554 cm) has a dating range of c. 2000 years in the early Holocene; comparable to the chronology of VC003 and VC004. Physical, geochemical and microfossil results are presented here for these three sediment cores. Depth intervals are used in describing the results.

5.5.1 Physical data

Parameters obtained from the MSCL include p-wave velocity, gamma density and magnetic susceptibility. MSCL results for VC002, VC003 and VC004 are represented in Figure 5.17 a-c. Laser diffraction grain size analysis (LDGSA) was only performed on sediment core VC003.

The p-wave velocity in sediment core VC002 ranges from 849 m/s to 1900 m/s and there is a decreasing trend upcore. This is a marked difference from the p-wave parameter in VC003, where it remains stable throughout the core with a mean of 1542 m/s and a peak of 1577 m/s. The p-wave data for this core had gaps occurring in the data at the following intervals: 0-48 cm; 130-170 cm; 180-190 cm and 230-260 cm. It is most likely that gaps in sediment core VC003 occur where sections had either distorted liners or where significant air gaps occur inside the liner and the sediment. In VC004, p-wave velocity ranges from 831 m/s to 1921 m/s and has the largest range of all four cores. While there is no distinct trend; there are sections of the core where high variability and great peaks and depressions are visible. This may be due to insufficient coupling between the core sediment and the core liner as a result of voids and micro-cracks in these areas (exhibited from 430 cm to 390 cm; 230 cm to 190 cm; 90 cm to 70 cm and 40-0 cm). Gamma densities in cores VC002 and VC003 have similar patterns and reflect the consolidated homogenous sediments found in these cores. Gamma density levels in VC002 range from 1.29 g/cm^3 to 1.94 g/cm^3 and fluctuate from 5.5-3.8 m with lowest levels occurring as extreme points at 4.9 m (1.29 g/cm^3) and 3.8 m (1.41 g/cm^3). Levels remain steady, maintaining an approximate range between 1.70 g/cm^3

to 1.90 g/cm^3 until a decrease in the upper core from 40 cm-0. VC003 shows a similar pattern to VC002 with a gamma density range of 1.41 g/cm^3 to 2.07 g/cm^3. The lowest levels occurring in the lower half of the core and the highest levels are in the upper 0.50 m of the core. In VC004, gamma density ranges from 1.29 g/cm^3 to 2.02 g/cm^3 and exhibits no real trend throughout the core. The troughs at 3.9 m and 0.88 m are most likely the result of sediment shifting adjacent to section joints.

Magnetic susceptibility in sediment core VC002 displays a decreasing trend ranging from 4.9 SI to 0.921 SI and reaches the lowest levels at 26 cm at the top of the core. From 29-18 cm, a layer consisting of several whole shells mixed with dense shell hash is a disturbance layer as indicated by the chronology (Table 5.2) and may be a contributing factor to the low magnetic susceptibility here. Changes in magnetic susceptibility, a measure of the concentration of magnetic minerals, indicates environmental changes associated with this type of sediment and can signpost varying transport and deposition conditions. A similar upcore trend is exhibited in VC003 and the magnetic susceptibility here ranges from 0.24 SI to 7.16 SI. There are three distinct peaks which occur at 490 cm, 350 cm and 230 cm and these correlate to smaller peaks seen in VC002 at 490 cm, 380 cm and 210 cm. Sediment core VC004 has a similarly low magnetic susceptibility range to VC002, ranging from 0.99 SI to 6.14 SI with a significant peak at the bottom of the core where the highest level of 6.14 SI is recorded. Lower SI is evident in most of VC004 when compared to VC002 with the exception of the lower 25 cm. The peak at the bottom of VC004 (460 cm) is close in core depth to downcore peaks of both VC002 and VC003, but where VC002 and VC003 have variation upcore, VC004 exhibits little change.

The mean grain size in sediment core VC003 is additionally presented in Figure 5.17 (b). Similarities exist between the mean grain size and the gamma density most notably at the top of the core around 50 cm.

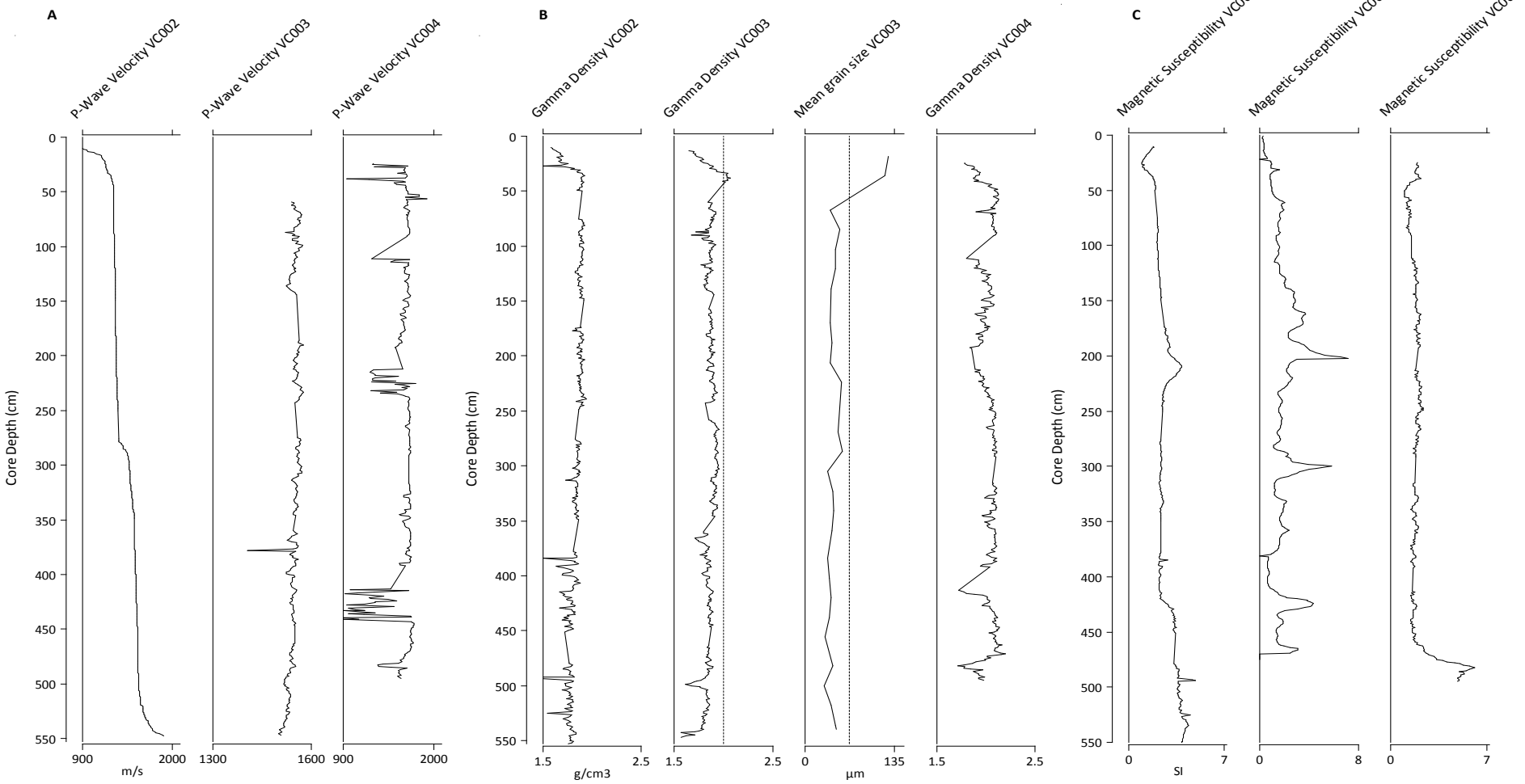

Figure 5.17: Results of the MSCL analysis for: (A) p-wave VC002, VC003, VC004; (B) gamma density VC002, VC003, VC004 and Mean grain size VC003; (C) magnetic susceptibility VC002, VC003 and VC004.

5.5.2 Geochemical (XRF) analysis

Seven elemental ratios used for proxy investigation (Ca/Ti, K/Ti, Si/Ti, Zr/Ti, Fe/Mn, Br/Cl and Sr/Ca) and for VC002, VC003 and VC004 are presented in Figure 5.19 and Appendix C. Br/Cl reflects changes in marine organic matter in a sediment core. In VC002 and VC003, there is a similar Br/Cl profile with a decrease in the lower core until 500 cm and highly fluctuating levels upcore, exhibiting no particular pattern, until recent sediment from 50-0 cm (c. 400-0 cal years BP) where the measurements increase. The Br/CL measurements for VC004 had extensive areas of the core where no reading was taken (zero values) and data are not presented here. The Sr/Ca measurements are related to sediment provenance and biogenic markers. Sr/Ca is high at the base of VC003 c. 10000-9000 cal years BP and for three samples at the base of VC002 (c. 9000 cal years BP). These are likely turbidite sediments. VC002 sees relatively steady Sr/Ca upcore until a prominent increase at the sediment hiatus layer (68-50 cm). VC003 has notable change in the basal sediments and exhibits greater fluctuation than Sr/Ca in VC002 with several increases from 150-0 cm, most notable c. 130 cm. In the upper core, VC004 exhibits limited change in the Sr/Ca measurements. Ca/Ti is a good proxy for measuring changes in terrigenous sediment contribution to a sample and gauging the calcium carbonate content. Ca/Ti has little change in VC002 with the exception of the recent sediment in the upper core (above 40 cm); the hiatus layer is clearly visible with this proxy. In VC003, the Ca/Ti has notable change in the basal sediments of the core and the recent sediment deposition on top. Ca/Ti in VC004 also has lower values in the bottom of the core and little change upcore. A slight increase at 175 cm and in the upper 50 cm is seen. Si/Ti, which is an indicator of biogenic silica, has little change in VC002 and VC003 with the exception of the upper sediments (above 70 cm) where there are higher fluctuations in VC002 and an increasing trend in VC003. Si/Ti is low at the base of the core for 25 cm then increases. There is a general decreasing trend upcore thereafter with very low measurements again, particularly in the upper 150 cm.

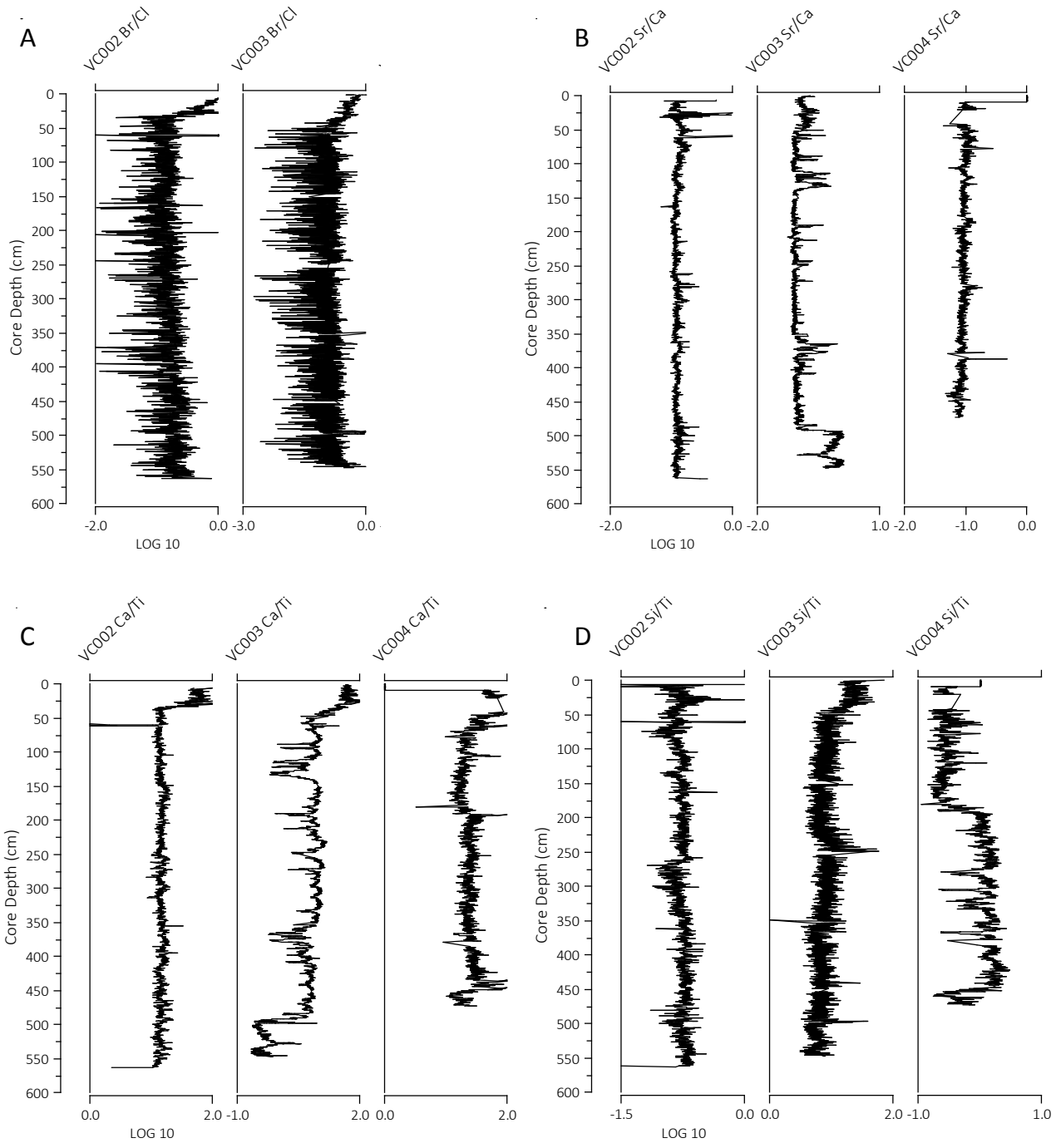

Figure 5.18: Results of selected geochemical proxies for sediment cores VC002, VC003 and VC004 based on the PCA (axis 1): A) Br/Cl (VC002 and VC003 only); B) Sr/Ca; C) Ca/Ti and D) Si/Ti.

In order to determine which of the ratios are the most relevant in each sediment core, a principle component analysis (PCA) was carried out (Figure 5.19). The axis 1 eigenvalue of VC002 is 0.5198 and indicates the most influential geochemical driver is Br/Cl. The axis 1 eigenvalue of VC003 is 0.6093 and indicates Ca/Ti is the most influential geochemical driver. In VC004, axis 1 has an eigenvalue of 0.7743 and the Br/Cl is the driving geochemical factor here. Appendix G has the relevant tables with all PCA loadings for sediment cores VC002, VC003 and VC004.

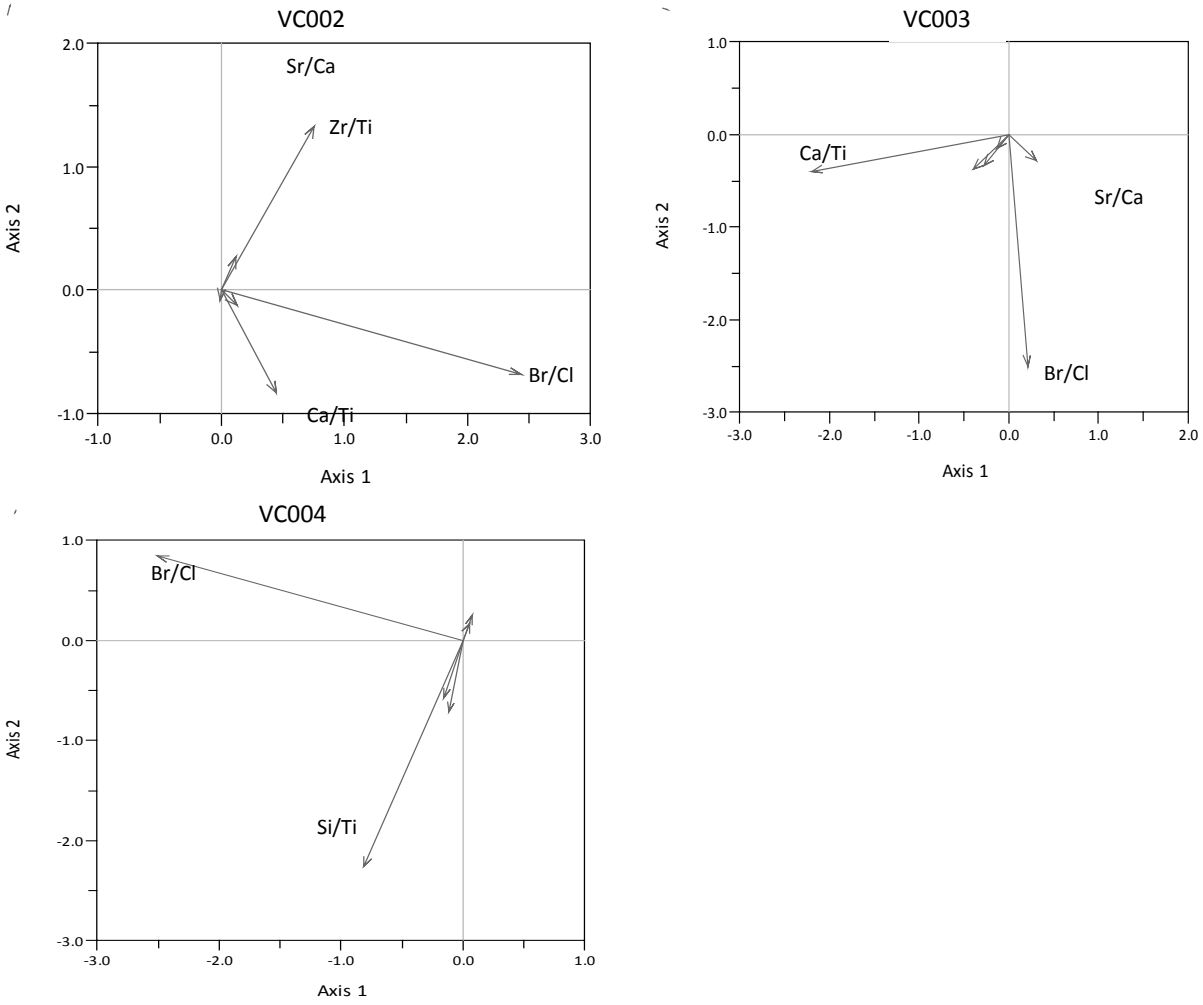

Figure 5.19: Results of the principle component analysis (PCA) for the geochemical elemental ratios on VC002, VC003 and VC004.

5.5.3 Diatoms VC003 and VC004

Diatoms were sampled initially in sediment core VC001 to examine estuary conditions and in VC003 to examine inner bay conditions. When the individual frustule counts for VC003 resulted in low valve numbers (<300), VC004 was also sampled. Full diatom results for sediment cores VC003 and VC004 are presented here. In sediment core VC003 a total of 56 samples were examined resulting in 116 genus varieties and 96 taxa identified to species level. Subsamples were originally taken at 20 cm intervals. After lithological analysis, sampling intensity was increased at sediment change points. A summary diatom profile of species with >2% occurrence is presented in Figure 5.20 with the radiocarbon dates for VC003; full diatom results are included in Appendix D. CONISS constrained cluster analysis was carried out on square root transformed data and revealed nine clusters. Samples with <50 frustules were excluded from the analysis. Of those included, nine samples had <100 frustules and 23 had <200 frustules. This resulted in the exclusion of all samples between 104 and 19 cm. Due to this, cluster analysis results are not an accurate reflection of change in the sediment core and are not presented.

Diatom concentration in VC003 ranges from 1.2×10^4 (486 cm) to 3.9×10^5 (378 cm) frustules with 92 taxa identifiable to species level. This is lower relative to VC001. In total 56 sediment samples were processed for diatom enumeration and sampling frequency ranges from 20 cm to 2 cm in areas of higher diatom concentrations. Generally, concentrations are more variable in the lower core from 532 cm to 331 cm and then there is little change up-core with a slight dip in concentration seen at 223 cm and 81 cm and a steep rise in concentration from 3-0 cm where concentrations are 2.2×10^5 in the upper 2 cm of VC003. The number of valves enumerated was low throughout VC003 and only eight sediment samples had counts of over 300 diatoms (532, 498, 496, 436, 382, 380, 378 and 376 cm). Due to this factor, observations of diatom variability will be presented semi-quantitatively and further analysis was limited to semi quantitative analysis. The low numbers of fossil diatoms and poor representation in the modern training set precluded application of the DI salinity model.

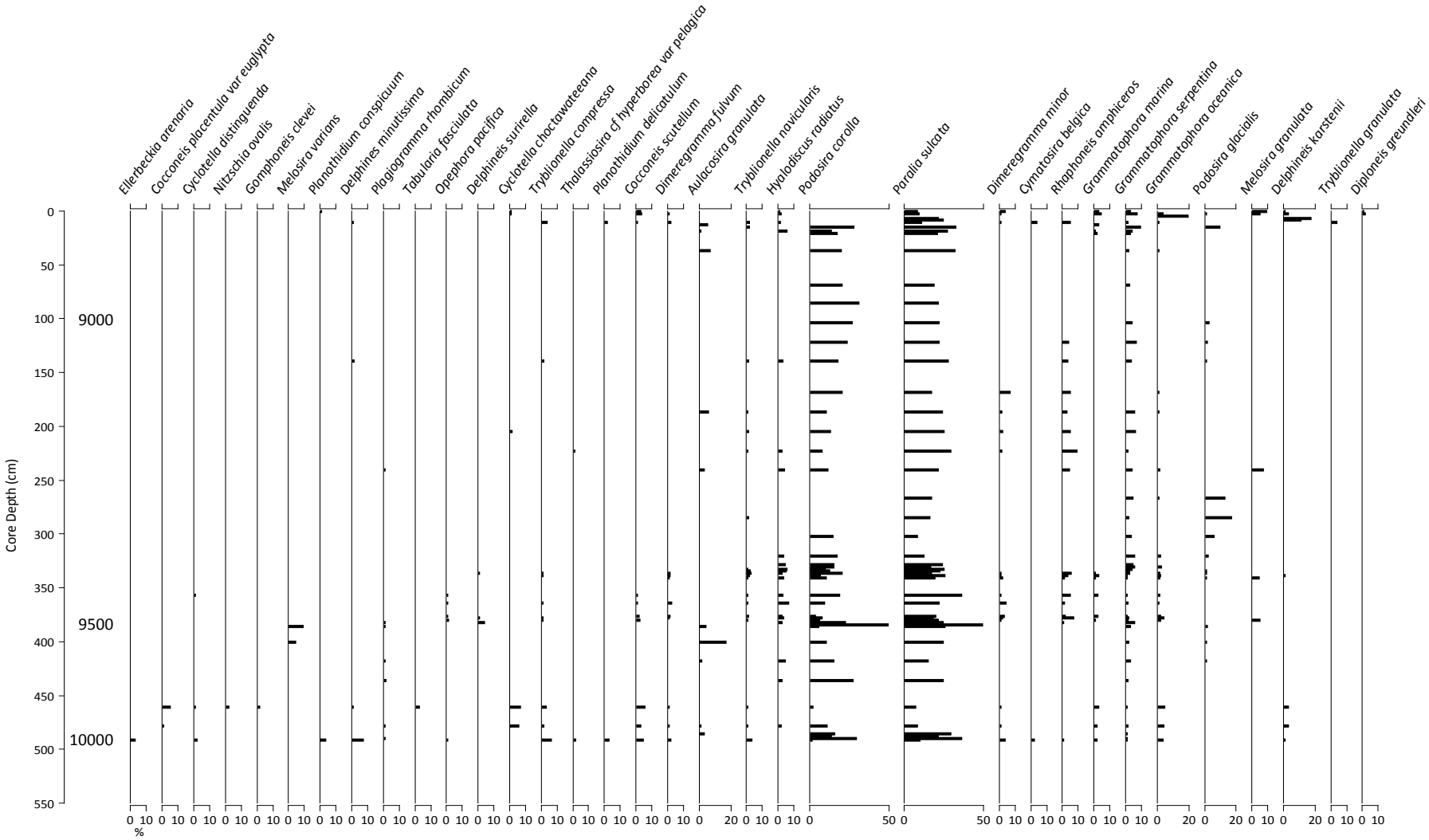

Figure 5.20: Diatoms >2% occurrance from VC003. Radiocarbon dates (cal years BP) are shown on the vertical axis.

Diatom metrics can be found in Figure 5.21. The morphological dissolution F index for VC003 shows a medium level of dissolution (F index 0.588) in the lower core and remaining steady for approximately 100 cm where it drops to 0.367 indicating high levels of dissolution from 400 to 325 cm. Upcore to 13 cm dissolution levels are low indicated by a high F index ranging from 0.696 to 0.788. At 13 cm there is one data point where the lowest F index (0.323) occurs. Breakage follows a similar pattern to dissolution in this core with slightly elevated levels averaging 0.733 from 542 cm to 300 cm. From 300 to 69 cm there is a slight upward trend with the highest breakage index at 69 cm with an index level of 0.8841. This reflects a high level of frustule preservation observed. In the upper core where diatoms counts were very low, the breakage index is low, and in the upper four centimeters where count numbers are over 150 individuals, the breakage index returns to a mid level of 0.569. Total percent of unknown diatoms parallels the morphological dissolution index, and where dissolution is higher, there is a higher percentage of unknown diatoms. The diversity index, Hill's N2, has an increasing trend upcore through VC003 indicating very low diversity in the lower and middle core and in the top of the core a significantly higher diversity index. Planktonic diatoms dominate sediment core VC003; from 514-488 cm and 205-86 cm planktonic diatoms represent more than 90% of the total frustules with the exception of 532 and 498 cm samples which have benthic diatoms in the majority. From 69-19 cm benthic diatoms represent more than 50% of the total samples and the top of the core planktonic diatoms have higher percentage (c. 72%).

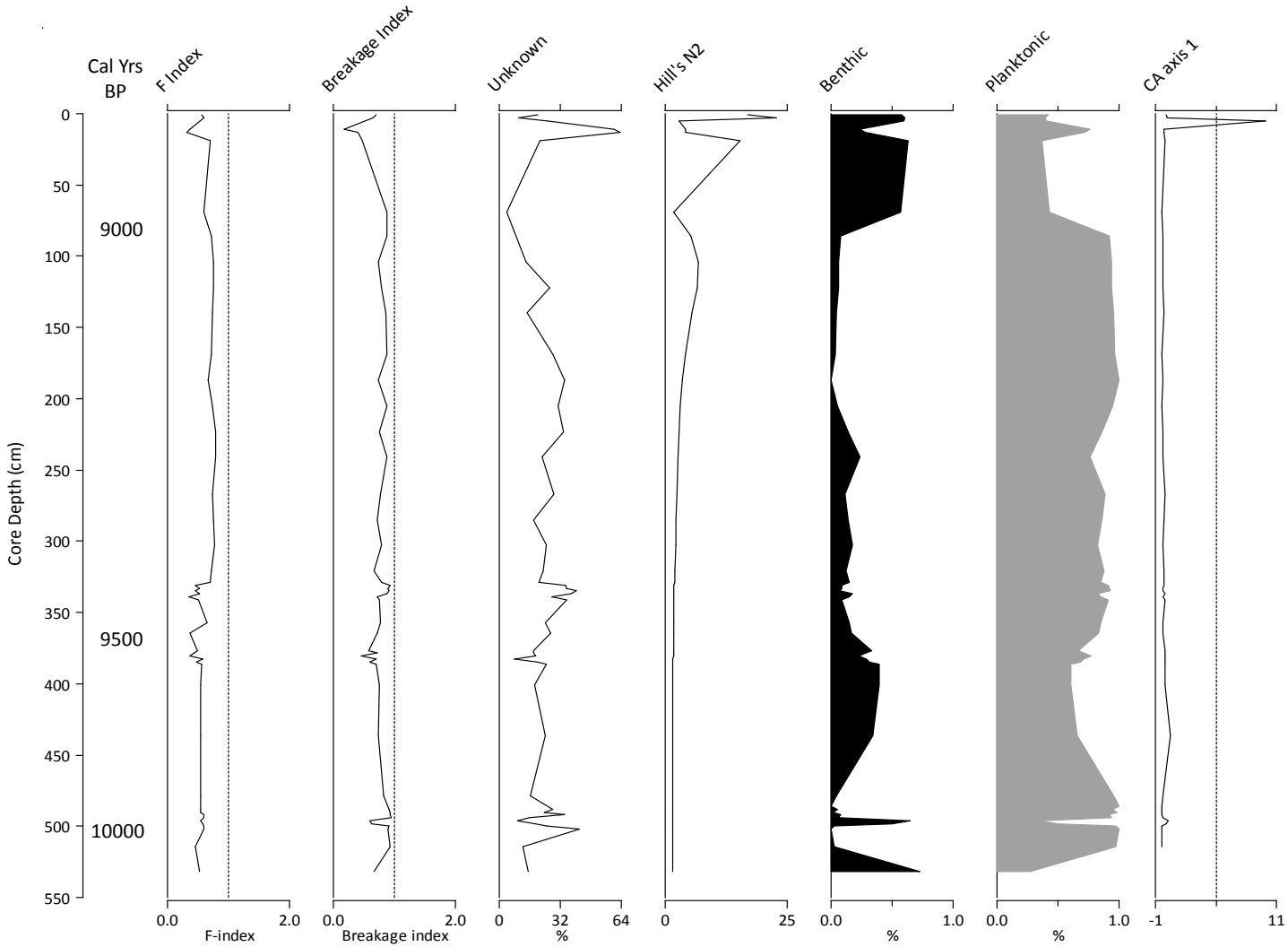

Figure 5.21: Diatom metrics for sediment core VC003 including the F-index, Breakage index, % unknown, Hill'sN2 and benthic:planktonic ratio.

Sediment core VC004 had a very limited number of diatoms fossils observed. From 478 cm to 449 cm diatom frustule concentration ranged from 2.4 x 10^4 (449 cm) to 5.8 x 10^5 at the bottom of the core (478 cm) but all counts were below 300 individuals. From 449 cm to the top of the core (0 cm) no diatoms were found with the exception of a few (<20 individual frustules) scattered valves observed at 181 cm, 141 cm and 1 cm. Sampling frequency throughout the core was 20 cm from 449 to 0 cm and was increased to 2 cm intervals where diatoms were observed (478-449); in areas where no diatoms were found, samples were processed twice (at 20 cm intervals) to ensure this was not a laboratory error. A total of 59 taxa were identified to species level and are included in Appendix D. Each sediment sample in VC004 was processed twice in order to eliminate sampling error as cause for the lack of diatom presence. Results from VC004 will be used in a limited fashion as they only correspond to a limited sampling area of VC001 and VC003.

5.5.4 Foraminifera VC003

There were 27 samples examined for foraminifera in sediment core VC003 and this yielded 33 individual taxa. Figure 5.22 shows foraminifera (>2% occurrence) in the sediment core samples. From 532-460 cm no foraminifera were found and from 460 to 360 cm only one species, *Jadammina macrescens*, was present in low numbers (11 and 18 individuals at sampling points 460 and 432 cm, 287 and 250 individuals at 414 and 396 cm and 89 and 72 at 378 and 360 cm). Species assemblages become more diverse from 332-232 cm with an average of 21 species per sample in this section but with count numbers remaining below 300 individual tests (45-227 tests counted in this area). In this area, *Haynesina germanica, Elphidium* spp., *Trochammina inflata, Haplophragmoides bradyii, Textularia sagittula, Stainsforthia fusiformis* and *Nonionella labrador* are present in the samples from 332-232 cm. From 214-60 cm foraminifera again disappear from the fossil record until the top of the sediment core where samples at 46 and 28 cm have high test counts (370 and 369 individuals respectively). Here, the species assemblage is more diverse with 28 species represented including *H. bradyii* (15%), *Lobatula lobatulus* (11%), *Elphidium williamsonii* (8%), *Bulimina gibba* (8%) and *H. germanica* (6%). Quantitative analysis was not carried out due to low count numbers and an inconsistency in samples with foraminifera present.

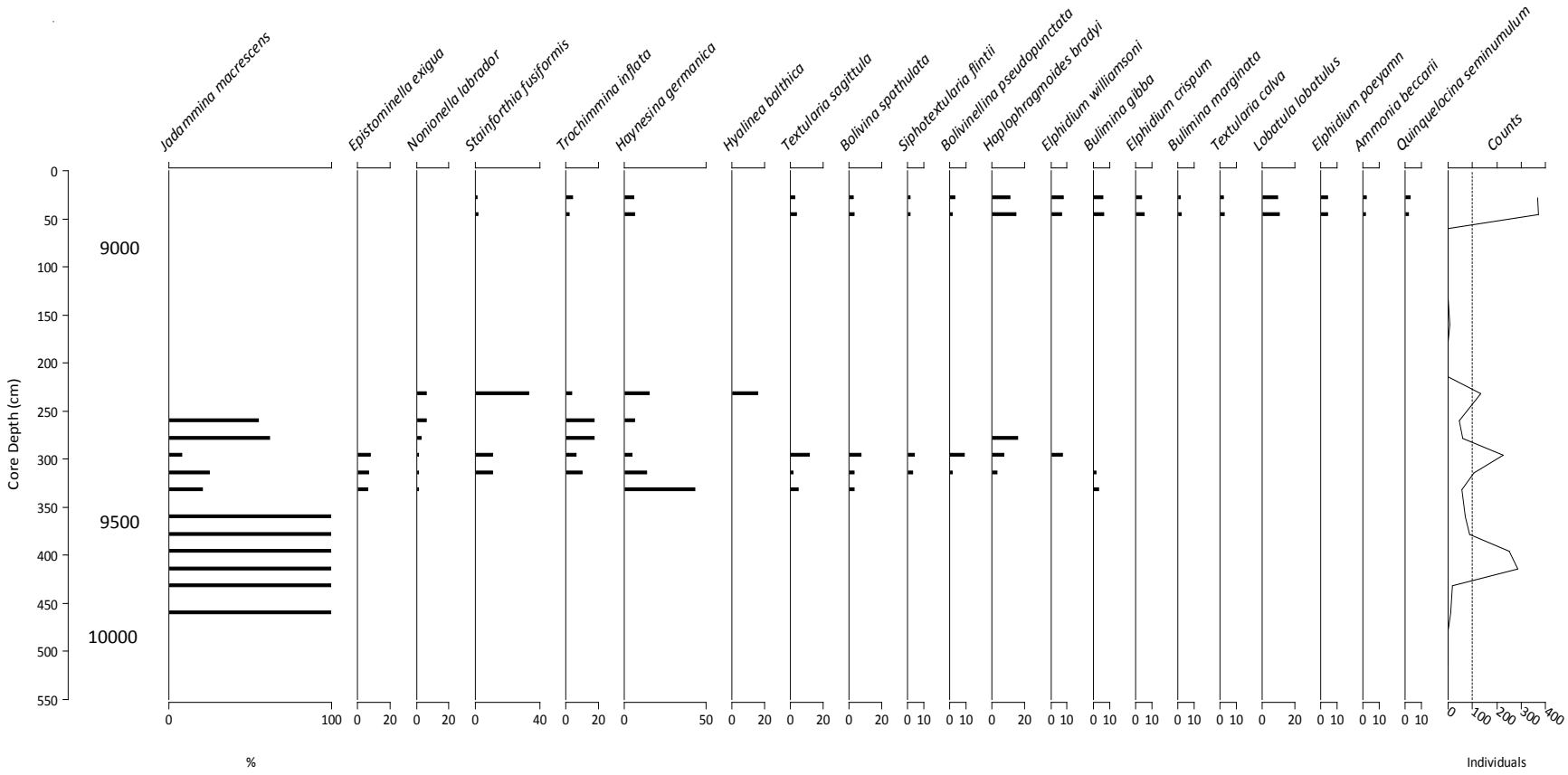

Figure 5.22: Foraminifera present in sediment core VC003; shown here are those present in >2% of the individual sample. Total counts numbers are presented on the right.

5.5.5 Summary of results for sediment cores VC002, VC003 and VC004

Sediment cores VC002, VC003 and VC004 were extracted in water depths ranging from 12.4 to 13.5 m and have similar chronologies encompassing 10000-8000 cal years BP. VC002 has one date of c. 350 cal years BP in the upper core confirming a sediment hiatus of c. 7500 years. This contrasts with the c. 5000 year hiatus identified in VC001. Physical proxies in these sediment cores reveal little change throughout the cores with the exception of the uppermost sediment (c. 60-0 cm) of VC002 and VC003; most obvious in the gamma density (VC002 and VC003) and mean grain size (VC003) data results. A PCA was carried out on the geochemical elemental ratios indicating the most influential driver for sediment cores VC002 and VC004 is Br/Cl and the most influential driver for VC003 is Ca/Ti. Microfossil evidence was poor in sediment core VC003 (diatom and foraminifera) and VC004 (diatom) but foraminifera results for VC003 revealed assemblages associated with distinct habitat changes from 556 to 150 cm. The upper sediment of VC002 and VC003 have similar lithology, gamma density and selected geochemical profiles indicating the upper sediment of VC003 is likely also recent material, however, this could not be confirmed with radiocarbon dating.

CHAPTER 6: Discussion

Introduction

Coastal environments are complex systems which are connected to open-ocean, terrestrial and atmospheric forces. Aeolian and meteorological conditions affect tides, currents, geomorphology, freshwater inputs, water level and temperature. On the western coast of Ireland, in Galway Bay, the modern behaviour of currents is well understood and recent depositional patterns can be predicted from this information. However, historical dynamics (e.g.: sea levels, geomorphology and ecological conditions) can only be inferred with the use of proxy evidence. The primary aim of the current research is to reconstruct paleoenvironmental conditions in Galway Bay. This chapter discusses the sediment chronology and lithology, diatom and foraminiferal stratigraphy and evaluates the potential lines of evidence for Holocene environmental change in Galway Bay.

6.1 Synthesis of Data

Sediment cores VC001 and VC003 yielded a higher amount of proxy evidence and as such are used as the primary representative cores of Holocene changes along the east to west transect in the Inner Bay and the Corrib Estuary. Synthesis tables are offered of VC001 (Figure 6.1) and VC003 (Figure 6.2) to summarise salient evidence acquired from each sediment core. Marine transgression is captured in the basal sediment of both cores and while the Corrib estuary core (VC001) experiences high sedimentation rates from 9000 to 8000 cal years BP, sediment accumulation rates slow considerably from 8000 to 6000 cal years BP before a sediment hiatus occurs. In the Inner Bay core (VC003), sedimentation rates continue at rapid rates throughout resulting in c. 1,000 years of early Holocene sediment. Radiocarbon dating indicates the three western cores (VC002, VC003 and VC004) experience a similar sedimentation rate and captures the early Holocene and as such VC003 offers a good representation of Inner Bay conditions while VC001 reflects the changes which occurred in the Corrib Estuary.

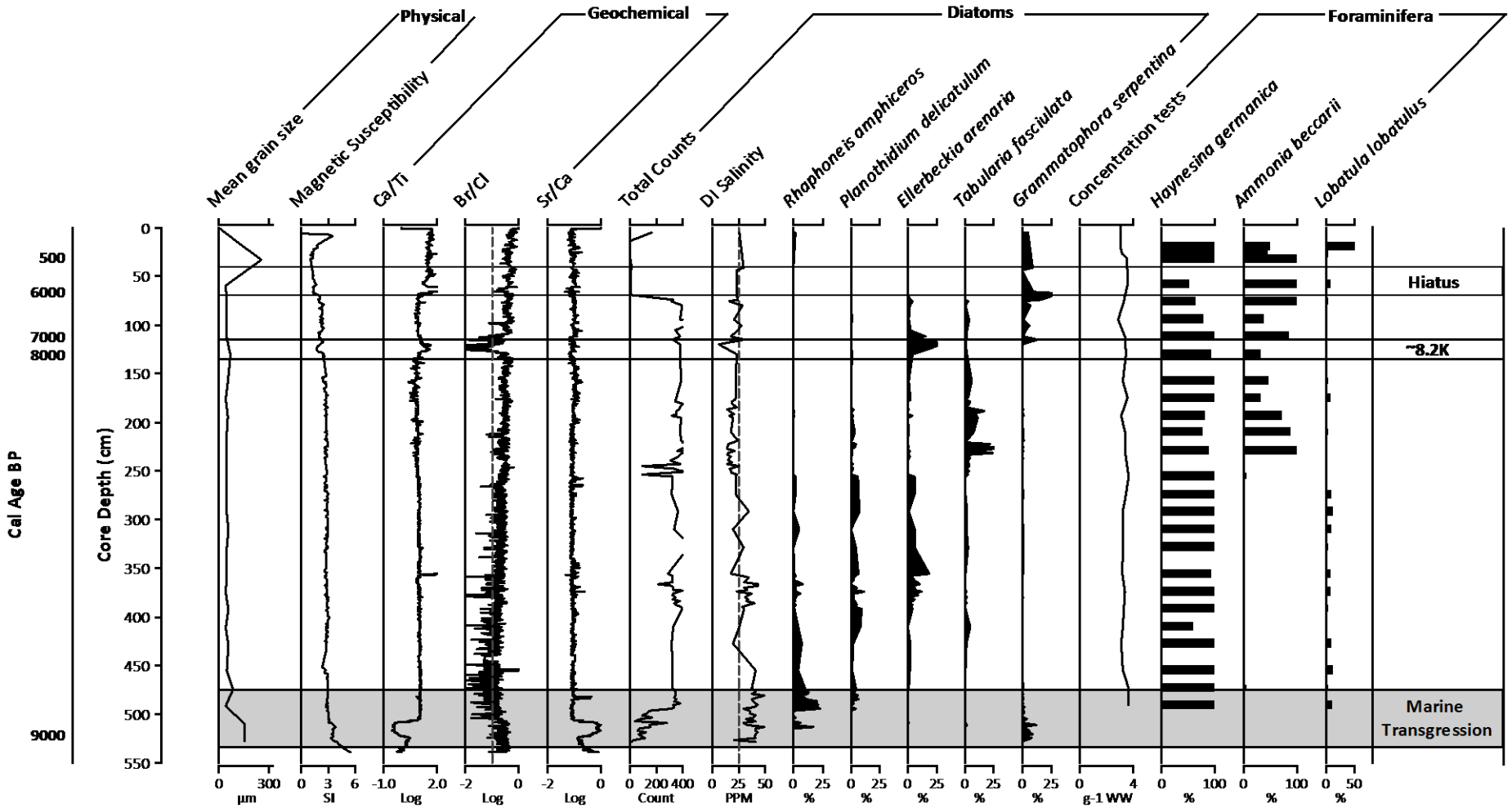

Figure 6.1: Synthesis plot for sediment core VC001. The primary y-axis gives sediment core depth and the secondary y-axis gives radiocarbon dates in Cal Age BP. A representative sample of the physical (mean grain size and magnetic susceptibility), geochemical (Ca/Ti, Br/Cl and Sr/Ca ratios), diatoms (frustule counts, inferred salinity and selected species) and foraminiferal (test concentrations and selected species) results. In the column on the right the zones of marine transgression, 8.2K cold event and hiatus are indicated.

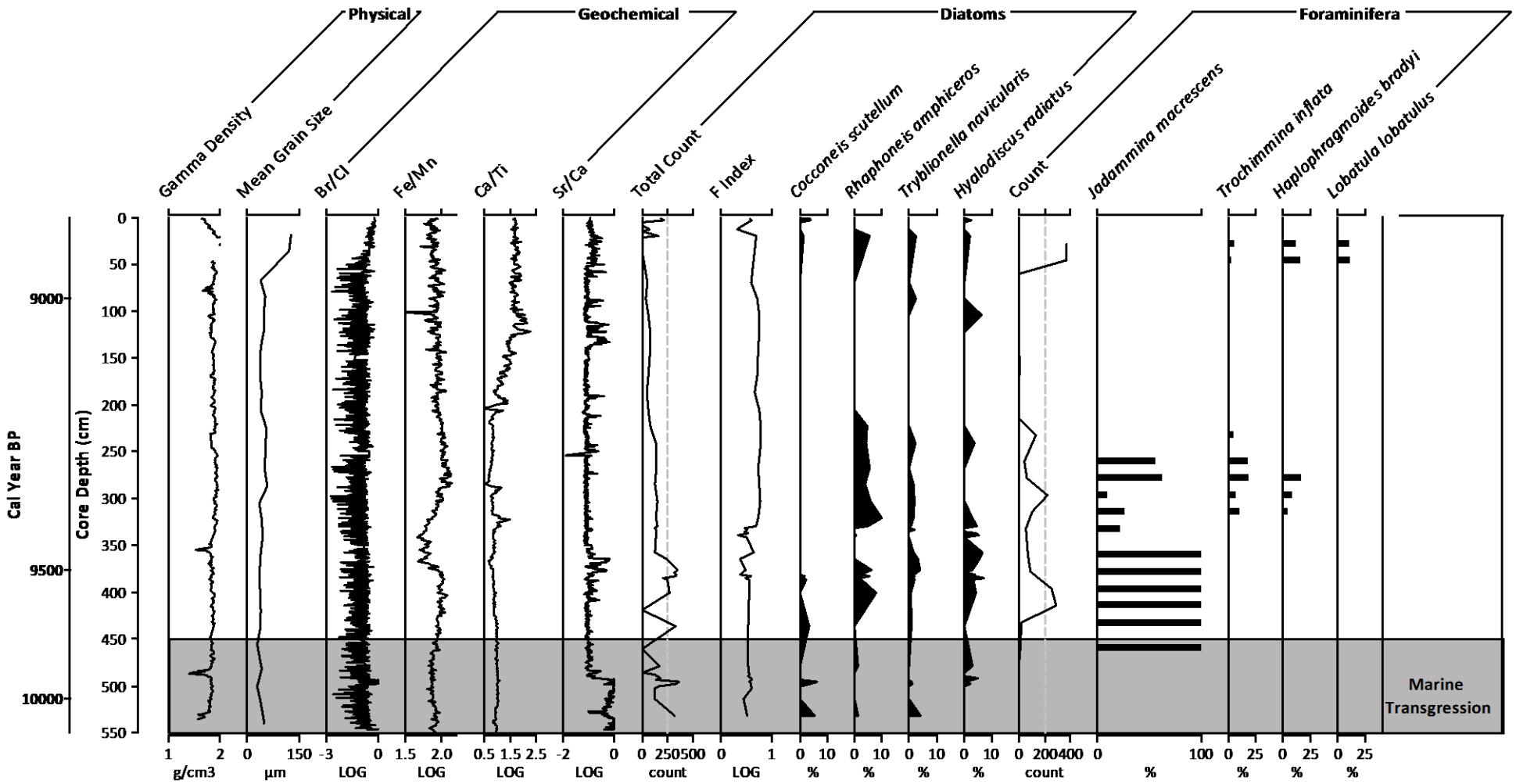

Figure 6.2: Synthesis plot for VC003. The primary y-axis gives sediment core depth and the secondary y-axis gives radiocarbon dates in Cal years BP. A representative sample of the physical (gamma density and mean grain size), geochemical (Br/Cl, Fe/Mn, Ca/Ti and Sr/Ca ratios), diatoms (frustule counts, f-index, and selected species) and foraminiferal (test counts and selected species) results. In the column on the right marine transgression is indicated.

6.2 Sediment chronology

The chronological record for the four sediment cores extracted from Galway Bay reveals a complex stratigraphy with incomplete Holocene profiles. The four six meter cores include mainly sandy-silt profiles, with sporadic layers of shell hash and laminations, organic wood fragments, and interruptions and truncations in the sediment sequence continuity. Despite the chronological complexity, many of the changes evident can potentially be linked to a changing coastal geomorphology and bathymetry, with altering marine and freshwater inputs, possible lagoon formation, and marine transgression associated with sea level rise across a tidal flat and low marsh system during the Holocene period.

The Quaternary literature uses a wide variety of Holocene sub-divisions but the most common usage is early, middle and late Holocene periods. Walker *et al.* (2012; 2014) provides a guideline for Holocene subdivisions; an early Holocene timeframe of 11700 to 8200 cal BP, a middle Holocene boundary from 8200 to 4200 a BP and a late Holocene division from 4200 cal BP to present. These boundaries are used here in the discussion of the Galway Bay results which span 10235 cal years BP to present. Table 6.1 provides a summary of data generated in this research and groups the data according to the appropriate Holocene subdivision.

Table 6.1: Summary data table. An overview of the physical, geochemical and microfossil results in this study. The corresponding Holocene time periods are given along with the paleoenvironmental conditions assessed based on proxy evidence.

Time Period	Western Inner Bay → Eastern Transitional Waters			
	VC004	**VC003**	**VC002**	**VC001**
Early Holocene **10.2 k-8.2 k** **cal years BP**	**Physical**			
	Extremely high sedimentation rate → High sedimentation rate Basal sediments sandy silt → Basal sediment sandy Large increase p-wave and magnetic susceptibility (mag sus) in basal sediments in all sediment cores. P-wave, gamma density and mag sus -little change above c. 9.8 Gamma density increase c. 8.2k			
	Geochemical			
	← c. 10.2-9.8k prominent changes in Sr/Ca, Ca/Ti & Br/Cl in base of all cores → ← Above c. 9.8k elemental ratios display little change until 8.2k → Ca/Ti, Si/Ti & Br/Cl increase c. 8.2ka (VC001)			
	Microfossil			
	Diatoms present in a small limited section, abundances low (marine/brackish).	Foraminifera appear c. 9.8k – largely agglutinated (abundance <300) Diatom abundances low (M/B)		Foraminifera appear c. 9k - largely calcareous (abundance >300). Diatom abundances low in basal sediments; high after c. 9k. (M/B/F)
	Paleoenvironmental change			
	Marine intrusion c. 10.2 k cal yrs BP → c. 9 k cal yrs BP ***Tidal Ranges*** ← EHW to MHHW to MHW → ***Environments*** Terrestrial to High marsh to Low marsh → Terrestrial to Low marsh to Mudflat			
Mid Holocene **8.2 k-6 k** **cal years BP**	**Physical**			
	No sediment	No sediment	No sediment	p-wave, mag sus no change; gamma density decrease
	Geochemical			
	No sediment	No sediment	No sediment	No change all elements
	Microfossil			
	No sediment	No sediment	No sediment	Foraminifera largely calcareous; Diatom counts high (M/B)
	Paleoenvironmental change			
	n/a	n/a	n/a	*Lagoon to open intertidal*
Sediment Hiatus	**n/a**	**Suspected Hiatus** (8K-500 yr BP)	**Hiatus** (8K-500 yr BP)	**Hiatus** (6K-500 yr BP)
Late Holocene **500-0 cal years BP**	**Physical**			
	No sediment	Gravelly sediment → Sandy sediment ← Low sedimentation rate - sediment starved →		
	Geochemical			
	No sediment	Prominent changes in Br/Cl & Ca/Ti		change in Br/Cl
	Microfossil			
	No sediment	Foram. shelf spp Low diatom counts	No data	Foram. intertidal & shelf spp Low diatom counts
	Paleoenvironmental change			
	No data	*Possible shelf seas*	*Shelf seas*	*Shelf seas*

Figure 6.3 uses the photographic images to summarise the estimated Galway Bay sediment core chronology. Due to the complex nature of the stratigraphical chronology, a colour scheme has been employed in this figure to give clarity to the corresponding sections of the sediment cores which will be considered in the discussion. The colour coding is as follows: green lines link the oldest sediment (10000-9000 cal years BP), blue lines link sediment ranging from 9000 to 8000 cal years BP, yellow lines indicate sediment 8000-6000 cal years BP, red areas indicate a sediment hiatus and purple lines link recent sediment (500-0 cal years BP). The dashed box outlines on VC003 indicate a probable sediment hiatus overlain with probable recent sediment and the possible correlation to sediment core VC002 is denoted with a question mark (?). This probable hiatus and recent sediment in VC003 is not confirmed by the chronology but correlations can be made from proxy evidence. All other links are confirmed. Sediment cores VC002, VC003 and VC004 span c. 1500 years in the early Holocene and exhibit rapid sediment deposition. This same period is incorporated in the bottom 2 m of VC001. Sediment core VC004 spans 9642-8572 cal years BP in its entirety. The mid Holocene is only reflected in sediment core VC001. A sediment hiatus is confirmed in sediment cores VC001 and VC002. Sediment deposition above the hiatus in the upper cores, radiocarbon dated to less than c. 500 cal years BP, is referred to as recent material and is confirmed in VC001 and VC002.

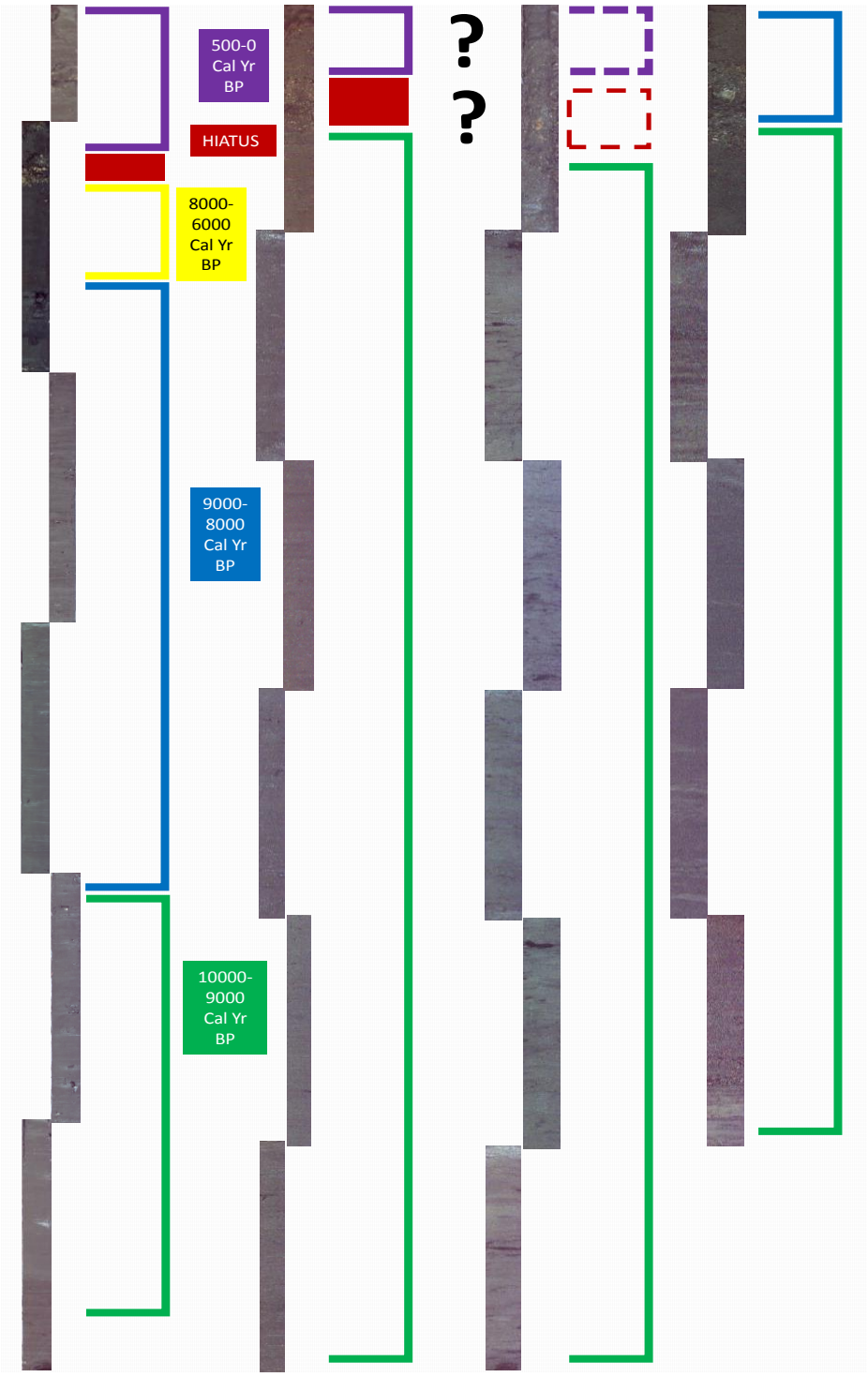

Figure 6.3: High resolution photographs of the sediment cores VC001, VC002, VC003 and VC004 from North Inner Galway Bay. Colours indicate correlating chronologies as follows: green, 10000-9000 cal year BP; blue, 9000-8000 cal year BP; yellow, 8000-6000 cal year BP; red, hiatus; purple, 500-0 cal year BP. Probable chronological links between VC002 and VC003 are indicated by question marks (?) and dashed boxes.

The lack of post-8500 cal years BP sediments in two of the four Galway bay cores is indicative of a major environmental change. A wash out of sediment c. 6000 cal years BP (VC001), c. 8500 cal years BP (VC002 and VC004) and c. 9000 cal years BP (VC003) is postulated in this research. A washout is defined as the removal of sediment from hydrological forces (Neuendorf, 2005). Sediment cores VC001 and VC002 have recent sediment deposited above the sediment washout. This indicates that the washout caused a major hiatus in the chronology of approximately 5000 to 7000 years. Sediment core VC004 has no recent deposition of material and the chronology here shows a complete washout of material deposited after 8978-8572 cal years BP. A review of the available seismic data looked at by Clarke (unpublished MSc, 2014) identifies a paleo deltaic system (identified as 'proto Corrib delta') in the modern estuary and inner bay and includes a paleo-estuarine channel. Sediment cores VC001, VC002 and VC003 fall outside of this paleo-estuarine channel and VC004 is within; this may explain the lack of recent sediments in VC004. If this was the main channel for both the Corrib River outflow and the route of initial marine intrusion, a continual movement of water would have acted as a control on sediment deposition here. Nearly all sediments from the mid and late Holocene have been washed out of VC002 and VC003 and all have been washed out from VC004. The inner-most core (VC001) has a continuous record until c. 6000 cal years BP before the hiatus presents itself.

6.2.1 Hiatus

Radiocarbon dating confirms the existence of a hiatus in sediment cores VC001 and VC002. Dates obtained from VC001 suggest the hiatus occurred between c. 6200 and c. 375 cal years BP (6409-6063 cal years BP and 492-259 cal years BP). This layer is identified by a 13 cm shell layer, many largely intact and some broken. Dates obtained from VC002 suggest the hiatus occurred between c. 9000 and c 350 cal years BP (9294-8798 cal years BP and 493-244 cal years BP). The layer is 12 cm in depth, consisting of largely broken shell material with few intact shells. A less pronounced shell layer is present from c. 40-20 cm in sediment core VC003 but no radiocarbon dates were obtained here. Figure 6.4 shows the photographs taken of sediment cores VC001, VC002 and VC003 of the hiatus and postulated hiatus (VC003) sections. Physical and geochemical evidence confirm similarities in the

surface sediments of VC002 and VC003 suggesting that the disturbance becomes less prominent with westward progression.

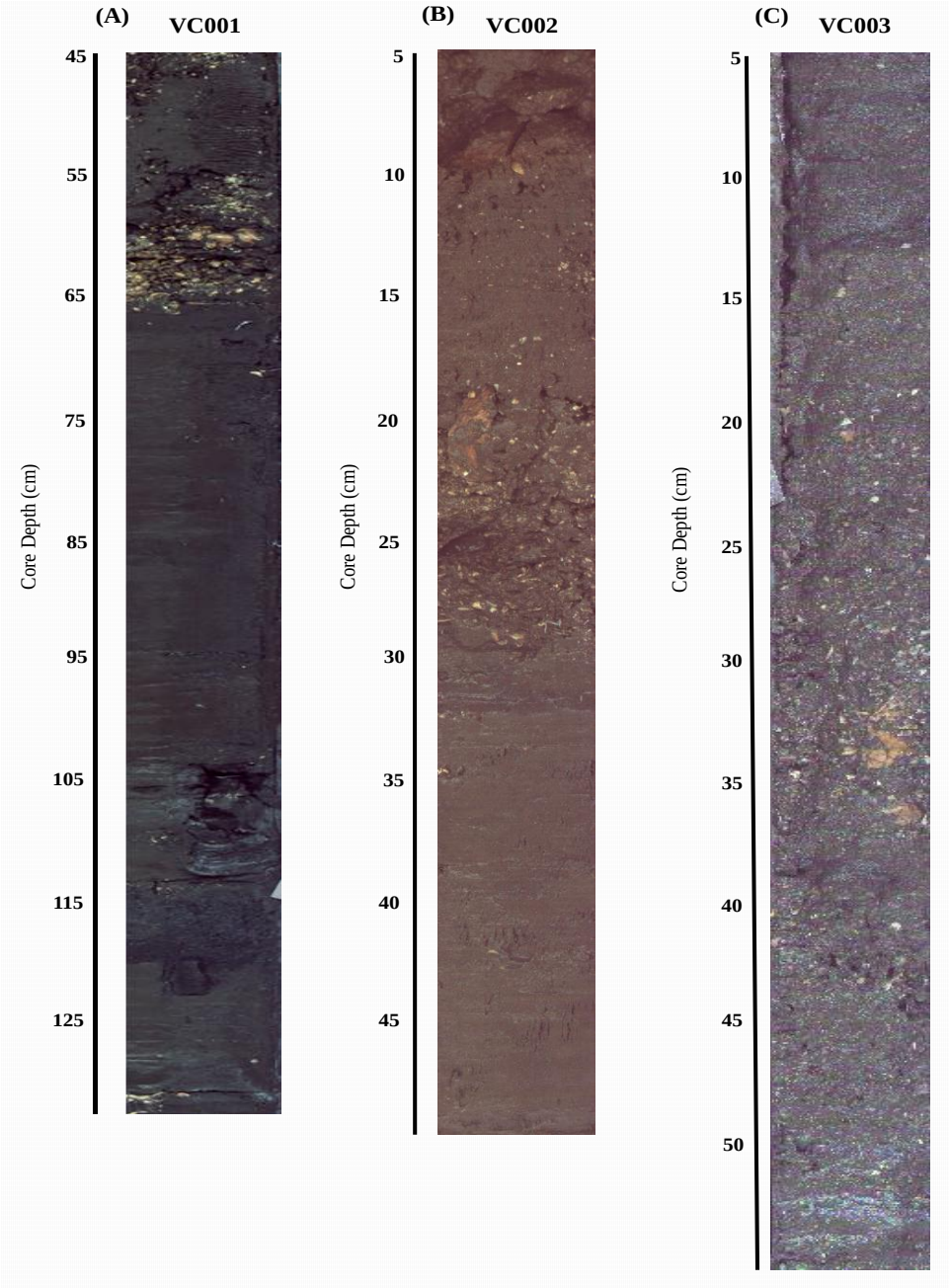

Figure 6.4: Photographs of the hiatus section of sediment cores. A) VC001, hiatus 68-55 cm; B) VC002, hiatus 30-18 cm; C) VC003, suspected hiatus 37-27 cm. The Corrib Estuary sediment core (VC001) displays the most prominent disturbance layer and the disturbance becomes less prominent with westward progression.

The correlation coefficient (r) was determined using select physical and geochemical proxies illustrating common trends in the upper (50 cm) cores of VC002 and VC003. In reviewing observable trends (Figures 5.17 and 5.18) in gamma density and Ca/Ti, K/Ti and Br/Cl for these two sediment cores, commonality was observed in the upper cores. As a result, a stratigraphic correlation (correlation coefficient (r)) was established to determine the strength of these similarities. The physical proxy, gamma density, has a moderate correlation between the two sediment cores (r=0.58) and likely reflects grain size similarities. Ca/Ti is commonly used as a stratigraphic correlation parameter in marine cores (Goudeau *et al*., 2014) and in VC002 and VC003 there is a strong correlation (r=0.70). The proxies K/Ti and Br/Cl have moderately strong correlations (r=0.62 and r=0.57 respectively) and reflect the similarities in these sections of VC002 and VC003 and are associated with sediment provenance and marine influence in these sections (Rothwell and Rack, 2006; Croudace *et al.,* 2006). The coefficient of correlation is used to give an indication of the strength of a relationship between two parameters. Here it allows for a strong to moderate positive relationship between the sediment in the upper 50-10 cm of VC002 and VC003. This, in turn, gives relevance to the existence of a sediment hiatus in VC003.

The time scale represented by the hiatus in all three sediment cores is expansive and spans c. 5000 to 7000 years, until modern sediment deposits are seen in the top of the cores (VC001 and VC002) dating from c. 400 cal years BP. The shell species found in VC001 are identified as *Spisula* cf *subtruncata*, a low intertidal and near shore shelf species living in depths up to 200 m along the coasts of the UK and Ireland (Cardoso *et al.,* 2007). Shell and shell hash deposits identified in VC002 and VC003 could not be identified due to poor preservation.

Four possible hypotheses are offered to explain the hiatus and deposition of shells and shell hash evident in the top 1 m (Figure 6.4). Figure 6.5 is a schematic diagram of the varying hypotheses discussed. The first possibility (hypothesis 1; H1) is that the shell laden deposit indicates a sudden and turbulent impact just prior to the modern deposit. This could reflect the onset of the cold period (the Little Ice Age (LIA)). The 15^{th} to 19^{th} centuries were the coldest of the millennium over the Northern Hemisphere (Mann *et al*., 1998; Jones *et al*., 1998) with increased precipitation and cold conditions varying in different regions

(D'Andrea *et al*., 2012). Lund *et al*. (2006) identifies diminished oceanic heat transport as a main contributor to LIA cooling in the North Atlantic and high Gulf Stream surface salinity, suggesting a tight linkage between the Atlantic Ocean circulation and hydrologic cycle during the past millennium. Rodrigo *et al*. (1998) analysed climatic information in private correspondence of the Jesuit order in Spain from 1634 to 1648. They showed a prevalence of intense rainfall and cold waves in Spain during that time. Araújo (2007) links the LIA with increased storms and a greater influence of flooding and discusses strong winds and great sand storms which acted upon coastal land regions in Portugal, resulting in increased sedimentation by rivers into littoral zones. She goes on to say that downstream and inside the estuaries, a sea level drop allowed sediments to migrate towards the sea and allowed rivers to make deposits close to river mouth forming river terraces.

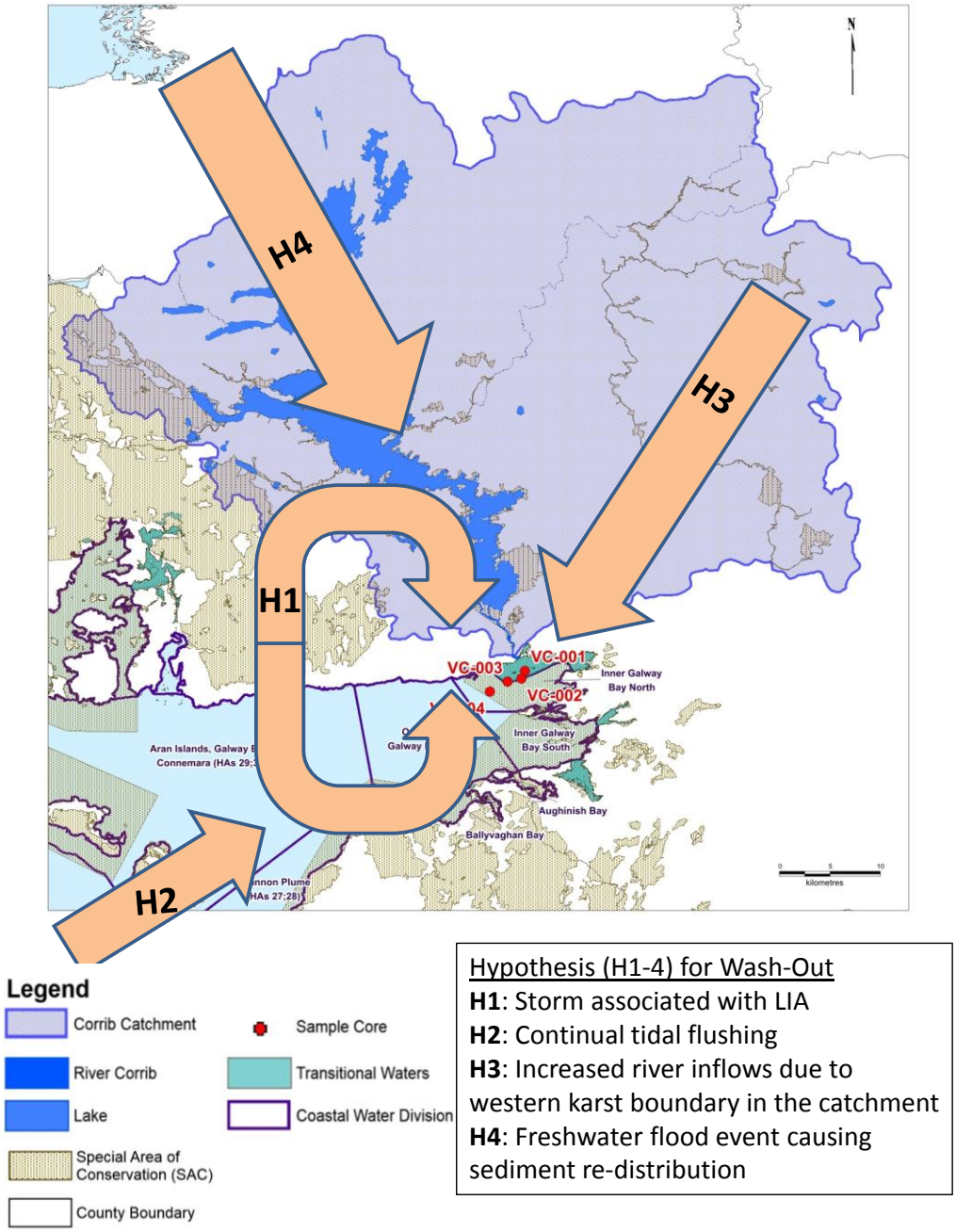

Figure 6.5: Schematic drawing of possible hypothesis which led to the sediment washout seen in sediment cores VC001, VC002 and VC003. Arrows indicate directional hydrological forcings and imply fluvial or marine influences.

Overwhelming evidence of the LIA and increased storminess points to the possibility of a storm event c. 1600 which created the prominent shell deposit in the estuary and the combination of fluvial and marine forces resulted in the deposit being so pronounced in the

estuary and less so in inner bay sediment cores VC002 and VC003. During this time period, one severe storm is on record in 1588 which reportedly wrecked 24 ships of the Spanish Armada off of the Western coast of Ireland (Lamb, 1991; 1995; Douglas, 2009). A definitive link between the deposit in the Corrib Estuary and this storm cannot be made as the severity of the storm has not been quantified and much of the evidence available is anecdotal. Additional coring of Lough Corrib and Inner Galway Bay could shed light on major storm events during the LIA and their implications for the Bay.

In an unpublished thesis, Wood (2011) examined nine sediment cores from Galway Bay. Largely outer Bay deposits, with three of the cores located in Southern Inner Galway Bay. The Southern Bay cores exhibited similar dating profiles with a large sediment deposit in the early-mid Holocene, a hiatus layer over lain by recent material. A further two sediment cores sampled by Woods in the outer bay along the northern coastline, as well, had recent materials in the top 200 cm and a large section of mid – early Holocene in the lower core. Radiocarbon dating was not straightforward, however, and anomalies exist in several of these sediment cores and it is suggested that re-working is the reason for the dating anomalies. The second hypothesis (H2) explored is that tidal forcing, a known culprit of reworking in many coastal environments (Edwards, 2013; Devoy, 1990; 2008) results in extensive reworking causing the hiatus seen in the sediment cores in this study. As sea level rose in the Corrib Estuary and Inner Galway Bay and low energy marsh systems slowly became intertidal areas, a continual tidal energy would have been exerted on this area. This would explain the lack of sediment deposition (hiatus) and the deposition of shells and shell hash. It is the opinion of this author, however, that the condition, arrangement and quantity of the shells found in the deposition in the Corrib Estuary, indicate a single depositional event, possibly at the end of a period of extensive re-working.

A third hypothesis (H3) explored to explain the hiatus relates to the karstic geology underlying the western side of the Corrib catchment which offers another possibility for freshwater intrusion into this system. Cave and Henry (2011) discuss subaqueous discharge into Southern Galway Bay via the highly karstified geology underlying surrounding catchments and the elevated levels of freshwater they expel into Kinvarra Bay. This could offer additional insight into the freshwater system of the Corrib Catchment and the opening

of a karstic channel during the Holocene. A freshwater signal noted in the DI salinity just prior to the hiatus could be a remnant of such a Corrib River deposit. It is however doubtful that this occurrence on its own would lead to enough hydrological forcing to break a large sediment barrier in the Estuary but it could contribute to the fluvial deposition. Conditions in the Corrib River and Lough Corrib should be investigated further for evidence of flooding and barrier breakage that would cause such a large freshwater influx. As well, paleo channels may reveal additional fluvial inputs to the estuary.

The wash out of these cores may have greatly affected paleo currents, tidal ranges and the paleoecology of the inner bay. Still other evidence of storm deposition in Galway bay during the Holocene shows that paleo storms, and possibly tsunamis, exerted great enough force in this area to transform bathymetry; thus changing the geomorphology of this section of Galway Bay frequently (Cox *et al.*, 2013). We know that coastlines are dynamic and change often due to several different forcings, the heightened climatological conditions during the early Holocene would have exacerbated this occurrence. Holmes et al., (2016) who looks at pollen and isotope proxies on western lakes, including Lough Corrib makes no note of an event in the sediment record c. 7,800-7,300. However, the focus of this study was the 8,200 event and data from earlier than 8,000 cal years BP is not included in the publication for Lough Corrib. A fourth hypothesis (H4) is that the changing hydrological conditions in the bay were heavily influenced by the changing bathymetry during this time and resulted in the wash out. Inundation by seawater coupled with greater mixing with freshwater from the Corrib estuary which surely would have taken place during this time, led to rapid changes in spatial sediment deposition. This altering of the Galway Bay floor could have caused the creation and dismantling of several sediment barriers over time. This would have opened up the estuary to greater tidal forcings and indeed left it vulnerable to storm events which are known to have a great affect on sediment distribution in Galway Bay (Cox *et al.*, 2012; Hall *et al.*, 2006; Williams *et al*., 2004). As sea levels rose and water levels increased, re-deposition took place and modern sediments began to re-accumulate.

6.2 The Early Holocene (10235-8200 cal years BP)

Coastlines are dynamic and change often due to several different forcings, and the heightened climatological conditions during the early Holocene would have exacerbated change. The early Holocene is defined as 11700-8200 (Walker, 2012; 2014) and sediment recovered in this study has a chronology encompassing 10235-8200 of early Holocene sediment.

The early Holocene in Europe is marked by a warm period initiated by the pre-Boreal Oscillation leading to the Holocene Thermal Maximum (HTM). The pre-Boreal Oscillation persisted until 10750 cal years BP (Fisher *et al.*, 2002) and signified the end of Late Glacial type environments in Ireland. The input of meltwater into the North Western Atlantic eventually led to changes in pack ice position on the North Atlantic and Arctic Oceans that likely affected ocean circulation and caused a rapid increase in atmospheric temperatures in Ireland and North West Europe (Diefendorf, 2005). The HTM was not a uniform phenomenon, however, and seems to vary spatially in Europe (Kaufman *et al*., 2004) with studies from Sweden (Laroque and Hall, 2003), North-West Russia (Ilyashuk *et al.* 2005) and the Austrian Alps (Ilyashuk *et al*. 2011) putting the HTM between 10000 and 9000 cal years BP and other European studies in Norway (Velle *et al.* 2005), Fennoscandia (Seppa *et al*. 2002), Northern Sweden (Rosen *et al.* 2001), Iceland (Caseldine *et al.* 2006) and Scotland (Edwards *et al.* 2007) giving the time frame for the HTM later, between 8000-7000 cal years BP. Studies from Ireland indicate a HTM ranging from 10800 cal years BP (Deifendorf, 2005) to 10000-9000 cal years BP (McKeown, 2013; Ghilardi and O'Connell, 2013).

6.2.1 Marine transgression

Marine transgression is inferred from sedimentological evidence in the bottom of cores VC001, VC002 and VC003 as the sea encroached on the inner area of Galway Bay. Basal sandy silts and sands with deposits of shell hash are evident at the base of sediment cores VC001, VC002 and VC003 (c. 10235-9040 cal years BP) and are evidence of either a fluvial deposit or deposition of sandy silt material as a result of tidal incursion into the inner bay. Sediment cores obtained using cable percussion borehole drilling, as part of the Galway

Harbour Extension project, were taken in the Corrib estuary in 2014 (Dunlop, 2014). While no dates were recorded, stratigraphical evidence obtained from these records have similar profiles to VC001 and VC002 with largely silty material, sandy silts and sands with areas of shell hash. One core in particular is in close proximity to VC001 in the Corrib Estuary and has terrestrial deposits (peat) less than one metre below the base of VC001. This peat layer is overlain with sandy silt material as seen in the basal layer of VC001, VC002 and VC003. In sediment core VC001, Mylotte *et al.* (2014) describe a lignin presence in the basal sediment which would indicate a terrestrial input between c. 10000-9000 cal years BP. Lignin is a chemical compound found in plants and indicates contributions from terrestrial organic matter (plant material). Initial interpretations were of a deltaic environment with a possible fluvial deposit but other proxy evidence does not fully support this hypothesis. An argument can be made that this is potentially marine deposited sediment during the early phase of marine transgression as sand was beginning to enter the terrestrial environment by occasional tidal forcing. Microfossil evidence from the basal sediments of VC001 and VC003 supports the theory that this was a largely terrestrial environment with low level marine influence. Diatom abundances here were low, ranging from 14-164 individuals with only one sample recording 276 taxa. Marine and brackish diatoms dominate the assemblage and breakage is high; foraminifera are not present, suggesting a semi-terrestrial environment with early stage marine transgression occurring c. 10000 cal years BP in the Inner Bay and c. 9000 cal years BP in the Corrib Estuary.

Poor diatom preservation and high breakage are also a potential indication of depositional conditions and offer another piece of evidence that a changing environment existed (Hemphill-Haley, 1995). In addition to the hypothesis that continual low level tidal forcing caused these conditions, this could mean that these diatoms are the result of storm deposition due to an increase in storm frequency associated with the increased temperatures of the HTM (McKeown, 2013). Occasional deposition from increased storm wave activity would potentially deposit a higher proportion of broken valves (Pilarczyk *et al.,* 2014). Semi-quantitative diatom evidence tells us that diatom taxa recorded are marine, brackish diatoms and are tychoplanktonic and/or episammic. Diatom assemblages at 10000 cal years BP are dominated by *P. sulcata, Delphineis minutissima, Tryblionella compressa* and *Cocconeis*

scutellum which are all marine species with a tolerance for brackish waters. Their deposition is most likely the result of their attachment to sediment that had been transported during this time and deposited by wind and during storm surges and this facies likely represents extreme high water (EHW), above the extent of the Highest Astronomical Tide (HAT) (Hemphill-Haley, 1995). Generally, DI-salinity is highest in the basal sediment of VC001 and very low levels of freshwater diatoms suggest that the estuary environment was not heavily influenced by the Corrib as it is in modern times and the diatoms are the result of marine deposition.

However, one sample in the inner bay (at the base of VC003) revealed the presence of *Ellerbeckia arenaria*, *Encyonema minutium* and *Fallacia pygmaea*, freshwater diatom species that would indicate a fluvial deposit. As this facies of the core is c. 1000 cal years BP older than the estuary core, this could be a reflection of earlier conditions where the fluvial channels of a paleo deltaic environment extended to this area. Another alternative is that the inner bay was separated from the modern estuary during this time and had differing environments as a result. Williams and Doyle (2014) discuss the existence of an Oak-pine forest on the central western seaboard of Ireland with two relevant radiocarbon dates from storm exposed *Pinus* (7466-7414 cal years BP) and *Quercus* (6281-6183 cal years BP) tree stumps from Spiddeal to Blackrock on the northern shore of Galway Bay. It is possible that this forest extended out towards one or more of the sediment core sampling positions used in this research. Initial marine transgression was probably slow and highly variable along the coastline, exhibiting itself in the fossil record with varying periods of fluvial and marine dominance as the coastline becomes more inundated. The geochemical signals in the basal sediments indicate changes associated with the onset of a marine environment as well. The rise in the Ca/Ti ratio c. 10000 cal years BP to 9000 cal years BP, indicates an increase of marine biogenic material (Goudeau *et al.,* 2014) and the fall in the Sr/Ca levels during the same interval is interpreted as a severe change in water depth associated with the sudden influence of deeper marine waters (Croudace *et al.,* 2006). Sr/Ca gives an indication of $CaCO_3$ mineralogy – high values when aragonite predominates, low values when calcite predominates (Bischoff *et al.,* 2005). The high Sr/Ca ratio in this area is reflected in the lack of calcareous foraminifera (calcite) and possibly indicates changes in hydrological conditions. The paleoenvironmental change here is likely repeated high tides, which increased the shear stress on the bed, enough to erode the cohesive (silt, clay) sediments

despite being armoured with small amounts of sand (Cooper *et al*., 2009). This is seen in the sediment profile of VC001 as the sandy basal sediment deposit is overlain with silty material c. 9000 cal years BP (500 cm) (Appendix A). The base fluvial diatom deposit recorded in VC003 can be seen as the last evidence of the pre-existing conditions prior to the marine transgression in the inner bay. This could possibly have a link to the Galway Bay EIS sediment cores (Dunlop, 2014) which were 8 m cores and exhibited peat deposits c. 7 m in an adjacent area.

Existing sea level models published in Edwards and Craven (2017) discuss the use of Primary/Secondary Limiting Dates and Primary/Secondary SLIPs (Sea Level Index Points). Galway Bay has limited data available for the Irish RSL model discussed here with only one radiocarbon date in Galway Bay listed as a 'Primary Limiting Date.' This date is likely the tree stump discussed in Williams and Doyle (2014). The basal dates taken from sediment cores VC001 and VC003 can contribute to the existing RSL models as SLIPs. In Figure 6.6 a sea level curve has been generated using the data from V001 and VC003 and presented with the RSL curve available for Galway Bay.

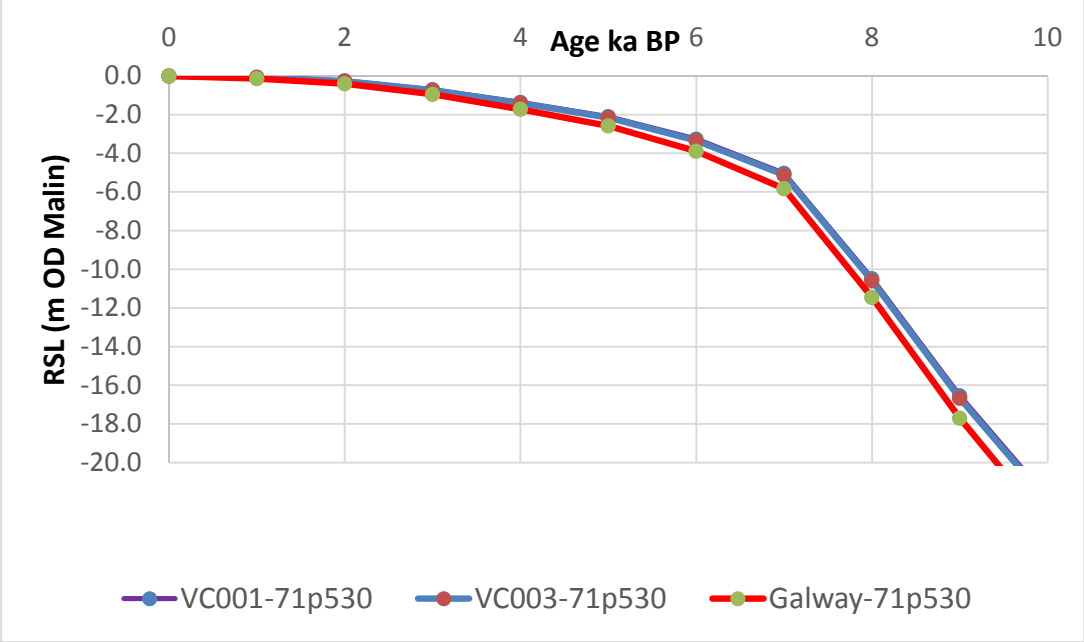

Figure 6.6: RSL curve generated based on Edwards and Craven (2017). The red line indicates the existing curve based on data from Galway Bay and VC001 and VC003 data is represented on the second curve.

There is a slight offset between RSL indicated by the cores used in this research and the existing information for Galway Bay indicating that there is a 1 to 2 m difference in RSL c. 9000 ka BP. This difference becomes smaller by c. 6000 ka BP where there is <1m of a difference between the two data sets and a nil difference inferred c. 4000 ka BP. Contributing this new data to existing models can only serve to strengthen the accuracy of such models. Additionally, The Glacial Isostatic Adjustment (GIA) model presented in Bradley *et al*. (2011) can also infer RSL and cores VC001 and VC003 have been input into this model to hypothesise sea level rise in Galway Bay. Figure 6.7 shows GIA in Ireland at 10kyr, 9kyr, 7kyr BP and 4 kyr BP. Again here, we see an offset between RSL generated by the model and actual marine transgression indicated by the data used here. Data acquired from sediment cores VC001 and VC003 indicate a sea level of -20 to -18 m c. 10000 cal years BP where the GIA gives a level of -22 m. The contribution of this data to these models can assist in generating data with higher spatial accuracy along the western coast of Ireland; specifically Galway Bay where data is lacking. This can only serve to improve models relating to GIA and RSL in Western Ireland where existing data for this purpose is scarce. As well, it helps to understand the spatial and temporal variation in marine transgression on the west coast of Ireland.

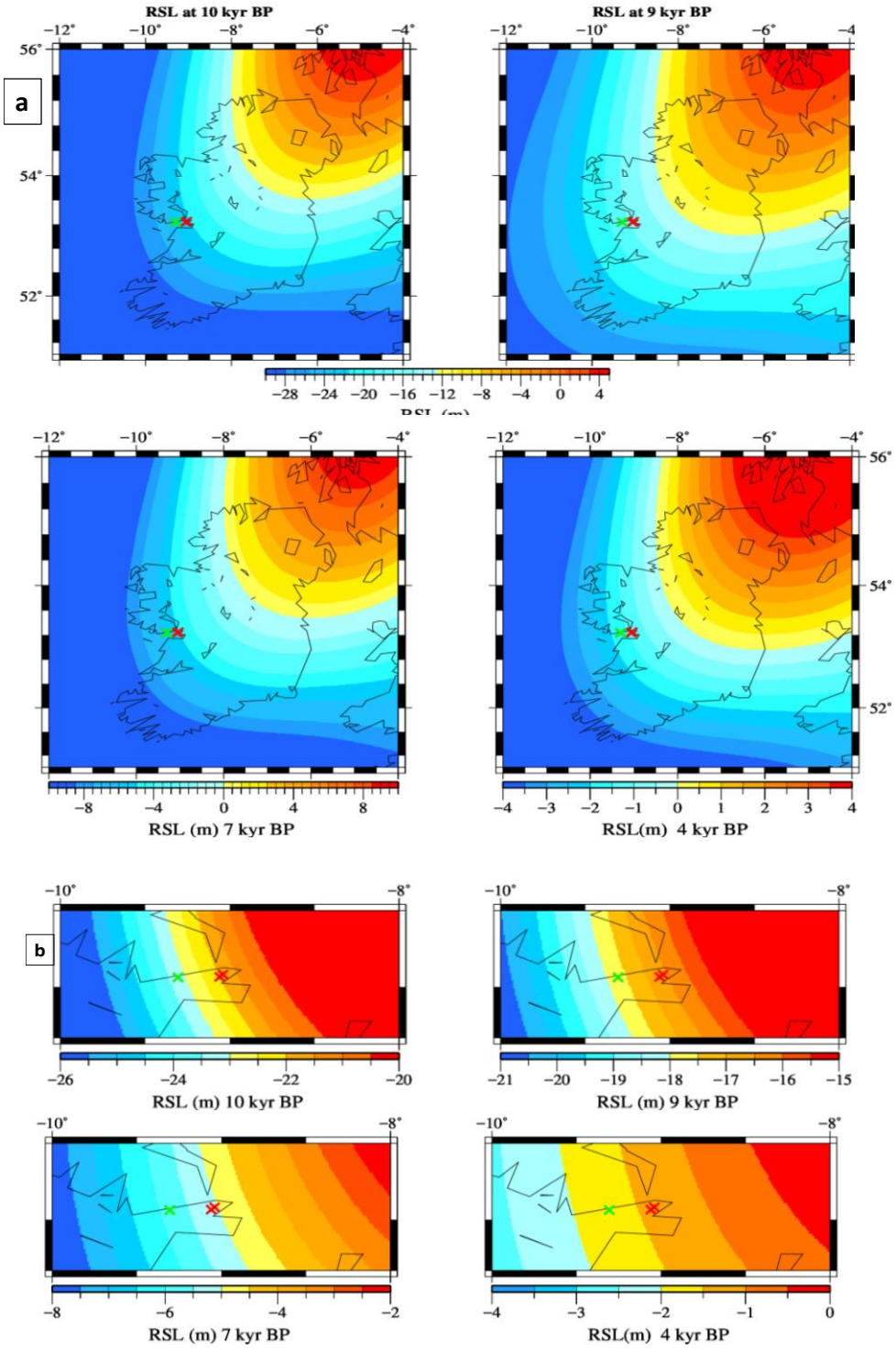

Figure 6.7: Sediment cores VC001 and VC003 in the Glacoal Isostatic Adjustment (GIA) Model (Bradley *et al*., 2011). The green 'x' is the existing primary limiting point identified in Edwards and Craven (2017); the two red 'x' marks are VC001 and VC003. (a) Ireland RSL for 10, 9, 7 and 4 kyr BP; (b) Galway Bay RSL for 10, 9, 7 and 4 kyr BP.

6.2.2 Early Holocene paleoenvironmental coastline changes

The sediment cores demonstrate that a large amount of sediment (5-6 meters) was deposited during the early Holocene from c. 10000-8000 cal years BP in northern inner Galway bay after marine transgression. This is common in coastal zones during Early Holocene sea level rise (Edwards, 2013) and can potentially be attributed to marine incursions, storm deposits and/or fluvial deposition on a paleo-coastline. For example, Wood (2011) attributed observed inversions of sediment dating to re-working associated with tidal forcing.

Sediments deposited in coastal environments are influenced by several mechanisms including aeolian processes, speed and directionality of tidal forcing and intertidal wave action. Tibert *et al*. (2007) examined ostracod oxygen isotope and carbon isotope values from a sediment core in Lough Corrib and determine early Holocene conditionswere dominated by cold lake water heavily influenced by carboniferous limerstone in the watershed. The high levels of sediment deposition displayed in VC002, VC003 and VC004 from c. 10235 cal years BP to c. 8572 cal years BP, are possibly indicative of a low energy tidal/mud flat environment or a high marsh environment as it transforms into a low marsh or tidal flat environment with limited freshwater influnce. Lake studies indicate that the climate during this time in Western Ireland is cool and arid (Diefendorf *et al*., 2006; Tibert *et al*., 2007). Sediment core VC001 experienced a lower sedimentation rate during this period and becomes intermittently less saline and more heavily influenced by the freshwater outflow of the Corrib River; a deduction based on microfossil evidence. This could be attributed to the influence of discreet coastal geomorphology and bathymetry changes, which caused varying freshwater inputs. The discreet ecological changes in habitat and geomorphology are driven not only by climate changes but also by the resulting changes to bathymetry in the inner Bay. Some studies have pointed to the possible existence of a paleo-drowned drumlin field in inner Galway Bay (McCabe and Dardis, 1989; Williams and Doyle, 2014). This offers one possibility of a varying bathymetry in the inner bay, which would have greatly affected paleo currents, tidal ranges and the overall paleoecology. Other evidence of storm deposition in Galway Bay during the Holocene shows that paleo storms, and possibly tsunamis, exerted enough force in this area to transform bathymetry thus changing the geomorphology frequently (Cox *et al.*, 2013). The rapidly increasing temperatures culminating with the

HTM in Ireland (c. 10800-9000 cal years BP) (Deifendorf, 2005; McKeown, 2013; Ghilardi and O'Connell, 2013), would have meant greater variation in precipitation and climatic changes. This area of the inner bay would have experienced changing patterns of sediment transport and deposition as a result.

The appearance of foraminifera in the sediment record can help determine the tidal zone; the distribution of foraminifera in the intertidal zone is usually a direct function of elevation relative to the tidal frame, with the duration and frequency of intertidal exposure as the most important controlling factors (Horton and Edwards, 2006). The early Holocene is generally regarded as a period of marine low stand conditions in Ireland (McCabe *et al.,* 2007; Williams, 2012). Foraminifera first appear in the sediment record c. 9800 cal years BP in VC003 (Figure 5.22) and c. 9000 cal years BP in VC001 (Figure 5.13). In VC003, these foraminifera are representative of high marsh environments. The silty substrate, with a 9-15% clay fraction, supports a monospecific population of the agglutinated foraminifera *Jadammina macrescens*. Haake (1982) gives account of marsh foraminifera living in areas not connected to the sea in inland marshes with salt rich waters in northern Germany, and Patterson *et al*. (1990) in salt springs in Canada (Patterson *et al.,* 1990) where *J. macrescens* appears as a single taxon in the fossil record. As well, Haslett *et al*. (2007) discuss a monospecific *J. macrescens* assemblage present immediately after an interval devoid of foraminifera as indicative of the HHW extending to the MHHW. The distinctive assemblage could therefore potentially represent the uppermost paleotide level in the early Holocene in the inner Bay. It is here also that diatoms see their highest concentration in the VC003 sediment core with polyhalobian, epiphytic species dominating the assemblage. Species indicative of mud/tidal flats and marsh environments are found here (i.e.: *C. scutellum, G. oceanica* and *T. compressa*). As the foraminifera *Trochammina inflata* begins to appear as a significant part of the assemblage along with *H. germanica* c. 9500 cal years BP, the ecology changes to typical Mean High Water (MHW) conditions suggesting tidal/mud flats (Murray, 2006). Diatom profiles change here as well with a strong freshwater signal as evinced by the appearance of *Hyalodiscus radiata, Aulacosira granulata* and *Melosira varians*, all freshwater planktonic species indicating a fluvial deposit at this point.

By c. 9400 cal years BP, diatom microfossil evidence is present in VC001, VC003 and VC004 . The most western sediment core (VC004) only has diatoms in a limited number of samples at the base of the core (9642-9287 cal years BP). These diatoms, however, were largely tychoplanktonic with 64% comprised of *Campylosira cymbelliformis, Cymatosira belgica* and, *Raphoneis amphiceros* and benthic cosmopolitan species *Delphineas minutissima* and *Dimeregramma minor* (Hasle and Syvertsen, 1996; Witkowski *et al.* 2000). According to Hasle & Syvertsen (1996), *D. minutissima* and *R. amphiceros* are often stirred up in turbulent waters and become part of the benthic plant communities. Denys (1989) relates these diatom assemblages to intertidal and subtidal sand and mud flats. Intertidal environments are characterized by extensive tidal flats intermixed with a series of interconnected channels (Mariotti and Fagherazzi, 2012). The sedimentary dynamics in this type of environment are changeable on a temporal and spatial scale (de Swart and Zimmerman, 2009) and may be why diatoms are seen only in one section of VC004; gentle wave action and tidal currents resulted in the redistribution and remobilization of sediment in intertidal environments (Edwards, 2013) and could have altered the placement of the channel or resulted in increased sediment raising the area above sea level leaving it no longer affected by direct hydrological influences. The diatom assemblages in samples from VC001 c. 9400 cal years BP have a similar profile but the DI-salinity shows a freshwater pulse here. While a low percentage of freshwater species occur at this interval (e.g.: *E. arenara* and *Encyonema silesiacum*; <10%), it is possible that low sampling frequency and diminished count numbers (250-290 individuals) have exaggerated the drop in salinity (from 40 PPM to 19 PPM). It is more likely the environments surrounding VC001 and VC004 had comparable intertidal environments during this time. The majority of diatom assemblages found in VC001 offer potential evidence of the paleotidal regime in the North Inner Bay as inundation increases in the early Holocene. Individual diatom frustule counts in VC003 are very low (39-137) and foraminifera disappear from the fossil record. The environment around VC003 was experiencing lower marine influence, possibly a regression in sea level likely due to geomorphological conditions; or a raised area due to sediment deposition, and thus the creation of a barrier adjacent to this core. This also may be attributed to the intertidal environment and a change in channel placement.

Diatom taxa increase c. 8800 cal years BP (VC001), with all counts exceeding 300 frustules, with the exception of three samples. This section of diatom Zone 2 (Figure 5.9) has a varied assemblage with *D. minor* and *P. sulcata* representing the highest percentage of diatoms; found as part of this assemblage also is *Tryblionella compressa, R. amphiceros, Cymatosira belgica, Planothidium delicatulum, Ellerbeckia arenaria, Cocconeis peltoides* and *Grammatophora oceanica*. *E. arenaria* was abundant in a limited area here in a clayey silt band. The deposit of clayey material coupled with the appearance of *E. arenaria*, a ubiquitous, planktonic, freshwater species most likely indicates a fluvial deposit (Berglund *et al*., 2005). This evidence corresponds with a freshwater spike at the same interval in the DI-salinity. One possible scenario is that the lower temperatures in the North Atlantic region that contributes to increased rain in lakes preceeding the 8.2 kyr cold event (Tibert *et al*., 2007) are seen in the sediment record here. This may have caused flooding of the Corrib River and may have resulted in this deposit. Head *et al*., (2006) investigated a coastal sediment core on Achill Island in County Mayo, Ireland and discuss a sustained disruption to vegetation over hundreds of years before and after the 8.2 kyr cold event. They determined that the landscape was impacted by a long-term cooling event in the early Holocene, and not the single century length 8200-year meltwater event proposed in many other records in the North Atlantic region. This offers another possibility to cold, freshwater pulses toward the end of the early Holocene.

Thalassionema nitzschioides, a species indicating relatively warmer waters (Jiang *et al.*, 2001; Ren *et al*., 2009), appears c. 8500 cal years BP (229 cm) as 13% of the assemblage. A possible warm water pulse and a period of DI-salinity fluctuation could indicate greater storm frequency and therefore higher precipitation. This is further reinforced with the presence of *Tabularia fasciculata* (229 cm) as 20% of the assemblage. *T. fasciculata* is a river diatom with a tolerance for brackish waters (Mills *et al.,* 2009) and higher nutrient levels (Fluin *et al*., 2009) and thus potential evidence of Corrib River input. It is apparent that c. 8500 cal years BP was highly variable climatically and mixed levels of tidal and wave energy were acting upon the inner Bay at this time. During this time, Europe experienced widespread cooling, culminating with the well documented 8200 abrupt cooling event (Alley *et al*., 1997; McDermott *et al.,* 2001; Magny and Bégeot, 2004; Veski *et al.,* 2004; Diefendorf, 2005; Diefendorf *et al.,* 2006). The pattern of cooling implies that heat transfer

from the ocean to the atmosphere was reduced in the North Atlantic, possibly altering atmospheric circulation and intensifying westerly winds. This caused highly localised responses in Europe with Scandinavia and along the North Atlantic seaboard, experiencing an increase in precipitation (Barber *et al*., 1999; Hammarlund *et al.,* 2005; Hede *et al.,* 2010) and other areas, for example Ireland (e.g.: McDermott *et al.,* 1999; Baldini *et al.,* 2002, 2007; Molloy and O'Connell, 2004; Ghilardi and O'Connell, 2013; O'Connell *et al.,* 2014; Holmes *et al*., 2016) and southern England (e.g.: Rousseau *et al*., 1998; Garnett *et al.,* 2004), experiencing a reduction in precipitation.

The sediment from cores VC002, VC003 and VC004 pre-date the 8.2 ka cooling event, however, a possible signature of this event can be seen in the estuary core (VC001). The sediment profile exhibits a sandy deposit with disturbed white laminations in the sediment dated between 8801-8393 cal years BP and 8140-7825 cal years BP. Supporting physical and geochemical proxy evidence is presented in Figure 6.8, which shows the upper 200 cm of sediment core VC001 and selected proxies. The event is not captured in the foraminiferal record; possibly due to the sampling resolution. A change in p-wave velocity, gamma density and magnetic susceptibility coupled with the decrease in organic carbon and a freshwater pulse seen in the DI-salinity could be a signal from this event. Lough Corrib was experiencing cool and humic conditions with relatively high precipitation rates during the 8.2 kyr cold event which contributed to hydrological open conditions (Tibert *et al*., 2007). This is likely the cause of the strong freshwater signal seen here in the DI salinity. As well, the Ca/Ti increase and K/Ti decrease indicates a change in sediment provenance with Ca/Ti reflecting detrital input (Lacka *et al.,* 2015). The rise in Si/Ti could mean an increase in biogenic silicia, which can be linked to higher productivity associated with colder waters (Cantarero, 2013). The lowering of Br/Cl at this interval possibly reflects a freshwater pulse and is supported by a decrease in DI-salinity. The evidence is not conclusive but it is likely these signals could relate to the known 8.2 kyr cold event which signals the end of the Early Holocene (Walker, 2012; 2014).

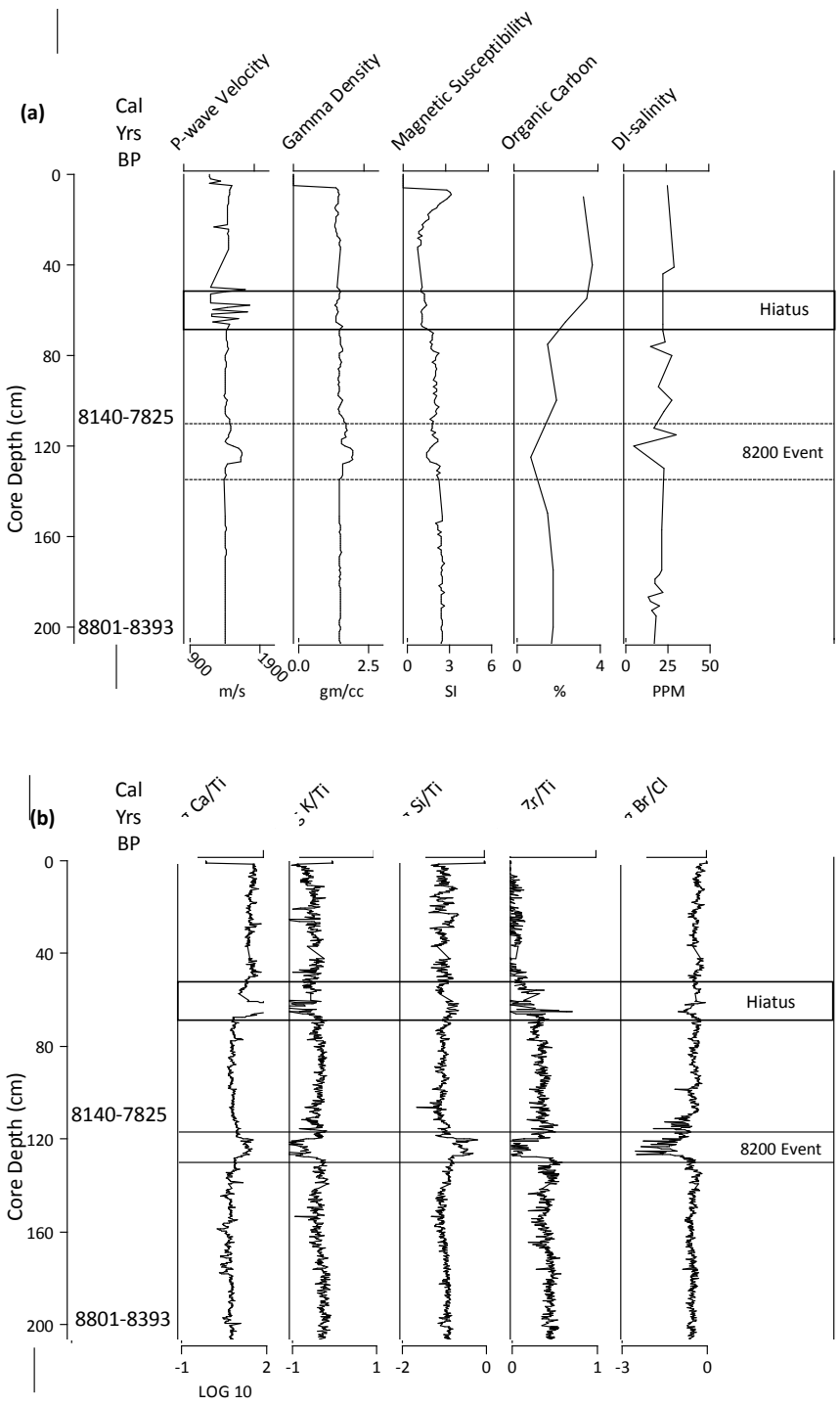

Figure 6.8: The upper 200 cm of VC001 is displayed showing possible evidence of the 8.2 ka cold with selected physical and geochemical proxies. A) Physical evidence: p-wave velocity (m/s), gamma density (g/cm^3), magnetic susceptibility (SI), organic carbon (%) and DI-salinity (PPM). B) Geochemical evidence: Ca/Ti, K/Ti, Si/Ti, Zr/Ti and Br/Cl.

In summary, the diatom and foraminiferal results can be interpreted as a paleo-tidal regime that changes from EHW to HHW and then as water levels rise, from MHHW to MHW with high to middle marsh and mudflat environments existing during the early Holocene in the inner bay.

6.3 The Mid Holocene (8200-6063 cal years BP)

The mid Holocene ranges from the end of the 8200 cold event to the 4200 event (Walker 2012; 2014) but the chronology in this study only encompasses sediment from 8200 cal years BP to 6063 cal years BP. The 8200 cold event is discussed as the close of the early Holocene. This section will discuss sediment that has an age range from 8140-6063 cal years BP as the mid Holocene sediment.

The changing climatic conditions during the mid Holocene are not straightforward (Steig, 1999). While major trends are widely accepted across Europe (HTM, mid Holocene cooling and mid - late Holocene warming trends) studies carried out in Ireland have shown a number of climate events, including at 5200–5100 cal. years BP, believed to be linked to increased storm activity (Caseldine *et al.*, 2005) and the 4200 cal. years BP event, which has been linked to wetter conditions (Swindles *et al*., 2012). As well, Ireland based studies have also revealed discreet changes over varying spatial and temporal scales. This can often be due to varying paleoecological proxies used in the studies (e.g.: pollen, Ghilardi and O'Connell (2012); oxygen isotope, Deifendorf (2007) and chironomids, McKeown (2013)). In other instances, variations in local hydrology and geomorphology create an environment where certain events are not recorded in the sediment and fossil record. Hede (2010) found evidence of high accumulation of minerogenic sediment during high precipitation conditions with an inferred shift to more humid conditions, which would lead to water level rise.

Mid-Holocene temperature decreases have been documented at a range of sites in Ireland. McKeown (2013) records a temperature decrease during the mid-Holocene at Lough Nakeeroge, Ireland and reaching the lowest values between 7800 cal. years BP and 7500 cal years BP. Head *et al*. (2007) and Edwards *et al*. (2007) also identify a temperature decrease with a 320 year prolonged cool period in western Ireland and Scotland from 7790 cal. years BP to 7470 cal. years BP. Atmospheric warming in Europe begins to take place c. 8000-

7000 cal years BP (Bassetti *et al*., 2016) and increased winter precipitation between 7550 to 7250 cal years BP is noted by Magny and Bégeot (2004) and Diefendorf *et al*. (2006).

6.3.1 Mid Holocene paleoenvironmental coastline changes

Sediment core VC001 is the only core with sedimentary evidence from the mid Holocene (Figure 6.1). Diatom and foraminiferal abundances are high at the onset of the mid Holocene c. 8100-7500 cal years BP. Microfossil evidence during this time reflects a change in environment, with agglutinated foraminifera nearly disappearing from the fossil record. *H. germanica* dominates the foraminiferal assemblage while *Ammonia beccarii* appears in the fossil record at 229 cm. *A. beccarii* prefers a muddy, silt lagoon and has been used as an indicator of cooler sea surface temperatures and higher salinity (Hodell *et al.*, 2005). An assemblage including *A. beccarii, Textularia sagittula* and *Stainforthia fusiformis* (also indicators of higher salinity) suggest the environment is moving away from a low marsh system in the supratidal zone to a more inundated, intertidal environment (Murray, 2006). Diatom abundances remain high with counts of over 300 individual frustules during this mid-Holocene period and assemblages see a shift to more species sharing dominance with lower percentages. *Cocconeis scutellum, Tabularia fasciulata, P. sulcata, Cocconeis placentula var euglypta, Cyclotella choctawateeana* and *Tryblionella compressa* appear as the drivers of this assemblage shift accompanied by *Grammatophora oceanica, G. marina, Eunotogramma leave* and *Delphines karstenii*. *C. scutellum, T. fasciculata* and *C. placentula var euglypta* and are all common brackish lagoon species (Vos and de Wolf, 1993; De Stefano *et al.*, 2000; Fluin *et al*., 2009). At c. 7500 cal years BP the inner estuary was likely a lagoon environment with increasing water depth, as demonstrated also by the presence of *Cyclotella choctowaneeana* (Witkowski, 1994; Weckstrom and Juggins, 2005). *C. scutellum* can also be an indicator of rising sea levels. Burić *et al.* (2004) found that higher abundance of this species was an indicator of decreased vegetation available for attachment as water levels rose. *C. scutellum* is an epiphytic species and as the plant material disappeared, they fell to the seabed.

The microfossil evidence combined with the presence of dark silty sediment with a clayey band here could be evidence of a paleo brackish lagoon. In coastal areas, lagoons are created by a barrier or partial barrier that separates a small area of water from the ocean. They are

generally short lived features formed during the Holocene (Kjerfve, 1986) and represent unique habitats vulnerable to climate change (Cassina *et al.,* 2013). Various possibilities exist as to what may have caused a potential barrier and formed a lagoon in the inner bay. Two possibilities are presented in Figure 6.4. One possibility which could have created the physical barriers necessary for the presence of a lagoon environment in the possible drumlin field discussed in O'Carra *et al.* (2014). McCabe and Dardis (1989) first describe the stratigraphy of an intertidal exposed drumlin in Inner Galway Bay, located in Rusheen Bay roughly 3 km west of the study cores. O'Carra *et al.* (2014) goes on to postulate that eroded rocky barriers which can be identified on recent LIDAR imaging of Galway Bay formed part of a field of drowned drumlins. As well, Driscoll (2013) discusses the possibility of the Rusheen drumlins, identified by McCabe and Dardis (1989) and discussed in O'Carra *et al.* (2014), as being part of an originally more extensive drumlin field in Galway Bay. It is possible that the drumlins acted as sediment traps, building up sediment to create a lagoon. If extensive drumlinoid landforms dominated the coastline of the inner bay they would have provided protection for low energy environments; salt marshes and embayments (Curtis and Skeffington, 1998). When these barriers are washed away the lagoon environment changes. The drumlins are not identified specifically but are speculated by O'Carra *et al.* (2014) and there is no corroborating radiocarbon dates to confirm this theory or offer a time frame for their presence. However, Marine Institute LIDAR imagery is presented here and some possible drumlin remains are indicated in Figure 6.9 (a). Possible drumlins are demarcated in purple along with the three drumlins identified by McCabe and Dardis (1989) outlined in red. Sediment cores VC001, VC002, VC003 and VC004 are labelled accordingly. It is not the aim of this research to identify drumlins or other glacial landforms. However, the possibility of a paleo drumlin field is put forward here as one paleo landscape that could have created the hydrological conditions necessary for the lagoon environment suggested by the microfossil assemblages at this location during the mid Holocene. Further sediment coring is necessary to confirm the existence of drumlins in inner Galway Bay.

A second possibility is that the changing hydrological conditions in the inner bay were heavily influenced by the changing bathymetry during this time, and this was the driving factor in lagoon formation and disappearance. Figure 6.9 (b) delineates a theoretical paleo-barrier which would have created lagoonal conditions. This delineation is based on current

bathymetry and one possible way in which paleo barriers would have been connected. Inundation by seawater coupled with greater precipitation and mixing with freshwater from the Corrib River, which potentially took place during the mid Holocene, would have led to rapid changes in spatial sediment deposition. This could have caused the creation of a barrier able to facilitate the formation of a brackish lagoon and also the subsequent destruction of the barrier several hundred years later. Studies from Lough Inchiquin (Diefendorf *et al.*, 2006) and Lough Corrib (Tibert *et al.*, 2007) indicate a cool episode from c. 7.3-6.7 specific to Western Ireland which could have resulted in a change in hydrological conditions in this region as well. A bathymetric alteration causing the removal of a barrier could have opened up the inner bay to greater tidal forcings and indeed leave it vulnerable to storm events which are known to have a great effect on sediment distribution in Galway Bay (Cox *et al.*, 2012; Hall *et al.*, 2006; Williams and Hall, 2004). Alternatively, continual tidal flushing or a single storm event could have resulted in a paleo tidal channel which would have opened the lagoon. In either scenario, an increased force (whether from storm events, subsequent freshwater inundation or frequency from tidal flushing) could have also played a role in the occurrence of the hiatus layer confirmed in VC001 and VC002 in the mid-Holocene.

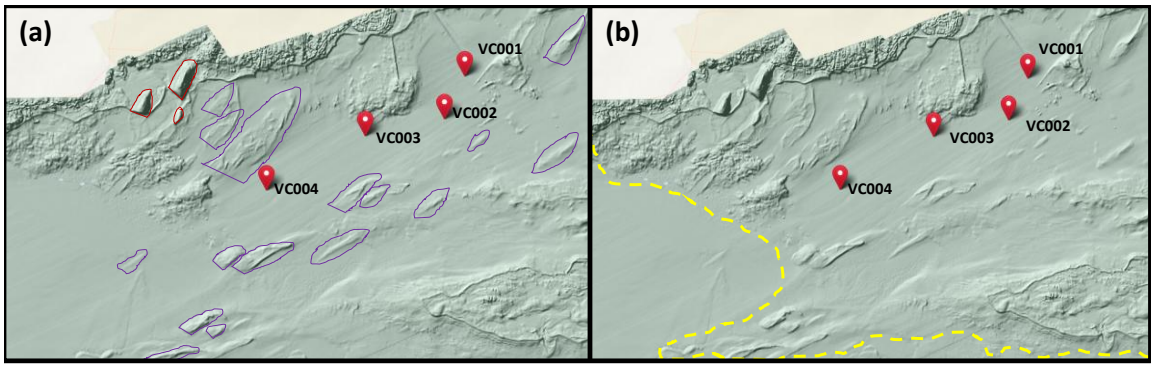

Figure 6.9: Marine Institute LIDAR imagery of inner Galway Bay, accessed on 12/9/2016 from the INFOMAR bathymetry mapping system on the Marine Institute website. Sediment cores VC001, VC002, VC003 and VC004 are marked accordingly. (a) Drumlins identified by McCabe and Dardis (1989) are outlined in red and potential, unconfirmed drumlins are outlined in purple. (b) A potential paleo lagoon in Inner Galway Bay during the mid-Holocene is indicated with a yellow dashed line. This is a theoretical delineation and postulated here as one possible paleo lagoon barrier.

The atmospheric warming in Europe c. 8000-7000 potentially changes hydrological conditions in the inner bay. There is clear physical change in VC001 sediment core (in the

sediment log) and in the microfossil evidence at this time from 7500 to 6000 cal years BP (from 100 to 68 cm). Diatom assemblages in Galway Bay change to a potentially more open, intertidal environment from 6409-6063 cal years BP with the disappearance of *T. fasciculata* and *Thallasionema nitzioides* from the diatom profile and the dominance of pelagic species *P. sulcata, Grammataphora serpentina* and *G. oceanica* indicating deeper intertidal conditions (Fluin *et al*., 2009). The departure of *T. fasciculata* from the diatom profile occurs during increased salinity suggesting that conditions were moving toward more marine, open intertidal conditions (Mills *et al*., 2009). An initial rise in salinity from c. 7000 cal years BP (94 to 80 cm) is punctuated by a strong freshwater pulse at c. 6500 cal years BP (70 cm). *A. beccarii* reaches maximum abundance and *Elphidium* spp. disappear during this time reflecting a change from a marsh/lagoonal environment to a more open, intertidal environment from c. 7000 to 6000 cal years BP. *H. germanica* is present in lower numbers and *T. sagittula* and *S. fusiformis* disappear from the profile c. 6800 cal years BP (76 cm). The departure of these two species is an indicator of decreased salinity (Murray, 2006) that corresponds with the freshwater signal seen in the DI-salinity during this same interval just prior to the hiatus at c. 6000 BP. Climatic conditions inferred during this time see rising temperatures in Western Europe. Davis *et al*. (2003) suggest the temperatures in northwest Europe were highest c. 6000 cal. years BP. The warm mid Holocene (between 8.2 and 4.2 ka cal BP; Walker *et al.*, 2012) is punctuated by several cold phases, including events at 6.4, 5.3 and 4.2 ka cal BP which are the most significant in terms of temperature change (Wanner *et al*., 2011). Stolze *et al*. (2012) associated the elevated summer temperatures and low rainfall from 5800 to 5500 cal years BP with an increase in human settlement. Palynological records from western Ireland broadly suggest a warmer, more hospitable climate between 6000 cal. years BP and 5600 cal. years BP in line with an increase in human activities (Verrill and Tipping, 2010; Stolze, 2013).

An additional consideration is that the freshwater input into the Corrib estuary is a catalyst for change in the inner bay during the mid Holocene. Dynamics in fluvial systems since the last interglacial have strong implications for freshwater input and associated transgressive and regressive preservation potential of coastal sedimentology (Harris *et al.,* 2013). The karstic geology underlying the western side of the Corrib catchment is a possible contributor to freshwater input into this system. Cave and Henry (2011) discuss subaqueous discharge

into Southern Galway Bay via the highly karstified geology underlying surrounding catchments and the elevated levels of freshwater they expel into Kinvarra Bay. The same karstic geology exists in the western Corrib catchment and the opening of a karstic channel could have seen additional freshwater input from the Corrib catchment during the Holocene, possibly even flooding events. Gaining a quantitative understanding of how the groundwater hydrology of the catchment affects the bay over time is key to understanding localised environmental change, specifically how the underlying karstic hydrogeology changed during the Holocene.

The upper sediment facies of VC003, where it has been discussed as a possible modern sediment deposit, sees individual foraminiferal counts >350 and diatom counts ranging from 180 to 250 frustules and is discussed further with modern sediments from VC001 and VC002.

6.4 The Late Holocene (4200 to date)

Late Holocene sediments (4200 a BP to present; Walker 2012; 2014) are largely missing from the Galway Bay sediment cores. Only recent sediment post c. 500 cal years BP was identified in VC001 and VC002 and potentially in VC003. This precludes detailed inferences for this time period. The hypothetical scenarios for lagoon formation and subsequent breach outlined included a possible paleo drumlin field and paleo sediment barrier which were possibly removed with increased tidal forcing, storm events or heightened fluvial inputs. These scenarios were offered as possible events to account for mid Holocene paleoenvironmental changes (c. 8000-6000 cal years BP). However, these scenarios would also have created an environment where the coastline here was susceptible to increased climatic and oceanic forcings that could have caused the washing out of sediment which resulted in the hiatus in the sediment profiles of VC001, VC002 and possibly VC003 (Figures 6.1 and 6.2). The mid to late Holocene sees gradual climatic cyclicity in 1500 year periods after c. 6000 BP (Sorrell *et al*., 2012). This is attributed to changing ocean dynamics associated with the slowing of sea-level rise and cessation of meltwater fluxes. (Debret *et al.,* 2009). Coastal sediment sequences from two sites in France on the North Atlantic reveal late Holocene storm deposits at 4500-3950, 3300-2700, 1600-1250 and 600-300 cal BP (Billeaud *et al.*, 2009; Sorrell *et al.*, 2009). Sorrell *et al*. (2012)

identifies five mid to late Holocene storm periods based on these and coastal sediment cores from six other northern European locations. It is possible that conditions in the inner Bay after this last storm period allowed for the re-deposition of sediment in the intertidal zone. da Assunção Araújo (2007) also links the time period (600-300 cal years BP) with increased storms and flooding which resulted in increased sedimentation by rivers into littoral zones. The combination of fluvial and marine forces during this time may have resulted in the shell deposits in VC001, VC002 and VC003. The deposit in VC001 is more pronounced and less so in inner bay sediment cores (VC002 and VC003) and this could be due to increased storms and river flooding and could also possibly indicate that the washout of sediment is generated by terrestrial and fluvial drivers more so than marine influences. Sediment begins to be re-deposited as sea levels rise in inner Galway Bay and the impacts of storm periods and tidal forcing is lowered.

6.4.1 Modern sediment deposits

Modern North Inner Galway Bay is a marine transgressed continental margin and, as is typical of this type of environment, is sediment starved (Riggs *et al.,* 1998, Harris *et al*., 2013). Clarke (2014) reports that the Corrib outflow currently acts as a confined channel that flows in a wide arc around Mutton Island and opens out to a less confined plain. Fine grained sediments are found in the modern post c. 500 cal years BP deposits of sediment cores VC001, VC002 and VC003 suggesting fluvial deposits. Sediment cores from the Galway Harbour Expansion EIS (Dunlop, 2014) are composed of similar thick sequences of fine to medium sandy silt. Organic carbon levels are at their highest (3.72% OC) in the modern deposit in VC001. Microfossil assemblages are distinctly varied in these sediments (VC001 diatom Zone 4, Figure 5.9; foraminifera Zone 5, Figure 5.13) and in the upper sediments of VC002 and VC003, reflecting the deeper ocean intertidal and shelf assemblages indicative of modern conditions in inner Galway Bay. The foraminiferal record here is overwhelmingly dominated by *A. beccarii* with *H. germanica, Lobatula lobatula, Bulimina gibba* and *E. excavatum* comprising the rest of the assemblage. This is a typical brackish estuarine assemblage (Murray, 2006) with the dominant *A. beccarii* indicating warmer waters (Scott *et al.,* 2001). Notably, *Stainsforthia fusiformis* disappeared from the assemblage, possibly representing an increased water depth (Murray, 2006). *S. fusiformis* is

an opportunistic species that often represents frontal systems; the departure of this species from the assemblage indicates a change from typical shallow estuarine stratification to more open water conditions (Murray, 2006). However, the diatom record here is poor; only two of the ten samples examined in the modern sediments have diatom occurrences and a maximum of just 11 frustules. The surface sediment sample has a count of 161 individual diatom taxa and an assemblage composed primarily of *C. scutellum, C. peltoides, P. sulcata* and *G. serpentina*; indicative of brackish marine conditions. *C. peltoides* is a common coastal diatom in marine brackish water, with an affinity for marine conditions (Mills *et al.*, 2009). *P. sulcata* is common in coastal environments with high salinity variation (Zong, 1997). A major component of benthic communities in coastal, estuarine and lagoon environments, it is susceptible to tidal or wind disturbance and thus may be prone to re-distribution to shallower waters (Fluin *et al*., 2009).

Modern water currents were examined using unpublished 2015 data from the Marine Institute to gauge the pattern of modern sediment deposition (Map 4.3). Previously, Ren *et al*. (2015) and O'Donncha *et al.* (2015) have investigated surface currents in Galway Bay with a focus on aeolian driven processes. The Marine Institute data is the mean of surface and bottom water currents and therefore gives a more accurate description of water movement in the inner bay (pers comm. K. Lyons, MI). It is clear from the map that two small gyres dominate the north inner bay current and this would likely have an influence on sediment distribution. Clarke (2014) discusses Mutton Island as a possible sediment trap for estuarine and fluvial sediment and Dunlop (2014) indicates inner Bay sediment could also be deposited near Rusheen Bay or washed into the tidal channel. The sediment cores used in this research are all influenced by this circulatory pattern and this likely has a great effect on the modern sediment seen in the upper deposits of VC001, VC002 and possibly VC003. The lack of modern sediment in VC004 may be attributed to its location closer to the main tidal channel (as defined in Dunlop, 2014). All four sediment cores used in this project were extracted along a transect that was designed to avoid known dredging channels and so this is eliminated as a reason for the absence of recent sediment deposition. Whether continual tidal flushing is the reason for restricted sediment deposition in VC004 throughout the mid and late Holocene cannot be determined with certainty. The variable nature of modern sediment deposition seems to act in a directional manner with higher, more pronounced deposition in

the eastern-most core (VC001), closer to the Corrib River outflow and no deposition in the western-most core (VC004). This could indicate that in the modern environment, cores VC001 and VC002 are more influenced by freshwater sediments and cores VC003 and VC004 are more affected by marine forces.

Summary

The Holocene time period in coastal environments is characterized, in part, by highly variable climatic change that varies temporally and spatially, sea level rise and changing geomorphology. Figure 6.10 offers a schematic representation of the paleoenvironmental changes discussed in this study.

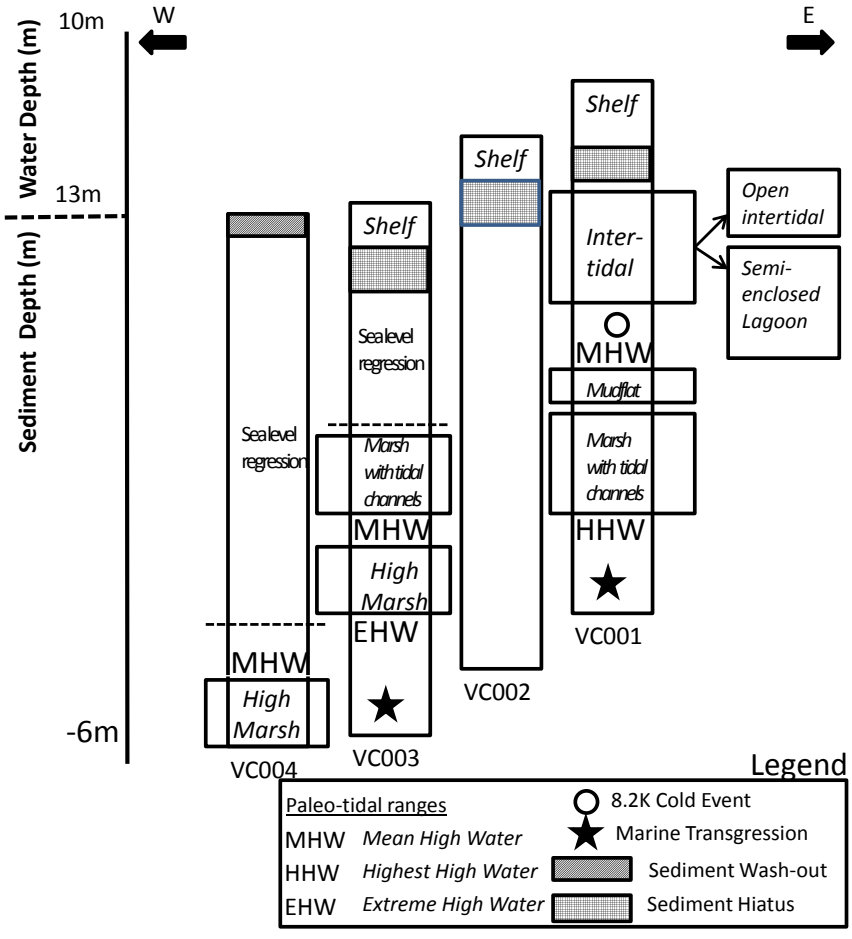

Figure 6.10: A schematic diagram of paleoenvironmental changes in Inner Galway Bay during the Holocene. Here, environmental changes, paleotidal changes, sea level and the 8.2K cold event are noted. Additionally water levels and sediment depths are indicated.

In Inner Galway Bay during the early Holocene sediment deposition is high and paleo-tidal regimes are distinct, ranging from terrestrial environments which experience EHW during storm events to MHW in high/mid marsh and mudflat environments. The mid Holocene is only observable in sediment core VC001, located in the modern Corrib estuary; sediment is missing from VC002, VC003 and VC004 for this time period. VC001 sees increasing seas and a move from mud and tidal flats to a more intertidal environment influenced by freshwater phases as a result of Corrib River outflows. A hiatus is confirmed in sediment cores VC001 and VC002 and suspected in VC003 where whole and broken shell material is deposited. Modern sediment deposition occurs and is indicative of more open intertidal conditions. Sediment core VC004 has no sediment deposition after the early Holocene. While a complex sediment stratigraphy with incomplete Holocene profiles was identified, a spatial trajectory of chronological, physical, chemical and biological change is confirmed from outer to inner bay in the Galway deposits.

CHAPTER 7: Conclusion

This research provides novel and valuable paleoenvironmental data from the transitional waters adjacent to the Corrib River outflow and the more saline coastal waters of inner Galway Bay. The overall aim of this research was to track sediment responses to environmental changes during the Holocene period with the use of physical, chemical and biological proxies. Four objectives were outlined at the beginning of this project: to produce a chronological profile, the creation of a significant data set, to examine the trajectory of change between the transitional waters of the Corrib Estuary and the Inner, more saline modern bay and to establish baseline data in Inner Galway Bay North in the form of identifying paleoenvironmental changes.

The west-east transect of Inner Galway Bay North was targeted to investigate natural variation in coastal evolution as the sediment cores decreased in proximity to the freshwater outflow of the Corrib River. This has implications for regional coastal zone management. The first objective of this research, to establish a chronological profile that was temporally accurate, was achieved. The radiocarbon dates in this study range from 10235 to 0 cal years BP over the four sediment cores. Extensive sediment deposition occurs during the early Holocene in all cores from c. 10235 to 8000 cal years BP with c. 300-500 m of sediment deposited during this time in all cores. Mid Holocene sediment is only present in the Corrib Estuary core (VC001). A temporally extensive sediment hiatus was identified which was confirmed in the two eastern sediment cores (VC001 and VC002) and suspected in the inner bay core VC003. No hiatus is present in the western most core, VC004, and this core contains only early Holocene sediment. This chronology limited detailed analysis to the early Holocene in sediment cores VC002, VC003 and VC004 with late Holocene observations (c. 500-0 cal years BP) possible in VC002 and VC003 (suspected).

Various proxies were targeted in this research to create a valuable and informative data set. Extracting information that was both useful and beneficial to the project and generating a dataset that could prove useful to others was a key component of this work. Physical, geochemical and microfossil proxies were targeted as follows:

- Physical proxies were generated on all four sediment cores using the Multi Scanner Core Logger (MSCL) and included p-wave velocity, gamma density and magnetic susceptibility. Grain size analysis was carried out on VC001 and VC003 as a representation of estuarine (VC001) and more saline inner bay (VC003) conditions. Basal sediments in VC001 are sandy and more pronounced than those found at the base of VC003. Both sediment cores are silty but VC001 is comprised of sandy silts with clayey silt deposits and VC003 is predominantly silt material. A confirmed shell layer overlain with modern sediment is clear in the stratigraphic record of VC001 and VC003 displays a shell hash layer with several whole shells, and a possible modern deposit at the top of the core which was not confirmed with radiocarbon dating.
- Geochemical proxies were generated using X-Ray Fluorescence (XRF) scanning. Of the 32 individual elemental profiles generated seven elemental ratios were used for analysis. In VC001 changes in Ca/Ti and Sr/Ca in the basal sediments indicates a change in marine versus terrestrial input and a shallow water source. A slight decrease in Br/Cl here has implications for salinity variation during this time. A notable decrease in Br/Cl and K/Ti and an increase in Si/Ti c. 8200 cal years BP may be a record of the 8200 climate event. A PCA was used to determine the significance of elemental ratios in VC002, VC003 and VC004. The PCA indicates Br/Cl is the most influential driver in all three sediment cores possibly indicating marine influence as the driver of change in these cores.
- Diatoms were analysed for environmental conditions. In the inner transitional waters (VC001), diatoms were present throughout the sediment core. The basal, sandy sediment contained very low numbers of marine diatoms such as *Paralia sulcata* and *Podosira corolla* and these experienced high breakage and dissolution. The diatom assemblage changes c. 9300 cal years BP as individual counts and floristic diversity increase. The core consists of benthic, brackish diatoms such as *Delphineis minutissima, Dimmeregramma minor, Cymatosira belgica, Tryblionella compressa* and *Cocconeis peltoides* and is punctuated by freshwater pulses characterised by the presence of *Ellerbeckia areanaria*. The diatom assemblage alters c. 8500 cal years BP where *Cyclotella choctawateeana, Delphineis karstenii* and *Cocconeis scutellum* are dominant in the assemblage and a departure of *D. minutissima, D. minor* and *C. belgica* is

witnessed. From c. 8000 to 6000 cal years BP the floristic profile changes again and the assemblage is dominated by *Grammatophora serpentina* and *G. oceanica*. Modern sediment overlaying the shell disturbance layer has low diatom counts and encompasses brackish diatoms such as *C. peltoides* and *G serpentina*. The diatom data from VC001 allowed for successful quantitative analysis resulting in DI-salinity which showed salinity as one of the driving forces through time. In the inner Bay (VC003) this was not the case as diatoms were impoverished, the number of valves enumerated was low throughout and only eight sediment samples had counts of over 300 diatoms. No diatoms are present in the basal sediment and appear c. 9800 cal years BP with *P. sulcata* and *P. corolla* dominant throughout the core. The lower core c. 9500 is characterized by *Hyalodiscus radiatus, C. scutellum* and *Planothidium delicatulum* and contains some samples with freshwater influence represented by *Melosira variens* and *Aulacosira granulata*. The upper core c. 9000 cal years BP is characterized by *Rhaphoneis amphiceros, G. serpentina* and *D. minor*. Sediment at the top of the core, where it is suspected there is a modern sediment deposit is dominated by *P. sulcata, G. serpentina, G. marina, D. karstenii* and *Melosira granulata*.

- Foraminifera were analysed for environmental conditions. In the transitional waters of sediment core VC001, there are no foraminifers in the basal sediments indicating limited or no marine influence in this sediment. They appear c. 9300 cal years BP and the assemblage is dominated by *Haynesinia germanica, Ammonia aberdovenysis* with *Elphidium* spp., *Bolivina spathulata, Stainsforthia fusiformis, Textularia sagittula* and *Haplophragmoides bradyii*. This changes c. 8500 cal years BP when the assemblage alters with *H. germanica* and *Ammonia beccarii* dominating and *Aubigyna hamblensis, Fissurina subformosa Stainforthia fusiformis* and *T. sagittula* comprising the main assemblage. The modern sediment deposit represents deeper, more open water conditions with *H. germanica, Lobatula lobatula, Cibidies reflugens, A. beccarri, Epistominella exigua, Rosalina anomala, Textularia tenusa* and *Quinquelocina seminulum* represented. In the Inner Bay (VC003), individual counts of foraminifers were low throughout the core. Foraminifera does not appear in the stratigraphy until c. 9800 cal years BP and then there is a single species, *Jadammina macrescens*, until c. 9500 cal years BP. This likely indicates the period of marine intrusion followed by a

high marsh environment. From c. 9500 to 9300 cal years BP, the assemblage is comprised predominately of *J. macrescens, Trochammina inflata, H. germanica, Nonionella labrador, S. fusiformis* and *Haplophragmoides bradyii.* No foraminifers appear in the sediment profile from c. 9300 to 9000 cal years BP. This could be the result of changing coastal geomorphology during this time. The suspected modern sediment deposit over laying this material has individual counts > 300 and is dominated by *H. germanica, L. lobatula, H. bradyii, Bulimina gibba* and *Elphidium* spp. possibly indicative of deeper, more saline waters.

Parameters for early, mid and late Holocene are provided and results are discussed in this context. A summary of these results is as follows:

- Sediment from the early Holocene encompasses a record of marine intrusion into inner Galway Bay. Marine intrusion occurred c. 9800 cal years BP in the inner bay and c. 9000 cal years BP in the inner transitional waters near the Corrib river outflow. The c. 800 year time lag is likely due to the c. 2.5 km difference between sediment cores VC004 (inner bay) and VC001 (transitional estuarine waters) and marine transgression in response to sea level rise. The sediment cores demonstrate that a large amount of sediment (5-6 meters) was deposited c. 10000-8000 cal years BP after marine transgression. Salinity levels are highly variable throughout the early Holocene in inner Galway Bay North. This is evident in the microfossil record from VC001 where the DI salinity infers freshwater pulses at several intervals including c. 9300, 9100, 8900 and 8200 cal years BP. A record of paleoenvironmental change during the early Holocene shows that after marine intrusion, inner Galway Bay North (represented by sediment cores VC002, VC003 and VC004) was likely a high marsh environment with a tidal range of EHW to MHHW progressing over time to a tidal/mudflat environment with typical tidal condition associated with MHW conditions. The eastern transitional waters of inner Galway Bay North (represented by sediment core VC001) was likely an intertidal environment (mud/sand flats intermixed with a series of tidal channels) after marine intrusion and the progression from high marsh to tidal flat environment is not likely to have occurred here. A possible record of the 8200 cold event occurs at the end of the early Holocene as seen in selected proxies in the Corrib Estuary sediment core

(VC001). An examination of the upper 200 cm of sediment in this core revealed a short pulse of increased p-wave velocity, gamma density, Ca/Ti and Si/Ti and decreased magnetic susceptibility, % OC, DI salinity, K/Ti, Zr/Ti and Br/Cl during this time.

- Mid Holocene sediments are only represented in VC001. As water levels continue to rise in the inner transitional waters, deeper intertidal conditions occur and a paleo lagoon is postulated as a possible paleo environment at this sampling point. Several possibilities are offered for the theorised creation and subsequent destruction of this lagoon including a paleo drumlin field, a deeper and more powerful tidal channel and geomorphological change as a result of sediment redistribution. DI salinity infers a freshwater pulse at c. 6000 cal years BP. A depositional hiatus is confirmed in the two innermost sediment cores VC001 and VC002 and a suspected hiatus is discussed in VC003. In VC001, the hiatus is c. 5500 years long and is characterised by a shell layer comprised largely of intact shells and broken shell material. In sediment core VC002 the hiatus is c. 8000 years. As sea levels rose, continual tidal energy would have been exerted and reworked sediments in this area. This could potentially explain the lack of sediment deposition (hiatus) and the deposition of shells and shell hash. It is postulated, however, that the condition, arrangement and quantity of the shells found in the deposition in the eastern-most core (VC001), indicate a single depositional event, likely at the end of a period of extensive re-working.
- Late Holocene sediments are largely missing from the Galway Bay sediment cores. Only recent sediment post c. 500 cal years BP was identified in VC001 and VC002 and potentially in VC003. This precludes detailed inferences for this time period. Modern currents are discussed as modes of sediment transport and the resultant discreet environmental changes. The more open coastline which resulted after events in the mid Holocene was susceptible to increased climatic and oceanic forcings that could have caused the continual washing out of sediment which resulted in the lack of early Holocene sediment. Microfossil evidence from the modern sediment deposit is indicative of a brackish marine environment and changes in foraminiferal assemblages indicate a departure from shallow water marine to a warmer, more open marine environment.

This research successfully gauged sediment responses to environmental changes during the Holocene period using a multi proxy approach. It should be noted that the recent availability

of equipment such as MSCL and XRF scanners for paleoenvironmental research in Ireland was highly beneficial to the current research. These non-invasive techniques allowed the sediment cores to remain intact for additional measurement and usage (e.g.: microfossil extraction) throughout the duration of the project. It is hoped that this research will be used in future coastal planning and as a base for paleoenvironmental research in the wider Galway Bay area. To this end, the following further recommendations are offered:

- Conditions in the Corrib River, Lough Corrib and the upper catchment could be investigated further for evidence of flooding and paleoenvironmental change that would cause such a large freshwater influx – especially as major points of freshwater pulses were identified in this study. The eastern border of the Corrib catchment is geologically defined by a limestone base and the frequency and volumes of freshwater entering Lough Corrib and the Corrib River via subaqueous methods in this area are unknown. Quantifying the amount and paleo-flow patterns of freshwater into the catchment will assist in current and future water quality and quantity planning as well as creating flood defence plans.
- On-going research in Galway Bay will likely yield more sediment cores and resultant data regarding paleoenvironmental conditions in the Bay. In an effort to make future research cost effective and maximise the research potential of future endeavours the creation of a sediment core database in the Marine Institute is recommended. This metadatabase could parallel the EPA SAFER-Data archive. This would allow for researchers to learn from each other and facilitate partnerships based on what data is produced and what data is still needed to construct beneficial future projects in the field of coastal paleoenvironmental research.

CHAPTER 8: References

Aitchison, J. and Egozcue, J.J., 2005. Compositional data analysis: where are we and where should we be heading?. *Mathematical Geology*, *37*(7), pp.829-850.

Al-Yamani, F.Y. and Saburova, M.A., 2011. Illustrated guide on the benthic diatoms of Kuwait's marine environment. *Kuwait Institute for Scientific Research, Lucky Press, Kuwait*.

Albani, A., Vachard, D., Kuhnt, W. and Thurow, J., 2001. The role of diagenetic carbonate concretions in the preservation of the original sedimentary record. *Sedimentology*, *48*(4),875-886.

Alley, R. B., Mayewski, P. A., Sowers, T., Stuiver, M., Taylor, K. C. and Clark, P. U..1997. Holocene climate instability: a prominent, widespread event 8200 years ago. Geology, Vol. 25, pp 483-486.

Andersen C., Koc N., Jennings A., Andrews J.T., 2004. Non-uniform response of the major surface currents in the Nordic Seas to insolation forcing: implications for the Holocene climate variability. Paleoceanography 19.

Andersen, J.H., Conley, D.J., Hedal, S., 2004. Palaeoecology, reference conditions and classification of ecological status: the EU Water Framework Directive in practice. Marine Pollution Bulletin 49: 283–290.

Anderson, K., Svenssona, A., Johnsena, S., Rasmussena, S., Biglera, M., Ro¨thlisbergerb, R., Ruthc, U., Siggaard-Andersena, M., Steffensena, J., Dahl-Jensena, D., Vinthera, B., Clausen, H., 2006. The Greenland Ice Core Chronology, 15–42 ka. Part 1: constructing the time scale. Quaternary Science Reviews 25 3246–3257.

Anderson, N.J. and Vos, P., 1992. Learning from the past: Diatoms as palaeoecological indicators of changes in marine environments. Netherlands Journal of Aquatic Ecology 26(1): 19-30.

Anderson, N.J., Bugmann, H., Dearing J.A., Gaillard M.J., 2006. Linking palaeoenvironmental data and models to understand the past and to predict the future. Trends in Ecology and Evolution 21(12): 696-704.

Andreev, A, Tarasov, P.E., Ilyashuk, B.P., Ilyashuk, E.A.,Cremer, H., Hermichen, W.D., Wischer, F., Hubberten, H. W., 2005**.** Holocene environmental history recorded in Lake Lyadhej-To sediments, Polar Urals, Russia. *Palaeogeography, Palaeoclimatology, Palaeoecology*, 223(3-4**)**, 181-203.

Andrén, E., Clarke, A.L., Telford, R.J., Weckström, K., Vilbaste, S., Aigars, J., Conley, D., Johnsen, T., Juggins, S., Korhola, A., 2007. Defining reference conditions for coastal areas in the Baltic Sea. TemaNord 583, 81.

Andrews, J.T., Caseldine, C.,Weiner, N.J. and Hatton, J., 2001. Late Holocene (ca. 4 ka) marine and terrestrial environmental change in Reykjarfjördur, north Iceland: climate and/or settlement?. *Journal of Quaternary Science*, *16*(2), pp.133-143.

Anninou, P. and Cave, R. 2009. How conservative is arsenic in coastal marine environments? A study in Irish coastal waters. Estuarine, Coastal and Shelf Science 82 (2009) 515-524.

Appenzeller, C., Stocker, T.F., Anklin, M. 1998. North Atlantic Oscillation dynamics recorded in Greenland ice cores. Science 282: 446-449.

Armstrong, H.A. and Brasier, M.D., 2005. Foraminifera. Microfossils, Second Edition, pp.142-187.

Ashley, G.M. and Driese, S.G., 2000. Paleopedology and paleohydrology of a volcaniclastic paleosol interval: implications for early Pleistocene stratigraphy and paleoclimate record, Olduvai Gorge, Tanzania. *Journal of Sedimentary Research, 70*(5), pp.1065-1080.

Bahr, A., Lamy, F., Arz, H., Kuhlmann, H. and Wefer, G., 2005. Late glacial to Holocene climate and sedimentation history in the NW Black Sea. *Marine Geology, 214*(4), pp.309-322.

Balascio, N.L. and Bradley, R.S., 2012. Evaluating Holocene climate change in northern Norway using sediment records from two contrasting lake systems. *Journal of paleolimnology*, *48*(1), pp.259-273.

Baldini, J.U., McDermott, F. and Fairchild, I.J., 2002. Structure of the 8200-year cold event revealed by a speleothem trace element record. *Science,296*(5576), pp.2203-2206.

Baldini, L.M., 2007. *An investigation of the controls on the stable isotope signature of meteoric precipitation, cave seepage water, and Holocene stalagmites in Europe*. University College Dublin.

Ballantyne CK, McCarroll D, Stone JO. 2006. Vertical dimensions and age of the Wicklow Mountains ice dome, Eastern Ireland, and implications for the extent of the last Irish Ice Sheet. Quaternary Science Reviews 25: 2048–2058.

Ballantyne, C.K., McCarroll, D. and Stone, J.O., 2011. Periglacial trimlines and the extent of the Kerry-Cork Ice Cap, SW Ireland. Quaternary Science Reviews, 30(27), pp.3834-3845.

Barber, D.C., Dyke, A., Hillaire-Marcel, C., Jennings A. E., Andrews J. T., Kerwin, M. W., Bilodeau, G., McNeely, R., Southon, J., Morehead, M.D., Gagnon, J.M., 1999. Forcing of the cold event of 8,200 years ago by catastrophic drainage of Laurentide lakes. Nature 400, 344-34.

Barber, R.T., Murray Jr, J.W. and McCarthy, J.J., 1994. Biogeochemical interactions in the equatorial Pacific. *Ambio. Stockholm*, *23*(1), pp.62-66.

Barber, H.G. and Haworth, E.Y., 1981. *A guide to the morphology of the diatom frustule: with a key to the British freshwater genera*. Freshwater Biological Association.

Bard, E., 1988. Correction of accelerator mass spectrometry 14C ages measured in planktonic foraminifera: paleoceanographic implications. Paleoceanography, 3(6), pp.635-645.

Barlow, L.K., Rogers, J.C., Serreze, M.C. and Barry, R.G., 1997. Aspects of climate variability in the North Atlantic sector: Discussion and relation to the Greenland Ice Sheet Project 2 high-resolution isotopic signal. *Journal of Geophysical Research: Oceans*, *102*(C12), pp.26333-26344.

Barrett, C., 1998. Benthic foraminifera and their oceanographic parameters, Dingle Bay, South West Ireland. Unpublished Master of Science thesis. National University of Ireland.

Barth, A.M., Clark, P.U., Clark, J., McCabe, A.M. and Caffee, M., 2016. Last Glacial Maximum cirque glaciation in Ireland and implications for reconstructions of the Irish Ice Sheet. Quaternary Science Reviews, 141, pp.85-93.

Bartholdy, J., 2000. Processes controlling import of fine-grained sediment to tidal areas: A simulation model, p. 13–30. In K. Pye and J. R. L. Allen (eds.), Coastal and Estuarine Environments: Sedimentology, Geomorphology, and Geoarchaeology, Volume 175. Geological Society, Special Publications, London, U.K.

Bassetti, M.A., Berné, S., Sicre, M.A., Dennielou, B., Alonso, Y., Buscail, R., Jalali, B., Hebert, B. and Menniti, C., 2016. Holocene hydrological changes in the Rhône River (NW Mediterranean) as recorded in the marine mud belt. *Climate of the Past Discussions*, *12*(7), pp.1539-1553.

Bassinot, F.C., 1993. Sonostratigraphy of tropical Indian Ocean giant piston cores: toward a rapid and high resolution tool for tracking dissolution cycles in Pleistocene carbonate sediments. Earth Planet. Sci. Lett. 120: 327-344

Battarbee, R.W., Jones, V.J., Flower, R.J., Cameron, N.G., Bennion, H., Carvalho, L. and Juggins, S., 2002. *Diatoms* (pp. 155-202). Springer Netherlands.

Battarbee R., Jones V., Flower R., Cameron N., Bennion H., Carvalho L., Juggins S., 2001. Diatoms. In: J. P. Smol, H. J. B. Birks & W. M. Last (eds.), Tracking Environmental Change Using Lake Sediments. Volume 3: Terrestrial, Algal, and Siliceous Indicators. Kulwer Academic Publishers, Dordrecht, The Netherlands.

Battarbee, R.W., Charles, D.F., Dixit, S. and Renberg, I., 1999. Diatoms as indicators of surface water acidity.

Battarbee, R.W., 1986, January. The Eutrophication of Lough Erne Inferred from Changes in the Diatom Assemblages of ^{210} Pb-and ^{137} Cs-Dated Sediment Cores. In *Proceedings of the Royal Irish Academy. Section B: Biological, Geological, and Chemical Science* (pp. 141-168). Royal Irish Academy.

Behrenfeld, MJ., Boss, E., Siegel, D.A., Shea, D.M., 2005. Carbon- based ocean productivity and phytoplankton physiology from space. Global Biogeochemical Cycle.

Benetti, S. (ed.), 2007. INFOMAR: Ground Truthing and Sampling Strategy. Integrated Mapping for the Sustainable Development of Ireland's Marine Resource.

Bennett, K.D., Tzedakis, P.C. and Willis, K.J., 1991. Quaternary refugia of north European trees. Journal of Biogeography, pp.103-115.

Bennion, H., Battarbee, R., 2007. The European Union Water Framework Directive: opportunities 733 for palaeolimnology. J. Paleolimnol. 38, 285-295.

Berglund, B.E., 2003. Human impact and climate changes—synchronous events and a causal link?. *Quaternary International*, *105*(1), pp.7-12.

Berglund, B.E., Barnekow, L., Hammarlund, D., Sandgren, P. and Snowball, I.F., 1996. Holocene forest dynamics and climate changes in the Abisko area, northern Sweden: the Sonesson model of vegetation history reconsidered and confirmed. *Ecological Bulletins*, pp.15-30.

Berglund, B.E., Sandgren, P., Barnekow, L., Hannon, G., Jiang, H., Skog, G. and Yu, S.Y., 2005. Early Holocene history of the Baltic Sea, as reflected in coastal sediments in Blekinge, southeastern Sweden.*Quaternary International*, *130*(1), pp.111-139.

Bersch, M., 2002. North Atlantic Oscillation–induced changes of the upper layer circulation in the northern North Atlantic Ocean. Journal of Geophysical Research: Oceans, 107.

Beyens, L., L. Denys, 1982. Problems in diatom analysis of deposits: allochthonous valves and fragmentation. Geologie Mijnb. 61: 159–162.

Bianchi, G.G. and McCave, I.N., 1999. Holocene periodicity in North Atlantic climate and deep-ocean flow south of Iceland. *Nature*, *397*(6719), pp.515-517.

Biastoch, A., Böning, C.W., Getzlaff, J., Molines, J.M. and Madec, G., 2008. Causes of interannual-decadal variability in the meridional overturning circulation of the midlatitude North Atlantic Ocean. Journal of Climate, 21(24), pp.6599-6615.

Billeaud, I, Tessier, B. and Lesueur, P., 2009. Impacts of Late Holocene rapid climate change as recorded in a macrotidal coastal setting (Mont-Saint-Michel Bay, France). Geology 37, 1031-1034.

BIM, 2012. Environmental impact statement for deep sea fish farm development in Galway Bay, Technical Report. Irish Sea Fisheries Board.

Birks, H.H., Eide, W., Birks, H.J.B., 1999. Early Holocene atmosphere CO2 concentrations. Science, 286, 1815-1816.

Birks, H.J.B., 1995. Quantative paleoenvironmental reconstruction. In D. Maddy and J.S. Brew (Eds.), Statistical modelling of Quaternary science data (pp. 161-254). Canbridge: Quaternary Research Association.

Birks, H. J. B., 1996. Contributions of Quaternary palaeoecology to nature conservation. Journal of Vegetation Science 7:89–98.

Bischoff, J.L., Cummins, K. and Shamp, D.D., 2005. *Geochemistry of sediments in cores and sediment traps from Bear Lake, Utah and Idaho* (No. 2005-1215).

Bjerknes, J., 1964. Atlantic air-sea interaction. Advances in Geophysics. 10, 1–82.

Blaauw, M., 2010. Methods and code for 'classical'age-modelling of radiocarbon sequences. *quaternary geochronology*, *5*(5), pp.512-518.

Blaauw, M. and Christen, J.A., 2011. Flexible paleoclimate age-depth models using an autoregressive gamma process. *Bayesian Analysis*, *6*(3), pp.457-474.

Blake, CB., 2005. Use of maerl as a biogenic archive. PhD thesis. Biological Sciences, Queen's University Belfast.

Bloemsma, M.R., 2010. Semi-automatic core characterisation based on geochemical logging data (Doctoral dissertation, TU Delft, Delft University of Technology).

Boelens, R., Minchin, D., O'Sullivan, G., 2005. Climate Change: Implications for Ireland's Marine Environment and Resources, Marine Foresight Series No 2, Marine Institute.

Booth, D. A. 1975. *The water structure and circulation of Killary Harbour and of Galway Bay*. Unpublished M. Sc. thesis, National University of Ireland.

Bond, G., Showers, W., Cheseby, M., Lotti, R., Almasi, P., Priore, P., Cullen, H., Hajdas, I. and Bonani, G., 1997. A pervasive millennial-scale cycle in North Atlantic Holocene and glacial climates. *science*, *278*(5341), pp.1257-1266.

Bond, G., Kromer, B., Beer, J., Muscheler, R., Evans, M.N., Showers, W., Hoffmann, S., Lotti-Bond, R., Hajdas, I. and Bonani, G., 2001. Persistent solar influence on North Atlantic climate during the Holocene. Science,294(5549), pp.2130-2136.

Bonatti, E. and Gartner, S., 1973. Caribbean climate during Pleistocene ice ages. *Nature*, *244*, pp.563-565.

Boomer, I. and Horton, B.P., 2006. Holocene relative sea-level movements along the North Norfolk Coast, UK. *Palaeogeography, Palaeoclimatology, Palaeoecology*, *230*(1), pp.32-51.

Borja, A., Galparsoro, I., Solaun, O., Muxika, I. Tello, E.M., Uriarte, A. & Valencia, V., 2006. The European Water Framework Directive and the DPSIR, a methodological approach to assess the risk of failing to achieve good ecological status. Estuarine, Coastal and Shelf Science 66: 84-96.

Borja, A., Josefson, A.B., Miles, A., Muxika, I., Olsgard, F., Phillips, G., Rodriguez, J.G., Rygg, B., 2007. An approach to the intercalibration of benthic ecological status assessment in the North Atlantic ecoregion, according to the European Water Framework Directive. Marine Pollution Bulletin 55, 42–52.

Boulton, C.A., Allison, L.C. and Lenton, T.M., 2014. Early warning signals of Atlantic Meridional Overturning Circulation collapse in a fully coupled climate model. Nature communications, 5.

Bouma, A.H., 1969. Methods for the Study of Sedimentary Structures. Wiley-Interscience, New York, 458 pp.

Bowen, D.Q., Rose, J., McCabe, A.M. and Sutherland, D.G., 1986. Correlation of quaternary glaciations in England, Ireland, Scotland and Wales. Quaternary Science Reviews, 5, pp.299-340.

Bower, A.S., Lozier, M.S., Gary, S.F. and Böning, C.W., 2009. Interior pathways of the North Atlantic meridional overturning circulation. *Nature*, *459*(7244), pp.243-247.

Boyle, J., 2001. Redox remobilization and the heavy metal record in lake sediments: a modelling approach. *Journal of Paleolimnology*, *26*(4), pp.423-431.

Braconnot, P., Harrison, S.P., Kageyama, M., Bartlein, P.J., Masson-Delmotte, V., Abe-Ouchi, A., Otto-Bliesner, B. and Zhao, Y., 2012. Evaluation of climate models using palaeoclimatic data. Nature Climate Change, 2(6), pp.417-424.

Bradley, R.S., 1988. The explosive volcanic eruption signal in Northern Hemisphere continental temperature records. *Climatic Change*, *12*(3), pp.221-243.

Bradley, R.S., 1999. *Paleoclimatology: reconstructing climates of the Quaternary* (Vol. 68). Academic Press.

Bradley, R.S., 2008. Holocene perspectives on future climate change. In: R.W. Battarbee and H.A. Binney (eds.) Natural Climate Variability and Global Warming: a Holocene Perspective. Wiley-Blackwell, Chichester, 254-268.

Bradley, R.S. and Jonest, P.D., 1993. 'Little Ice Age' summer temperature variations: their nature and relevance to recent global warming trends. *The Holocene*, *3*(4), pp.367-376.

Breitzke, M., H. Grobe, G. Kuhn, P. Muller, 1996. Full waveform ultrasonic transmission seismic grams: a fast new method for the determination of physical and sedimentological parameters for marine sediment cores. J. Geophysics. Res. 101: 22, 123-22, 124.

Briggs, R.W., Engelhart, S.E., Nelson, A.R., Dura, T., Kemp, A.C., Haeussler, P.J., Corbett, D.R., Angster, S.J. and Bradley, L.A., 2014. Uplift and subsidence reveal a nonpersistent megathrust rupture boundary (Sitkinak Island, Alaska). *Geophysical Research Letters*, *41*(7), pp.2289-2296.

Broecker, W.S., 1991. The great ocean conveyor. *Oceanography*, *4*(2), pp.79-89.

Brooks, S., Parr, A. and Mill, P., 2007. Dragonflies as climate-change indicators. *British Wildlife*, 9 (2), p.85.

Brooks, A. and Edwards, R., 2006. The development of a sea-level database for Ireland. *Irish Journal of Earth Sciences*, pp.13-27.

Brooks, A.J., Bradley, S.L., Edwards, R.J., Milne, G.A., Horton, B., Shennan, I., 2008. Postglacial relative sea-level observations from Ireland and their role in glacial rebound modelling. J. Quat. Sci. 23, 175–192.

Brown, K. J., and Pasternack, G.B., 2005. A paleoenvironmental reconstruction to aid in the restoration of floodplain and wetland habitat on an upper deltaic plain, California, USA. Environmental Conservation 32:1–14.

Brown, E.T., Johnson, T.C., Scholz, C.A., Cohen, A.S. and King, J.W., 2007. Abrupt change in tropical African climate linked to the bipolar seesaw over the past 55,000 years. *Geophysical Research Letters*, *34*(20).

Bryden, H.L., Longworth, H.R. and Cunningham, S.A., 2005. Slowing of the Atlantic meridional overturning circulation at 25 N. Nature, 438(7068), pp.655-657.

Buric, Z., Caput, K. and Vilicic, D., 2004. Distribution of the diatom *Cocconeis scutellum* in the karstic estuary (Zrmanja, eastern Adriatic Sea). *BIOLOGIA-BRATISLAVA-*, *59*(1), pp.1-8.

Butler, C.J., Coughlin, A.D.S., Fee, D.T., 1999. Precipitation at Armagh Observatory 1838-1997. Biology and Environment: Proceedings of the Royal Irish Academy 98B: 123-40.

Butler, Paul G., James D. Scourse, Christopher A. Richardson, Alan D. Wanamaker Jr., Charlotte L. Bryant, James D. Bennell. 2009. Continuous marine radiocarbon reservoir calibration and the 13C Suess effect in the Irish Sea: Results from the first multi-centEarth and Planetary Science Letters, 279 230-241.

Calvert, S.E. and Pedersen, T.F., 2007. Chapter fourteen elemental proxies for palaeoclimatic and palaeoceanographic variability in marine sediments: interpretation and application. *Developments in Marine Geology*, *1*, pp.567-644.

Cann, J.H., Harvey, N., Barnett, E.J., Belperio, A.P. and Bourman, R.P., 2002. Foraminiferal biofacies eco-succession and Holocene sealevels, Port Pirie, South Australia. *Marine Micropaleontology*, *44*(1), pp.31-55.

Cantarero, S., 2013. *Multiproxy paleoclimatic record from geochemical analyses of Lake Chalco sediments, a closed basin lake in central Mexico* (Doctoral dissertation, University of Minnesota).

Caraco, N.F., Cole, J.J., Likens, G.E., 1989. Evidence for sulphate-controlled phosphorus release from sediments of aquatic systems. Nature 341: 316-318.

Cardoso, J., Witte, J., van der Veer, H., 2007. Growth and reproduction of the bivalve *Spisula subtruncata* (da Costa) in Dutch coastal waters. Journal of Sea Research, 57.4, pp. 316-324.

Carlson A.E., 2013. The Younger Dryas Climate Event. In: Elias S.A. (ed.) The Encyclopedia of Quaternary Science, vol. 3, pp. 126-134.

Carter, T.R., R.N. Jones, X. Lu, S. Bhadwal, C. Conde, L.O. Mearns, B.C. O'Neill, M.D.A. Rounsevell and M.B. Zurek, 2007: New Assessment Methods and the Characterisation of Future Conditions. Climate Change 2007: Impacts, Adaptation and Vulnerability. Contribution of Working Group II to the Fourth Assessment Report of the Intergovernmental Panel on Climate Change, M.L. Parry, O.F. Canziani, J.P. Palutikof, P.J. van der Linden and C.E. Hanson, Eds., Cambridge University Press, Cambridge, UK, 133-171.

Caseldine, C., Thompson, G., Langdon, C. and Hendon, D., 2005. Evidence for an extreme climatic event on Achill Island, Co. Mayo, Ireland around 5200–5100 cal. yr BP. *Journal of Quaternary Science*, *20*(2), pp.169-178.

Caseldine, C., Langdon, P. and Holmes, N., 2006. Early Holocene climate variability and the timing and extent of the Holocene thermal maximum (HTM) in northern Iceland. Quaternary Science Reviews, 25(17), pp.2314-2331.

Cassina, F., Dalton, C., Dillane, M., De Eyto, E., Poole, R. and Sparber, K., 2013. A multi-proxy palaeolimnological study to reconstruct the evolution of a coastal brackish lake (Lough Furnace, Ireland) during the late Holocene.Palaeogeography, Palaeoclimatology, Palaeoecology, 383, pp.1-15.

Cassina, F., 2012. A late-Holocene palaeolimnological assessment of two Irish coastal lagoons. PhD thesis. Mary Immaculate College, University of Limerick, Ireland.

Cave, R.R. and Henry, T., 2011. Intertidal and submarine groundwater discharge on the west coast of Ireland. Estuarine, Coastal and Shelf Science 92 iss. 3. p415-423

Cearreta, A., Cachão, M., Cabral, M.C., Bao, R. and de Jesus Ramalho, M., 2003. Lateglacial and Holocene environmental changes in Portuguese coastal lagoons 2: microfossil multiproxy reconstruction of the Santo André coastal area. *The Holocene*, *13*(3), pp.447-458.

Chahinian, N., Tournoud, M.G., Perrin, J.L. and Picot, B., 2011. Flow and nutrient transport in intermittent rivers: a modelling case-study on the Vène River using SWAT 2005. Hydrological Sciences Journal–Journal des Sciences Hydrologiques, 56(2), pp.268-287.

Chappell, J. and Polach, H., 1991. Post-glacial sea-level rise from a coral record at Huon Peninsula, Papua New Guinea.

Chi, J. and J. Mienert 1996. Linking physical property records of Quaternary sediments to Heinrich events. Mar. Geol. 131:57-73.

Chiverrell, R.C. and Thomas, G.S., 2010. Extent and timing of the Last Glacial Maximum (LGM) in Britain and Ireland: a review. Journal of Quaternary Science, 25(4), pp.535-549.

Christiansen and Ljungqvist, 2012. The extra-tropical Northern Hemisphere temperature in the last two millennia: reconstructions of low-frequency variability. Climate of the Past, 8, 765-786.

Clark, C.D. and Meehan, R.T., 2001. Subglacial bedform geomorphology of the Irish Ice Sheet reveals major configuration changes during growth and decay. *Journal of Quaternary Science*, *16*(5), pp.483-496.

Clark, C.D., Hughes, A.L.C., Greenwood, S.L., Jordan, C., Sejrup, H.P., 2012. Pattern and timing of retreat of the last British–Irish Ice Sheet. Quat. Sci. Rev. 44, 112–146.

Clark, P.U., Dyke,A.S., Shakun, J.D., Carlson, A.E., Clark, J.,Wohlfarth, B., Mitrovica, J.X., Hostetler, S.W., McCabe, A.M., 2009. The Last Glacial maximum. Science, 325, pp. 710–714.

Clarke, A.L., Juggins, S., Conley, D., 2003.. A 150-year reconstruction of the history of coastal eutrophication in Roskilde Fjord, Denmark. Marine Pollution Bulletin 46: 1615–1629

Clarke, A.L., Weckstrom, K., Conley, D.J., Anderson, N.J., Adser, F., Andre´n, E., de Jonge, V.N., Ellegaard, M., Juggins, S., Kauppila, P., Korhola, A., Reuss, N., Telford, R.J., 2006. Long-term trends in eutrophication and nutrients in the coastal zone. Limnolugy and Oceanography, 51 (1, part 2), 385–397.

Clarke, C., 2014. An Interpretation of the Single Channel High Frequency Seismic Reflection Datasets of Galway Bay, Ireland. Unpublished MSc Thesis. National University of Ireland, Galway.

Cleve-Euler, A., 1923. *Försök till analys av Nordens senkvartära nivåförändringar*, Geologiska Föreningens i Stockholm Förhandlingar. Vol 45. Issue 1-2.

Cleve-Euler, A., 1943. *Natur und Alter der Strandflächen Finnlands: Eine spätquartäre Rekonstruktion*. Sweded, 89pp.

Cohen, A.L. and McConnaughey, T.A., 2003. Geochemical perspectives on coral mineralization. *Reviews in mineralogy and geochemistry*, *54*(1), pp.151-187.

Coleman, M.A., 2002. Small-scale spatial variability in intertidal and subtidal turfing algal assemblages and the temporal generality of these patterns. *Journal of Experimental Marine Biology and Ecology*, *267*(1), pp.53-74.

Colman, S.M., Baucom, P.C., Bratton, J.F., Cronin, T.M., McGeehin, J.P., Willard, D., Zimmerman, A.R. and Vogt, P.R., 2002. Radiocarbon dating, chronologic framework, and changes in accumulation rates of Holocene estuarine sediments from Chesapeake Bay. *Quaternary Research, 57*(1), pp.58-70.

Colman R., 2003. A comparison of climate feedbacks in general circulation models. Clim. Dyn. 20:865–73.

Cooper, J.A.G., Jackson, D.W.T., 2003. Geomorphological and dynamic constraints on mesoscale coastal response to storms, Western Ireland. *Coastal Sediments* (Vol. 3, pp. 3015-3024).

Cooper, J.A.G., Jackson, D.W.T. and Kelley, J.T, 2009. Late Holocene Beach Evolution: Sediment Starvation under a Falling Sea Level. Journal of Coastal Research. SI 56 (Proceedings of the 10th International Coastal Symposium). 594-598.

Cooper, L.H.N., 1960. Some theorems and procedures in shallow water oceanography applied to the Celtic Sea. Journal of the Marine Biological Association of the United Kingdom 39: 155-171.

Cooper, S.R., 1999. Estuarine paleoenvironmental reconstructions using diatoms. In: Stoermer, E.F., Smol, J.P. (Eds.), The Diatoms: Application for the Environmental and Earth Sciences, Cambridge University Press, Cambridge, 352-373.

Cooper, S.R., Wachnicka, A., Gaiser, E., 2010. Estuarine and paleoenvironmental reconstructions using diatoms. In: Smol, J.P. and Stoemar, E.F. (Eds), *The Diatoms: Applications for the Environmental and Earth Sciences*, p.324.

Coughlan, C. and Stips, A., 2015. Modelling the tides on the North West European Shelf.

Cox, R., Zentner, D.B., Kirchner, B.J. and Cook, M.S., 2012. Boulder ridges on the Aran Islands (Ireland): recent movements caused by storm waves, not tsunamis. The Journal of geology, 120(3), pp.249-272.

Cremer, H., Bunnik, F.P. and Lammens, E.H.R.R., 2007. Diatom paleoecology of Lake IJssel, The Netherlands. *Diatomededelingen 31*, p.39.

Cronin, T.M., Gemery, L., Briggs, W.M., Jakobsson, M., Polyak, L. and Brouwers, E.M., 2010. Quaternary Sea-ice history in the Arctic Ocean based on a new Ostracode sea-ice proxy. *Quaternary Science Reviews*,*29*(25), pp.3415-3429.

Croudace IW, Rindby A, Rothwell RG. 2006. ITRAX: description and evaluation of a new multi-function X-ray core scanner. In New Techniques in Sediment Core Analysis, Rothwell RG (ed.). Special Publication 267, Geological Society: London; 51–63.

Croudace, I.W., Romano, E., Ausili, A., Bergamin, L. and Rothwell, R.G., 2015. X-ray core scanners as an environmental forensics tool: a case study of polluted harbour sediment (Augusta Bay, Sicily). In *Micro-XRF studies of sediment cores* (pp. 393-421). Springer Netherlands.

Cullen, H.M., Hemming, S., Hemming, G., Brown, F.H., Guilderson, T. and Sirocko, F., 2000. Climate change and the collapse of the Akkadian empire: Evidence from the deep sea. *Geology*, *28*(4), pp.379-382.

Culleton, B.J., 2006. Implications of a freshwater radiocarbon reservoir correction for the timing of late Holocene settlement of the Elk Hills, Kern County, California. *Journal of Archaeological Science*, *33*(9), pp.1331-1339.

Cunningham, W.L., Leventer, A., Andrews, J.T., Jennings, A.E. and Licht, K.J., 1999. Late Pleistocene-Holocene marine conditions in the Ross Sea, Antarctica: evidence from the diatom record. *The Holocene*, *9*(2), pp.129-139.

Curry, Ruth G., and Michael S. McCartney, 2001. Ocean gyre circulation change associated with the North Atlantic Oscillation. Journal of Physical Oceanography, 31(12), 3374−3400.

Curtis, T.G.F. and Skeffington, M.S., 1998, December. The salt marshes of Ireland: an inventory and account of their geographical variation. In *Biology and Environment: Proceedings of the Royal Irish Academy* (pp. 87-104). Royal Irish Academy.

Dahl-Jensen, D., Mosegaard, K., Gundestrup, N., Clow, G.D., Johnsen, S.J., Hansen, A.W. and Balling, N., 1998. Past temperatures directly from the Greenland ice sheet. *Science*, *282*(5387), pp.268-271.

Dalton, C., Mylotte, R., Hayes, M., McCarron, S., Edwards, R., Turner, J., 2010. Using coastal paleoenvironmental records to examine past climate variation and track anthropogenic influences. INFOMAR Project # INF-09-19-DAL. Unpublished report.

Dansgaard, W., Johnsen, S.J., Clausen, H.B., Dahl-Jensen, D., Gundestrup, N.S., Hammer, C.U., Hvidberg, C.S., Steffensen, J.P., Sveinbjörnsdottir, A.E., Jouzel, J. and Bond, G., 1993. Evidence for general instability of past climate from a 250-kyr ice-core record. *Nature*, *364*(6434), pp.218-220.

Daultry, S. 1996. The influences of the North Atlantic oscillation, El Nino/Southern oscillation and the Quasi-Biennial Oscillation on winter precipitation in Ireland. In J.A.A.

Davis, O. K., 2001. Palynology: an important tool for discovering historic ecosystems. Pages 229–256 In: D. Egan and E. Howell (eds.) The historical ecology handbook: a restorationist's guide to reference ecosystems. Island Press, Washington, D.C.

Davis, B.A., Brewer, S., Stevenson, A.C. and Guiot, J., 2003. The temperature of Europe during the Holocene reconstructed from pollen data.*Quaternary Science Reviews*, *22*(15), pp.1701-1716.

D'Andrea, W.J., Vaillencourt, D.A., Balascio, N.L., Werner, A., Roof, S.R., Retelle, M. and Bradley, R.S., 2012. Mild Little Ice Age and unprecedented recent warmth in an 1800 year lake sediment record from Svalbard. *Geology*,*40*(11), pp.1007-1010.

da Assunção Araújo, M., 2007. Climatic and coastal evolution during little ice age: some considerations. European Seaport Systems in the Early Modern Age-A comparative approach, Internaitonal Workshop, Proceedings. Porto, IHM-UP, pp. 79-83.

da Costa E M, 1778. *Historia Naturalis Testaceorum Britanniae* London: Millan, White, Elmsley & Robson. 254pp, 17pls.

de Menocal, P.B., Raymo, M., Lynch-Stieglitz, J. and Philander, G., 2006. Pliocene-Pleistocene shifts in tropical Atlantic Ocean-atmosphere coupling. In: *AGU Fall Meeting Abstracts* (1), p.02.

de Menocal, P.B., 2001. Cultural responses to climate change during the late Holocene. *Science* New York, NY), 292(5517), pp.667-673.

de Menocal, P., Ortiz, J., Guilderson, T. and Sarnthein, M., 2000a. Coherent high-and low-latitude climate variability during the Holocene warm period. *Science*,*288*(5474), pp.2198-2202.

de Menocal, P., Ortiz, J., Guilderson, T., Adkins, J., Sarnthein, M., Baker, L. et al., 2000b. Abrupt onset and termination of the African humid period: rapid climate responses to gradual insolation forcing. Quaternary Science Reviews 19, 347±361.

De Stefano, M., Marino, D. & Mazzella, L. 2000. Marine taxa of Cocconeis on leaves of Posidonia oceanica, including a new species and two new varieties. European Journal of Phycology, 35:225-242.

De Swart, H. E., and J. T. F. Zimmerman, 2009. Morphodynamics of tidal inlet systems, *Annual Review Fluid Mechanics*, 41,203–229

de Vries, H., 1958. Atomic bomb effect: variation of radiocarbon in plants, shells, and snails in the past 4 years. Science, 128(3318), pp.250-251.

De Wolf, H.; Backeljau, T.; Breugelmans, K.; Brito, C., 1993. Population genetics in *Littorina striata* on a microgeographical scale. *Belg. J. Zool. 123(Suppl. 1)*: 22-23.

Debret, M., Sebag, D., Crosta, X., Massei, N., Petit, J.R., Chapron, E. and Bout-Roumazeilles, V., 2009. Evidence from wavelet analysis for a mid-Holocene transition in global climate forcing. *Quaternary Science Reviews*, *28*(25), pp.2675-2688.

Deitrich G., K. Kalle, W. Krauss, and G. Siedler., 1980. General Oceanography. 2nd ed. Translated by Susanne and Hans Ulrich Roll. New York: John Wiley and Sons (Wiley- Interscience).

Delaney, C. and Devoy, R., 1995. Evidence from sites in Western Ireland of late Holocene changes in coastal environments. Marine Geology 124 (1995) 273-287.

Delworth, T.L. and Mann, M.E., 2000. Observed and simulated multidecadal variability in the Northern Hemisphere. *Climate Dynamics*, *16*(9), pp.661-676.

Dengler, M., Schott, F.A., Eden, C., Brandt, P., Fischer, J. and Zantopp, R.J., 2004. Break-up of the Atlantic deep western boundary current into eddies at 8 S. *Nature*, *432*(7020), pp.1018-1020.

Denys, L., 1985. Diatom analysis of an Atlantic-Subboreal core from Slijpe (western Belgian coastal plain). *Review of palaeobotany and palynology*,*46*(1), pp.33-53.

Denys, L., 1989. Observations on the transition from Calais deposits to surface peat in the western Belgian Coastal plain. Results of a paleoenvironmental diatom study. *Professional Paper Belgische Geologische Dienst*, *241*, pp.20-43.

Denys, L., 1994. Diatom assemblages along a former intertidal gradient: A palaeoecological study of a subboreal clay layer (Western coastal plain, Belgium). *Netherland Journal of Aquatic Ecology*, *28*(1), pp.85-96

Denys, L., H. de Wolf, 1999. Diatoms as indicators of coastal paleoenvironments and relative sea-level change. In Stoermer, E. F. & J. P. Smol (eds.) The Diatoms: Applications for the Environmental and Earth Sciences. Cambridge University Press, Cambridge: 277–297.

Devoy, R.J.N., 1990. Sea-level changes and Ireland. Technology Ireland, 22, 24–30.

Devoy, RJN 2000. Climate warming and the links to the coast. Inland Coastal Estuarine Waters (3).

Devoy, R., 2008. Coastal vulnerability and the implications of sea-level rise for Ireland. Journal of Coastal Research 24(2): 325– 341.

Diefendorf, A.F., 2005. Late-Glacial to Holocene climate variability in western Ireland (Doctoral dissertation), University of Saskatchewan Saskatoon.

Diefendorf, A.F., Patterson, W.P., Mullins, H.T., Tibert, N. and Martini, A., 2006. Evidence for high-frequency late Glacial to mid-Holocene (16,800 to 5500 cal yr BP) climate variability from oxygen isotope values of Lough Inchiquin, Ireland. *Quaternary Research*, *65*(1), pp.78-86.

Dietrich G., K. Kalle, W. Krauss, and G. Siedler., 1980. General Oceanography. 2nd ed. Translated by Susanne and Hans Ulrich Roll. New York: John Wiley and Sons (Wiley- Interscience).

Dillon, W.R.; Goldstein, M., 1984. Multivariate Analysis: methods and application. New York: John Wiley and Sons.

Dixon, J.L., Heimsath, A.M. and Amundson, R., 2009. The critical role of climate and saprolite weathering in landscape evolution. Earth Surface Processes and Landforms, 34(11), pp.1507-1521.

Douglas, K., 2009. *The Downfall of the Spanish Armada in Ireland: The Grand Armada Lost on the Irish Coast in 1588*. Gill & Macmillan Ltd.

Drinkwater, K.F., Mueter, F., Friedland, K.D., Taylor, M., Hunt, G.L., Hare, J. and Melle, W., 2009. Recent climate forcing and physical oceanographic changes in Northern Hemisphere regions: A review and comparison of four marine ecosystems. Progress in Oceanography, 81(1), pp.10-28.

Driscoll, K., 2006. The early prehistory in the west of Ireland: Investigations into the social archaeology of the Mesolithic, west of the Shannon, Ireland. Unpublished M.Litt. Department of Archaeology National University of Ireland, Galway.

Driscoll, K., 2013. Coastal communities in earlier prehistoric Ireland: ploughzone survey and the Tawin/Maree stone axes, Galway Bay. Proceedings of the Royal Irish Academy, Section C, 113, 29-65.

Duck, R.W. and McManus, J., 2003. The effects of frontal systems on mixing in estuaries. ECSA 8 Mixing/Modelling, 6, pp.151-155.

Duffy, M.J. and Devoy, R.J.N., 1999. Contemporary process controls on the evolution of sedimentary coasts under low to high energy regimes: western Ireland. Geologie en Mijnbouw, 77, 333–349.

Dunkerton, T.J., 2001. Quasi-biennial and subbiennial variations of stratospheric trace constituents derived from HALOE observations. Journal of the atmospheric sciences, 58(1), pp.7-25.

Dunlop, D.P., 2014. Causeway Geotechnical Report. Galway Harbour Extension Environmental Impact Statement to An Bórd Planála, 2C: Appendices to EIS – [Part 2 of 3 Parts].

Durack, P.J. and Wijffels, S.E., 2010. Fifty-year trends in global ocean salinities and their relationship to broad-scale warming. Journal of Climate,23(16), pp.4342-4362.

Duxbury, *et al*., 2002. Fundamentals of Oceanography, 4th edition. New York: McGraw Hill. pp. 344.

Dyer, K.R. 1986. Coastal and Estuarine Sediment Dynamics. John Wiley, Chichester, 342pp.

Dyke, A. S., *et al*., 2003. Deglaciation of North America, Geol. Sum. Can. Open File Rep., 1574.

Edwards, A.B., 1951 Wave action in shore platform formation. Geological Magazine 88, 41-49.

Edwards, R.J. 2007a Sea levels: resolution and uncertainty. *Progress in Physical Geography* **31 (6)**, 621-632.

Edwards, R.J., 2007b. Sedimentary indicators of relative sea-level changes - low energy. in Scott A. Elias (ed.)*Encyclopedia of Quaternary Science*. Elsevier. pp 2994-3005.

Edwards, R.J., 2013. Sedimentary Indicators of Relative Sea-Level Changes - Low Energy. In: Elias, S.A. (ed.) The Encyclopedia of Quaternary Science vol. 4, pp. 396-408. Amsterdam: Elsevier.

Edwards, R.J. and Horton, B.P., 2000. Reconstructing relative sea-level change using UK salt-marsh foraminifera. *Marine Geology*, *169*(1), pp.41-56.

Edwards, R.J. and Horton, B.P., 2006. Developing detailed records of relative sea-level change using a foraminiferal transfer function: an example from North Norfolk, UK. *Philosophical Transactions of the Royal Society of London A: Mathematical, Physical and Engineering Sciences*, *364*(1841), pp.973-991.

Edwards, R.J. and Brooks, A.J., 2008. The Island of Ireland: Drowning the Myth of an Irish Land-bridge? In: Davenport, J.J., Sleeman, D.P., Woodman, P.C. (eds.) *Mind the Gap: Postglacial Colonisation of Ireland. Special Supplement to The Irish Naturalists' Journal.* pp 19-34.

Edwards, R.J. and Wright, A.J., 2015. Foraminifera. In: Shennan, I., Long, A.J., Horton, B.P. (eds.) *The Handbook of Sea-Level Research*. John Wiley & Sons: Chichester.

EEA, 2001. Eutrophication in Europe's coastal waters. European Environment Agency. Copenhagen, pp 86.

Egbert, G.D. and Ray, R.D., 2001. Estimates of M2 tidal energy dissipation from TOPEX/Poseidon altimeter data. Journal of Geophysical Research: Oceans, 106(C10), pp.22475-22502.

Eldevik, T., Nilsen, J. E. O., Iovino, D., Olsson, K. A., Sando, A. B., and Drange, H. 2009. Observed sources and variability of Nordic seas overflow. Nature Geoscience, 2: 405–409.

Enfield, D. B., A. M. Mestas-Nunez, and P. J. Trimble, 2001: The Atlantic multidecadal oscillation and its relation to rainfall and river flows in the continental U.S. Geophys. Res. Lett., 28, 2077–2080.

Engstrom, D.R. and Wright Jr, H.E., 1984. Chemical stratigraphy of lake sediments as a record of environmental change. *Lake sediments and environmental history: studies in palaeolimnology and palaeoecology in honour of Winifred Tutin/edited by EY Haworth and JWG Lund.*

Enters, D., Kirilova, E., Lotter, A.F., Lücke, A., Parplies, J., Jahns, S., Kuhn, G. and Zolitschka, B., 2010. Climate change and human impact at Sacrower See (NE Germany) during the past 13,000 years: a geochemical record. *Journal of paleolimnology*, *43*(4), pp.719-737.

EPA, 2006. Ireland. Water Framework Directive Monitoring Programme. Environmental Protection Agency.

Erdmann, W., Kelletat, D., Scheffers, A.M. and Haslett, S., 2015. *Origin and Formation of Coastal Boulder Deposits at Galway Bay and the Aran Islands, Western Ireland*. Springer.

Eshel, G. G.J. Levy, U. Mingelgrin, M.J. Singer, 2004. Critical Evaluation of the use of laser diffraction for particle size distribution analysis. Soil Sci. Soc. Of Amer. Jour. 68: 736-743.

Evans DJ, Johnes PJ, Lawrence DS., 2004. Physico-chemical controls on phosphorus cycling in two lowland streams. Part 2. — the sediment phase. Sci Total Environ 329:165–82.

Evans, D.J. and Cofaigh, C.O., 2003. Depositional evidence for marginal oscillations of the Irish Sea ice stream in southeast Ireland during the last glaciation. Boreas, 32(1), pp.76-101.

Fahey, J., 1900. Galway and Its Surroundings in the Pre-Norman Period. *Journal of the Galway Archaeological and Historical Society*, *1*(1), pp.49-56.

Fernandes, L. M. J. *A study of the oceanography of Galway Bay, mid-western coastal waters (Galway Bay to Tralee Bay), Shannon Estuary and the River Shannon plume*. Diss. Ph. D. thesis, unpublished. University College Galway, 1988.

Fisher, T.G., Smith, D.G. and Andrews, J.T., 2002. Preboreal oscillation caused by a glacial Lake Agassiz flood. *Quaternary Science Reviews*, *21*(8), pp.873-878.

Fischer, H. and Mieding, B., 2005. A 1,000-year ice core record of interannual to multidecadal variations in atmospheric circulation over the North Atlantic. *Climate Dynamics*, *25*(1), pp.65-74.

Fleitmann, D., Burns, S.J., Mudelsee, M., Neff, U., Kramers, J., Mangini, A. and Matter, A., 2003. Holocene forcing of the Indian monsoon recorded in a stalagmite from southern Oman Science, 300 (5626), pp.1737-1739.

Flower, R. J., 1993. Diatom preservation: experiments and observations on dissolution and breakage in modern and fossil material. Hydrobiologia 269/270: 473–484.

Flower R., Lokhoshway Y., 1993. An investigation of diatom preservation in Lake Baikal. In: M. A. Grachev (ed.) Fifth Workshop on Diatom Algae, Russian Botaincal Society, Irkutsk.

Flower R.J., Ryves D.B., 2009. Diatom preservation: differential preservation of sedimentary diatoms in two saline lakes. Acta Botanica Croatica 68: 381-399.

Fluin, J., Haynes, D. and Tibby, J., 2009. An environmental history of the Lower Lakes and the Coorong. *Report Commissioned by the South Australian Department of Environment and Heritage, Adelaide*.

Folk, R.L.1954. The distinction between grain size and mineral composition in sedimentary-rock nomenclature. Journal of Geology 62, 344-359.

Folland, C. K., D. E. Parker, and T. N. Palmer, 1986: Sahel rainfall and worldwide sea temperatures 1901–85. Nature, 320, 602– 607.

Folland, C. K., D. E. Parker, and T. N. Palmer and Coauthors, 2001. Observed climate variability and change. Climate Change 2001: The Scientific Basis, J. T. Houghton et al., Eds., Cambridge University Press, 99–181.

Folland, C.K., Knight, J., Linderholm, H.W., Fereday, D., Ineson, S. and Hurrell, J.W., 2009. The summer North Atlantic Oscillation: past, present, and future. Journal of Climate, 22(5), pp.1082-1103.

Forsythe, W., Breen, C., Callaghan, C. and McConkey, R., 2000. Historic storms and shipwrecks in Ireland: a preliminary survey of severe synoptic conditions as a causal factor in underwater archaeology. *The International Journal of Nautical Archaeology*, *29*(2), pp.247-259.

Francus, P., Lamb, H., Nakagawa, T., Marshall, M. and Brown, E., 2009. The potential of high-resolution X-ray fluorescence core scanning: applications in paleolimnology. *PAGES (Past Global Changes) News*, *17*(3), pp.93-95.

Frankcombe, L.M., Von Der Heydt, A. and Dijkstra, H.A., 2010. North Atlantic multidecadal climate variability: an investigation of dominant time scales and processes. Journal of climate, 23(13), pp.3626-3638.

Freeman, T. W., 1957. Galway—the key to west Connacht. *Irish Geography* 3.4: 194-205.

Fretwell, P.T., Hodgson, D.A., Watcham, E.P., Bentley, M.J. and Roberts, S.J., 2010. Holocene isostatic uplift of the South Shetland Islands, Antarctic Peninsula, modelled from raised beaches. *Quaternary Science Reviews*, *29*(15), pp.1880-1893.

Friedland, K.D., MacLean, J.C., Hansen, L.P., Peyronnet, A.J., Karlsson, L., Reddin, D.G., Maoiléidigh, N.Ó. and McCarthy, J.L., 2009. The recruitment of Atlantic salmon in Europe. ICES Journal of Marine Science: Journal du Conseil, 66(2), pp.289-304.

Fritz, S. C., 1996. Paleolimnological records of climate change in North America. Limnological Oceanography, Vol. 41(5), pp 882-889.

Fryxell, G.A., 1991. Comparison of winter and summer growth stages of the diatom Eucampia antarctica from the Kerguelen Plateau and south of the Antarctic Convergence Zone. In *Proceedings of the Ocean Drilling Program, scientific results* (Vol. 119, pp. 675-685).

Garnett, E.R., Andrews, J.E., Preece, R.C. and Dennis, P.F., 2004. Climatic change recorded by stable isotopes and trace elements in a British Holocene tufa. *Journal of Quaternary Science*, *19*(3), pp.251-262.

Gehrels, W.R., Roe, H.M. and Charman, D.J., 2001. Foraminifera, testate amoebae and diatoms as sea level indicators in UK saltmarshes: a quantitative multiproxy approach. *Journal of Quaternary Science*, *16*(3), pp.201-220.

Gehrels, W.R., Belknap, D.F., Black, S. and Newnham, R.M., 2002. Rapid sea-level rise in the Gulf of Maine, USA, since AD 1800. *The Holocene*, *12*(4), pp.383-389.

Gehrels WR, Kirby JR, Prokoph A, Newnham RM, Achterberg EP, Evans H, et al., 2005. Onset of recent rapid sea-level rise in the western Atlantic ocean. Quaternary Science Review, 24:2083–100.

Gehrels, W.R., Marshall, W.A., Gehrels, M.J., Larsen, G., Kirby, J.R., Eiríksson, J., Heinemeier, J. and Shimmield, T., 2006. Rapid sea-level rise in the North Atlantic Ocean since the first half of the nineteenth century. *The Holocene*, *16*(7), pp.949-965.

Geyer WR. 2010. Estuarine salinity structure and circulation. In: Contemporary Issues in Estuarine Physics, ed. A Valle-Levinson, pp. 12–26. Cambridge, UK: Cambridge Univ. Press.

Geyer, W.R. and MacCready, P., 2014. The estuarine circulation. Annual review of fluid mechanics, 46(1), p.175. Valle-Levinson, A. ed., 2010. Contemporary issues in estuarine physics. Cambridge University Press.

Gherardi, J.M., Labeyrie, L., McManus, J.F., Francois, R., Skinner, L.C. and Cortijo, E., 2005. Evidence from the Northeastern Atlantic basin for variability in the rate of the meridional overturning circulation through the last deglaciation. Earth and Planetary Science Letters, 240(3), pp.710-723.

Ghilardi, B. and O'Connell, M., 2013. Early Holocene vegetation and climate dynamics with particular reference to the 8.2 ka event: pollen and macrofossil evidence from a small lake in western Ireland. Vegetation History and Archaeobotany, Vol. 22, pp 99-114.

Gil, I.M., Keigwin, L.D. and Abrantes, F., 2015. The deglaciation over Laurentian Fan: History of diatoms, IRD, ice and fresh water. *Quaternary Science Reviews*, *129*, pp.57-67.

Giralt, S., Moreno, A., Bao, R., Sáez, A., Prego, R., Valero-Garcés, B.L., Pueyo, J.J., González-Sampériz, P. and Taberner, C., 2008. A statistical approach to disentangle environmental forcings in a lacustrine record: the Lago Chungará case (Chilean Altiplano). *Journal of Paleolimnology*, *40*(1), pp.195-215.

Glew John R., Smol, John P., Last, William M., 2001. Sediment Core Collection and Extrusion. In W.M. Last and J.P. Smol (eds.), 2001. Tracking Environmental Change Using Lake Sediments. Volume 1: Basin Analysis, Coring and Chronological Techniques. Kluwer Academic Publishers, Dordrecht, The Netherlands.

Goddijn, L.M. & White M. (2006). Digital camera measurements of water quality parameters in Galway Bay, Ireland. Estuarine, Coastal and Shelf Science 66(3-4): 429-436.

Goldenberg, S.B., Landsea, C.W., Mestas-Nuñez, A.M. and Gray, W.M., 2001. The recent increase in Atlantic hurricane activity: Causes and implications. *Science*, *293*(5529), pp.474-479.

Goudeau, M.L.S., Grauel, A.L., Bernasconi, S.M. and de Lange, G.J., 2013. Provenance of surface sediments along the southeastern Adriatic coast off Italy: An overview. *Estuarine, Coastal and Shelf Science*, *134*, pp.45-56.

Goudeau, M.L.S., Grauel, A.L., Tessarolo, C., Leider, A., Chen, L., Bernasconi, S.M., Versteegh, G.J., Zonneveld, K.A., Boer, W., Alonso-Hernandez, C.M. and De Lange, G.J., 2014. The Glacial–Interglacial transition and Holocene environmental changes in sediments from the Gulf of Taranto, central Mediterranean. *Marine Geology*, *348*, pp.88-102.

Gray, S.T., Graumlich, L.J., Betancourt, J.L. and Pederson, G.T., 2004. A tree- ring based reconstruction of the Atlantic Multidecadal Oscillation since 1567 AD. *Geophysical Research Letters*, *31*(12).

Greenwood, S.L. and Clark, C.D., 2009. Reconstructing the last Irish Ice Sheet 2: a geomorphologically-driven model of ice sheet growth, retreat and dynamics. Quaternary Science Reviews, 28(27), pp.3101-3123.

Gregory, K.J and Walling, D.E., 1976. Drainage Basin Form and Process Ed. Arnold, 458 pp. London.

Grootes, P.M., 1993. Interpreting continental oxygen isotope records.*Climate change in continental isotopic records*, pp.37-46.

Guilizzoni P., Oldfield F., guest eds. 1996. Palaeoenvironmental Analysis of Italian Crater lake and Adriatic Sediments (PALICLAS). Memorie Isl

Guiry, M.D.; Guiry, G.M. 2016. AlgaeBase. World-wide electronic publication, National University of Ireland, Galway. http://www.algaebase.org.

Gupta, B.K.S. ed., 2003. *Modern foraminifera* (pp. 1-6). Kluwer Academic Publishers.

Haake, F.W., 1982. Occurrence of living and dead salt marsh foraminifera in the interior of Northern Germany. *Senckenbergiana maritima.* 14: 217-225.

Haberzettl, T., Wille, M., Fey, M., Janssen, S., Lücke, A., Mayr, C., Ohlendorf, C., Schäbitz, F., Schleser, G.H. and Zolitschka, B., 2006. Environmental change and fire history of southern Patagonia (Argentina) during the last five centuries. *Quaternary international*, *158*(1), pp.72-82.

Haberzettl, T., Corbella, H., Fey, M., Janssen, S., Lücke, A., Mayr, C., Ohlendorf, C., Schäbitz, F., Schleser, G.H., Wille, M. and Wulf, S., 2007. Lateglacial and Holocene wet—dry cycles in southern Patagonia: chronology, sedimentology and geochemistry of a lacustrine record from Laguna Potrok Aike, Argentina. *The Holocene*, *17*(3), pp.297-310.

Haggart, B.A., 1988. The stratigraphy, depositional environment and dating of a possible tidal surge deposit in the Beauly Firth area, northeast Scotland. *Palaeogeography, palaeoclimatology, palaeoecology*, *66*(3-4), pp.215-230.

Häkkinen, S. and Rhines, P.B., 2004. Decline of subpolar North Atlantic circulation during the 1990s. Science, 304(5670), pp.555-559.

Halden, B. 1935. Diatomaceanalys. Nordisk Familjebok, 3:e uppl.

Hall, A.M., 2010 Storm wave currents, boulder movement and shore platform development: A case study from East Lothian, Scotland. Marine Geology 283.

Hall, A.M., Hansom, J.D., Williams, J.D., Jarvis, J. 2006 Distribution, geomorphology and lithofacies of cliff top storm deposits: Examples from the high energy coasts of Scotland. Marine Geology 232 131 –155.

Hall, A.M., Hansom, J.D. and Williams, D.M., 2010. Wave-emplaced coarse debris and megaclasts in Ireland and Scotland: boulder transport in a high-energy littoral environment: a discussion. The Journal of Geology, 118(6), pp.699-704.

Hammarlund, D., Björck, S., Buchardt, B. and Thomsen, C.T., 2005. Limnic responses to increased effective humidity during the 8200 cal. yr BP cooling event in southern Sweden. *Journal of Paleolimnology*, *34*(4), pp.471-480.

Hammer, Ø., Harper, D.A.T. and Ryan, P.D., 2001. PAST: Paleontological Statistics Software Package for education and data analysis. Palaeontolia Electronica 4.

Harkness, D D, 1983. The extent of the natural 14C deficiency in the coastal environment of the United Kingdom, Journal of the European Study Group on Physical, Chemical and Mathematical Techniques Applied to Archaeology PACT 8 (IV.9):351-364.

Harris, M. S., Sautter, L. R., Johnson, K. L., Luciano, K. E., Sedberry, G. R., Wright, E. E., Siuda, A. N. S., 2013. Continental shelf landscapes of the Southeastern United States since the last interglacial. Geomorphology, 203, 6-24.

Hartley, B., Ross, R. and Williams, D.M., 1986. A check-list of the freshwater, brackish and marine diatoms of the British Isles and adjoining coastal waters. *Journal of the Marine Biological Association of the United Kingdom*, *66*(03), pp.531-610.

Hasle, G.R., Syvertsen, E.E., Steidinger, K.A., Tangen, K. and Tomas, C.R., 1996. *Identifying marine diatoms and dinoflagellates*. Academic Press.

Hasle, G.R.; Syvertsen, E.E., 1997. Marine Diatoms, In: *Identifying marine phytoplankton*, Carmelo Tomas (ed). Academic Press.

Haslett, S.K. and Bryant, E.A., 2007. Reconnaissance of historic (post-AD 1000) high-energy deposits along the Atlantic coasts of southwest Britain, Ireland and Brittany, France. *Marine geology*, *242*(1), pp.207-220.

Haslett, S.K., Strawbridge, F., Martin, N.A., Davies, C.F.C., 2001 Vertical Saltmarsh Accretion and its Relationship to Sea-level in the Severn Estuary, U.K.: An Investigation using Foraminifera as Tidal Indicators. Estuarine, Coastal and Shelf Science 52, 143–153.

Harrington, S.T. and Harrington, J.R., 2014. Dissolved and particulate nutrient transport dynamics of a small Irish catchment: the River Owenabue. Hydrology and Earth System Sciences, 18(6), pp.2191-2200.

Hass, H.C., 1997. The benthic foraminiferal response to late Holocene climate change over northern Europe. *In: Hass, HC & Kaminski, MA (eds.)(1997): Micropaleontology and Paleoceanology of the North Atlantic.-Grzybowsky Foundation Special Publication*, *5*, pp.199-216.

Hátún, H., Sandø, A.B., Drange, H., Hansen, B. and Valdimarsson, H., 2005. Influence of the Atlantic subpolar gyre on the thermohaline circulation. Science, 309(5742), pp.1841-1844.

Haug, G.H., Hughen, K.A., Sigman, D.M., Peterson, L.C. and Röhl, U., 2001. Southward migration of the intertropical convergence zone through the Holocene. *Science*, *293*(5533), pp.1304-1308.

Hawkes, A.D. and Horton, B.P., 2012. Sedimentary record of storm deposits from Hurricane Ike, Galveston and San Luis Islands, Texas. *Geomorphology*,*171*, pp.180-189.

Hay, W.W., 1994. Pleistocene-Holocene fluxes are not the earth's norm. In Hay, W. W., ed. Global sedimentary geofluxes. Washington, DC, National Academy of Sciences Press, p. 15–27.

Hayes, M.O., Brown, P.J. and Michel, J.M., 1976. *Coastal Morphology and Sedimentation, Lower Cook Inlet, Alaska: With Emphasis on Potential Oil Spill Impacts*. Coastal Research Division, Department of Geology, University of South Carolina.

Haynes, J.R., 1981. *Foraminifera*. John Wiley & Sons, Ltd.

Hayward, B.W., Neil, H., Carter, R., Grenfell, H.R. and Hayward, J.J., 2002. Factors influencing the distribution patterns of Recent deep-sea benthic foraminifera, east of New Zealand, Southwest Pacific Ocean. *Marine Micropaleontology*, *46*(1), pp.139-176.

Hayward, B.W., Scott, G.H., Grenfell, H.R., Carter, R. and Lipps, J.H., 2004. Techniques for estimation of tidal elevation and con" nement (~ salinity) histories of sheltered harbours and estuaries using benthic foraminifera: examples from New Zealand. *The Holocene*, *14*(2), pp.218-232.

Hayward, B.W., Figueira, B.O., Sabaa, A.T. and Buzas, M.A., 2014. Multi-year life spans of high salt marsh agglutinated foraminifera from New Zealand. *Marine Micropaleontology*, *109*, pp.54-65.

Head K, Turney CSM, Pilcher JR, Palmer JG, Baillie MGL, 2007. Problems with identifying the '8200-year cold event' in terrestrial records of the Atlantic seaboard: a case study from Dooagh, Achill Island, Ireland. Journal of Quaternary Science 22:65–75.

Healy, M. and Hickey, K.R., 2002. Historic land reclamation in the intertidal wetlands of the Shannon estuary, western Ireland. In The 7th International Coastal Symposium, ICS 2002; Northern Ireland. Coastal Education and Research Foundation (CERF).

Hede MU, Rasmussen P, Noe-Nygaard N, Clarke AL, Vinebrooke RD, Olsen J., 2010. Multiproxy evidence for terrestrial and aquatic ecosystem responses during the 8.2 ka cold event as recorded at Højby Sø, Denmark. Quat Res 73:485–496.

Hegarty, S., 2004. Limits of Midlandian glaciation in south-eastern Ireland.Irish Geography, 37(1), pp.60-76.

Heier-Nielsen, S., Kuijpers, A. and Laier, T., 1995. Holocene sediment deposition and organic matter burial in the upwelling zone off Yemen, Northwest Indian Ocean. *Netherlands Indian Ocean Programme: Tracing a Seasonal Upwelling*, pp.111-119.).

Helm, K.P., Bindoff, N.L. and Church, J.A., 2010. Changes in the global hydrological cycle inferred from ocean salinity. Geophysical Research Letters, 37(18).

Hemphill-Haley, E., 1995. High Productivity and Upwelling in the California Current during Oxygen-Isotope Stage 3: Diatom Evidence. *Climate Variability of the Eastern North Pacific and Western North America*, (40), p.119.

Hemphill-Haley, E., 1996. Diatoms as an aid in identifying late-Holocene tsunami deposits. *The Holocene*, *6*(4), pp.439-448.

Hendey, N.I., 1964. *An introductory account of the smaller algae of British coastal waters, part V: Bacillariophyceae (Diatoms)*. HM Stationery Office.

Hennekam, R. and de Lange, G., 2012. X-ray fluorescence core scanning of wet marine sediments: methods to improve quality and reproducibility of high-resolution paleoenvironmental records. *Limnol. Oceanogr. Methods*,*10*(12), pp.991-1003.

Hibbert, F.D., Austin, W.E., Leng, M.J. and Gatliff, R.W., 2010. British Ice Sheet dynamics inferred from North Atlantic ice rafted debris records spanning the last 175 000 years. Journal of Quaternary Science, 25(4), pp.461-482.

Hiemstra, J.F., Evans, D.J., Scourse, J.D., McCarroll, D., Furze, M.F. and Rhodes, E., 2006. New evidence for a grounded Irish Sea glaciation of the Isles of Scilly, UK. Quaternary Science Reviews, 25(3), pp.299-309.

Hill, A. E. 2005. Buoyancy effects in coastal and shelf seas. In The Global Coastal Ocean: Processes and Methods, pp. 21–62. Ed. By K.H. Brinka and A.R. Robinson. Harvard University Press, Cambridge, MA. 628 pp.

Hodell, D.A., Brenner, M., Curtis, J.H., Medina-González, R., Can, E.I.C., Albornaz-Pat, A. and Guilderson, T.P., 2005. Climate change on the Yucatan Peninsula during the little ice age. *Quaternary Research*, *63*(2), pp.109-121.

Hoek, C., Mann, D. and Jahns, H.M., 1995. *Algae: an introduction to phycology*. Cambridge university press.

Holliday, N.P., 2003. Air sea interaction and circulation changes in the northeast Atlantic. Journal of Geophysical Research: Oceans, 108.

Holliday, N. P., Hughes, S. L., Bacon, S., Beszczynska,Moller, A., Hansen, B., Lavin, A., Loeng, H., et al.,2008. Reversal of the 1960s to 1990s freshening trend in the northeast NorthAtlantic and No rdic Seas. Geophysical Research Letters 35: L03614.

Holliday, N.P., Quante, M., Sherwin, T., Nolan, G., Mork, K.A., Cannaby, H. and Berry Jones, D., 2011. North Atlantic circulation and atmospheric forcing. In: Reid, P.C. and Valdés, L. (eds) ICES status report on climate change in the North Atlantic. ICES Cooperative Research Report No. 310, 262pp.

Holmes, J.A., Tindall, J., Roberts, N., Marshall, W., Marshall, J.D., Bingham, A., Feeser, I., O'Connell, M., Atkinson, T., Jourdan, A.L. and March, A., 2016. Lake isotope records of the 8200-year cooling event in western Ireland: Comparison with model simulations. *Quaternary Science Reviews*, *131*, pp.341-349.

Holt, J., Proctor, R., 2008. The seasonal circulation and volume transport on the northwest European continental shelf: A fine- resolution model study. Journal of Geophysical Research: Oceans, 113(C6).

Horton, B.P., Edwards, R.J., 2005. The application of local and regional transfer functions to the reconstruction of Holocene sea levels, north Norfolk, England, The Holocene. 15 (2). 216-228.

Horton, B.P., Edwards, R.J., 2006. Quantifying Holocene sea level change using intertidal foraminifera: lessons from the British Isles.

Horton, B.P., Edwards, R.J. and Lloyd, J.M., 1999. A foraminiferal-based transfer function: implications for sea-level studies. *The Journal of Foraminiferal Research*, *29*(2), pp.117-129.

Horton, B.P., Edwards, R.J. and Lloyd, J.M., 2000. Implications of a microfossil-based transfer function in Holocene sea-level studies. *Geological Society, London, Special Publications*, *166*(1), pp.41-54.

Horton, B.P., Peltier, W.R., Culver, S.J., Drummond, R., Engelhart, S.E., Kemp, A.C., Mallinson, D., Thieler, E.R., Riggs, S.R., Ames, D.V. and Thomson, K.H., 2009. Holocene sea-level changes along the North Carolina Coastline and their implications for glacial isostatic adjustment models. *Quaternary Science Reviews*, *28*(17), pp.1725-1736.

Horton, B.P., Sawai, Y., Hawkes, A.D. and Witter, R.C., 2011. Sedimentology and paleontology of a tsunami deposit accompanying the great Chilean earthquake of February 2010. *Marine Micropaleontology*,*79*(3), pp.132-138.

Hostetler, S.W., Bartlein, P.J., Clark, P.U., Small, E.E. and Solomon, A.M., 2000. Simulated influences of Lake Agassiz on the climate of central North America 11,000 years ago. Nature, 405(6784), pp.334-337.

House, W. 2003. Geochemical cycling of phosphorus in rivers. Appl. Geochem., 18: 739–748.

House, W. and Denison, F. 2002. Total phosphorus content of river sediments in relationship to calcium, iron and organic matter concentrations. Sci. Total Environ., 282-283: 341–351.

Hu, Q. and Feng, S., 2008. Variation of the North American summer monsoon regimes and the Atlantic multidecadal oscillation. *Journal of Climate*, *21*(11), pp.2371-2383.

Hubeny, J.B., King, J.W. and Santos, A., 2006. Subdecadal to multidecadal cycles of Late Holocene North Atlantic climate variability preserved by estuarine fossil pigments. *Geology*, *34*(7), pp.569-572.

Hughes, S. L., Holliday, N. P., Colbourne, E., Ozhigin, V., Valdimarsson, H., Østerhus, S., and Wiltshire, K. 2009. Comparison of in situ time-series of temperature with gridded sea surface temperature datasets in the North Atlantic. – ICES Journal of Marine Science, 66: 1467–1479.

Hughes, S. L., Holliday, N. P., Gaillard, F., and the ICES Working Group on Oceanic Hydrography, 2012. Variability in the ICES/NAFO region between 1950 and 2009: observations from the ICES Report on Ocean Climate. – ICES Journal of Marine Science, 69: 706–719.

Humayun, M., Qin, L. and Norman, M.D., 2004. Geochemical evidence for excess iron in the mantle beneath Hawaii. *Science*, *306*(5693), pp.91-94.

Hurrell, J.W. 1995. Decadal trends in North Atlantic Oscillation, regional temperatures and precipitation. Science 269:676-679.

Hurrell, J.W. and van Loon, H., 1997. Decadal trends in climate associated with the North Atlantic Oscillation. Climate Change 36: 301-326.

Hurrell, J. W., Hack, J. J., Shea, D., Caron, J. M., and Rosinski, J., 2008. A new sea surface temperature and sea ice boundary dataset for the Community Atmosphere Model. Journal of Climate, 21: 5145–5153.

Hustedt F., 1953. Die Systematik der Diatomeen in ihren Beziehungen zur Geologie und Ökologie nebst einer Revision des Halobien-Systems. Svensk Botanisk Tidskrift 47: 509-519 (in German).

Hustedt, F., 1927-1966. Die Kieselalgen Deutschlands. Osterreichs und der Schweiz. In Dr I Rabenhorsdt's Kryptogamen-Flora von Deutschland. Oserreich und der Schweitz 7. Leipzig: Akademische Verlagsgesellschaft.

Hutchinson, I., James, T.S., Reimer, P.J., Bornhold, B.D., Clague, J.J., 2004. Marine and limnic radiocarbon reservoir corrections for studies of late- and postglacial environments in Georgia Basin and Puget Lowland, British Columbia, Canada and Washington, USA. Quaternary Research 61, 193 – 203.

Ilyashuk, B. P. and Ilyashnk, E. A., 2001. Response of alpine chironomid communities (Lake Chuna, Kola Penninsula, northwestern Russia) to atmospheric contamination. Journal of Paleolimnology, Vol. 25(4), pp 467-475.

Ilyashuk, E.A., Ilyashuk, B.P., Hammarlund, D. and Larocque, I., 2005. Holocene climatic and environmental changes inferred from midge records (Diptera: Chironomidae, Chaoboridae, Ceratopogonidae) at Lake Berkut, southern Kola Peninsula, Russia. The Holocene, Vol. 15, pp 897-914.

Ilyashuk, E.A., Koinig, K.A., Heiri, O., Ilyashuk B.P. and Psenner, R., 2011. Holocene temperature variations at a high-altitude site in the Eastern Alps: a chironomid record from Schwarzsee ob Sölden, Austria. Quaternary Science Reviews, Vol. 30, pp 176-191.

Imbrie, J., Imbrie, K.P., 1979. Ice Ages: Solving the Mystery. London. Macmillan.

Ingram, B.L. and Southon, J.R., 1996. Reservoir ages in eastern Pacific coastal and estuarine waters. Radiocarbon, 38(3), pp.573-582.

Imbrie, J., Kipp, N.G., 1971. A new micropaleontological method for quantitative paleoclimatology: application to a late Pleistocene Caribbean core. In *The late Cenozoic glacial ages* (Vol. 3, pp. 71-181). New Haven: Yale University Press.

Innes, J.B. and Frank, R.M., 1988. Palynological evidence for late Flandrian coastal changes at Druridge Bay, Northumberland. *The Scottish Geographical Magazine*, *104*(1), pp.14-23.

Ip, C.C., Li, X.D., Zhang, G., Wai, O.W. and Li, Y.S., 2007. Trace metal distribution in sediments of the Pearl River Estuary and the surrounding coastal area, South China. Environmental Pollution, 147(2), pp.311-323.

IPCC, 2007. Climate Change 2007, Synthesis Report: Contribution of Working Groups I, II and III to the Fourth Assessment Report of the Intergovernmental Panel on Climate Change. Pachauri, R.K. and Reisinger, A. (Eds.). IPCC, Geneva, Switzerland.

IPCC, 2013: Climate Change 2013: The Physical Science Basis. Contribution of Working Group I to the Fifth Assessment Report of the Intergovernmental Panel on Climate Change [Stocker, T.F., D. Qin, G.-K. Plattner, M. Tignor, S.K. Allen, J. Boschung, A. Nauels, Y. Xia, V. Bex and P.M. Midgley (eds.)]. Cambridge University Press, Cambridge, United Kingdom and New York, NY, USA.

Irino, T. and Tada, R., 2000. Quantification of aeolian dust (Kosa) contribution to the Japan Sea sediments and its variation during the last 200 ky. *Geochemical Journal*, *34*(1), pp.59-93.

Jahnke, R., 2010. A Global Synthesis. Springer-Verlag. chapter In: Carbon 912 and Nutrient Fluxes in Continental Margins: A Global Synthesis. pp. 913 597–615.

Jalali, B., Sicre, M.-A., Bassetti, M.-A., and Kallel, N., 2016. Holocene climate variability in the North-Western Mediterranean Sea (Gulf of Lions), Clim. Past, 12, 91–101.

Jansen, J.H.F., Van der Gaast, S.J., Koster, B. and Vaars, A.J., 1998. CORTEX, a shipboard XRF-scanner for element analyses in split sediment cores. *Marine Geology*, *151*(1), pp.143-153.

Jennings, A.E. and Weiner, N.J., 1996. Environmental change in eastern Greenland during the last 1300 years: evidence from foraminifera and lithofacies in Nansen Fjord, 68 N. *The Holocene*, *6*(2), pp.179-191.

Jennings, E., Allott, N., McGinnity, P., Poole, R., Quirke, W., Twomey, H., George, G. 2000a. The north Atlantic oscillation: effects on freshwater systems in Ireland. Biology and Environment: Proceedings of the Royal Irish Academy. Vol 100B, No3: 149-157.

Jennings, A., Syvitski, J., Gerson, L., Grönvold, K., Geirsdóttir, Á., Hardardóttir, J., Andrews, J. and Hagen, S., 2000b. Chronology and paleoenvironments during the late Weichselian deglaciation of the southwest Iceland shelf. *Boreas*, *29*(3), pp.163-183.

Jiang, H., Seidenkrantz, M.S., Knudsen, K.L. and Eirıksson, J., 2001. Diatom surface sediment assemblages around Iceland and their relationships to oceanic environmental variables. *Marine Micropaleontology*, *41*(1), pp.73-96.

Jiang, H., Seidenkrantz, M.-S., Knudsen, K.L. and Erıksson, J., 2002. Late-Holocene summer sea-surface temperatures based on a diatom recor from the north Icelandic shelf. Holocene 12, 137– 147.

Johns, W. E., Baringer, M. O., Beal, L. M., Cunningham, S. A., Kanzow, T., Bryden, H. L., Hirschi, J. J.-M., Marotzke, J., Meinen, C. S., Shaw, B., and Curry, R., 2011. Continuous, array-based estimates of Atlantic Ocean heat transport at 26.5◦ N, Journal of Climate, 24, 2429– 2449.

Johnson, T.C., Brown, E.T., McManus, J., Barry, S., Barker, P. and Gasse, F., 2002. A high-resolution paleoclimate record spanning the past 25,000 years in southern East Africa. *Science*, *296*(5565), pp.113-132.

Jones, J.A.A. 1997. Global Hydrology-Processes, Resources and Environmental Management. Addison Wesley Longman, England.

Jones, R.W. and Brady, H.B., 1994. *The challenger foraminifera*. Oxford University Press, USA.

Jones, C. Liu, M.K. Woo and H.T. Kung, 1998. Regional hydrological response to climate change, 213-236. Dordrecht. Kluwer Academy Publishers.

Jones, K.B., Hodgins, G.W., Dettman, D.L., Andrus, C.F.T., Nelson, A. and Etayo-Cadavid, M.F., 2007. Seasonal variations in Peruvian marine reservoir age from pre-bomb Argopecten purpuratus shell carbonate. *Radiocarbon*, *49*(2), pp.877-888.

Jones, V.J., Stevenson, A.C. and Battarbee, R.W., 1989. Acidification of lakes in Galloway, south west Scotland: a diatom and pollen study of the post-glacial history of the Round Loch of Glenhead. *The Journal of Ecology*, pp.1-23.

Joshi, S., Duffy, G., Brown, C., Grehan A., 2011. Coupled hydrodynamic-sediment transport modelling and habitat modelling in Galway Bay, West of Ireland. 54th Irish Geological Research Meeting.

Juckes, M.N., Allen, M.R., K. R. Briffa, K.R., Esper, J., Heger, G.C., Moberg, A., Osborn, T.J. Weber, S.L. 2007. Millennial temperature reconstruction intercomparison and evaluation. Climate of the Past 3, 591–609.

Juggins, S., 1992. Diatoms in the Thames Estuary, England: Ecology, Palaeoecology, and Salinity Transfer Function. Bibliotheca Diatomologica, Volume 25, 216 pp.

Juggins, S., 1991-2007. C2 Version 1.5: software for ecological and palaeoecological data analysis and visualisation. *University of Newcastle, Newcastle upon Tyne.*

Kaczmarska, I., Barbrick, N.E., Ehrman, J.M. and Cant, G.P., 1993. Eucampia Index as an indicator of the Late Pleistocene oscillations of the winter sea-ice extent at the ODP Leg 119 Site 745B at the Kerguelen Plateau. *Hydrobiologia*, *269*(1), pp.103-112.

Kastner, S., Ohlendorf, C., Haberzettl, T., Lücke, A., Mayr, C., Maidana, N.I., Schäbitz, F. and Zolitschka, B., 2010. Southern hemispheric westerlies control the spatial distribution of modern sediments in Laguna Potrok Aike, Argentina. *Journal of Paleolimnology*, *44*(4), pp.887-902.

Kaufman, D. S., Ager, T. A., Anderson, N. J., Anderson, P. M., Andrews, J. T., Bartlein, P. J., Brubaker, L. B., Coats, L. L., Cwynar, L. C., Duvall, M. L., Dyke, A. S., Edwards, M. E., Eisner, W. R., Gajewski, K., Geirsdóttir, A., Hu, F. S., Jennings, A. E., Kaplan, M. R., Kerwin, M. W., Lozhkin, A. V., MacDonald, G. M., Miller, G. H., Mock, C. J., Oswald, W. W., Otto-Bliesner, B. L., Porinchu, D. F., Rühland, K., Smol, J. P., Steig, E. J. and Wolfe, B. B., 2004. Holocene thermal maximum in the western Arctic (0-180°C). Quaternary Science Reviews, Vol. 12, pp 115-140.

Keller, Edward A., 1985. *Environmental Geology, 4th Ed.* Charles E. Merril Publishing., 480 pp

Kemp, A.E., Pearce, R.B., Koizumi, I., Pike, J. and Rance, S.J., 1999. The role of mat-forming diatoms in the formation of Mediterranean sapropels. *Nature*, *398*(6722), pp.57-61.

Kemp, A.E.S., J. Dean, R. Pearce, J. Pike, 2001. Recognition and analysis of bedding and sediment fabric features. In W.M. Last & J.P. Smol (eds.), 2001. Tracking Environmental Change Using Lake

Sediments. Volume 1: Basin Analysis, Coring and Chronological Techniques. Kluwer Academic Publishers, Dordrecht, The Netherlands.

Kemp AC, Horton B, Donnelly JP, Mann ME, Vermeer M, Rahmstorf S., 2011. Climate related sea-level variations over the past two millennia. Proc Natl Acad Sci. 108:11017–22.

Kemp AC, Bernhardt CE, Horton BP, Vane CH, Peltier WR, Hawkes AD, *et al*., 2014. Late Holocene sea- and land-level change on the U.S. Southeastern Atlantic coast. Mar Geol. 357: 90–100.

Kemp, A.C., Dutton, A. and Raymo, M.E., 2015. Paleo constraints on future sea-level rise. Current Climate Change Reports, 1(3), pp.205-215.

Kennett, J.P., 1982. Marine Geology, 813 pp.

Kennington, K., 2002. The environmental applications of diatoms.*Quaternary Environmental Micropalaeontology. Arnold, London*, pp.166-184.

Kennington, K., Allen, J.R., Wither, A., Shammon, T.M. and Hartnoll, R.G., 1999. Phytoplankton and nutrient dynamics in the north-east Irish Sea. In*Biological, Physical and Geochemical Features of Enclosed and Semi-enclosed Marine Systems* (pp. 57-67). Springer Netherlands.

Kido, Y., Koshikawa, T. and Tada, R., 2006. Rapid and quantitative major element analysis method for wet fine-grained sediments using an XRF microscanner. *Marine Geology*, *229*(3), pp.209-225.

Kilbourne, K.H., Quinn, T.M., Webb, R., Guilderson, T., Nyberg, J. and Winter, A., 2008. Paleoclimate proxy perspective on Caribbean climate since the year 1751: Evidence of cooler temperatures and multidecadal variability.*Paleoceanography*, *23*(3).

Kjerfve B., 1986. Comparative oceanography of coastal lagoons. In: D. A. Wolfe (ed.) Estuarine variability. Academic Press, New York, 63-81.

Knight, J., 2014. Subglacial hydrology and drumlin sediments in Connemara, western Ireland. *Geografiska Annaler: Series A, Physical Geography*, *96*(3), pp.403-415.

Knight, J., 2011. Subglacial processes and drumlin formation in a confined bedrock valley, northwest Ireland. Boreas, 40(2), pp.289-302.

Knight, J.R., Allan, R.J., Folland, C.K., Vellinga, M. and Mann, M.E., 2005. A signature of persistent natural thermohaline circulation cycles in observed climate. *Geophysical Research Letters*, *32*(20).

Knudsen, M.F., Seidenkrantz, M.S., Jacobsen, B.H. and Kuijpers, A., 2011. Tracking the Atlantic Multidecadal Oscillation through the last 8,000 years.Nature Communications, 2, p.178.).

Kolbe R.W. (1927). Zur Ökologie, Morphologie und Systematik der BrackwasserDiatomeen. Pflanzenforschung 7: 1-146.

Krammer K. & Lange-Bertalot H., 1986. Bacillariophyceae. Naviculaceae. Heidelberg & Berlin: Spektrum Akademisher Verlag.

Krammer K. & Lange-Bertalot H., 1988. Bacillariophyceae. Bacillariaceae, Epithemiaceae, Surerillaceae. Heidelberg & Berlin: Spektrum Akademisher Verlag.

Krammer K. & Lange-Bertalot H., 1991a. Bacillariophyceae. Centrales, Fragilariaceae, Eunotiaceae. Heidelberg & Berlin: Spektrum Akademisher Verlag.

Krammer K. & Lange-Bertalot H., 1991b. Bacillariophyceae. Achnanthaceae. Heidelberg & Berlin: Spektrum Akademisher Verlag.
Kreveld, S.V., Sarnthein, M., Erlenkeuser, H., Grootes, P., Jung, S., Nadeau, M.J., Pflaumann, U. and Voelker, A., 2000. Potential links between surging ice sheets, circulation changes, and the Dansgaard Oeschger cycles in the Irminger Sea, 60–18 kyr. *Paleoceanography*, *15*(4), pp.425-442.

Kylander, M.E., Ampel, L., Wohlfarth, B. and Veres, D., 2011. High- resolution X- ray fluorescence core scanning analysis of Les Echets (France) sedimentary sequence: new insights from chemical proxies. *Journal of Quaternary Science*,*26*(1), pp.109-117.

Labudová, L., Šťastný, P. and Trizna, M., 2013. The north atlantic oscillation and winter precipitation totals in Slovakia. Moravian Geographical Reports, 21(4), pp.38-49.

Lacka, M., Pawlowski, J., Zajaczkowski, M. (2015) New Methods in the reconstruction of Arctic Marine Paleoenvironments IN: Impact of Climate Changes on Marine Environments

Lagerloef, G., Boutin, J., Chao, Y., Delcroix, T., Font, J., Niiler, P., Reul, N., Riser, S.J., Schmitt, R., Stammer, D. and Wentz, F., 2010. Resolving the global surface salinity field and variations by blending satellite and in situ observations. In OceanObs 09 pp. 587-597.

Lamb, H.H., 1995 "Climate, History and the Modern World. (2nd Edition).433pp.

Lamb, H.H., Gasse, F., Benkaddour, A., Roberts, C.N. 1995. Relation between century-scale Holocene arid intervals in tropical and temperate zones. Nature 373:134-137.

Lamb, A. L., Wilson, G. P., and Leng, M. J., 2006. A review of coastal palaeoclimate and relative sea-level reconstructions using δ13C and C/N ratios in organic material. Earth-Science Reviews 75, 29-57.

Lambeck, K., Smither, C. and Johnston, P., 1998. Sea-level change, glacial rebound and mantle viscosity for northern Europe. *Geophysical Journal International*, *134*(1), pp.102-144.

Lambeck, K., Esat, T.M. and Potter, E.K., 2002. Links between climate and sea levels for the past three million years. *Nature*, *419*(6903), pp.199-206.

Lambeck, K., Purcell, A., Zhao, J. and Svensson, N.O., 2010. The Scandinavian ice sheet: from MIS 4 to the end of the Last Glacial Maximum. Boreas, 39(2), pp.410-435.

Lambeck, K., Rouby, H., Purcell, A., Sun, Y. and Sambridge, M., 2014. Sea level and global ice volumes from the Last Glacial Maximum to the Holocene.Proceedings of the National Academy of Sciences, 111(43), pp.15296-15303.

Lancelot, C. and Muylaert, K., 2011. Trends in estuarine phytoplankton ecology, in: Wolanski, E. et al. Treatise on Estuarine and Coastal Science: 7. Functioning ecosystems at the land-ocean interface. pp. 5-15.

Lane, P., Donnelly, J.P., Woodruff, J.D. and Hawkes, A.D., 2011. A decadally-resolved paleohurricane record archived in the late Holocene sediments of a Florida sinkhole. *Marine Geology*, *287*(1), pp.14-30.

Lansky, D.E., B.W. Logan, R.G. Brown, A.C. Hine, 1979. A new approach to portable Vibrocoring underwater and on land. J. Sed. Petrol. 654-657.

Largier, J.H. 1993. Estuarine fronts: How important are they? Estuaries, 16, 1-11.

Larocque, I. and Hall, R. I., 2003. Chironomids as quantitative indicators of mean July air temperature: validation by comparison with century long meteorological records from northern Sweden. Journal of Paleolimnology, Vol. 29, pp 475-493.

Last, W., 2001 Textural Analysis of Lake Sediments. In W.M. Last and J.P. Smol (eds.), 2001. Tracking Environmental Change Using Lake Sediments. Volume 1: Basin Analysis, Coring and Chronological Techniques. Kluwer Academic Publishers, Dordrecht, The Netherlands.

Le Roux, V., Lee, C.T. and Turner, S.J., 2010. Zn/Fe systematics in mafic and ultramafic systems: Implications for detecting major element heterogeneities in the Earth's mantle. *Geochimica et Cosmochimica Acta*,*74*(9), pp.2779-2796.

Lei, W., 1995. Three Dimensional Hydrodynamic Modelling in Galway Bay. PhD Thesis, National University of Ireland, Dublin.

Leorri, E., Cearreta, A., 2004. Holocene environmental development of the Bilbao estuary, northern Spain: sequence stratigraphy and foraminiferal interpretation. Marine Micropaleontology 51, 75-94.

Leorri, E., Cearreta, A. and Milne, G., 2012. Field observations and modelling of Holocene sea-level changes in the southern Bay of Biscay: implication for understanding current rates of relative sea-level change and vertical land motion along the Atlantic coast of SW Europe. Quaternary Science Reviews,42, pp.59-73.

Leuschner, D.C. and Sirocko, F., 2000. The low-latitude monsoon climate during Dansgaard–Oeschger cycles and Heinrich events. *Quaternary Science Reviews*, *19*(1), pp.243-254.

Lewis, J., 2011. Holocene Environmental Change in Coastal Denmark: interactions between land, sea and society. PhD Thesis, Loughboro University.

Lewis, J.P., Ryves, D.B., Rasmussen, P., Knudsen, K.L., Petersen, K.S., Olsen, J., Leng, M.J., Kristensen, P., McGowan, S. and Philippsen, B., 2013. Environmental change in the Limfjord, Denmark (ca 7500–1500 cal yrs BP): a multiproxy study. *Quaternary Science Reviews*, *78*, pp.126-140.

Libby, W. F., Anderson, E. C., & Arnold, J. R., 1949. Age determination by radiocarbon content: world-wide assay of natural radiocarbon. Science, 109(2827), 227-228.

Liu, D., Sun, J., Zhang, J. and Liu, G., 2008. Response of the diatom flora in Jiaozhou Bay, China to environmental changes during the last century.*Marine Micropaleontology*, *66*(3), pp.279-290.

Liu, J., Milne, G.A., Kopp, R.E., Clark, P.U. and Shennan, I., 2016. Sea-level constraints on the amplitude and source distribution of Meltwater Pulse 1A.Nature Geoscience, 9(2), pp.130-134.

Loehle C, McCulloch H., 2008. Correction to: a 2000 Year global temperature reconstruction based on non-tree ring proxy data. Energ Environ 19:93–100.

Long, A.J. and Shennan, I., 1994. Sea-level changes in Washington and Oregon and the" earthquake deformation cycle". *Journal of Coastal Research*, pp.825-838.

Lowe, J.J. and Walker, M.J., C, 1997. Reconstructing Quaternary environments. *Longman, London*.

Lowe, J.J. and Walker, M.J.C., 2000. Radiocarbon dating the last glacial-interglacial transition (Ca. 14-9 14C ka BP) in terrestrial and marine records: the need for new quality assurance protocols. *Radiocarbon*, *42*(1), pp.53-68.

Löwemark, L., Chen, H.F., Yang, T.N., Kylander, M., Yu, E.F., Hsu, Y.W., Lee, T.Q., Song, S.R. and Jarvis, S., 2011. Normalizing XRF-scanner data: a cautionary note on the interpretation of high-resolution records from organic-rich lakes. *Journal of Asian Earth Sciences*, *40*(6), pp.1250-1256.

Lozano, I.; Devoy, R.J.N.; May, W., and Andersen, U., 2002. Storminess and associated cyclone tracks along the Atlantic coastlines of Europe: evolution during the last six decades and modelling an CO2-induced climate scenario. EOS Transactions, 82(20), Spring Meeting Supplement, Abstract.

Lozier, M.S., 2010. Deconstructing the conveyor belt. *Science*, *328*(5985), pp.1507-1511.

Lund, D.C., Lynch-Stieglitz, J. and Curry, W.B., 2006. Gulf Stream density structure and transport during the past millennium. *Nature*, *444*(7119), pp.601-604.

Lundqvist, G., Thomasson, H., 1923. Diatomaceekologien och kvartärgeologien. Geologiska föreningen i Stockholm Förhandlingar, 45, 379-385.

Magny, M., Bégeot, C., Guiot, J., and Peyron, O., 2003. Contrasting patterns of hydrological changes in Europe in response to Holocene climate cooling phases, Quaternary Sci. Rev., 22, 1589–1596.

Magny, M. and Bégeot, C., 2004. Hydrological changes in the European midlatitudes associated with freshwater outbursts from Lake Agassiz during the Younger Dryas event and the early Holocene. *Quaternary Research*, *61*(2), pp.181-192.

Magny, M. and Haas, J. N., 2004. A major widespread climatic change around 5300 cal. yr BP at the time of the Alpine Iceman, J. Quaternary Sci., 19, 423–430.

Magny, M., Combourieu-Nebout, N., de Beaulieu, J. L., BoutRoumazeilles, V., Colombaroli, D., Desprat, S., Francke, A., Joannin, S., Ortu, E., Peyron, O., Revel, M., Sadori, L., Siani, G., Sicre, M. A., Samartin, S., Simonneau, A., Tinner, W., Vannière, B., Wagner, B., Zanchetta, G., Anselmetti, F., Brugiapaglia, E., Chapron, E., Debret, M., Desmet, M., Didier, J., Essallami, L., Galop, D., Gilli, A., Haas, J. N., Kallel, N., Millet, L., Stock, A., Turon, J. L., and Wirth, S., 2013. North-south palaeohydrological contrasts in the central Mediterranean during the Holocene: tentative synthesis and working hypotheses, Climates Past, 9, 2043– 2071.

Mann, M.E., Bradley, R.S. and Hughes, M.K., 1998. Global-scale temperature patterns and climate forcing over the past six centuries. *Nature*,*392*(6678), pp.779-787.

Marine Institute, 2016. http://www.infomar.ie/surveying/Bays/Galway.php#Overview

Marine Institute, 2006. Sea Change (2007-2013) PART II: Marine Foresight Exercise for Ireland.

Mariotti, G. and Fagherazzi, S., 2012. Channels, tidal flat sediment exchange: The channel spillover mechanism. *Journal of Geophysical Research: Oceans*, *117*(C3).

Mariotti, G. and Fagherazzi, S., 2012. Channels-tidal flat sediment exchange: The channel spillover mechanism. *Journal of Geophysical Research: Oceans*, *117*(C3).

Maslin, M. and Tzedakis, C., 1996. Sultry last interglacial gets sudden chill .*EOS, Transactions American Geophysical Union*, *77*(37), pp.353-354.

Maslin, M.A., Stickley, C. and Ettwein, V., 2001. Paleo-oceanography: Holocene Climate variability. In: Encyclopedia of Ocean Sciences; John Steele, Stephen Thorpe and Karl Turkian (eds) Academic Press, p1210-1217.

Maslin, M.A., Vilela C., Mikkelsen, N. and Grootes, P., 2005. Causation of the Quaternary catastrophic failures of the Amazon Fan deduced from stratigraphy and benthic foraminiferal assemblages." Quaternary Science Review, volume 24, Issue 20-21, 2180-2193.

Mayewski, P.A., Meeker, L.D., Twickler, M.S., Whitlow, S., Yang, Q., Lyons, W.B. and Prentice, M., 1997. Major features and forcing of high latitude northern hemisphere atmospheric circulation using a 110,000 year long glaciochemical series. *Journal of Geophysical Research: Oceans*, *102*(C12), pp.26345-26366.

M^{c}Cabe, A.M., 1987. Quaternary deposits and glacial stratigraphy in Ireland.Quaternary Science Reviews, 6(3-4), pp.259-299.

M^{c}Cabe, A.M., 2008. Glacial Geology and Geomorphology: The Landscapes of Ireland Dunedin Academic Press;.

M^{c}Cabe, AM and O'Cofaigh, C., 1995. *Late Pleistocene morainal bank facies at greystones, eastern ireland - an example of sedimentation during ice marginal re-equilibration in an isostatically depressed basin.* Sedimentology, 42 (4). pp. 647-663.

M^{c}Cabe, A.M. and Dardis, G.F., 1989. Sedimentology and depositional setting of late Pleistocene drumlins, Galway Bay, western Ireland. *Journal of Sedimentary Research*, *59*(6).

M^{c}Cabe, A.M., Clark, P.U. and Clark, J., 2005. AMS 14 C dating of deglacial events in the Irish Sea Basin and other sectors of the British–Irish ice sheet.Quaternary Science Reviews, 24(14), pp.1673-1690.

M^{c}Cabe, A.M., Cooper, J.A.G. and Kelly, J.T. 2007 Relative sea level changes from NE Ireland during the last glacial termination. Journal of the Geological Society 164, 1059-63.

M^{c}Cabe, M., Knight, J. and McCarron, S., 1998. Evidence for Heinrich event 1 in the British Isles. Journal of Quaternary Science, 13(6), pp.549-568.

McCalpin, JP., Carver, GA., 2009. Paleoseismology of compressional tectonic environments, in: J.P. McCalpin (Ed.), Paleoseismology, International Geophysics, vol. 95 (2009), pp. 315–419.

McDermott, F., Mattey, D.P. and Hawkesworth, C., 2001. Centennial-scale Holocene climate variability revealed by a high-resolution speleothem δ18O record from SW Ireland. *Science*, *294*(5545), pp.1328-1331.

McDowell, D.M. and O'Connor, B.A., 1977. Hydraulic behavior of estuaries. Wiley.

McGinnity, P., Prodo¨hl, P., Ferguson, A., Hynes, R., O´ Maoile´idigh, N., Baker, N., Cotter, D., O'Hea, B., Cooke, D., Rogan, G., Taggart, J. and Cross, T., 2003. Fitness reduction and potential extinction of wild populations of Atlantic salmon Salmo salar as a result of interactions with escaped farm salmon. Proceedings of the Royal Society of London B 270, 2443/50.

McKeown, M., 2013. A Palaeolimnological Assessment of Human and Climate Influences on Chironomid Communities in Western Ireland. PhD Thesis. National University of Ireland, Galway.

McKillup, S. and Dyar, M.D., 2010. Geostatistics Explained, An introductory guide for earth scientists. Cambridge University Press.

McManus, J. 2000. Sedimentation associated with estuarine frontal systems. In K. Pye and J.R.L. Allen (Eds.) Coastal and Estuarine Environments: Sedimentology, Geomorphology and Geoarchaeology, Geological Society of London, Special Publication, 175, 5-11.

McManus, J. 2003. Salinity variations in the Tay Estuary. Continental Shelf Research.

McQuoid, M.R., Nordberg K., 2003. The diatom Paralia sulcata as an environmental indicator species in coastal sediments Estuarine, Coastal and Shelf Science 56: 339–354.

Millero, F. J. and Poisson, A., 1981. International one-atmosphere equation of state of seawater. Deep-Sea Research 28, 625-629.

Mills, K., Mackay, A.W., Bradley, R.S. and Finney, B., 2009. Diatom and stable isotope records of late-Holocene lake ontogeny at Indrepollen, Lofoten, NW Norway: a response to glacio-isostasy and Neoglacial cooling. *The Holocene*, *19*(2), pp.261-271.

Molloy, K. and O'Connell, M., 2004. Holocene vegetation and land-use dynamics in the karstic environment of Inis Oirr, Aran Islands, western Ireland: pollen analytical evidence evaluated in light of the archaeological record. *Quaternary International*, Vol. 113, pp 41-64

Moreno, A., Giralt, S., Valero-Garcés, B., Sáez, A., Bao, R., Prego, R., Pueyo, J.J., González-Sampériz, P. and Taberner, C., 2007. A 14kyr record of the tropical Andes: the Lago Chungará sequence (18 S, northern Chilean Altiplano). *Quaternary International*, *161*(1), pp.4-21.

Moreno, A., Valero-Garcés, B.L., González-Sampériz, P. and Rico, M., 2008. Flood response to rainfall variability during the last 2000 years inferred from the Taravilla Lake record (Central Iberian Range, Spain). *Journal of paleolimnology*,*40*(3), pp.943-961.

Morrison, L., Baumann, H.A., Stengel D.B., 2008. An assessment of metal contamination along the Irish coast using the seaweed Ascophyllum nodosum (Fucales, Phaeophyceae) Environmental Pollution 152: 293-303.

Murray, J. W., 1991. Ecology and Palaeoecology of Benthic Foraminifera. Longman, Harlow: 397 pp.
Murray, John W., 2003. An illustrated guide to the benthic foraminifera of the Hebridean shelf, west of Scotland, with notes on their mode of life. Palaeontologia Electronica 5(1):31pp.

Murray, J.W., 2001. The niche of benthic foraminifera, critical thresholds and proxies. *Marine Micropaleontology*, *41*(1), pp.1-7.

Murray, J., 2006. Ecology and Applications of Benthic Foraminifera. Cambridge: Cambridge University Press, UK.

Mylotte, R., 2014. Isolation and characterisation of organic components in sediments from an estuarine environment. PhD Thesis, University of Limerick.

Mylotte, R., Verheyen, V., Reynolds, A., Dalton, C., Patti, A.F., Chang, R.R., Burdon, J. and Hayes, M.H., 2015. Isolation and characterisation of recalcitrant organic components from an estuarine sediment core. *Journal of Soils and Sediments*, *15*(1), pp.211-224.

NPWS 2013. National Parks and Wildlife. *Galway Bay Complex SAC (site code: 0268) Conservation objectives supporting document - Marine habitats and species* Department of Arts, Heritage and the Gaeltacht. Dublin. 34pp.

Naylor, L. A., Stephenson, W. J. S., 2010. On the role of discontinuities in mediating shore platform erosion. Geomorphology, 114, 89 – 100.

Nees, S., 1997. High-resolution benthic foraminiferal records of the last glacial termination in the northern North Atlantic.

Neff, U., Burns, S.J., Mangini, A., Mudelsee, M., Fleitmann, D. and Matter, A., 2001. Strong coherence between solar variability and the monsoon in Oman between 9 and 6 kyr ago. Nature, 411(6835), pp.290-293.

Nelson, A.R. and Kashima, K., 1993. Diatom zonation in southern Oregon tidal marshes relative to vascular plants, foraminifera, and sea level.*Journal of Coastal Research*, pp.673-697.

Nelson, AR., Kashima, K., Bradley, L.A., 2009. Fragmentary evidence of great-earthquake subsidence during Holocene emergence, Valdivia estuary, south central Chile. Bulletin of the Seismological Society of America, 99 (1) pp. 71–86.

Nelson, D.M., Hu, F.S., Scholes, D.R., Joshi, N. and Pearson, A., 2008. Using SPIRAL (Single Pollen Isotope Ratio AnaLysis) to estimate C 3-and C 4-grass abundance in the paleorecord. Earth and Planetary Science Letters,269(1), pp.11-16.

Neuendorf, K.K., 2005. *Glossary of geology*. Springer Science & Business Media.

Nicholls, R.J., P.P. Wong, V.R. Burkett, J.O. Codignotto, J.E. Hay, R.F. McLean, S. Ragoonaden and C.D. Woodroffe, 2007: Coastal systems and low-lying areas. Climate Change 2007: Impacts, Adaptation and Vulnerability. Contribution of Working Group II to the Fourth Assessment Report of the Intergovernmental Panel on Climate Change, M.L. Parry, O.F. Canziani, J.P. Palutikof, P.J. van der Linden and C.E. Hanson, Eds., Cambridge University Press, Cambridge, UK, 315-356.

NOAA, 2016. Tidal datums. https://tidesandcurrents.noaa.gov/datum_options.html. Accessed 25/10/2016.

O'Carra, B., Williams, D.M., MerCer, B. and Wood, B., 2014. Evidence of environmental change since the earliest medieval period from the inter-tidal zone of Galway Bay. *Irish Naturalists' Journal*, *33*(Part 2), p.83.

O'Cofaigh, C.Ó., Evans, D.J., 2001. Sedimentary evidence for deforming bed conditions associated with a grounded Irish Sea glacier, southern Ireland. Journal of Quaternary Science, 16(5), pp.435-454.

O´Cofaigh C, Telfer MW, Bailey RM, Evans DJA., 2010. Late Pleistocene chronostratigraphy and ice sheet limits, southern Ireland. Quaternary Science Reviews.

O'Connell, M., Ghilardi, B. and Morrison, L., 2014. A 7000-year record of environmental change, including early farming impact, based on lake-sediment geochemistry and pollen data from County Sligo, western Ireland.*Quaternary Research*, *81*(1), pp.35-49.

O'Donncha, F., Hartnett, M., Nash, S., Ren, L., Ragnoli, E., 2015. Journal of Marine Systems, v. 142; 96–110.

O'Hanlon, L., 2002. Making waves. *Nature*, *415*(6870), pp.360-362.

Oldfield, F., 2005. *Environmental change: key issues and alternative perspectives*. Cambridge University Press.

Olsson, I., 1979. A warning against radiocarbon dating of samples containing little carbon. Boreas, 8(2), pp 203-207.

Oswald, W.W., Anderson, P.M., Brown, T.A., Brubaker, L.B., Hu, F.S., Lozhkin, A.V., Tinner, W. and Kaltenrieder, P., 2005. Effects of sample mass and macrofossil type on radiocarbon dating of arctic and boreal lake sediments. The Holocene, 15(5), pp.758-767.

Palmer, A.J. and Abbott, W.H., 1986. Diatoms as indicators of sea-level change. In *Sea-level Research* (pp. 457-487). Springer Netherlands.

Palmer, T.A., Montagna, P.A., Pollack, J.B., Kalke, R.D. and DeYoe, H.R., 2011. The role of freshwater inflow in lagoons, rivers, and bays.Hydrobiologia, 667(1), pp.49-67.

Patterson, R.T., Scott, D.B., McKillop, W.B., 1990. Recent marsh-type agglutinated foraminifera from inland salt springs, Manitoba, Canada. In: Hemblen, C., Kaminski, M.A., Kuhnt, W. and Scott, D.B. eds. Paleoecology, Biostratigraphy, Paleoceanography and Taxonomy of Agglutinated Foriminfera. Dordrecht: Kluwer, pp. 765-81.

Patterson, R.T., Hutchinson, I., Guilbault, J.-P., Clague, J.J., 2000. A comparison of the vertical zonation of diatom, foraminifera, and macrophyte assemblages in a coastal marsh: implications for greater paleo-sea level resolution. Micropaleontology 46 (3), 229–244.

Patterson, R.T., Prokoph, A. and Chang, A., 2004. Late Holocene sedimentary response to solar and cosmic ray activity influenced climate variability in the NE Pacific. *Sedimentary Geology*, *172*(1), pp.67-84.

Patterson, R.T., Prokoph, A., Kumar, A., Chang, A.S. and Roe, H.M., 2005. Late Holocene variability in pelagic fish scales and dinoflagellate cysts along the west coast of Vancouver Island, NE Pacific Ocean. *Marine Micropaleontology*,*55*(3), pp.183-204.

Peck VL, Hall IR, Zahn R, Grousset F, Hemming SR, Scourse JD. 2007. The relationship of Heinrich events and their European precursors over the past 60 ka BP: a multi-proxy ice rafted debris provenance study in the North East Atlantic. Quaternary Science Reviews 26:862–875.

Peiser, B.J., 1998. Comparative Analysis of Late Holocene Environmental and Social Upheaval: Evidence for a Global Disaster in the Late 3rd Millennium BC. In *Natural Catastrophes During Bronze Age Civilisations: Archaeological, Geological, Astronomical and Cultural Perspectives* (p. 117).

Pelling, H.E., Green, J.M. and Ward, S.L., 2013. Modelling tides and sea-level rise: To flood or not to flood. *Ocean Modelling*, *63*, pp.21-29.

Peltier, W.R., 1998. Postglacial variations in the level of the sea: implications for climate dynamics and solid-Earth geophysics, Rev. Geophysics, 36(4), 603–689.

Peltier, W.R., 2004. Global glacial isostasy and the surface of the ice-age Earth: the ICE-5G (VM2) model and GRACE, Annu. Rev. Earth Pl. Sc., 32, 111–149.

Peltier, W.R. and Fairbanks, R.G., 2006. Global glacial ice volume and Last Glacial Maximum duration from an extended Barbados sea level record, Quaternary Science Review, 25(23–24), 3322–3337.

Peltier, W.R., Shennan, I., Drummond, R., Horton, B.P., 2002. On the postglacial isostatic adjustment of the British Isles and the shallow viscoelastic structure of the Earth, Geophys. J. Int., 148(3), 443–475.

Peltier, W.R., Argus, D.F., Drummond, R., 2015. Space geodesy constrains ice-age terminal deglaciation: the global ICE-6G_C (VM5a) model, J. geophys. Res.: Solid Earth, 119.

Petchey F., A. Anderson, A. Zondervan, S. Ulm, A. Hogg., 2008. New marine Î”R values for the South Pacific subtropical gyre region. Radiocarbon 50(3):373-397.

Peterson, L.C., Haug, G.H., Hughen, K.A. and Röhl, U., 2000. Rapid changes in the hydrologic cycle of the tropical Atlantic during the last glacial. *Science*,*290*(5498), pp.1947-1951.

Peterson, L.C. and Haug, G.H., 2006. Variability in the mean latitude of the Atlantic Intertropical Convergence Zone as recorded by riverine input of sediments to the Cariaco Basin (Venezuela). *Palaeogeography, Palaeoclimatology, Palaeoecology*, *234*(1), pp.97-113.

Pidgeon, E. J., and Winant, C.D., 2005. Diurnal variability in currents and temperature on the continental shelf between central and southern California, Journal of Geophysical Research, 110.

Pidwirny, M., 2006. Coastal and Marine Processes and Landforms. *Fundamentals of Physical Geography, 2nd Edition*.

Pilarczyk, J.E., Dura, T., Horton, B.P., Engelhart, S.E., Kemp, A.C. and Sawai, Y., 2014. Microfossils from coastal environments as indicators of paleo-earthquakes, tsunamis and storms. *Palaeogeography, Palaeoclimatology, Palaeoecology*, *413*, pp.144-157.

Pilcher, J., Bradley, R. S., Francus, P. & Anderson, L., 2005. A Holocene tephra record from the Lofoten Islands, Arctic Norway. Boreas, Vol. 34, pp. 136–156.

Pillar, H.R., Heimbach, P., Johnson, H.L. and Marshall, D.P., 2016. Dynamical attribution of recent variability in Atlantic overturning. Journal of Climate, 29(9), pp.3339-3352.

Pinet, P.R., 1998. Invitation to Oceanography. Sudbury, MA.: Jones and Bartlett Publishers. 596 pp. Sudbury, MA.

Plets, R.M., Callard, S.L., Cooper, J.A.G., Long, A.J., Quinn, R.J., Belknap, D.F., Edwards, R.J., Jackson, D.W., Kelley, J.T., Long, D. and Milne, G.A., 2015. Late Quaternary evolution and sea-level history of a glaciated marine embayment, Bantry Bay, SW Ireland. Marine Geology, 369, pp.251-272.

Potter, R. A., and Lozier, M. S., 2004. On the warming and salinification of the Mediterranean outflo w waters in the North Atlantic. Geophysical Research Letters, 31: L01202.

Praeg, D., McCarron, S., Clarke, C., Dove, D., Evans, W., O'Cofaigh C., Romeo, R., Scott, G. Exploring submerged glacial landscapes south and west of Ireland: preliminary results from the GATEWAYS campaign. Irish Geological Research Meeting, 2013 University of Ulster. 64.

Pritchard, D. and Hogg, A. J., 2003. Suspended sediment transport under seiches in circular and elliptical basins**:** *Coastal Engineering* 49: 43–70.

Pritchard, D.W., 1967. Estuaries: Sediment transport and sedimentation in estuaries. In G.H. Lauff (Ed.) Estuaries, American Association for the Advancement of Science, 158-179.

Pugh, D.T., 1982. A comparison of recent and historical tides and mean sea levels off Ireland. Geophysical Journal of the Royal Astronomical Society, 71, 809–815.

Pyle, L., Cooper, S.R. and Huvane, J.K., 1998. *Diatom paleoecology Pass Key Core 37, Everglades National Park, Florida Bay*. US Geological Survey.

Qin, L. and Humayun, M., 2008. The Fe/Mn ratio in MORB and OIB determined by ICP-MS. *Geochimica et Cosmochimica Acta*, *72*(6), pp.1660-1677.

Rashid, T., Suzuki, S., Monsaur, M.H., Saha, S.K., 2013. Relative sea-level changes during the Holocene in Bangladesh. *Journal of Asian Earth Sciences*. 64, pp. 136-150.

Rashid, T., 2014. Holocene Sea-level Scenarios in Bangladesh, Springer Briefs in Oceanography.

Rasmussen, S.O., Andersen, K.K., Svensson, A.M., Steffensen, J.P., Vinther, B.M., Clausen, H.B., Siggaard, Andersen, M.L., Johnsen, S.J., Larsen, L.B., Dahl- Jensen, D. and Bigler, M., 2006. A new

Greenland ice core chronology for the last glacial termination. Journal of Geophysical Research: Atmospheres, 111(D6).

Reimer, P J and Reimer, R W., 1987-2014. A marine reservoir correction database and on-line interface. Radiocarbon 43:461-463. (supplemental material URL:http://www.calib.org).

Reimer, P.J., Baillie, M.G., Bard, E., Bayliss, A., Beck, J.W., Blackwell, P.G., Bronk, R.C., Buck, C.E., Burr, G.S., Edwards, R.L. and Friedrich, M., 2009. IntCal09 and Marine09 radiocarbon age calibration curves, 0-50,000 years cal BP. Radiocarbon, 51(4), pp.1111-1150.

Reimer, P. J., Bard, E., Bayliss, A., Beck, J. W., Blackwell, P. G., Bronk Ramsey, C., Grootes, P. M., Guilderson, T. P., Haflidason, H., Hajdas, I., HattŽ, C., Heaton, T. J., Hoffmann, D. L., Hogg, A. G., Hughen, K. A., Kaiser, K. F., Kromer, B., Manning, S. W., Niu, M., Reimer, R. W., Richards, D. A., Scott, E. M., Southon, J. R., Staff, R. A., Turney, C. S. M., & van der Plicht, J., 2013. IntCal13 and Marine13 Radiocarbon Age Calibration Curves 0-50,000 Years cal BP. Radiocarbon, 55(4).

Ren, J., Jiang, H., Seidenkrantz, M.S. and Kuijpers, A., 2009. A diatom-based reconstruction of Early Holocene hydrographic and climatic change in a southwest Greenland fjord. *Marine Micropaleontology*, *70*(3), pp.166-176.

Reverdin, G., 2010. North Atlantic subpolar gyre surface variability (1895-2009). Journal of climate, 23(17), pp.4571-4584.

Richerson, P. J., T. H. Suchanek, R. A. Zierenberg, D. G. Slotton, C. A. Eagles-Smith, and C. E. Vaughn., 2008. Anthropogenic stressors and changes in the Clear Lake ecosystem as recorded in sediment cores. Ecological Applications 18:A257–A283.

Richter, T.O., Van der Gaast, S., Koster, B., Vaars, A., Gieles, R., de Stigter, H.C., De Haas, H. and van Weering, T.C., 2006. The Avaatech XRF Core Scanner: technical description and applications to NE Atlantic sediments. *Geological Society, London, Special Publications*, *267*(1), pp.39-50.

Rick, Torben C., Gregory A. Henkes, Darrin L. Lowery, Steven M. Colman, Brendan J. Culleton, 2012. Marine radiocarbon reservoir corrections (Î”R) for Chesapeake Bay and the Middle Atlantic Coast of North America ,Quaternary Research 77 205-210.

Riethdorf, J.R., Thibodeau, B., Ikehara, M., Nürnberg, D., Max, L., Tiedemann, R. and Yokoyama, Y., 2016. Surface nitrate utilization in the Bering sea since 180kA BP: Insight from sedimentary nitrogen isotopes.*Deep Sea Research Part II: Topical Studies in Oceanography*, *125*, pp.163-176.

Riggs, S. R., Ambrose, W. G., Cook, J. W., Snyder, S. W., 1998. Sediment Production on Sediment-Starved Continental Margins: The Interrelationship Between Hardbottoms, Sedimentological and Benthic Community Processes, and Storm Dynamics. Journal of Sedimentary Research, Section A: Sedimentary Petrology and Processes, 68, 155-168.

Rindi, F., Sartoni, G. and Cinelli, F., 2002. A floristic account of the benthic marine algae of Tuscany (Western Mediterranean Sea). Nova Hedwigia, 74(1-2), pp.201-250.

Roberts, N., 1998. The Holocene: An Environmental History, 2nd Edition. Wiley-Blackwell; 328pp.

Roberts, D.H., Dackombe, R.V. and Thomas, G.S., 2007. Palaeo- ice streaming in the central sector of the British—Irish Ice Sheet during the Last Glacial Maximum: evidence from the northern Irish Sea Basin. *Boreas*,*36*(2), pp.115-129.

Roberts, N., Brayshaw, D., Kuzucuoglu, C., Perez, R., and Sadori, 2011. The mid-Holocene climatic transition in the Mediterranean: Causes and consequences, Holocene, 21, 3–13.

Rodrigo, F.S., Esteban-Parra, M.J. and Castro-Diez, Y., 1998. On the use of the Jesuit order private correspondence records in climate reconstructions: A case study from Castille (Spain) for 1634–1648 AD. *Climatic Change*, *40*(3-4), pp.625-645.

Roe, H.M., Doherty, C.T., Patterson, R.T. and Swindles, G.T., 2009. Contemporary distributions of saltmarsh diatoms in the Seymour–Belize Inlet Complex, British Columbia, Canada: Implications for studies of sea-level change. Marine Micropaleontology, 70(3), pp.134-150.

Rosén, P., Segerstrom, U., Eriksson, L., Renberg, I. and Birks, H. J. B., 2001. Holocene climate change reconstructed from diatoms, chironomids, pollen and nearinfrared spectroscopy at an alpine lake (Sjuodjijaure) in northern Sweden. The Holocene, Vol. 11(5), pp 551-562.

Ross, D., 1995. Introduction to Oceanography. New York: HarperCollins College Publishers. pp. 199-226, 339-343.

Rossby, T., Flagg, C. and Donohue, K., 2010. On the variability of Gulf Stream transport from seasonal to decadal timescales. Journal of Marine Research, 68, 503–522.

Rothwell, R.G., Hoogakker, B., Thomson, J., Croudace, I.W. and Frenz, M., 2006. Turbidite emplacement on the southern Balearic Abyssal Plain (western Mediterranean Sea) during Marine Isotope Stages 1–3: an application of ITRAX XRF scanning of sediment cores to lithostratigraphic analysis. *Geological Society, London, Special Publications*, *267*(1), pp.79-98.

Round, F.E., Crawford, R.M. and Mann, D.G., 1990. *Diatoms: biology and morphology of the genera*. Cambridge University Press.

Rousseau, D.D., Preece, R. and Limondin-Lozouet, N., 1998. British late glacial and Holocene climatic history reconstructed from land snail assemblages. *Geology*, *26*(7), pp.651-654.
Ruiz, F., González-Regalado, M.L., Pendón, J.G., Abad, M., Olías, M. and Muñoz, J.M., 2005. Correlation between foraminifera and sedimentary environments in recent estuaries of southwestern Spain: applications to Holocene reconstructions. *Quaternary International*, *140*, pp.21-36.

Ryves D.B., Juggins S., Fritz S.C., Battarbee R.W. , 2001. Experimental diatom dissolution and the quantification of microfossil preservation in sediments. Palaeogeography, Palaeoclimatology, Palaeoecology 172: 99-113.

Ryves D.B., Battarbee R.W., Juggins S., Fritz S.C., Anderson J.N., 2006. Physical and chemical predictors of diatom dissolution in freshwater and saline lake sediments in North America and West Greenland. Limnology and Oceanography 51: 1355-1368.

Ryves D.B., Battarbee R.W., Fritz S.C., 2009. The Dilemma of Disappearing Diatoms: Incorporating Diatom Dissolution Data into Paleoenvironmental Modeling and Reconstruction. Quaternary Science Reviews 28: 120-136.

Sanders, J.E. and J. Imbrie, 1963. Continuous cores of Bahamian calcareous sands made by vibrodrilling. Geol Soc. Amer. Bull. 74: 1287-1292.

Sarnthein, M., Stattegger, K., Dreger, D., Erlenkeuser, H., Grootes, P., Haupt, B.J., Jung, S., Kiefer, T., Kuhnt, W., Pflaumann, U. and Schäfer-Neth, C., 2001. Fundamental modes and abrupt changes in North Atlantic circulation and climate over the last 60 ky—concepts, reconstruction and numerical modeling. In *The Northern North Atlantic* (pp. 365-410). Springer Berlin.

Sawai, Y., Namegaya, Y., Okamura, Y., Satake, K. and Shishikura, M., 2012. Challenges of anticipating the 2011 Tohoku earthquake and tsunami using coastal geology. *Geophysical Research Letters*, *39*(21).

Schaller, T. and Wehrli, B., 1996. Geochemical-focusing of manganese in lake sediments—an indicator of deep-water oxygen conditions. *Aquatic Geochemistry*, *2*(4), pp.359-378.

Schrader, H., Isrenn, K., Swanberg, N., Paetzel, M. and Sæthre, T., 1993. Early Holocene diatom pulse in the Norwegian Sea and its paleoceanographic significance. *Diatom research*, *8*(1), pp.117-130.

Scott, D.B. and Medioli, F.S., 1980. Quantitative studies of marsh foraminiferal distributions in Nova Scotia; implications for sea level studies. *Special Publications-Cushman Foundation for Foraminiferal Research*.

Scott, D.B., Medioli, F.S. and Schafer, C.T., 2001. *Monitoring in coastal environments using foraminifera and thecamoebian indicators*. Cambridge University Press.

Scourse, J.D., 1991. Late Pleistocene stratigraphy and palaeobotany of the Isles of Scilly. *Philosophical Transactions of the Royal Society of London B: Biological Sciences*, *334*(1271), pp.405-448.

Scourse, J., 2013. Quaternary sea- level and palaeotidal changes: a review of impacts on, and responses of, the marine biosphere, Oceanography and Marine Biology: An Annual Review, 2013, 51, 1-70.

Scourse, J.D., Austin, W.E.N., Bateman, R.M., Catt, J.A., Evans, C.D.R., Robinson, J.E. and Young, J.R., 1990. Sedimentology and micropalaeontology of glacimarine sediments from the central and southwestern Celtic Sea. *Geological Society, London, Special Publications*,*53*(1), pp.329-347.

Scourse, J.D., Haapaniemi, A.I., Colmenero-Hidalgo, E., Peck, V.L., Hall, I.R., Austin, W.E.N., Knutz, P.C. and Zahn, R., 2009. Initiation, dynamics, and deglaciation of the last British-Irish Ice Sheet: the deep-sea ice-rafted detritus record. Quaternary Science Reviews 28, 3066-3084.

Sejrup, H.P., Haflidason, H., Aarseth, I., Forsberg, C.F., King, E., Long, D., Rokoengen, K., 1994. Late Weichselian glaciation history of the northern North Sea. Boreas 23, 1–13.

Sejrup, H.P., Hjelstuen, B.O., Dahlgren, K.T., Haflidason, H., Kuijpers, A., Nygård, A., Praeg, D., Stoker, M.S. and Vorren, T.O., 2005. Pleistocene glacial history of the NW European continental margin. Marine and Petroleum Geology, 22(9), pp.1111-1129.

Seppä, H. and Birks, H. J. B., 2002. Holocene climate reconstructions from the Fennoscandian Tree-line area based on pollen data from Toskaljavri. Quaternary Research, Vol. 57(2), pp 191-199.

Seppä, H., Nyman, M., Korhola, A. and Weckström, J., 2002. Changes of treelines and alpine vegetation in relation to post glacial climate dynamics in northern Fennoscandia based on pollen and chironomid records. *Journal of Quaternary Science*, *17*(4), pp.287-301.

Shennan, I., 1992. Late Quaternary sea-level changes and crustal movements in eastern England and eastern Scotland: an assessment of models of coastal evolution. *Quaternary International*, *15*, pp.161-173.

Shennan, I., Innes, J.B., Long, A.J. and Zong, Y., 1994. Late Devensian and Holocene relative sealevel changes at Loch nan Eala, near Arisaig, northwest Scotland. *Journal of Quaternary Science*, *9*(3), pp.261-283.

Shennan, I., Lambeck, K., Flather, R., Horton, B., McArthur, J., Innes, J., Lloyd, J., Rutherford, M. and Wingfield, R., 2000a. Modelling western North Sea palaeogeographies and tidal changes during the Holocene. *Geological Society, London, Special Publications*, *166*(1), pp.299-319.

Shennan, I., Lambeck, K., Horton, B., Innes, J., Lloyd, J., McArthur, J., Purcell, T. and Rutherford, M., 2000b. Late Devensian and Holocene records of relative sea-level changes in northwest Scotland and their implications for glacio-hydro-isostatic modelling. Quaternary Science Reviews, 19(11), pp.1103-1135.

Shennan, I., Peltier, W.R., Drummond, R., Horton, B., 2002. Global to local scale parameters determining relative sea-level changes and the post-glacial isostatic adjustment of Great Britain. Quaternary Science Reviews,21(1), pp.397-408.

Shennan, I., Bradley, S., Milne, G., Brooks, A., Bassett, S. and Hamilton, S., 2006. Relative sea level changes, glacial isostatic modelling and ice sheet reconstructions from the British Isles since the Last Glacial Maximum. Journal of Quaternary Science, 21(6), pp.585-599.

Shennan, I., Bruhn, R. and Plafker, G., 2009. Multi-segment earthquakes and tsunami potential of the Aleutian megathrust. *Quaternary Science Reviews*, *28*(1), pp.7-13.

Shennan, I., Barlow, N., Carver, G., Davies, F., Garrett, E. and Hocking, E., 2014. Great tsunamigenic earthquakes during the past 1000 yr on the Alaska megathrust. *Geology*, *42*(8), pp.687-690.

Shennan, I., Long, A. J., and Horton, B. P. (Eds.), 2015: Handbook of SeaLevel Research, Wiley Blackwell.

Shepard, F.P., 1954. Nomenclature based on sand-silt-clay ratios. *Journal of Sedimentary Research*, *24*(3).

Sherrod, B.L., Rollins, H.B. and Kennedy, S.K., 1989. Subrecent intertidal diatoms from St. Catherines Island, Georgia: taphonomic implications.*Journal of Coastal Research*, pp.665-677.

Shi, Y., Davis, K., Duffy, C., Yu, X., 2013 Development of a Coupled Land Surface Hydrologic Model and Evaluation at a Critical Zone Observatory. Journal of Hydrometeorology, 14, 1401—1420.

Shindell, D., Rind, D., Balachandran, N., Lean, J. and Lonergan, P., 1999. Solar cycle variability, ozone, and climate. Science, 284(5412), pp.305-308.

Simpson, J. H. 2005. Tidal processes in shelf seas. In The Global Coastal Ocean: Processes and Meth -ods, pp. 113–151. Ed. by K.H. Brink, A.R. Robinson . Harvard University Press, Cambridge 628 pp.

Simpson, J. H., Sharples, J., 2012. *Introduction to the physical and biological oceanography of shelf seas.* Cambridge: Cambridge University Press, UK.

Simonsen, R., 1969. Diatoms as indicators in estuarine environments.*Veröffentlichungen Institut für Meeresforschung zu Bremershaven*, *11*, pp.287-291.

Sirocko, F., Sarnthein, M., Lange, H. and Erlenkeuser, H., 1991. Atmospheric summer circulation and coastal upwelling in the Arabian Sea during the Holocene and the last glaciation. *Quaternary Research*, *36*(1), pp.72-93.

Skagseth, Ø., Furevik, T., Ingvaldsen, R., Loeng, H., Mork, K. A., Orvik, K. A., and Ozhigin, V. 200 8Volume and heat transports to the Arctic Ocean via the Norwegian and Barents Seas. In Arctic–Subarctic Ocean Fluxes: Defining the Role of the Northern Seas in Climate, pp. 45-64 Ed. B. Dickson, J. Meincke, and P. Rhines. Springer Verlag, Berlin. 736 pp.

Smith, D., Raper, S.B., Zerbini, S. and Sanchez-Arcilla, A., 2000. Sea level change and coastal processes: Implications for Europe. Office for Official Publications of European Communities, Luxembourg, pp. 247.

Smith, D.I. and Stopp, P., 1978. *The river basin: An introduction to the study of hydrology*.

Smith, D., Raper, S.B., Zerbini, S. and Sanchez-Arcilla, A., 2000. Sea level change and coastal processes: Implications for Europe. Office for Official Publications of European Communities, Luxembourg, 247p.

Smith, D.E., Davies, M.H., Brooks, C.L., Mighall, T.M., Dawson, S., Rea, B.R., Jordan, J.T., Holloway, L.K., 2010. Holocene relative sea levels and related prehistoric activity in the Forth lowland, Scotland, United Kingdom. Quaternary Science Reviews 29, 2382-2410.

Smith, T. M., Reynolds, R. W., and Lawrimore, J. 2008. Improvements to NOAA's historical merged land-ocean surface temperature analysis (1880–2006). Journal of Climate, 21: 2283–2296.

Smith, D.E., Harrison, S., Firth, C.R. and Jordan, J.T., 2011. The early Holocene sea level rise. *Quaternary Science Reviews*, *30*(15), pp.1846-1860.

Smith, G.J., Zimmerman, R.C. and Alberte, R.S., 1992. Molecular and physiological responses of diatoms to variable levels of irradiance and nitrogen availability: growth of Skeletonema costatum in simulated upwelling conditions. *Limnology and Oceanography*, *37*(5), pp.989-1007.

Smol, J.P., 1990. Paleolimnology: recent advances and future challenges.*Mem. Ist. ital. Idrobiol*, *47*, pp.253-276.

Snoeijs P., 1993. *Intercalibration and distribution of diatom species in the Baltic Sea*. Opulus Press Uppsala.

Snoeijs P. and Vilbaste S., 1994. *Intercalibration and distribution of diatom species in the Baltic Sea*. Opulus Press Uppsala.

Snoeijs P. and Potapova M., 1995. *Intercalibration and distribution of diatom species in the Baltic Sea* Opulus Press Uppsala. Opulus Press Uppsala.

Snoeijs P. and Kasperovičienė J., 1996. *Intercalibration and distribution of diatom species in the Baltic Sea*. Opulus Press Uppsala.

Snoeijs P. and Balashova N., 1998. *Intercalibration and distribution of diatom species in the Baltic Sea*. Opulus Press Uppsala.

Snoeijs P., 2004. Diatoms and environmental change in brackish waters. In: E. F. Stoermer and J. P. Smol (eds.), *The Diatoms: Applications for the Environmental and Earth Sciences.* Cambridge University Press.

Snoeijs P. and Weckström K., 2010. Diatoms and environmental change in large brackish water ecosystems. In: J. P. Smol and E. F. Stoermer (eds.), *The Diatoms - Applicationsfor the Environmental and Earth Sciences. Second Edition.* Cambridge University Press, 287-308.

Sobolev, N.V., Schertl, H.P., Neuser, R.D. and Shatsky, V.S., 2007. Relict unusually low iron pyrope-grossular garnets in UHPM calc-silicate rocks of the Kokchetav massif, Kazakhstan. *International Geology Review*, *49*(8), pp.717-731.

Sorrel, P., Tessier, B., Demory, F., Delsinne, N. and Mouazé, D., 2009. Evidence for millennial-scale climatic events in the sedimentary infilling of a macrotidal estuarine system, the Seine estuary (NW France). Quat. Sci. Rev. 28, 499-516.

Sperazza, M., Moore, J.N., and Hendrix, M.C., 2004. High-resolution particle size analysis of naturally occurring very fine-grained sediment through laser diffractometry. Journal of Sedimentary Reseach,74(5): 736-743.

Steig, E.J., 1999. Mid-Holocene climate change. *Science*, *286*(5444), pp.1485-1487.

Stewart, R. H. 2008. Introduction to Oceanography, September 2008 Edition. Texas: Department of Oceanography, Texas A&M University pp 73-101, 183-210, 293-312.

Stolze, S., Muscheler, R., Dörfler, W. and Nelle, O., 2013. Solar influence on climate variability and human development during the Neolithic: evidence from a high-resolution multi-proxy record from Templevanny Lough, County Sligo, Ireland. Quaternary Science Reviews, Vol. 67, pp 138-159.

Stuiver, M. and Reimer, P.J., 1993. Extended 14C data base and revised CALIB 3.0 14C age calibration program, Radiocarbon 35:215-230.

Stuiver, M. and Suess, H.E., 1966. On the relationship between radiocarbon dates and true sample ages. Radiocarbon, 8(1), pp.534-540.

Stuiver, M, Pearson, G W, and Braziunas, T F, 1986. Radiocarbon age calibration of marine samples back to 9000 cal yr BP. Radiocarbon 28:980-1021.

Sutherland, D.G., 1980. Problems of radiocarbon dating deposits from newly deglaciated terrain: examples from the Scottish Lateglacial. Studies in the Lateglacial of North-West Europe. Pergamon Press, Oxford, pp.139-149.

Sutton, R. T., and D. L. R. Hodson, 2005: Atlantic Ocean forcing of the North American and European summer climate. Science, 309, 115–118.

Swindles, G.T., Morris, P.J., Baird, A.J., Blaauw, M. and Plunkett, G., 2012. Ecohydrological feedbacks confound peat based climate reconstructions. *Geophysical Research Letters*, *39*(11).

Syvitski, J.P.M., 2003. Supply and flux of sediment along hydrological pathways: research for the 21st century. Global Planet. Change 39:1–11.

Syvitski, J.P., Kettner, A.J., Correggiari, A. and Nelson, B.W., 2005. Distributary channels and their impact on sediment dispersal. Marine Geology, 222, pp.75-94.

ter Braak, 1987. Ordination. In R.H.G. Jongman, C.J.F. ter Braak and O.F.R. van Tongeren (Eds.), Data Analysis in Community and Landscape Ecology (pp. 91-173). Wageningen:Pudoc.

ter Braak, C.J.F., Prentice, I.C., 1988. A theory of gradient analysis. *Advances in Ecological Research*, 18, 271-313.

Tada, R., 1991. Origin of rhythmical bedding in middle Miocene siliceous rocks of the Onnagawa Formation, northern Japan. *Journal of Sedimentary Research*,*61*(7), pp.1123-1145.

Taffs, K.H., Farago, L.J., Heijnis, H. and Jacobsen, G., 2008. A diatom-based Holocene record of human impact from a coastal environment: Tuckean Swamp, eastern Australia. *Journal of Paleolimnology*, *39*(1), pp.71-82.

Terasmaa, J., Puusepp, L., Marzecová, A., Vandel, E., Vaasma, T. and Koff, T., 2013. Natural and human-induced environmental changes in Eastern Europe during the Holocene: a multi-proxy palaeolimnological study of a small Latvian lake in a humid temperate zone. *Journal of paleolimnology*,*49*(4), pp.663-678.

Thomas, E. and Varekamp, J.C., 1991. Paleo-environmental analyses of marsh sequences (Clinton, Connecticut): evidence for punctuated rise in relative sealevel during the latest Holocene. *Journal of Coastal Research*, pp.125-158.

Thomas, G.S., Chiverrell, R.C. and Huddart, D., 2004. Ice-marginal depositional responses to readvance episodes in the Late Devensian deglaciation of the Isle of Man. *Quaternary Science Reviews*, *23*(1), pp.85-106.

Thomson, J., Croudace, I.W. and Rothwell, R.G., 2006. A geochemical application of the ITRAX scanner to a sediment core containing eastern Mediterranean sapropel units. *Geological Society, London, Special Publications*, *267*(1), pp.65-77.

Thurman, H., 1994. Introductory Oceanography, 7th edition. New York: Macmillan Publishing Company. pp. 172-222.

Tjallingii, R., Röhl, U., Kölling, M. and Bickert, T., 2007. Influence of the water content on X-ray fluorescence core-scanning measurements in soft marine sediments. *Geochemistry, Geophysics, Geosystems*, *8*(2).

Tomczak, M., Godfrey S., 2005. Regional Oceanography: An Introduction. Originally published: 1994 Oxford: Elsevier Science.

Tooley, M.J. and Shennan, I., 1987. Sea-Level Changes. Institute of British Geographers special publication.

Traykovski, P., Geyer, R. and Sommerfield, C., 2004. Rapid sediment deposition and fine scale strata formation in the Hudson estuary. Journal of Geophysical Research: Earth Surface, 109(F2).

Trenhaile, A.S., 1972 The shore platforms of the Vale of Glenmorgan, Wales. Transactions of the Institute of British Geographers, 56, 127-144.

Trouet, V., Scourse, J.D. and Raible, C.C., 2012. North Atlantic storminess and Atlantic Meridional Overturning Circulation during the last Millennium: Reconciling contradictory proxy records of NAO variability. Global and Planetary Change, 84, pp.48-55.

Turner, J.T.,1991. Zooplankton feeding ecology: do co-occurring copepods compete for the same food? Reviews in Aquatic Sciences 5, 101–195.

Uehara, K., Scourse, J.D., Horsburgh, K.J., Lambeck, K. and Purcell, A.P., 2006. Tidal evolution of the northwest European shelf seas from the Last Glacial Maximum to the present. Journal of Geophysical Research: Oceans,111(C9).

Unesco, 1981. Tenth Report of the Joint Panel on Oceanographic Tables and Standards. Unesco Technical Papers in Marine Science 36.

Valle-Levinson A. 2010. Definition and classification of estuaries. In Contemporary Issues in Estuarine Physics, ed. A Valle-Levinson, pp. 1–11.

Valle-Levinson, A. and O'Donnell, J., 1996. Tidal Interaction with Buoyancy Driven Flow in a Coastal Plain Estuary. Buoyancy Effects on Coastal and Estuarine Dynamics, pp.265-281.

Van Der Putten, N., Hébrard, J.P., Verbruggen, C., Van de Vijver, B., Disnar, J.R., Spassov, S., De Beaulieu, J.L., De Dapper, M., Kéravis, D., Hus, J. and Thouveny, N., 2008. An integrated palaeoenvironmental investigation of a 6200 year old peat sequence from Ile de la Possession, Iles Crozet, sub-Antarctica. *Palaeogeography, palaeoclimatology, palaeoecology*, *270*(1), pp.179-195.

Velle, G., Brooks, S. J., Birks, H. J. B. and Willassen, E., 2005. Chironomids as a tool for inferring Holocene climate: an assessment based on six sites in southern Scandinavia. Quaternary Science Reviews, Vol. 24, pp 1429-1462.

Vélez, M. I., Wille, M., Hooghiemstra, H., Metcalfe, S., Vandenberghe, J., and Van der Borg, K., 2001. Late Holocene environmental history of southern Chocó region, Pacific Colombia; sediment, diatom and pollen analysis of core El Caimito, Palaeogeogr. Palaeoecol., 173, 197–214.

Vellinga, M. and Wu, P., 2004. Low-latitude freshwater influence on centennial variability of the Atlantic thermohaline circulation. *Journal of Climate*, *17*(23), pp.4498-4511.

Verrill, L. and Tipping, R., 2010. Use and abandonment of a Neolithic field system at Belderrig, Co. Mayo, Ireland: Evidence for economic marginality. The Holocene, Vol. 20(7), pp 1011-1021.

Veski, S., Seppä, H. and Ojala, A.E., 2004. Cold event at 8200 yr BP recorded in annually laminated lake sediments in eastern Europe. *Geology*,*32*(8), pp.681-684.

Vos, P.C., deWolf, H., 1988. Methodological aspects of palaeoecological diatom research in coastal areas of the Netherlands. Geologie en Mijnbouw 67, 31–40.

Vos P.C., de Wolf, H., 1992. Diatoms as a tool for reconstructing sedimentary environments in coastal wetlands; methodological aspects. Hydrobiologia 269/270: 285-296.

Vos, P. C., H. de Wolf, 1993. Reconstruction of sedimentary environments in Holocene coastal deposits of the southwest Netherlands; the Poortvliet boring, a case study of palaeoenvironmental diatom research. Hydrobiologia 269/270: 297–306.

Walker, M.J.C., M. Berkelhammer, S. Björck, L.C. Cwynar, D.A. Fisher, A.J. Long, J.J. Lowe, R.M. Newnham, S.O. Rasmussen, H. Weiss, 2012. Formal subdivision of the Holocene Series/Epoch: a Discussion Paper by a Working Group of INTIMATE (Integration of ice-core, marine and terrestrial records) and the Subcommission on Quaternary Stratigraphy (International Commission on Stratigraphy). Journal of Quaternary Science, 27. Pp. 649-659.

Walker, M. J. C.; Gibbard, P. L.; Berkelhammer, M.; Björck, Svante **LU** ; Cwynar, L. C.; Fisher, D. A.; Long, A. J.; Lowe, J. J.; Newnham, R. M. and Rasmussen, S. O., *et al*., 2014. 1st International Congress on Stratigraphy (STRATI) In *STRATI 2013* p.983-987.

Walling DE, Owens PN, Carter J, Leeks GJL, Lewis S, Meharg AA, et al., 2003. Storage of sediment-associated nutrients and contaminants in river channel and floodplain systems. Applied Geochemistry, 18:195–220.

Wang, Y., Cheng, H., Edwards, R.L., He, Y., Kong, X., An, Z., Wu, J., Kelly, M.J., Dykoski, C.A. and Li, X., 2005. The Holocene Asian monsoon: links to solar changes and North Atlantic climate. Science, 308(5723), pp.854-857.

Wanner, H., Solomina, O., Grosjean, M., Ritz, S. P., and Jetel, M., 2011. Structure and origin of Holocene cold events, Quaternary Sci. Rev., 30, 3109–3123.

Warren, W.P., 1992. Drumlin orientation and the pattern of glaciation in Ireland. Sveriges Geologiska Underso¨kning 81, 359–366.

Watcham, E.P., Shennan, I. and Barlow, N.L., 2013. Scale considerations in using diatoms as indicators of sea- level change: lessons from Alaska.*Journal of Quaternary Science*, *28*(2), pp.165-179.

Weber, M.E., F. Niessen, G. Kuhn, M. Wiedicke 1997. Calibration and application of marine sedimentary physical properties using a multi sensor core logger. Mar. Geol. 136: 151-172.

Weckström, K., Juggins, S. and Korhola, A., 2004. Quantifying background nutrient concentrations in coastal waters: a case study from an urban embayment of the Baltic Sea. Ambio 33, 324–327.

Weckström K**.,** Korhola, A., Weckström, J., 2007. Impacts of eutrophication on diatom life forms and species richness in coastal waters of the Baltic Sea. *Ambio*36: 155-160.

Weckström K, Juggins S., 2005. Coastal diatom-environment relationships from the Gulf of Finland, Baltic Sea. Journal of Phycology p. 21–35. Vol. 42.

Weckström, K., Juggins, S., 2006. Coastal diatom–environment relationships from the Gulf of FIinland, Baltic Sea1. *Journal of Phycology*, *42*(1), pp.21-35.

Weisberg M. K., Prinz, M., Clayton, R. N., Mayeda, T. K., Sugiura, N., Zashu, S., and Ebihara, M., 2001. A new metalrich chondrite grouplet. Meteoritics and Planetary Science 36:401–418.

Weltje, G.J. and Tjallingii, R., 2008. Calibration of XRF core scanners for quantitative geochemical logging of sediment cores: theory and application.*Earth and Planetary Science Letters*, *274*(3), pp.423-438.

Wentworth, C.K., 1922. A scale of grade and class terms for clastic sediments. *The Journal of Geology*, *30*(5), pp.377-392.

Western River Basin District (WRBD), 2008. Help us plan - Draft River Basin Management Plan. http://www.westernrbd.ie/PDF/WesternRBD_RBMP.pdf

Wheeler, A.J.; Orford, J.D., and Dardis, O., 1999. Saltmarsh deposition and its relationship to coastal forcing over the last century on the north-west coast of Ireland. Geologie en Mijnbouw, 77, 295–310.

Willard, D. A., and T. M. Cronin. 2007. Paleoecology and ecosystem restoration: case studies from Chesapeake Bay and the Florida Everglades. Frontiers in Ecology and the Environment 5:591–498.

Williams, D.M., 1980. Evidence for glaciation in the Ordovician rocks of western Ireland. *Geological Magazine*, *117*(01), pp.81-86.

Williams, D.M., 2010. Mechanisms of wave transport of megaclasts on elevated cliff-top platforms: examples from western Ireland relevant to the storm-wave versus tsunami controversy. Irish Journal of Earth Sciences, pp.13-23.

Williams, D.M., 2011. Reply to Knight. Irish Journal of Earth Sciences,29, pp.25-26.

Williams, D.M. and Doyle, E., 2014. Dates from drowned mid-Holocene landscapes on the central western Irish seaboard. *Irish Journal of Earth Sciences*, *32*, pp.23-27.

Williams, D.M. and Hall, A.M., 2004. Cliff-top megaclast deposits of Ireland, a record of extreme waves in the North Atlantic—storms or tsunamis?. Marine Geology, 206(1), pp.101-117.

Withers, P.J.A. and Jarvie, H.P., 2008. Delivery and cycling of phosphorus in rivers: a review. Science of the total environment, 400(1), pp.379-395.

Witkowski, A., 1994. Recent and fossil diatom flora of the Gulf of Gdansk,-Southern Baltic Sea.

Witkowski, A., Lange-Bertalot, H., Metzeltin, D., 2000. Diatom flora of marine coasts I. A.R.G. Gantner Verlag K.G. , Ruggell, pp. 925.

Wood, B., 2010. Post-glacial environmental change in Galway Bay, Western Ireland; evidence from shallow marine sedimentary vibrocores. Unpublished MSc Thesis, National University of Ireland, Galway.

Woodcock, N., 2000. British Geological Survey. 1987–1999. Holiday Geology Guides and Maps. *Geological Magazine*, *137*(5), pp.596-597.

Woodroffe, C., 2002. Coasts: Form, Process and Evolution. Cambridge University Press, Cambridge.

Woodroffe, C.D. and Murray-Wallace, C.V., 2012. Sea-level rise and coastal change: the past as a guide to the future. Quaternary Science Reviews, 54, pp.4-11.

Wright, A.J., Edwards, R.J. and van de Plassche, O., 2011. Reassessing transfer-function performance in sea-level reconstruction based on benthic salt-marsh foraminifera from the Atlantic coast of NE North America. *Marine Micropaleontology*, *81*(1), pp.43-62.

Wunsch, C. and Heimbach, P., 2006. Estimated decadal changes in the North Atlantic meridional overturning circulation and heat flux 1993-2004. Journal of Physical Oceanography, 36(11), pp.2012-2024.

Yancheva, G., Nowaczyk, N.R., Mingram, J., Dulski, P., Schettler, G., Negendank, J.F., Liu, J., Sigman, D.M., Peterson, L.C. and Haug, G.H., 2007. Influence of the intertropical convergence zone on the East Asian monsoon.*Nature*, *445*(7123), pp.74-77.

Yarincik, K.M., Murray, R.W. and Peterson, L.C., 2000. Climatically sensitive eolian and hemipelagic deposition in the Cariaco Basin, Venezuela, over the past 578,000 years: Results from Al/Ti and K/Al. *Paleoceanography*, *15*(2), pp.210-228.

Yu, S.Y., Berglund, B.E., Sandgren, P. and Fritz, S.C., 2005. Holocene palaeoecology along the Blekinge coast, SE Sweden, and implications for climate and sea-level changes. *The Holocene*, *15*(2), pp.278-292.

Zielinski, T., Weslawski, M. and Kuliński, K. eds., 2015. *Impact of Climate Changes on Marine Environments*. Springer.

Zhang, R., 2010. Latitudinal dependence of Atlantic meridional overturning circulation (AMOC) variations. Geophysical Research Letters, 37(16).

Zhang, L. and Wang, C., 2013. Multidecadal North Atlantic sea surface temperature and Atlantic meridional overturning circulation variability in CMIP5 historical simulations. Journal of Geophysical Research: Oceans,118(10), pp.5772-5791.

Ziegler, M., Jilbert, T., de Lange, G.J., Lourens, L.J. and Reichart, G.J., 2008. Bromine counts from XRF scanning as an estimate of the marine organic carbon content of sediment cores. *Geochemistry, Geophysics, Geosystems*, *9*(5).

Zolitschka, B., Mingram, J., Van Der Gaast, S., Jansen, J., Naumann, R. 2001. Sediment logging techniques. In W.M. Last and J.P. Smol (eds.), 2001. Tracking Environmental Change Using Lake Sediments. Volume 1: Basin Analysis, Coring and Chronological Techniques. Kluwer Academic Publishers, Dordrecht, The Netherlands.

Zong, Y. 1997. Implications of Paralia sulcata abundance in Scottish isolation basins. Diatom Research, 2:1, 125-150.

Zong, Y., Shennan, I., Combellick, R.A., Hamilton, S.L. and Rutherford, M.M., 2003. Microfossil evidence for land movements associated with the AD 1964 Alaska earthquake. *The Holocene*, *13*(1), pp.7-20.

Appendix A: Grain Size Analysis

Table A: The results of Laser Diffraction Grain Size Analysis for sediment cores VC001 (left) and VC003 (right). This includes actual data results along with the sediment classification as per Shepard (1954).

VC001						VC003					
Core Position (m)	Gravel %	Sand %	Silt %	Clay %	Sediment Class	Core Position (m)	Gravel %	Sand %	Silt %	Clay %	Sediment Class
0.04		25.97	65.61	8.43	SANDY SILT	0.19	23.96	23.40	43.07	9.57	GRAVELLY SEDIMENT
0.22	8.36	51.30	36.59	3.75	SILTY SAND	0.37	21.20	29.25	41.09	8.46	GRAVELLY SEDIMENT
0.58		14.46	67.23	18.31	CLAYEY SILT	0.69		12.77	76.12	11.12	SILT
0.76		24.93	65.78	9.29	SANDY SILT	0.86		17.57	72.08	10.35	SANDY SILT
0.94		21.26	68.68	10.07	SANDY SILT	1.04		16.05	74.40	9.55	SANDY SILT
1.12		16.91	73.99	9.10	SANDY SILT	1.22		13.75	74.82	11.43	SANDY SILT
1.30		17.79	72.61	9.60	SANDY SILT	1.40		12.25	74.29	13.46	CLAYEY SILT
1.58		23.68	64.69	11.63	SANDY SILT	1.69		12.63	75.06	12.31	SILT
1.77		20.50	67.50	12.01	SANDY SILT	1.87		14.40	75.31	10.29	SILT
1.95		22.61	65.01	12.37	SANDY SILT	2.05		15.03	75.29	9.68	SILT
2.13		14.47	70.27	15.26	CLAYEY SILT	2.23		16.54	72.04	11.42	SANDY SILT
2.31	0.95	17.32	64.97	16.76	SANDY SILT	2.41		17.46	73.32	9.22	SANDY SILT
2.58	0.17	20.14	63.98	15.71	SANDY SILT	2.67		17.48	72.34	10.18	SANDY SILT
2.76		19.88	63.76	16.37	SANDY SILT	2.85		10.65	78.19	11.15	SILT
2.94		18.47	64.40	17.14	SANDY SILT	3.03		13.45	77.52	9.03	SILT
3.10		29.61	57.36	13.03	SANDY SILT	3.21		14.26	75.89	9.86	SILT
3.28		21.82	65.56	12.63	SANDY SILT	3.39		12.92	77.16	9.92	SILT
3.56		19.06	66.88	14.06	SANDY SILT	3.64		9.58	78.92	11.51	SILT
3.76	0.35	12.35	68.40	18.90	CLAYEY SILT	3.82		8.35	78.85	12.80	SILT
3.92	9.86	19.51	58.26	12.37	SANDY SILT	4.00		11.06	77.61	11.33	SILT
4.10		17.48	66.86	15.67	SANDY SILT	4.18		9.67	78.64	11.68	SILT
4.28	0.68	23.56	66.93	8.83	SANDY SILT	4.36		6.49	80.77	12.74	SILT
4.55		16.98	72.75	10.27	SANDY SILT	4.61		11.32	77.65	11.04	SILT
4.73	0.22	35.82	51.16	12.80	SANDY SILT	4.79		6.64	79.36	14.00	SILT
4.92		17.12	69.19	13.69	SANDY SILT	4.96		8.24	77.95	13.81	SILT
5.10	0.40	54.64	42.24	2.72	SILTY SAND	5.18		10.48	75.31	14.22	SILT
5.28		59.56	37.93	2.50	SILTY SAND	5.32		16.15	68.61	15.24	SANDY SILT

Appendix B: Age Depth Profiles VC003 and VC004

Age depth models run in R(ver. 3.0.1) with Bacon software (Blaauw and Christen, 2011)

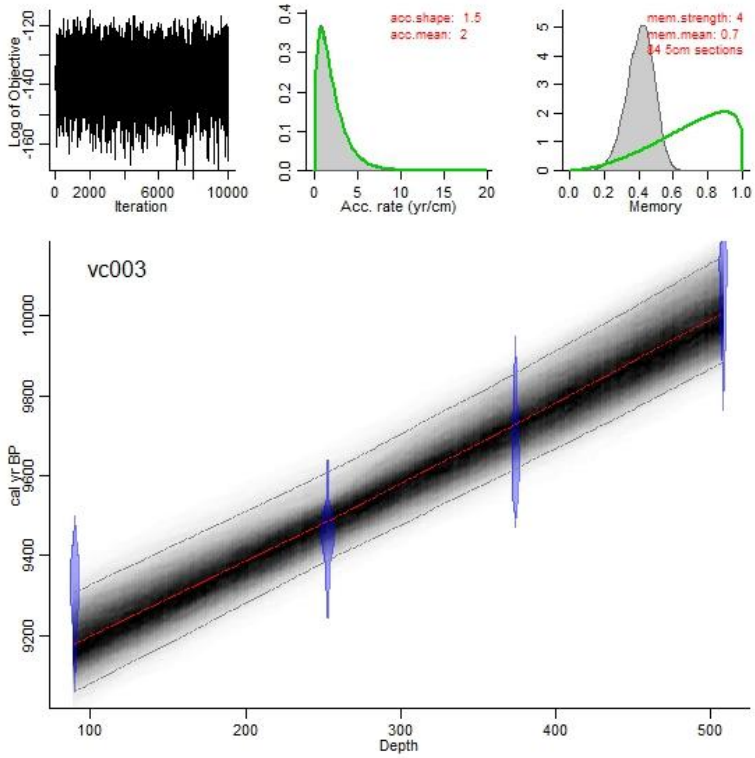

Figure B1: Age Depth Profile VC003

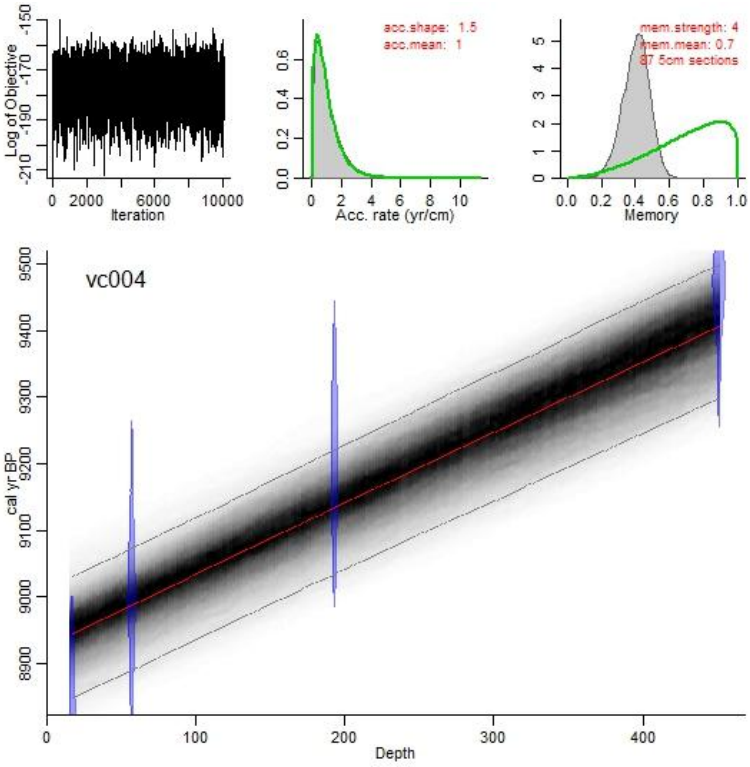

Figure B2: Age Depth Profile VC004

Appendix C: XRF Elemental Profiles VC001, VC002, VC003 and VC004

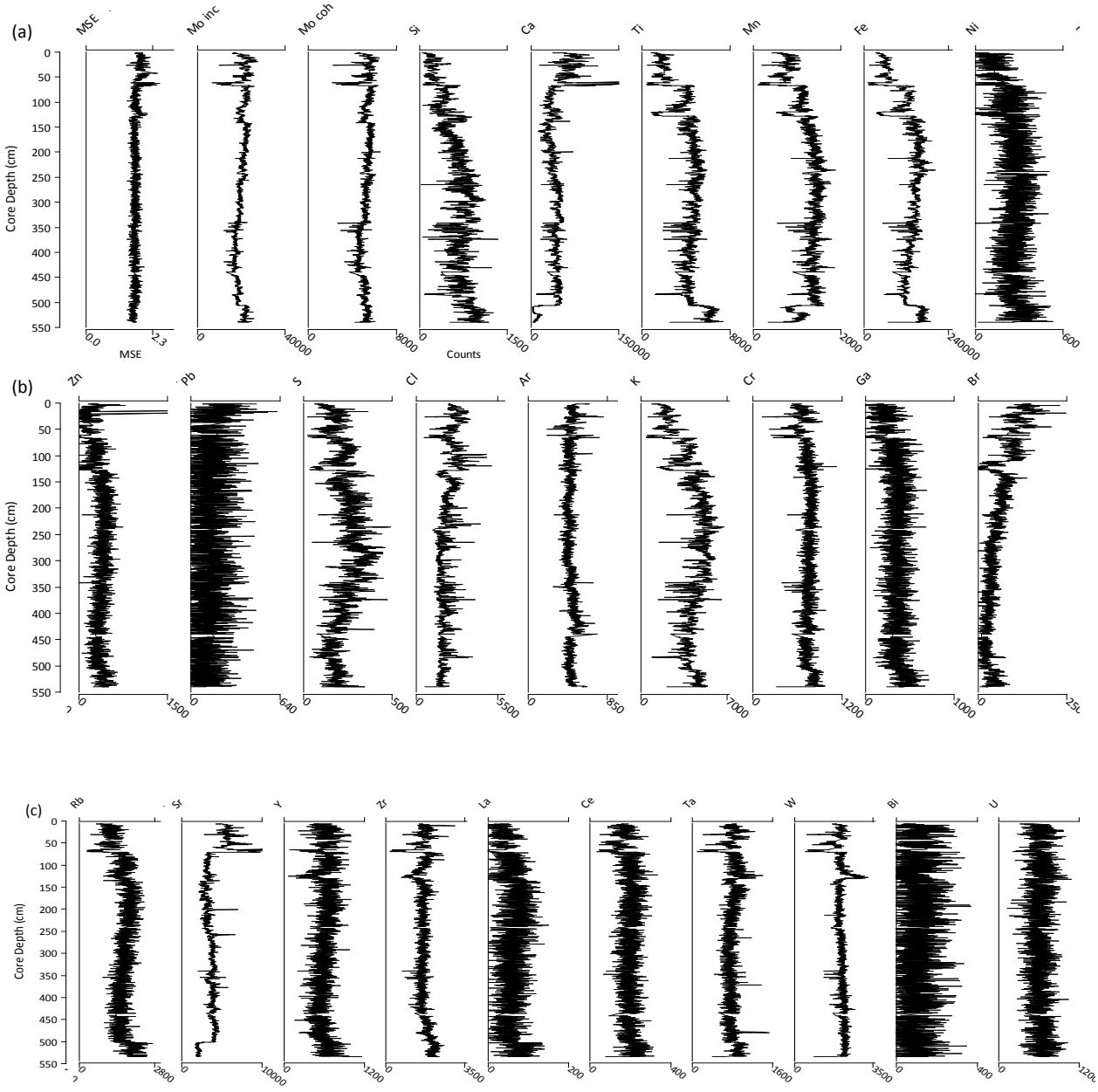

Figure C1: Single Elemental Profiles XRF VC001 (a): MSE, Mo inc, Mo coh, Si, Ca, Ti, Mn, Ni; (b): Zn, Pb, S, Cl, Ar, K, Cr, Ga, Br; (c): Rb, Sr, Y, Zr, La, Ce, Ta, W, Bl, U. The following elements are excluded due to extensive nil counts: Mg, Al, Cu, Ba, As.

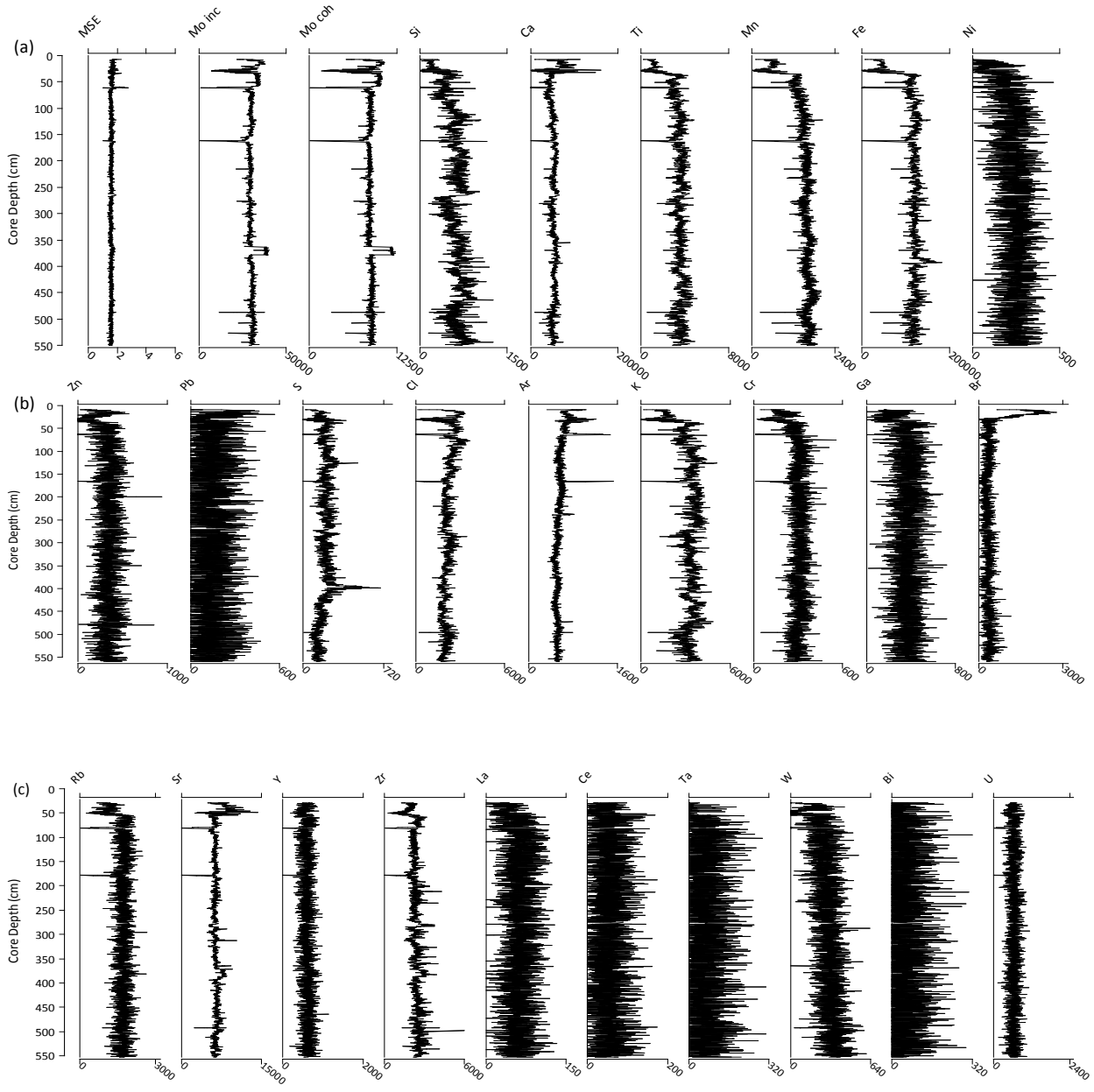

Figure C2: Single Elemental Profiles XRF VC002 (a): MSE, Mo inc, Mo coh, Si, Ca, Ti, Mn, Ni; (b): Zn, Pb, S, Cl, Ar, K, Cr, Ga, Br; (c): Rb, Sr, Y, Zr, La, Ce, Ta, W, Bl, U. The following elements are excluded due to extensive nil counts: Mg, Al, Cu, Ba, As.

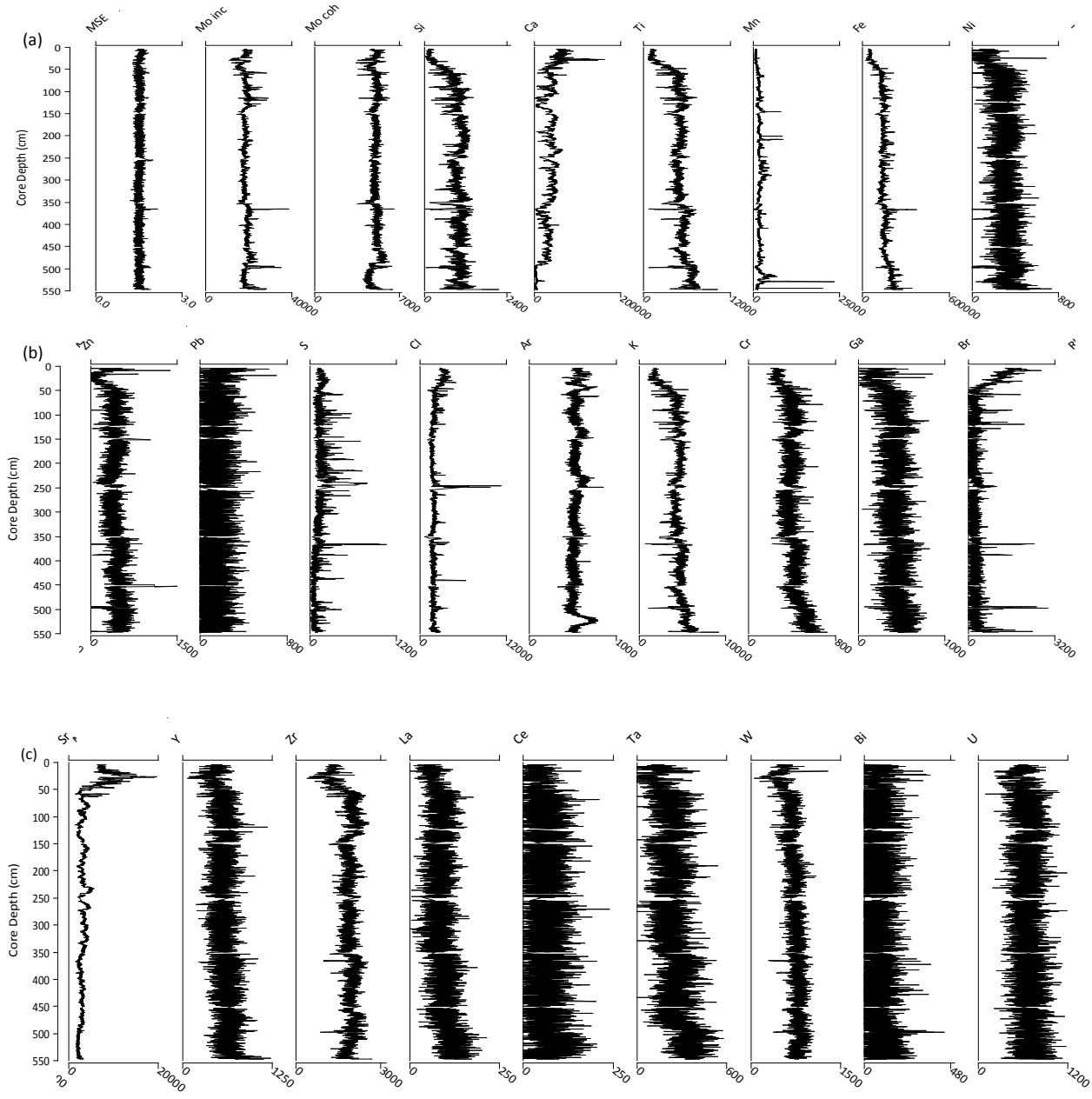

Figure C3: Single Elemental Profiles XRF VC003 (a): MSE, Mo inc, Mo coh, Si, Ca, Ti, Mn, Ni; (b): Zn, Pb, S, Cl, Ar, K, Cr, Ga, Br; (c): Rb, Sr, Y, Zr, La, Ce, Ta, W, Bl, U. The following elements are excluded due to extensive nil counts: Mg, Al, Cu, Ba, As.

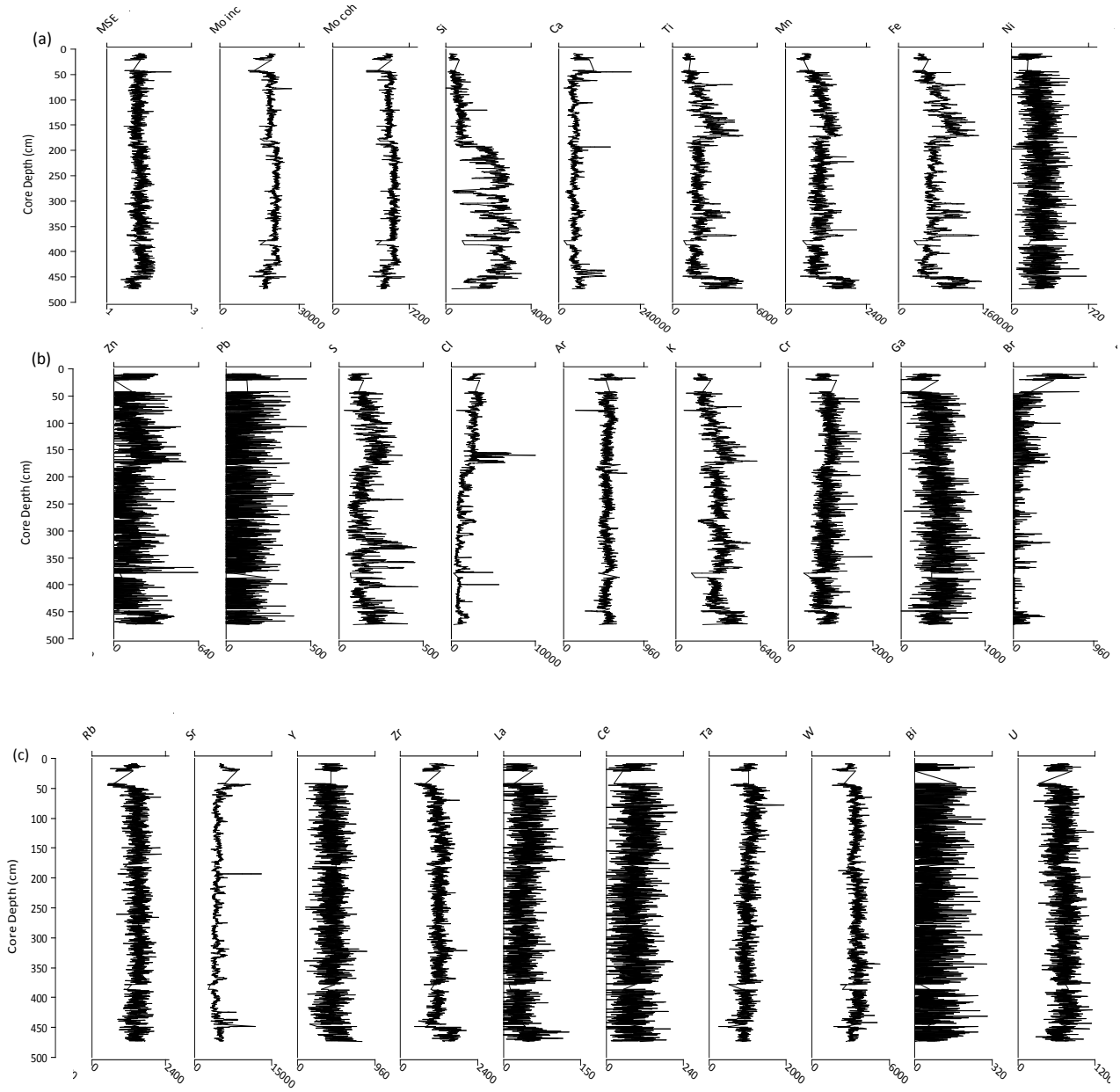

Figure C4: Single Elemental Profiles XRF VC004 (a): MSE, Mo inc, Mo coh, Si, Ca, Ti, Mn, Ni; (b): Zn, Pb, S, Cl, Ar, K, Cr, Ga, Br; (c): Rb, Sr, Y, Zr, La, Ce, Ta, W, Bl, U. The following elements are excluded due to extensive nil counts: Mg, Al, Cu, Ba, As.

Appendix D: Diatoms

Table D: Complete list of fossil diatom species found in sediment cores VC001, VC003 and VC004 from Inner Galway Bay; listed with taxonomic authority. Genus is included for diatoms where identification was limited due to dissolution and breakage and, as a result, some individuals were only identified to genus level. Included in this table also is the Sediment Core where species was identified (1: VC001; 3: VC003; 4: VC004), Frustule Group (C: centric; P: pennate), Habitat (B: benthic; PL: planktonic; T: tychoplanktonic), General Environment (F: freshwater; B: benthic; M: marine) and Life Form (PL: plankton; PR: periphyton; EL: epilithon; EPH: epiphyton; EP: epipelon; EPS: episammon). Ecological classification was based Hendey (1964); Krammer and Lange-Bertalot (1986, 1988, 1991a, 1991b); Round *et al*. (1990); Vos and De Wolf (1992); Witkowski (1994); Hasle and Syvertsen (1997); Witkowski *et al*. (2000); Guiry and Guiry (2016).

Taxon Name and Authority	Sediment Core	Frustule Group		Habitat			General Environment	Life Form
Achnanthidium coarctatum **Brébisson ex W.Smith 1855**	1,3,4		P	B			F	EP
Achnanthidium deflexum **(C.W.Reimer) J.C.Kingston 2000**	1,3,4		P	B			F	EP
Actinocyclus **Ehrenberg, 1837**	1	C			Pl		M	PL
Actinoptychus **Ehrenberg, 1843**	1,3,4	C			Pl		M	PL
Actinoptychus senarius **(Ehrenberg) Ehrenberg 1843**	1,3,4	C				T	M	PL
Actinoptychus splendens **(Shadbolt) Ralfs in Pritchard 1861**	3	C			Pl		M	PL
Amphora **Ehrenberg ex Kützing**	1,3		P	B			M, F	EPH, EL, EP
Amphora costata **W.Smith 1853**	1,3		P	B			M, F	EPH, EL, EP
Amphora cymbaphora **Cholnoky**	1		P	B			M	EPH, EL, EP
Amphora exigua **W.Gregory 1857**	3		P	B			M	EPH, EL, EP
Amphora ovalis **(Kützing) Kützing 1844**	1		P	B			F	EPH, EL, EP
Amphora spectabilis **Gregory 1857**	1,4		P	B			M	EPH, EL, EP
Amphora subangularis **Hustedt 1955**	1		P	B			M	EPH, EL, EP
Aneumastus **D.G.Mann & A.J.Stickle, 1990**	1,3,4		P	B			F	EP
Aneumastus tuscula **(Ehrenberg) D.G.Mann & A.J.Stickle**	1,3,4		P	B			F	EP
Aulacoseira granulata **(Ehrenberg) Simonsen**	3	C			Pl		F	PL
Auliscus caelatus **Bailey 1854**	1,3,4	C			Pl		M	PL
Auliscus sculptus **(W.Smith) Brightwell**	1	C			Pl		M	PL
Bacillaria paxillifer **(O.F.Müller) T.Marsson 1901**	1,3,4		P	B			M, B	EP, EL
Caloneis **Cleve, 1894**	1		P	B			F, B	EP
Caloneis bacillum **(Grunow) Cleve 1894**	1		P	B			F, B	EP
Caloneis clevei **(N.Lagerstedt) Cleve**	1		P	B			F, B	EP
Campylodiscus **Ehrenberg ex Kützing, 1844**	1,3		P	B			F, B, M	EP
Campylodiscus clypeus **(Ehrenberg) Ehrenberg ex Kützing**	1		P	B			F, B, M	EP
Campylosira cymbelliformis **(A.Schmidt) Grunow ex**	1,3,4		P			T	M	PL, EPS

Taxon Name and Authority	Sediment Core	Frustule Group		Habitat			General Environ-ment	Life Form
Van Heurck, 1885								
Capartogramma crucicula **(Grunow ex Cleve) Ross 1963**	1		P	B			F, B	EP
Catacombas gaillonii **(Bory) D.M.Williams & Round**	1,3		P	B			F, B	EPH
Cocconeis **Ehrenberg 1837**	1,3,4		P	B			M, B, F	EPH, EPS
Cocconeis guttata **Hustedt & Aleem 1951**	1,3		P	B			M	EPS
Cocconeis peltoides Hustedt 1939	1,3,4		P	B			M, B	EPS
Cocconeis placentula **Ehrenberg 1838**	1,3		P	B			M, B, F	EPH, EPS
Cocconeis placentula var euglypta **(Ehrenberg) Grunow 1884**	1,3,4		P	B			B	EPH, EPS
Cocconeis scutellum **Cocconeis scutellum**	1,3,4		P	B			M, B	EPH
Coscinodiscus **Ehrenberg, 1839**	1,4	C			Pl		M	PL
Cosinodiscus radiatus **Ehrenberg 1840**	4	C			Pl		M	PL
Coscinodiscus robustus **Greville 1866**	1	C			Pl		M	PL
Coscinodiscus symbolophorus **Grunow**	1	C			Pl		M	PL
Craticula halophila **(Grunow) D.G.Mann**	1,3		P	B			B	EP
Cyclostephanos damasii **(Hustedt) Stoermer & Håkansson**	1,3	C			Pl		F	PL
Cyclotella **(Kützing) Brébisson, 1838**	1,3,4		P	B			M, F, B	PL
Cyclotella antigua **W.Smith, 1853**	1,3	C			Pl		B	PL
Cyclotella bodanica **Eulenstein ex Grunow 1878**	1	C					F	PL
Cyclotella bodanica var affinis **Grunow**	1,3	C					F	PL
Cyclotella choctawhatcheeana **Prasad, 1990**	1,3,4	C			Pl		B	PL
Cyclotella comta **Kützing 1849**	1	C					F	PL
Cyclotella distinguenda **Hustedt**	1,3,4	C					M, F	PL
Cyclotella krammeri **Håkansson 1990**	1,3	C					B	PL
Cyclotella meneghiniana **Kützing 1844**	1	C			Pl		B	PL
Cyclotella ocellata **Pantocsek 1901**	1	C			Pl		F	PL
Cymatosira belgica **Grunow**	1,3,4		P	B			M	PL, EPS
Cymbella **C. Agardh, 1830**	1,3,4		P	B			F, B	EPH, EP, EL
Cymbella affinis **Kützing 1844**	1,3,4		P	B			F, B	EPH, EP, EL
Cymbella helvetica **Kützing 1844**	1,3		P	B			F, B	EPH, EP, EL
Cymbella pseudoaffinis **Tynni**	1,3,4		P	B			F	EPH, EP, EL
Cymbella turgidula **Grunow**	1,3,4		P	B			F	EPH, EP, EL
Delphineis **G.W.Andrews**	1,3,4		P	B	Pl		M	EPS, PL
Delphineis karstenii **(Boden) G.Fryxell 1978**	1,3,4		P		Pl		M	EPS
Delphineis minutissima **(Hustedt) Simonsen 1987**	1,3,4		P	B			M, F	EPS
Delphineis surirella **(Ehrenberg) G.W.Andrews 1981**	3		P			T	M	PL, EPS
Denticula distans **Gregory 1857**	4		P	B			M, F	EPS
Diatoma moniliformis **(Kützing) D.M.Williams**	1,3		P		Pl		F, B	PL
Dimeregramma **Ralfs, 1861**	1,3,4		P	B			M	EPS, EPH, EP
Dimeregramma dubium **Grunow**	1		P	B			M	EPS
Dimeregramma fulvum **(Gregory) Ralfs 1861**	1,3,4		P	B			M	EP
Dimeregramma minus **(W.Gregory) Ralfs 1861**	1,3,4		P	B			M	EPS, EPH

Taxon Name and Authority	Sediment Core	Frustule Group		Habitat			General Environment	Life Form
Diploneis **Ehrenberg ex Cleve, 1894**	1,3,4		P	B			M, B, F	EP
Diploneis aestuarii Hustedt 1939	1,4		P	B			M, B	EP
Diploneis decipiens var parallela **A. Cleve 1915**	3		P	B			M	EP
Diploneis didyma **(Ehrenberg) Ehrenberg 1839**	1,3		P	B			B	EP
Diploneis domblittensis **(Grunow) Cleve 1894**	1,3		P	B			M, F	EP
Diploneis gruendleri **(A.Schmidt) Cleve**	1,3		P	B			M	EP
Diploneis smithii var. rhombica **A.Cleve**	3		P	B			M	EP
Ellerbeckia arenaria **(G.Moore ex Ralfs) R.M.Crawford 1988**	1,3,4	C				T	F	EPS
Encyonema mesianum **(Cholnoky) D.G.Mann**	1,3,4		P	B			F	EP
Encyonema minutum **(Hilse) D.G.Mann**	1,3,4		P	B			F	EP, PR
Encyonema silesiacum **(Bleisch) D.G.Mann**	1,3		P	B			F	EP
Epithemia **Kützing, 1844**	1		P	B			F, B	EPH
Epithemia argus **(Ehrenberg) Kützing 1844**	1,3		P	B			F	EPH
Epithemia goeppertiana **Hilse 1860**	1,3		P	B			F, B	EPH
Epithemia sorex **Kützing 1844**	1,4		P	B			F, B	EPH
Eunotia **Ehrenberg, 1837**	1,3		P	B			F	EPH
Eunotia arcubus **Nörpel & Lange-Bertalot**	1,3		P	B			F	EPH
Eunotia pectinalis var undulata **(Ralfs) Rabenhorst 1864**	1,3		P	B			F	EPH
Eunotia tenella **(Grunow) Hustedt**	1		P	B			F	EPH
Eunotogramma laeve **Grunow in Cleve & Möller 1879**	1,3,4		P	B			M, B	EPS
Eunotogramma marinum **(W.Smith) H.Peragallo & M.Peragallo 1908**	1,3		P	B			M, B	EPS
Fallacia **Stickle & D.G.Mann, 1990**	1,3		P	B			B	EP
Fallacia litoricola **(Hustedt) D.G.Mann**	1		P	B			B	EP
Fallacia pygmaea **(Kützing) Stickle & D.G.Mann**	1,3,4		P	B			B	EP
Fragilaria **Lyngbye, 1819**	1,3		P	B	Pl		F, B	PL, EP
Fragilaria capucina var. vaucheriae **(Kützing) Lange-Bertalot 1980**	3		P			T	F	EP
Fragilaria construens **(Ehrenberg) Grunow 1862**	1		P			T	F, B	PL, EP
Glyphodesmis distans (Gregory) Grunow ex Van Heurck, 1881	1		P	B			M, B	EP, EPS
Gomphoneis clevei **(Fricke) Gil 1989**	1,3		P	B			F	EPH
Gomphonema **Ehrenberg, 1832**	1,3,4		P	B			FF	EPH
Gomphonema angustum **C. Agardh 1831**	1		P	B			F	EPH
Gomphonema angustatum var. sarcophagus **(W.Gregory) Grunow**	1		P	B			F	EPH
Gomphonema intricatum var vibrio **(Ehrenberg) Cleve 1894**	1		P	B			F	EPH
Gomphonema occultum **E.Reichardt & Lange-Bertalot 1991**	1		P	B			F	EPH
Gomphonemopsis exigua **(Kützing) Medlin**	1,3		P	B			M, B	EPH
Grammatophora marina **(Lyngbye) Kützing 1844**	1,3,4		P	B			M	EP
Grammatophora oceanica **Ehrenberg 1840**	1,3,4		P	B			M	EPH, EP
Grammatophora serpentina **Ehrenberg, 1844**	1,3,4		P			T	M	PL, EPH
Gyrosigma **Hassall, 1845**	1,3		P	B			M, B	EP
Gyrosigma balticum **(Ehrenberg) Rabenhorst 1853**	1		P	B			B	EP
Hantzschia marina **(Donkin) Grunow**	1,4		P	B			M, B, F	EP
Hantzschia **Grunow, 1877**	1,4		P	B			M, B, F	EP
Hyalodiscus **Ehrenberg, 1845**	1,3	C				T	M	EPH,

Taxon Name and Authority	Sediment Core	Frustule Group		Habitat			General Environ-ment	Life Form
								PL
***Hyalodiscus radiatus* (O'Meara) Grunow 1879**	3	C				T	M	EPH, PL
***Hyalodiscus scoticus* (Kützing) Grunow 1879**	1	C				T	M	EPH, PL
***Karayevia clevei* (Grunow) Round & Bukhtiyarova, 1999**	1		P	B			F	EL, EP
***Lyrella* Karajeva, 1978**	1,3		P	B			M	EP
***Lyrella abrupta* (Gregory) D.G.Mann**	1		P	B			M	EP
***Lyrella spectabilis* (Gregory) D.G.Mann**	3		P	B			M	EP
***Mastagloia* Thwaites ex W.Smith, 1856**	1,4		P	B			M, B, F	EP, EPH
***Mastogloia smithii var. lacustris* Grunow 1878**	1,4		P	B			M, B, F	EP, EPH
***Melosira granulata* (Ehrenberg) Ralfs**	3	C			Pl		M	EP
***Melosira varians* C. Agardh 1827**	3	C			Pl		F	EP
***Navicula* Bory, 1822**	1,3,4		P	B			M, B, F	EP
***Navicula cryptocephala* Kützing 1844**	1		P	B			M, B, F	EP
***Navicula digitoradiata* (W.Gregory) Ralfs**	1,3,4		P	B			M, B	EP
***Navicula directa* (W.Smith) Ralfs**	1,3,4		P	B			M	EP
***Navicula halophia* (Grunow) Cleve**	4		P	B			B, F	EP
***Navicula lanceolata* (C.Agardh) Kützing**	1		P	B			B	EP
***Navicula oppugnata* Hustedt**	1		P	B			F	EP
***Navicula tripuncta* (O.F.Müller) Bory**	1,4		P	B			B	EP
***Navicula vulpina* Kützing**	1		P	B			B	EP
***Navicula zosteretii* Grunow**	1		P	B			B	EP
***Nitzschia* Hassall, 1845**	1,3,4		P	B	Pl		M, B, F	EP or PL
***Nitzschia amphibioides* Hustedt 1942**	1,4		P	B			B	EP
***Nitzschia ovalis* H.J.Arnott in Cleve & Grunow 1880**	1,3,4		P	B			U	EP
***Nitzschia recta* Hantzsch ex Rabenhorst 1862**	1,3,4		P	B			B	EP
***Nitzschia sigma* (Kützing) W.Smith 1853**	1,3		P	B			B	EP
***Nitzschia wuellerstorffii* Lange-Bertalot**	1		P	B			B	EP
***Opephora marina* (W.Gregory) Petit 1888**	4		P	B			M	EPS
***Opephora mutabilis* (Grunow) Sabbe & Wyverman 1995**	1		P	B			M	EPS
***Opephora pacifica* (Grunow) Petit 1888**	1,3,4		P	B			B	EPS
***Paralia* Heiberg, 1863**	1,3	C			Pl		M	PL, EPH, EP, EPS
***Paralia sulcata* (Ehrenberg) Cleve 1873**	1,3,4	C			Pl		M	PL
***Peronia fibula* (Brébisson ex Kützing) R.Ross 1956**	1		P	B			F	EPH
***Petroneis humerosa* (Brébisson ex W.Smith) Stickle & D.G.Mann**	1,3		P	B			M	EP
***Petroneis marina* (Ralfs) D.G.Mann**	1,3		P	B			M	EP
***Plagiogramma* Greville, 1859**	1		P	B			M	EPS
***Plagiogramma pulchellum var pygmaeum* (Greville) H.Peragallo & M.Peragallo 1901**	1		P	B			B, M	EPS
***Plagiogramma rhombicum* Hustedt**	1,3,4		P	B			B, M	EPS
***Planktoniella blanda* (A.Schmidt) Syvertsen & Hasle**	1	C			Pl		M	PL
***Planothidium* Round & L.Bukhtiyarova, 1996**	1,3,4		P	B			B, F	EPS
***Planothidium conspicuum* (Ant.Mayer) Aboal**	1,3,4		P	B			F	EPS
***Planothidium delicatulum* (Kützing) Round &**	1,3,4		P	B			B	EPS

Taxon Name and Authority	Sediment Core	Frustule Group		Habitat			General Environ-ment	Life Form
Bukhtiyarova								
***Podosira* Ehrenberg, 1840**	1,3,4	C			Pl		M	PL
***Podosira corolla* A.W.F.Schmidt 1889**	1,3	C		B			M	EPH
***Podosira glacialis* (Grunow) Cleve 1896**	1,3	C			Pl		M	PL
***Podosira stelliger* (J.W.Bailey) A.Mann 1907**	1	C			Pl		M	PL
***Pseudopodosira westii* (W.Smith) Sheshukova-Poretzskaya**	1	C			Pl		M	PL
***Pseudostaurosira parasitica* (W.Smith) Morales**	1,3		P	B			F	EPH
***Rhabdonema arcuatum* (Lyngbye) Kützing 1844**	1,3,4		P	B			B	EPH
***Rhabdonema minutum* Kützing 1844**	1		P	B			B	EPH
***Rhaphoneis amphiceros* (Ehrenberg) Ehrenberg 1844**	1,3,4		P			T	M	PL, EPH, EPS
***Rhopalodia musculus* (Kützing) Otto Müller 1900**	1		P	B			B	EPH, EP
***Rossithidium lineare* (W.Smith) Round & Bukhtiyarova**	1		P	B			F, B	EPS, EL
***Sellaphora pupula* (Kützing) Mereschkovsky 1902**	3,4		P	B			F	EP
***Stauroneis finmarchica* Cleve & Grunow 1880**	4		P	B			F	EP
***Stauroneis glacialis* H.Heiden**	1		P	B			F	EP
***Stauroneis phoenicenteron* (Nitzsch) Ehrenberg**	3		P	B			M	EP
***Stephanodiscus alpinus* Hustedt**	3	C			Pl		F	PL
***Surirella* Turpin, 1828**	1,3,4		P	B			F, M	EP
***Surirella fastuosa* (Ehrenberg) Ehrenberg 1843**	1		P	B			B	EP
***Synedra* Ehrenberg, 1830**	4		P	B			F, B	PL, EPH
***Synedra ulna* (Nitzsch) Ehrenberg 1832**	1		P	B			B	EPH
***Tabularia* (Kützing) D.M.Williams & Round, 1986**	1,3		P	B			M, B	EPH, EL
***Tabularia fasciulata* (C.Agardh) D.M.Williams & Round 1986**	1,3,4		P	B			M, B	EPH, EL
***Thalassionema* Grunow ex Mereschkowsky, 1902**	4		P		Pl		M	PL
***Thalassionema nitzschioides* (Grunow) Merchkowsky 1902**	1		P		Pl		M	PL
***Thalassiosira hyperborea var pelagica* (A.Cleve) G.R.Hasle**	3	C			Pl		M	PL
***Thalassiosira decipiens* (Grunow ex Van Heurck) E.G.Jørgensen 1905**	1,3,4	C			Pl		M	PL
***Trachyneis aspera var. robusta* (Petit) Cleve**	1		P	B			B	EP, EPH
***Triceratium* Ehrenberg, 1839**	1,3	C			Pl		M	PL
***Triceratium archangelskianum* O.N.Witt**	1	C			Pl		M	PL
***Triceratium antediluvianum* (Ehrenberg) Grunow, 1868**	1	C			Pl		M	PL
***Triceratium pentacrinus* (Ehrenberg) Wallich**	1	C			Pl		M	PL
***Triceratium perplexum* J.A.Long, D.P.Fuge & J.Smith**	1	C			Pl		M	PL
***Triceratium reticulum* Ehrenberg**	1	C			Pl		M	PL
***Triceratium favus* Ehrenberg**	1,3	C			Pl		M	PL
Triceratium nitescens Greville	1	C			Pl		M	PL
***Tryblionella* W.Smith, 1853**	1,3,4		P	B			M, B	EP, EPS
***Tryblionella acuminata* W.Smith 1853**	1,4		P	B			M, B	EP
***Tryblionella apiculata* W.Gregory 1857**	1,3,4		P	B			B	EP
***Tryblionella coarctata* (Grunow) D.G.Mann**	1,3,4		P	B			M	EP, EPS
***Tryblionella compressa* (J.W.Bailey) Poulin**	1,3		P	B			M	EP

Taxon Name and Authority	Sediment Core	Frustule Group		Habitat			General Environ-ment	Life Form
Tryblionella granulata **(Grunow) D.G.Mann**	1,3,4		P	B			B	EP
Tryblionella navicularis **(Brébisson) Ralfs**	1,3,4		P	B			B	EP

Appendix E: DCA for diatoms in VC001

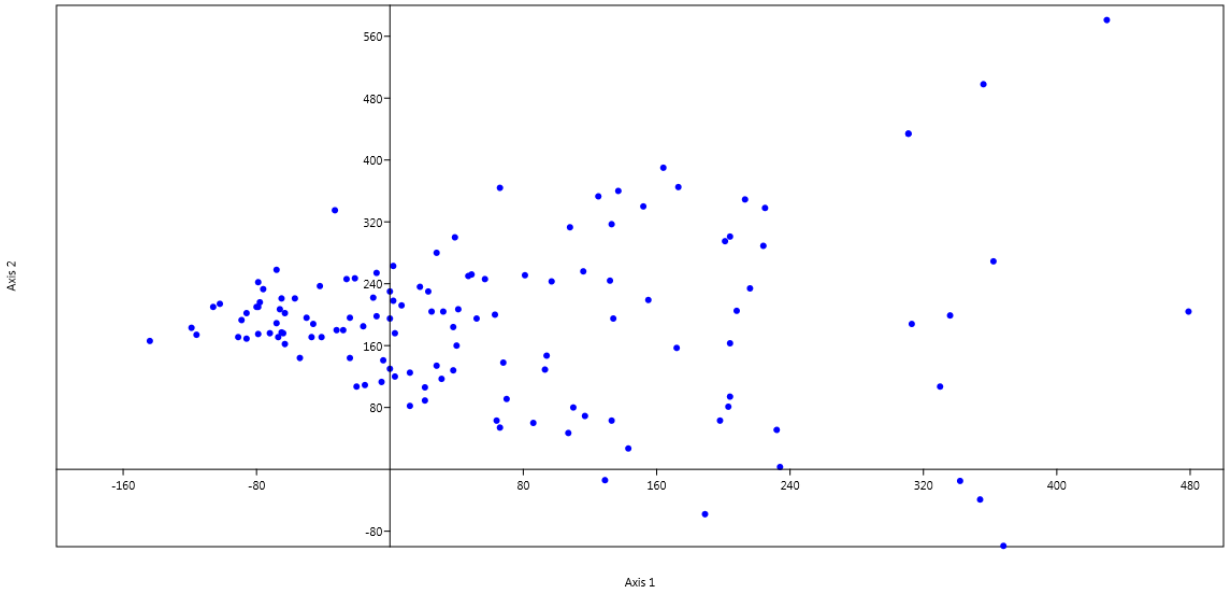

Figure E: Detrended Correspondence Analysis (DCA) for diatoms in sediment core VC001

Appendix F: DI Salinity Data

Table F: MOLTON/DEFINE Diatom Inferred (DI) salinity (Diatom taxonomy was harmonised with the Molten and Define project (http://craticula.ncl.ac.uk/Molten/jsp/ ; Andrén *et al*., 2007) includes the MOLTON code, the relevant species and the corresponding salinity optimum used for sediment core VC001.

MOLTEN code	Species	Salinity Optimum g L^{-1}
ActpSen	*Actinoptychus senarius*	22.16545232
AmpCym	*Amphora cymbaphora*	20.01336538
AmpOva	*Amphora ovalis*	11.75063553
BacPax	*Bacillaria paxillifer*	11.55816407
CalBac	*Caloneis bacillum*	5.141284154
CocPel	*Cocconeis peltoides*	17.58342943
CocPla	*Cocconeis placentula*	9.265022823
CocPla	*Cocconeis placentula var euglypta*	9.265022823
CocScu	*Cocconeis scutellum*	14.86218152
CycBod1	*Cyclotella bodanica*	6.743785734
CycCho	*Cyclotella choctawateeana*	7.177201741
CycComt	*Cyclotella comta*	17.6026398
CycMen	*Cyclotella meneghiniana*	3.511463732
CycOce	*Cyclotella ocellata*	5.4235889
CymAff	*Cymbella affinis*	2.839764226
CymHel	*Cymbella helvetica*	3.334495124
CymtBel	*Cymatosira belgica*	23.88912252
DelMin	*Delphineis minutissima*	25.03441183
DiaMon	*Diatoma moniliformis*	3.001764154
DimMin	*Dimeregramma minor*	19.56098293
DipDid	*Diploneis didyma*	14.23039818
EllAre	*Ellerbeckia arenaria*	4.155849188
EpiSor	*Epithemia sorex*	4.800656282
FraPar	*Pseudostaurosira parasitica*	5.914624
GlyDis	*Glyphodesmis distans*	13.2507648256
GomAngu	*Gomphonema angustum*	2.1488041744
GompExi	*Gomphynopsis exiguum var minutissima*	7.6295831089
GraOce	*Grammatophora oceanica*	16.6597034569
GyrBal	*Gyrosigma balticum*	17.92963524
HyaSco	*Hyalodiscus scoticus*	13.5050370064
KarCle	*Planothidium clevi*	3.42213001
MasSmi	*Mastagloia smithii var lacustrus*	4.2586925956
NavCryc	*Navicula cryptocephala*	4.436162688
NavDig	*Navicula digitoriata*	13.35061982
NavDir	*Navicula directa*	18.61413365
NavHal	*Craticula halophila*	15.60092004
NavLan	*Navicula lanceolata*	4.63334235
NavTrip	*Navicula tripuncta*	14.18102369
OpeMut	*Opephora mutabilis*	12.67303041
ParaSul	*Paralia sulcata*	19.56558289

MOLTEN code	Species	Salinity Optimum g L^{-1}
PlanDelG	*Planothidium delicatulum*	7.123080588
PlaSta	*Plagiogramma pulchellum var pygmaeum*	22.23282813
RhabMin	*Rhabdonema minutum*	18.79803435
SynUln	*Synedra ulna*	2.674271502
TabFasAG	*Tabularia fasciulata*	9.212742563
ThanNit	*Thalassionema nitzschoides*	20.23443299
TraAsp	*Trachaneas espera*	15.35605294
TryAcu	*Tryblionella acuminata*	20.03224855
TryApi	*Tryblionella apiculata*	12.47523592
TryCoa	*Tryblionella coarctata*	21.14031658
TryGra	*Tryblionella granulata*	4.905959204

Appendix G: Foraminifera

Table G: Complete list of fossil foraminifers found in sediment cores VC001 (1) and VC003 (3) from Inner Galway Bay; listed with taxonomic authority. Included in this table also is the Test Composition (C: calcareous; A: agglutinated; P: porcellaneous), Habitat Preference (I: infaunal; E: epifaunal), Growth Form and Environmental Preference. Ecological and environmental information was based on: Leobich and Tappan (1987); Scott *et al.* (2001); Murray (2003; 2006) and Horton and Edwards (2006).

Taxon Name and Authority	Core	Test Compo-sition	Habitat Preference	Growth Form	Environmental Preference
***Ammonia aberdovenysis* Haynes, 1973**	1	C	I	Trochospiral	Marine Inner shelf, muddy sand, brackish, warm temperate
***Ammonia beccarii* Linnaeus, 1758**	1,3	C	I	Trochospiral	Marine Inner shelf, muddy sand, brackish, warm temperate
***Ammonia* Brünnich, 1772**	1	C	I	Trochospiral	Marine Inner shelf, muddy sand, brackish, warm temperate
***Aubigyna hamblensis* Murray, Whittaker & Alve, 2000**	1	C	I	Trochospiral	Marine Inner shelf, sediment (lagoon), brackish, warm temperate
***Bolivina pseudoplicata* Heron-Allen & Earland, 1930**	1	C	I-E	Biserial	Marine Inner shelf-bathyal, cold-warm
***Bolivina spathulata* Williamson, 1858**	1,3	C	I-E	Biserial	Marine Inner shelf-bathyal, cold-warm
***Bolivinellina pseudopunctata* Höglund, 1947**	1,3	C	I	Biserial	Marine Inner shelf
***Brizalina variabilis* Williamson, 1858**	1,3	C	I	Biserial	Marine Inner shelf, intertidal, muddy, cold-temperate
***Buccella* Andersen, 1952**	1	C	I	Trochospiral	Marine Inner shelf, estuaries, lagoons, cold-temperate
***Bulimina elongata* d'Orbigny, 1826**	1	C	I	Triserial	Marine Inner shelf
***Bulimina gibba* d'Orbigny, 1826**	1,3	C	I	Triserial	Marine Inner shelf
***Bulimina inflata* Seguenza, 1862**	1	C	I	Triserial	Marine Inner shelf-deep sea
***Bulimina marginata d'*Orbigny, 1826**	1	C	I	Triserial	Marine Inner shelf
***Cassidulina carinata* Silvestri, 1896**	1,3	C	I	Biserial-planispiral	Marine Inner shelf
***Cibicides* de Montfort, 1808**	1,3	C	E	Trochospiral	Marine Inner shelf
***Cibicides refulgens* de Montfort, 1808**	1	C	E	Trochospiral	Marine Inner shelf, high energy
***Elphidium* de Montfort, 1808**	1,3	C	E	Planispiral	Marine, wide ranging
***Elphidium aculeatum* d'Orbigny,**	1,3	C	E	Planispiral	Marine Inner shelf

Taxon Name and Authority	Core	Test Compo-sition	Habitat Preference	Growth Form	Environmental Preference
1846					
***Elphibium bartletti* Cushman, 1933**	1	C	E	Planispiral	Marine Inner shelf, estuarine outer
***Elphidium crispum* Linnaeus, 1758**	1,3	C	E	Planispiral	Marine Inner shelf
***Elphidium earlandi* Cushman, 1936**	1	C	E	Planispiral	Marine intertidal, low marsh, tidal flat
***Elphidium excavatum* formae Terquem, 1875**	1,3	C	E	Planispiral	Marine intertidal, warm temperate
***Elphidium poeyamn* d'Orbigny, 1839**	3	C	E	Planispiral	Marine Inner shelf
***Elphidium williamsoni* Haynes, 1973**	1,3	C	E	Planispiral	Marine intertidal
***Epistominella exigua* Brady, 1884**	1,3	C	I	Trochospiral	Marine shelf seas-bathyal, temperate-cold
***Epistominella vitrea,* Parker, 1953**	1	C	I	Trochospiral	Marine shelf seas-bathyal, opportunistic
***Favulina squamosa* Montagu, 1803**	1	C	I	Spherical, ovoid	Marine Inner shelf, preference for muddy substrates
***Fissurina marginata* Montagu, 1803**	1,3	C	I	Rounded, ovoid	Marine Inner shelf - ectoparasitic
***Fissurina orbignyana* Seguenza, 1862**	1,3	C	I	Rounded, ovoid	Marine Inner shelf - ectoparasitic
***Fissurina subformosa* Parr, 1950**	1,3	C	I	Rounded, ovoid	Marine Inner shelf - ectoparasitic
***Gavelinopsis praegeri* Heron-Allen & Earland, 1913**	1,3	C	E	Trochospiral	Marine Inner shelf, clings to firm substrates
***Hansenisca soldanii* d'Orbigny, 1826**	1	C	E	Trochospiral	Marine Inner shelf-bathyal, cold
***Haplophragmoides bradyi* Robertson, 1891**	1,3	A	I	Planispiral	Marine Inner shelf, intertidal marsh
***Haynesina depressula* Walker & Jacob, 1798**	1	C	I	Planispiral	Marine Inner shelf, brackish, marsh, lagoon, cold-warm
***Haynesina germanica* Ehrenberg, 1840**	1,3	C	I	Planispiral	Marine Inner shelf, brackish, marsh, lagoon, cold-warm
***Haynesina obiculare* Brady, 1881**	1	C	I	Planispiral	Marine Inner shelf, brackish, marsh, lagoon, cold-warm
***Homalohedra williamsoni* Alcock, 1865**	1	C	I	Spherical, ovoid	Marine Inner shelf species, preference for muddy substrates
***Hyalinea balthica* Schröter, 1783**	3	C	E	Trochospiral	Marine Inner shelf, upper
***Jadammina macrescens* Brady, 1870**	3	A	E-I	Trochospiral	Marine marginal, high intertidal marsh
***Lagena doveyensis* Haynes, 1973**	1	C	I	Uniserial	Marine Inner shelf species, preference for muddy substrates
***Lagena substriata* Willianson, 1848**	1,3	C	I	Uniserial	Marine Inner shelf species, preference for muddy substrates
***Lagena sulcata* Walker & Jacob, 1798**	1,3	C	I	Uniserial	Marine Inner shelf species, preference for muddy substrates
***Laryngosigma lactea* Walker &**	1	C	E	Biserial	Marine Inner shelf

Taxon Name and Authority	Core	Test Compo-sition	Habitat Preference	Growth Form	Environmental Preference
Jacob, 1798					
***Lobatula lobatulus* Walker & Jacob, 1798**	1,3	C	E	Trochospiral	Marine Inner shelf species, high energy environments.
***Nonionella labradorica* Dawson, 1860**	3	C	I	Trochospiral	Marine Inner shelf, intertidal estuarine-cold temperate
***Patellina corrugata* Williamson, 1858**	1	C	E	Conical	Marine Inner shelf, cold-warm
***Procerolagena clavata* d'Orbigny, 1846**	1	C	I	Unilocular	Marine Inner shelf, bathyal
***Pyrgo williamsoni* Silvestri, 1923**	1	P	E	Planispiral	Marine Inner shelf species, preference for muddy substrates
***Quinqueloculina lata* Terquem, 1876**	1	P	E	Quinquelocu line	Marine Inner shelf, marsh, hypersaline lagoon, cold-warm
***Quinqueloculina seminulum* Linnaeus, 1758**	1,3	P	E	Quinquelocu line	Marine Inner shelf, marsh, hypersaline lagoon, cold-warm
***Reophax scorpiurus* de Montfort, 1808**	3	A	E	Uniserial	Marine Inner shelf, tidal flat, low marsh
***Rosalina anomala* Terquem, 1875**	1	C	E	Trochospiral	Marine Inner shelf, clings to seaweed & other firm substrates
***Siphotextularia flintii* Cushman, 1911**	1,3	A	E	Biserial	Marine Inner shelf, bathyal
***Siphotrochammina lobata* Saunders, 1957**	3	A	E	Trochospiral	Marine Inner shelf, marginal marine, marsh
***Spirillina vivipari* Ehrenberg, 1843**	1	C	E	Discoidal	Marine Inner shelf, opportunistic
***Spiroloculina* d'Orbigny, 1826**	1	P	E	Spiroloculine	Marine Inner shelf, attaches to substrate
***Stainforthia fusiformis* Williamson, 1848**	1,3	C	I	Triserial, biserial	Marine Inner shelf, opportunistic
***Textularia calva* Lalicker, 1940**	3	A	E	Biserial	Marine Inner shelf, lagoon-bathyal, cold-warm
***Textularia saggittula* Defrance, 1824**	1,3	A	E	Biserial	Marine Inner shelf, bathyal - open marine
***Textularia earlandi* Parker, 1952**		A	E	Biserial	Marine Inner shelf, marginal marine., estuaries, lagoons
***Trochimmina inflata* Montagu, 1808**	1,3	A	I	Trochospiral	Marine Inner shelf, marginal marine., high to mid marsh
***Vasiglobulina myristiformis* Williamson, 1858**	1	C	E	Ovoid	Marine Inner shelf, bathyal - open marine

APPENDIX H: PCA for Geochemical ratios

Table H: PCA Loadings of all sediment cores: (a) VC001, (b) VC002, (c) VC003, (d) VC004

a) VC001

Axis	Eigenvalue
Axis 1	0.46980805
Axis 2	0.27339987
Axis 3	0.13872999
Axis 4	0.05274829
Axis 5	0.03219521

FullName	Score01	Score02	Score03	Score04	Score05
Log Ca/Ti	-2.36274	-0.06722	-0.22334	-0.27278	-0.12743
Log K/Ti	0.314796	-0.36239	-1.77224	0.851264	0.402713
Log Si/Ti	-0.00398	0.497384	-0.62455	0.516522	-2.45099
Log Zr/Ti	0.598558	0.232077	-1.0685	0.318065	0.385991
Log Fe/Mn	-0.4537	-0.07616	0.8746	2.414508	0.305262
Log Br/Cl	0.041835	-2.55759	-0.04798	-0.05586	-0.47547
Log Sr/Ca	0.867472	-0.12592	1.228948	-0.00345	-0.58821

b) VC002

Axis	Eigenvalue
Axis 1	0.51982386
Axis 2	0.21095412
Axis 3	0.16172147
Axis 4	0.07220564
Axis 5	0.01729983

FullName	Score01	Score02	Score03	Score04	Score05
LOG Ca/Ti	0.447766	-0.8276	-2.12639	0.217827	0.320203
LOG K/Ti	0.132121	-0.11868	-0.62327	-0.24959	1.341591
LOG Si/Ti	0.120818	0.265301	-0.31386	-2.57043	-0.03209
LOG Zr/Ti	0.759905	1.328272	-1.17011	0.415232	-1.10335
LOG Fe/Mn	-0.00952	-0.07596	0.023234	0.299893	1.68641
LOG Br/Cl	2.436005	-0.68409	0.770755	-0.05503	0.009518
LOG Sr/Ca	0.505756	1.998135	0.166528	0.133215	1.017412

c) VC003

Axis	Eigenvalue
Axis 1	0.60932355
Axis 2	0.26392919
Axis 3	0.06601107
Axis 4	0.03348652
Axis 5	0.01948983

FullName	Score01	Score02	Score03	Score04	Score05
LOG Ca/Ti	-2.19827	-0.40215	0.493748	-0.18878	0.917933
LOG K/Ti	-0.12516	-0.149	0.33173	-0.00879	0.572114
LOG Si/Ti	-0.38868	-0.37947	1.678709	0.305985	-1.93785
LOG Zr/Ti	-0.27363	-0.3358	0.869535	-0.11304	0.727198
LOG Fe/Mn	0.306306	-0.28378	0.241289	-2.589	-0.19854
LOG Br/Cl	0.207761	-2.51398	-0.74397	0.242778	-0.15589
LOG Sr/Ca	1.337542	-0.39836	1.568537	0.309889	1.217492

d) VC004

Axis	Eigenvalue
Axis 1	0.77435786
Axis 2	0.14143103
Axis 3	0.04486702
Axis 4	0.01653727
Axis 5	0.01310722

FullName	Score01	Score02	Score03	Score04	Score05
LOG Fe/Mn	0.084528	0.267504	-0.1759	0.032967	0.09546
LOG K/Ti	-0.16694	-0.60687	0.465775	-0.32996	0.209185
LOG Sr/Ca	0.06195	0.179327	0.044229	-0.79286	1.422332
LOG Br/Cl	-2.6736	0.908138	0.16276	0.00956	-0.01544
LOG Ca/Ti	-0.11773	-0.7683	2.199096	0.057332	-1.27684
LOG Si/Ti	-0.87279	-2.36201	-1.14573	-0.2605	-0.16051
LOG Zr/Ti	-0.12932	-0.52418	1.172109	-1.12825	1.635443